



International Society for  
Therapeutic Ultrasound



# ISTU 2009

[www.istu2009.org](http://www.istu2009.org)

# FINAL PROGRAM





THE UNIVERSITY OF TOKYO

Department of Mechanical Engineering  
7-3-1 Hongo, Bunkyo-ku Tokyo 113-8656 JAPAN  
Phone : +81-3-5841-6286  
Fax : +81-3-5802-2947 e-mail : ymats@mech.t.u-tokyo.ac.jp

The Board of the International Society for Therapeutic Ultrasound  
is very pleased to present the 10th edition of  
the International Symposium on Therapeutic Ultrasound

Under the Chairmanship of

**YOICHIRO MATSUMOTO**  
Special Advisor to the President, Professor  
University of Tokyo

A handwritten signature in black ink, likely belonging to Yoichiro Matsumoto.

**ISTU 2010**  
**June 2 to 5, 2010**  
Hongo Campus  
The University of Tokyo  
Hongo, Bunkyo-ku  
Tokyo, Japan





## TABLE OF CONTENT

- Welcome Messages .....4
- General Information.....6
- General Map of the Congress Center .....7
- Registration Modalities .....8
- Technical Exhibition Information & Map .....9
- Poster Exhibition Information & Map ..... 11
- Invited Speakers.....15
- Program at a Glance .....16
- Detailed Program .....18
- Posters .....26
- Abstracts
  - Thursday, September 24.....33
  - Friday, September 25.....79
  - Saturday, September 26 .....117
  - Poster Communications.....131
- Authors Index .....183



**WELCOME MESSAGE FROM THE  
PRESIDENT OF ISTU**

On the behalf of the International Society of Therapeutic Ultrasound (ISTU) it is my pleasure to welcome you to the ninth International Symposium on Therapeutic Ultrasound.

Therapeutic ultrasound is a rapidly growing field, with a wide range of novel therapies being developed. Some areas of current interest in the field of therapeutic ultrasound include: tumor ablation, stroke, vascular malfunction, and targeted gene and drug delivery.

Numerous companies have been formed that are dedicated to developing technologies for various ultrasound-based therapies.

Tens of thousands of patients with tumors have been treated with therapeutic ultrasound in recent years. Given the recent advances in medical imaging and ultrasound technology, and the increased interest in minimally invasive medicine, this technology will no doubt continue to advance rapidly for years to come.

The purpose of ISTU is to promote international development and collaboration in the general field of therapeutic ultrasound including research, development, commercialization, clinical application, education, and standardization.

With that goal in mind this 9<sup>th</sup> International Symposium will foster communication among diverse multidisciplinary fields, provide an overview and basic background for clinical uses of ultrasound therapy, and share insights among researchers, clinical users and device manufacturers.

I would like to thank the organizers for the exciting program and I hope you enjoy the meeting and beautiful Southern France.

**Kullervo Hynynen, Ph.D.**  
**President**  
**International Society of Therapeutic Ultrasound**



**WELCOME MESSAGE FROM THE  
CHAIRMAN OF ISTU 2009**

Dear Colleagues and Friends,

Welcome in Provence!

We have been able to put together a very interesting program for this 9<sup>th</sup> edition of the ISTU annual symposium. We have tried to keep a good balance between clinically focused and scientific driven presentations. The major themes covered by the different talks will address the following topics:

- HIFU-mediated drug delivery,
- HIFU applications in the brain
- HIFU physics and bioeffects
- HIFU surgery, tissue ablation & erosion
- HIFU applications in the prostate
- HIFU-mediated sonothrombolysis
- Guidance techniques, monitoring, treatment planning & quality assessment.

The beautiful city of Aix-en-Provence is going to welcome us on the occasion of ISTU 2009. Aix-en-Provence is a city of Art and Culture with its two most famous citizens being the painter Paul Cezanne and the novelist Emile Zola. Today the City is celebrating Picasso and Cezanne in an exhibit at the Musée Granet in Aix-en-Provence. Years ago, Picasso bought a castle few miles out of Aix-en-Provence, the Castle of Vauvenargues, where he is now buried with his last wife Jacqueline. Through the acquisition of the castle located right under Montagne Sainte Victoire, a mountain painted by Cezanne at different time of the year, he wanted in fact to acquire the surroundings of Cezanne.

Aix-en-Provence is also a university city where humanities, literature, political science and law are being taught, the neighbouring metropolis of Marseille being focused at the academic level on sciences.

I hope you will enjoy your time in Aix-en-Provence and that this 9<sup>th</sup> symposium will fulfill your expectation from a scientific standpoint.

So once again welcome in Provence,  
Best Regards,

**Jacques Souquet, Ph.D.**  
**Chairman of ISTU 2009**



## GENERAL INFORMATION

### REGISTRATION & INFORMATION DESK

#### ➤ Opening hours

Wednesday, September 23-----	14:00 – 18:00
Thursday, September 24-----	07:00 – 19:00
Friday, September 25-----	07:30 – 18:30
Saturday, September 26-----	07:30 – 14:00

① **Contact: +33 (0)678 604 708**

### PREVIEW ROOM

#### ➤ Opening hours

Wednesday, September 23-----	16:00 – 18:00
Thursday, September 24-----	07:30 – 18:00
Friday, September 25-----	07:30 – 18:00
Saturday, September 26-----	07:30 – 13:00

### INTERNET LOUNGE

Two desktop computers are available in Picasso Room (ground floor) to stay tuned with your contacts.

#### ➤ Opening hours

Thursday, September 24-----	08:00 – 18:30
Friday, September 25-----	08:00 – 18:30
Saturday, September 26-----	08:00 – 13:00

**WIFI connection:** code to access free WIFI connection is **aixcongres13**

### PRODUCTS OF PROVENCE

The Aix-en-Provence Tourist Office will be very pleased to welcome you to its booth in the Picasso Room. A variety of local products including food and beverage will be presented there and available for purchase. This is a nice opportunity for attendees to bring souvenirs back home.

### OPENING CEREMONY

The ISTU 2009 Opening Ceremony will occur on Thursday, September 24, at 08:00, in the Cezanne Room, which is the amphitheatre of the Congress Center.

### **GALA DINNER**

Jacques Souquet, Chairman of ISTU 2009, is very pleased to invite you to join the ISTU 2009 Gala Dinner, on Friday, September 25, at 20:00, in the Chateau Pont Royal.

Full registration to ISTU 2009 includes a complimentary voucher to attend this Gala Dinner event. Extra tickets can be purchased at the Registration Desk at the price of 95 €.

Ground transportation to and back from the Chateau Pont Royal has been arranged for dinner attendees. Please confirm your seat at the Registration Desk on Thursday, September 24 at latest. The meeting point will be situated in front of the Congress Center on **Friday, September 25 at 19:15.**

### **BREAKS & LUNCHES**

Breaks in the morning include beverages, fresh fruits and «French viennoiseries».

Lunches: a buffet will be offered on the ground floor.

Breaks in the afternoon include beverages.

### **AWARDS CEREMONY**

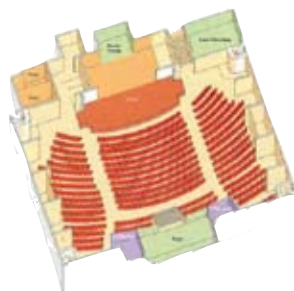
The International Society for Therapeutic Ultrasound is very pleased to announce the Awards Ceremony that will be held on the occasion of the Gala Dinner, in the Chateau Pont Royal, on Friday, September 25.

#### **Awards include:**

- The Fred Lizzi Early Career Award
- The William and Francis Fry Honorary Fellowship for Contributions to Therapeutic Ultrasound Award
- Student Prizes will be announced after the conference.



## **GENERAL MAPS OF THE CONGRESS CENTER**





## REGISTRATION MODALITIES

▀ INCLUDES:

- Entry to all sessions in Cezanne and Milhaud Rooms
- Access to the Poster Exhibition (Milhaud and Forbin Rooms)
- Access to the Technical Exhibition (Sainte Victoire and Picasso Rooms)
- Student and standard registrations include coffee breaks, lunches and one voucher for the Gala Dinner. Extra tickets can be purchased at the Registration Desk at the price of 95 €.





## TECHNICAL EXHIBITION INFORMATION

### ► OPENING HOURS:

- from 08:00 to 18:30 on Thursday, September 24
- from 08:00 to 18:30 on Friday, September 25
- from 08:00 to 13:00 on Saturday, September 26

ISTU 2009 thanks all its Sponsors and Partners for their contribution and support

### ► GOLD LEVEL SPONSOR

# PHILIPS

### ► SILVER LEVEL SPONSORS



Bringing New Horizons to Therapy

### ► BRONZE LEVEL SPONSORS

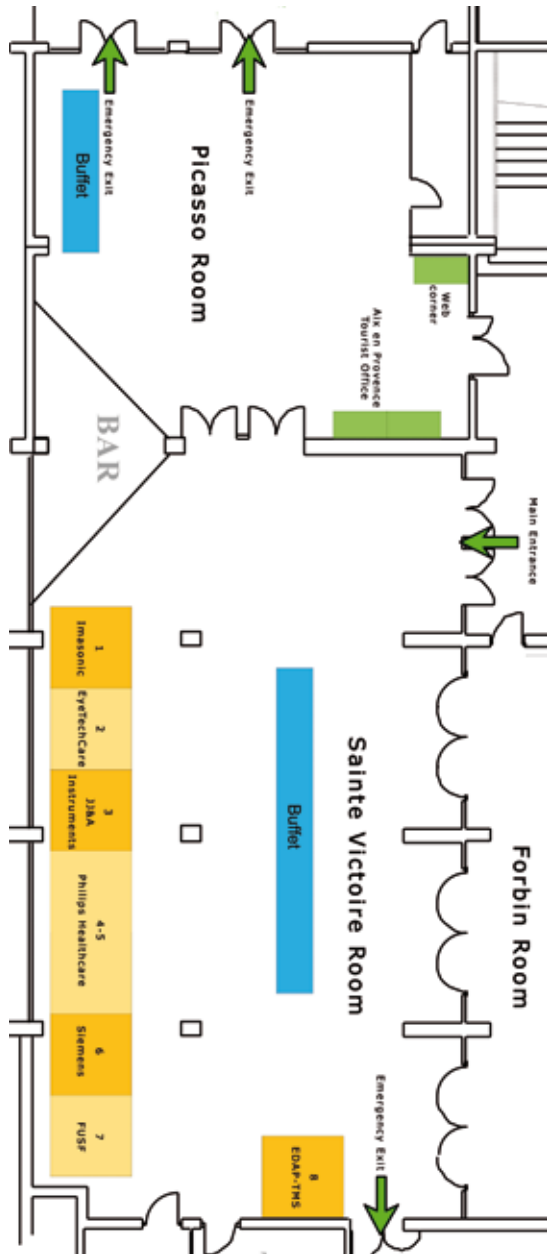


### ► INSTITUTIONAL PARTNERS





## MAP OF THE TECHNICAL EXHIBITION





## POSTER EXHIBITION INFORMATION

### ▼ OPENING HOURS:

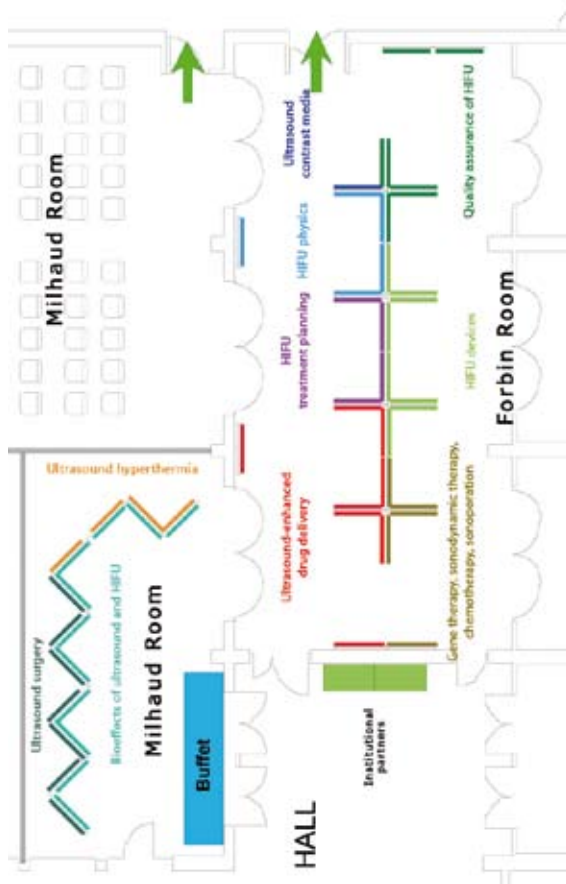
ISTU 2009 thanks all the authors who are presenting their work during this edition.

The Poster Exhibition at ISTU 2009 opens:

- from 08:00 to 18:30 on Thursday, September 24
- from 08:00 to 18:30 on Friday, September 25
- from 08:00 to 13:00 on Saturday, September 26



## MAP OF THE POSTER EXHIBITION





# Invited Speakers & Program

[www.istu2009.org](http://www.istu2009.org)



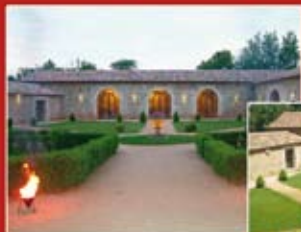
## *ISTU 2009 Gala Dinner*

*At the very heart of Provence,  
experience the French magnificence*

*The ISTU2009 Chairman invites you to a grandiose Gala dinner  
at the Chateau Pont Royal on September 25.*

*Buses departure at 19:15 in front of the Congress Center*

*Information & vouchers available at the front desk until September 24*







## INVITED SPEAKERS

- **Alexandre Carpentier**

Hôpital de la Salpêtrière  
Service de Neurochirurgie  
47/83, Bd de l'hôpital  
75651 Paris Cedex 13 - France  
alexandre.carpentier@psl.aphp.fr

- **Larry Crum**

University of Washington  
Center for Industrial and  
Medical Ultrasound  
Applied Physics Laboratory  
1013 NE 40<sup>th</sup> street  
Seattle, WA 98105 - USA  
lac@mail.apl.washington.edu

- **Mark Emberton**

UCLH/UCL  
Comprehensive Biomedical Center  
149 Tottenham Court Road  
London W1T 7NF - United Kingdom  
markemberton1@btinternet.com

- **Gerald Harris**

Food and Drug Administration  
Center for Devices  
and Radiological Health  
10903 New Hampshire Avenue  
Room WO62-2104  
Silver Spring, MD 20993-0002 - USA  
gerald.harris@fda.hhs.gov

- **Neal Kassell**

Focused Ultrasound Surgery Foundation  
213 7<sup>th</sup> Street, NE  
Charlottesville, VA 22902 - USA  
nfk8g@hscmail.mcc.virginia.edu

- **Pierre Khuri-Yakub**

Stanford University  
E. L. Ginzton Laboratory, room 11  
Stanford, CA 94305-4088 - USA  
khuri-yakub@stanford.edu

- **Stephen Meairs**

Department of Neurology,  
Universitätsmedizin Mannheim  
Mannheim - Germany  
meairs@neuro.ma.uni-heidelberg.de

- **William O'Brien**

University of Illinois  
at Urbana-Champaign  
Department of Electrical  
and Computer Eng.  
405 N. Mathews  
Urbana, IL 61801 - USA  
wdo@uiuc.edu

- **Bruno Quesson**

Université V Segalen Bordeaux 2  
UMR 5231  
146 rue Léo Saignat  
33076 Bordeaux Cedex - France  
b.quesson@imf.u-bordeaux2.fr

- **Gail ter Haar**

Royal Marsden Hospital  
Joint department of Physics  
Sutton  
Surrey SM2 5PT - United Kingdom  
gail.terhaar@jcr.ac.uk

- **Feng Wu**

The Churchill Hospital  
HIFU Unit  
Headington,  
Oxford OX3 7LJ - United Kingdom  
mfengwu@yahoo.com



## PROGRAM AT A GLANCE

**Thursday,  
September 24**

Cezanne Room	Milhaud Room
<b>08.00</b>	
OPENING CEREMONY	
<b>08.24</b>	
SESSION 1 Ultrasound surgery	
<b>10.12 Break</b>	
<b>10.48</b>	
SESSION 2A Sonothrombolysis	SESSION 2B HIFU tissue erosion
<b>12.36 Lunch</b>	
<b>13.36</b>	
SESSION 3A US-guided HIFU	SESSION 3B Contrast physics & drug delivery
<b>15.12 Break</b>	
<b>15.48</b>	
SESSION 4A HIFU surgery in the brain	SESSION 4B Principles for HIFU-mediated drug delivery

**Friday,  
September 25**

Cezanne Room	Milhaud Room
<b>08.00</b>	
SESSION 5 High intensity focused ultrasound physics	
<b>10.12 Break</b>	
<b>10.48</b>	
SESSION 6A Use of cavitation in HIFU	SESSION 6B Efficacy of HIFU-mediated drug delivery
<b>12.36 Lunch</b>	
<b>13.36</b>	
SESSION 7A Quality assessment & treatment planning	SESSION 7B Drug delivery & monitoring in the brain
<b>15.12 Break</b>	
<b>15.48</b>	
SESSION 8 HIFU transducers	





**DETAILED PROGRAM**

Thursday, September 24

**Cezanne Room**

▣ **OPENING CEREMONY**

08:00	Official welcome address .....	<i>J. Souquet</i>
08:12	Key factors of attractiveness in Provence .....	<i>P. Distinguin</i>

▣ **SESSION 1: ULTRASOUND SURGERY**

**CHAIRPERSONS:**  
F. WU & J. SOUQUET

<b>08:24</b>	<b>Invited lecture: Global clinical vision of the role of HIFU</b> .....	<i>F. Wu</i>
08:48	Optimal transthoracic targeting of liver tumors using dual-mode ultrasound arrays: a numerical and experimental study .....	<i>A. Casper</i>
09:00	Segmental liver resection assisted by HIFU: tissue precauterization using a toroidal-shaped HIFU transducer .....	<i>WA. N'Djin</i>
09:12	Efficacy and safety of focused ultrasound ablation for small hepatocellular carcinoma .....	<i>H. Fukuda</i>
09:24	MR guided focused ultrasound surgery for early breast cancer .....	<i>H. Furusawa</i>
09:36	Can extracorporeal HIFU adequately ablate small renal tumours? .....	<i>R. Ritchie</i>
09:48	Preliminary results: MR guided volumetric HIFU ablation of uterine fibroids with binary feedback control .....	<i>C. Mougnot</i>
10:00	Focused ultrasound to move kidney stones .....	<i>MR. Bailey</i>
10:12	Histotripsy for pediatric cardiac applications: in vivo piglet model .....	<i>R. Miller</i>

**10:24 >>> Break**

▣ **SESSION 2A: SONOTROMBOLYSIS**

**CHAIRPERSONS:**  
S. MEAIRS & K. HYNYNEN

<b>10:48</b>	<b>Invited lecture: Advances in sonothrombolysis</b> .....	<i>S. Meairs</i>
11:12	Acoustic fields involved in clinical trials of sonothrombolysis: investigation of the TRUMBI device .....	<i>JF. Aubry</i>
11:24	An investigation of the use of pulsed high intensity focused ultrasound for thrombolysis .....	<i>D. Goertz</i>
11:36	Enhancement of purely ultrasound thrombolysis efficiency using a bifrequency excitation .....	<i>I. Saletes</i>
11:48	The effects of microbubble size physical properties and acoustical properties on the efficacy of microbubble-ultrasound mediated sonothrombolysis .....	<i>MJ. Borrelli</i>
12:00	Transcranial clot lysis using high intensity focused ultrasound .....	<i>T. Hoelscher</i>
12:12	Penetration and diffusion of tissue plasminogen activator into whole blood clots following pulsed-high intensity focused ultrasound exposures .....	<i>G. Jones</i>

**12:36 >>> Lunch**

SESSION 3A: ULTRASOUND-GUIDED HIFU

CHAIRPERSONS:  
G. TER HAAR & E. EBBINI

13:36	<b>Invited lecture: Ultrasound guided HIFU: strength and weakness ....</b> <i>G. ter Haar</i>
14:00	Validating ultrasound-based HIFU lesion-size monitoring technique with MR thermometry and histology ..... <i>S. Zhou</i>
14:12	Real-time two-dimensional temperature imaging using ultrasound ..... <i>D. Liu</i>
14:24	Ultrasound-based mapping of elasticity and temperature during HIFU therapy: an ex vivo feasibility study ..... <i>E. Sapin</i>
14:36	Monitoring high intensity focused ultrasound therapy with backscattered ultrasound with a parametric treatment model ..... <i>G. Speyer</i>
14:48	Monitoring of thermal ablation during HIFU exposure using passive cavitation mapping ..... <i>M. Gyöngy</i>
15:00	HIFU Induced Displacement Estimation (HIDE) maps for monitoring the creation of thermal lesions ..... <i>C. Haw</i>
15:12	Real time motion correction for transcostal liver therapy: in vitro experiments ..... <i>F. Marquet</i>
15:24	An automated dosing method for a HIFU device containing multiple phased arrays ..... <i>X. Zeng</i>
15:36	Ultrasound-based monitoring technique to control lesion size during HIFU therapy ..... <i>A. Anand</i>
15:48	Ultrasound guided high intensity focused ultrasound (US-gFUS) therapy for uterine fibroids. Initial experiece in our center ..... <i>J. Insem Quitlet</i>

16:00 >>> Break

SESSION 4A: HIFU SURGERY IN THE BRAIN

CHAIRPERSONS:  
N. KASELL & M. FINK

16:36	<b>Invited lecture: Future clinical role of HIFU in the brain and the mission of the focused ultrasound surgery foundation</b> ..... <i>N. Kassell</i>
17:00	<b>Invited lecture: Experience in brain tissue necrosis using laser ...</b> <i>A. Carpentier</i>
17:24	MR-guided ultrasonic brain therapy: high frequency approach ..... <i>JF. Aubry</i>
17:36	Nonlinear ultrasound propagation through the skull ..... <i>G. Pinton</i>
17:48	Large-scale analysis of focused ultrasound in heterogeneous media ..... <i>J. Uebayashi</i>
18:00	Transcranial MR-guided high intensity focused ultrasound for non-invasive functional neurosurgery ..... <i>B. Werner</i>
18:12	MR guidance monitoring and control of brain HIFU therapy in small animals: in vivo demonstration in rats at 7T ..... <i>B. Larrat</i>
18:24	Real-time magnetic resonance temperature mapping in the brain ..... <i>A. Kickhefel</i>



**DETAILED PROGRAM**

Thursday, September 24

**Milhaud Room**

**SESSION 2B: HIFU TISSUE EROSION**

**CHAIRPERSON:**  
**M. TANTER**

10:48	Feasibility of HIFU tissue ablation in the presence of ribs using a 2D random phased array .....	<i>S. Bobkova</i>
11:00	A tissue phantom for evaluation of mechanical damage caused by cavitation .....	<i>A. Maxwell</i>
11:12	Tissue erosion using shock wave heating and millisecond boiling in high intensity focused ultrasound fields .....	<i>M. Canney</i>
11:24	Tissue ablation using cavitating bubbles triggered by high intensity ultrasound pulse .....	<i>S. Yoshizawa</i>
11:36	Why are short pulses more efficient in tissue erosion using pulsed cavitational ultrasound (histotripsy)? .....	<i>TY. Wang</i>
11:48	Evaluation of the contrast between tissues in rabbit in vivo and thermal lesions produced by HIFU using fast spin echo MRI sequences .....	<i>C. Damianou</i>
12:00	Adaptive volumetric MR-guided high-intensity focused ultrasound ablations in moving organs .....	<i>S. Hey</i>

**12:36 >>> Lunch**

**SESSION 3B: CONTRAST PHYSICS AND DRUG DELIVERY**

**CHAIRPERSON:**  
**M. BAILEY**

13:36	Development of a cannulated vessel model for the study of cell sonoporation in the presence of contrast agents .....	<i>A. Tokarczyk</i>
13:48	Validation of an acoustic cavitation dose in pulsed mode by the terephthalate dosimeter for in vitro drug delivery application .....	<i>L. Somaglino</i>
14:00	Cavitation-enhanced momentum transfer for drug delivery .....	<i>B. Rifai</i>
14:12	Correlation of ultrasound-mediated drug delivery with acoustical properties of the transducer by macroscopic fluorescence imaging .....	<i>M. Lepetit-Coiffe</i>
14:24	Ultrasound-inducible fluorescent particles for internal tattooing .....	<i>O. Couture</i>
14:36	Real-time monitoring of drug delivery with MRgHIFU and image-able low temperature sensitive liposomes .....	<i>A. Partanen</i>
14:48	Ultrasonic activation of thermally sensitive liposomes .....	<i>E. Mylonopoulou</i>

**16:00 >>> Break**

**SESSION 4B: PRINCIPLES OF HIFU-MEDIATED DRUG DELIVERY**

**CHAIRPERSON:**  
**L. CRUM**

16:36	Enhancement of antitumor effect by the combination of therapeutic ultrasound and immunotherapy ..... <i>N. Nishiie</i>
16:48	Sonoporation of cervical carcinoma cells affected with E6-oncoprotein for the treatment of uterine cancer ..... <i>L. Curiel</i>
17:00	Sonoporation outcome correlated with time-resolved measurements of microbubble dynamics ..... <i>Z. Fan</i>
17:12	Short-duration focused ultrasound stimulation of Hsp70 expression in vivo ..... <i>D. Kruse</i>
17:24	Ultrasound-enhanced nanotherapy of pancreatic cancer ..... <i>N. Rapoport</i>
17:36	Cancer gene therapy by the combination of liposomal bubbles and ultrasound ..... <i>R. Suzuki</i>
17:48	Investigations in to the influence of pulsed high intensity focused ultrasound on metastasis in a murine model ..... <i>H. Hancock</i>
18:00	Pulsed-HIFU enhanced delivery and therapy using radiolabeled monoclonal antibodies ..... <i>F. Razjouyan</i>
18:12	Therapeutic benefits of ultrasound delivery of anti-AB antibody in an Alzheimer's mouse model ..... <i>J. Jordao</i>
18:24	Virus-loaded microbubbles as a tool for targeted gene delivery ..... <i>B. Geers</i>



**DETAILED PROGRAM**

Friday, September 25

**Cezanne Room**

**SESSION 5: HIGH INTENSITY FOCUSED ULTRASOUND PHYSICS**

**CHAIRPERSONS:**  
W. O'BRIEN & C. DIEDERICH

08:00	<b>Invited lecture: HIFU dosimetry</b> .....	<i>W. O'Brien</i>
08:24	Non invasive transcostal focusing based on the decomposition of the time reversal operator: in vitro validation .....	<i>E. Cohard</i>
08:36	An analytical comparison of the thermal dose equation and the intensity-time product $I t^n$ for predicting tissue damage thresholds .....	<i>G. Harris</i>
08:48	Energy based adaptive focusing: optimal ultrasonic focusing using radiation force MR guidance .....	<i>B. Larrat</i>
09:00	The effect of electronically steering a phased-array transducer on proximal tissue heating .....	<i>A. Payne</i>
09:12	On the mathematical model of ultrasound propagation in liver .....	<i>G. Vilenskiy</i>
09:24	The effect of visco-elasticity on the stability of inertial cavitation .....	<i>D. Sinden</i>
09:36	Perfusion models for steep thermal gradients .....	<i>S. Woodford</i>
09:48	Fast ultrasound beam simulation in inhomogeneous tissue geometries for MRI-guided HIFU .....	<i>U. Vyas</i>
10:00	HIFU thermometry and acoustic calibration using a fibre-optic hydrophone .....	<i>J. Civalo</i>

**10:12 >>> Break**

**SESSION 6A: USE OF CAVITATION IN HIFU**

**CHAIRPERSONS:**  
L. CRUM & C. COUSSIOS

10:48	<b>Invited lecture: Cavitation during HIFU treatment</b> .....	<i>L. Crum</i>
11:12	Characterization of HIFU-induced cavitation activity and heating in porcine subcutaneous fat .....	<i>ZM. Kyriakou</i>
11:24	On cellular response to low intensity ultrasound .....	<i>N. Mizrahi</i>
11:36	Analysis of the microbubble dynamics under the ultrasound exposure .....	<i>Y. Nakamura</i>
11:48	A real-time controller for sustaining thermally relevant cavitation during HIFU exposure .....	<i>N. Hockham</i>
12:00	Characterization of perfluorocarbon droplets for focused ultrasound therapy .....	<i>K. Schad</i>
12:12	Temperature distribution heating experiment using HIFU and microbubble .....	<i>H. Utashiro</i>
12:24	Modelling oscillations of a microbubble in an elastic vessel .....	<i>S. Martynov</i>

**12:36 >>> Lunch**

SESSION 7A: QUALITY ASSESSMENT AND TREATMENT PLANNING

CHAIRPERSONS:  
G. HARRIS & G. TER HAAR

13:36	<b>Invited lecture: HIFU and regulatory challenges</b> .....	<i>G. Harris</i>
14:00	Realtime acousto-optical QA methods for high intensity fields .....	<i>I. Butterworth</i>
14:12	Effects of thermal dose-dependent absorption on temperature rise and lesion volume in HITU applications .....	<i>J. Soneson</i>
14:24	Spatially and temporally-controlled mild hyperthermia using a linear array .....	<i>CY. Lai</i>
14:36	Contrast agent ultrasonography before and after HIFU treatment of parathyroid glands .....	<i>F. Lacoste</i>
14:48	Tumor-specific immune response induced by HIFU therapy: a study in a mouse model .....	<i>T. Khokhlova</i>

15:12 >>> **Break**

SESSION 8: HIFU TRANSDUCERS

CHAIRPERSONS:  
P. KHURI-YAKUB & JY. CHAPELON

15:48	<b>Invited lecture: HIFU transducers - a vision for the future</b> .....	<i>P. Khuri-Yakub</i>
16:12	High power low impedance therapeutic intracavitary phased array .....	<i>A. Kukic</i>
16:24	Dual-mode 64-element array for interstitial ultrasound imaging and thermal ablation .....	<i>N. Owen</i>
16:36	Development of a new HIFU device for treating glaucoma: Preliminary results .....	<i>T. Charrel</i>
16:48	Design of a high intensity focused ultrasound multi-element phased array for transcostal treatment of liver tumours .....	<i>P. Gelat</i>
17:00	Thermal ablation of liver tumors by high intensity focused ultrasound using a toroid transducer. Results of animal experiments .....	<i>D. Melodelima</i>
17:12	Effects of respiratory motion on in-vivo HIFU treatments: a comparative study in the liver .....	<i>WA. N'Djin</i>
17:24	Criteria for modelling the capabilities of a 48 element phased array HIFU transducer .....	<i>I. Rivens</i>
17:36	Direct methods for free field characterization of HIFU transducers using acoustic streaming .....	<i>P. Hariharan</i>
17:48	Measurement of the total acoustic output power of HITU transducers .....	<i>KV. Jenderka</i>
18:00	Feasibility of a PVDF receiver for monitoring of transcranial therapy .....	<i>M. O'Reilly</i>



**DETAILED PROGRAM**

Friday, September 25

**Milhaud Room**

**SESSION 6B: EFFICACY OF HIFU-MEDIATED DRUG DELIVERY**

**CHAIRPERSON:  
B. WOOD**

10:48	In vivo and ex vivo assessment of pulsed HIFU-enhanced penetration of small molecules .....	<i>JH. Hwang</i>
11:00	Closed-loop controlled noninvasive ultrasonic glucose sensing and insulin delivery .....	<i>N. Smith</i>
11:12	Ultrasonic drug delivery in phase-shift nanoemulsions .....	<i>N. Rapoport</i>
11:24	Enhancement of doxorubicin effect on cancer cell mortality with ultrasound and microbubbles .....	<i>J. Piron</i>
11:36	Qualitative and quantitative evaluation of nanoparticles delivery into tumor tissue enhanced by focused ultrasound with microbubbles .....	<i>CY. Lin</i>
11:48	Controlled ultrasound-induced delivery of doxorubicin from liposomes on AT2-Dunning tumors: preliminary studies .....	<i>C. Lafon</i>
12:00	Inertial cavitation enhances the extravasation and therapy of an oncolytic adenovirus for breast cancer treatment .....	<i>M. Bazan-Peregrino</i>

**12:36 >>> Lunch**

**SESSION 7B: DRUG DELIVERY AND MONITORING IN THE BRAIN**

**CHAIRPERSON:  
E. KONOFAGOU**

13:36	Mechanism and safety at the threshold of BBB opening in vivo .....	<i>E. Konofagou</i>
13:48	Focused ultrasound induced blood-brain barrier to enhance chemotherapeutic drugs (BCNU) delivery for glioblastoma treatment .....	<i>HL. Liu</i>
14:00	Dual photon investigation of ultrasound induced BBB disruption: a threshold and dynamics study .....	<i>J. Drazic</i>
14:12	The dynamic of FUS-induced BBB opening in mouse brain assessed by contrast enhanced MRI .....	<i>JW. Jenne</i>
14:24	Identifying the inertial cavitation threshold of monodispersed microbubbles and skull effects in a vessel phantom using focused ultrasound .....	<i>YS. Tung</i>
14:36	Time reversal ultrasound system for enhanced drug delivery in rat brain .....	<i>L. Fillinger</i>
14:48	A high precision MR-compatible three-axis positioning system for focused ultrasound drug delivery in small animal models .....	<i>R. Chopra</i>

**15:12 >>> Break**



**DETAILED PROGRAM**

Saturday, September 26

**Cezanne Room**

**SESSION 9: HIFU IN THE PROSTATE**

**CHAIRPERSONS:**  
M. EMBERTON & E. BLANC

08:00	<b>Invited lecture: HIFU of the prostate: its challenges its strength and weakness</b> ..... <i>M. Emberton</i>
08:24	Primary prostate HIFU: local control and biochemical survival of 966 patients tracked with the @-registry ..... <i>A. Gelet</i>
08:36	Ten-year experience of high intensity focused ultrasound (HIFU) for localized prostate cancer..... <i>T. Uchida</i>
08:48	Analysis of acoustic access to the prostate through the abdomen and perineum for extracorporeal ablation ..... <i>T. Hall</i>
09:00	Histological evaluation of conformal 3D MRI-guided transurethral ultrasound therapy in the prostate..... <i>S. Vedula</i>
09:12	Ultrasound-activated microbubble enhancement of radiation response ..... <i>G. Czarnota</i>
09:24	Ultrasound properties of human tissues ..... <i>L. Retat</i>
09:36	Practical measures for evaluation of ultrasound therapies of the prostate ..... <i>I. Koblelevskiy</i>
09:48	Salvage therapy of high-intensity focused ultrasound (HIFU) ..... <i>S. Shoji</i>
10:00	HIFU partial treatment of localized prostate cancer: influence on erectile dysfunction (ED) ..... <i>A. Gelet</i>

**10:12 >>> Break**

**SESSION 10: MRI MONITORING DURING HIFU PROCEDURES**

**CHAIRPERSONS:**  
B. QUESSON & JH. HWANG

10:48	<b>Invited lecture: Rapid and volumetric MRI thermometry for monitoring HIFU ablation in the liver during breathing</b> ..... <i>B. Quesson</i>
11:12	Real time MR for in vivo monitoring of HIFU of the liver ..... <i>A. Holbrook</i>
11:24	Three dimensional motion compensation for real-time MRI guided focused ultrasound treatment of abdominal organs ..... <i>M. Ries</i>
11:36	Inter-costal liver ablation under real-time MR-thermometry with partial activation of a HIFU phased array transducer ..... <i>B. Quesson</i>
11:48	The optical sensing and imaging of HIFU lesions ..... <i>R. Roy</i>
12:00	Rapid MR-ARFI method for focal spot localization during focused ultrasound treatments ..... <i>E. Kaye</i>
12:12	Thermal analysis of the surrounding anatomy during 3D MRI-guided transurethral ultrasound prostate therapy ..... <i>M. Burtnyk</i>
12:24	Temperature mapping near the surface of ultrasound transducers using susceptibility-compensated magnetic resonance imaging ..... <i>A. Webb</i>
12:36	Alternative focal spot geometry for more efficient HIFU treatment assessment ..... <i>E. Kaye</i>
12:48	Robotically assisted MRgFUS system ..... <i>JW. Jenne</i>

**13:00 >>> Adjournment**



## P1 - Bioeffects of ultrasound and HIFU

- P1-1 A photoacoustic sensor for monitoring in situ temperature during HIFU exposures**  
Chitnis P. <sup>1</sup>, McLaughlan J.<sup>2</sup>, Mamou J.<sup>1</sup>, Murray T.<sup>2</sup>, Roy R.<sup>2</sup>  
<sup>1</sup>Riverside Research Institute, New York, USA  
<sup>2</sup>Boston University, Boston, USA
- P1-2 Ultrasound temperature monitoring in the scalp**  
Garapon P. <sup>1</sup>, Couture O.<sup>1</sup>, Tanter M.<sup>1</sup>  
<sup>1</sup>ESPCI, CNRS, Paris, France
- P1-3 Effect of low intensity pulsed ultrasound on transcriptional gene expression of calvarial bone**  
Gleizal A. <sup>1</sup>, Li S.<sup>2</sup>, Pialat J.<sup>2</sup>, Béra J.<sup>1</sup>, Lavandier B.<sup>2</sup>, Beziat J.<sup>1</sup>  
<sup>1</sup>Hopitaux Nord, LYON, France  
<sup>2</sup>INSERM, LYON, France
- P1-4 Detailed histological assessment of in vivo tissue exposed to high intensity focused ultrasound (HIFU)**  
Jayadewa C. <sup>1</sup>, Rivens I.<sup>1</sup>, Ter Haar G.<sup>1</sup>  
<sup>1</sup>Institute of Cancer Research, Sutton, UK
- P1-5 Does low intensity pulsed ultrasound accelerate calvarial bone defect reconstruction ? An experimental study in murine model**  
Lavandier B. <sup>1</sup>, Gleizal A.<sup>2</sup>, Béra J.<sup>1</sup>  
<sup>1</sup>INSERM, Lyon, France  
<sup>2</sup>Hôpitaux Nord, Lyon, France
- P1-6 Study of parameters affecting the level of ultrasound exposure with in vitro set-ups**  
Leskinen J. <sup>1</sup>, Hynynen K.<sup>2</sup>  
<sup>1</sup>University of Kuopio, Kuopio, Finland  
<sup>2</sup>University of Toronto and Sunnybrook Health Sciences Centre, Toronto, Canada
- P1-7 Dynamic analysis of irradiation of high intensity focused ultrasound (HIFU) to achieve a living tissue perforation**  
Mochizuki T. <sup>1</sup>, Kitazumi G.<sup>2</sup>, Katsuike Y.<sup>2</sup>, Hotta S.<sup>2</sup>, Maruyama H.<sup>3</sup>, Chiba T.<sup>2</sup>  
<sup>1</sup>Aloka Co. Ltd., Tokyo, Japan  
<sup>2</sup>National Center for Child Health and Development, Tokyo, Japan  
<sup>3</sup>Japan Broadcasting Corporation, Tokyo, Japan
- P1-8 Multi-frequency characterization of speed of sound for longitudinal transmission on freshly excised human skulls**  
Pichardo S. <sup>1</sup>, Hynynen K.<sup>2</sup>  
<sup>1</sup>Thunder Bay Regional Research Institute, Thunder Bay, Canada  
<sup>2</sup>Sunnybrook Research Institute, Toronto, Canada
- P1-9 New dynamical focusing method for HIFU therapeutic applications**  
Rybyanets A. <sup>1</sup>  
<sup>1</sup>South Federal University, Rostov on Don, Russia
- P1-10 Multi-frequency harmonic method for HIFU tissue treatment**  
Rybyanets A. <sup>1</sup>, Lugovaya M.<sup>1</sup>, Rybyanets A.<sup>1</sup>  
<sup>1</sup>South Federal University, Rostov on Don, Russia
- P1-11 QOL after HIFU for prostate cancer**  
Satoh M. <sup>1</sup>, Kuwahara M.<sup>1</sup>, Nakano O.<sup>1</sup>, Horinouchi T.<sup>1</sup>, Kudo T.<sup>1</sup>, Arai Y.<sup>2</sup>  
<sup>1</sup>Sen-en General hospital, Tagajo, Japan  
<sup>2</sup>Tohoku University, School of Medicine, Sendai, Japan,

## P2 - Ultrasound-enhanced drug delivery

- P2-1 In vitro models of thrombolysis of arterial bypass grafts with pulsed high-intensity focused ultrasound**  
Abi-Jaoudeh N.<sup>1</sup>, Jones G.<sup>2</sup>, Hancock H.<sup>1</sup>, Razjouyan F.<sup>1</sup>, Frenkel V.<sup>1</sup>, Wood B.<sup>1</sup>  
<sup>1</sup> National Institute of Health, Bethesda, USA  
<sup>2</sup> National Institute of Health, Rockville Pike, USA
- P2-2 Development of an acoustic droplet vaporization, ultrasound drug delivery emulsion**  
Fabiilli M.<sup>1</sup>, Sebastian I.<sup>2</sup>, Fowlkes J.<sup>1</sup>  
<sup>1</sup> University of Michigan, Ann Arbor, USA  
<sup>2</sup> University of Michigan, Miyagi, Japan
- P2-3 Delivery improvement into brain tissue with ultrasound sonication after blood-brain barrier opened temporarily by focused ultrasound with microbubbles**  
Lee Y.<sup>1</sup>, Hu S.<sup>2</sup>, Wu X.<sup>1</sup>, Lin W.<sup>1</sup>  
<sup>1</sup> National Taiwan University, Taipei, Taiwan  
<sup>2</sup> National Chiao Tung University, Hsinchu, Taiwan
- P2-4 Intravenous delivery of pDNA and siRNA into muscle with bubble liposomes and ultrasound**  
Negishi Y.<sup>1</sup>, Sekine S.<sup>2</sup>, Endo Y.<sup>1</sup>, Suzuki R.<sup>3</sup>, Maruyama K.<sup>3</sup>, Aramaki Y.<sup>1</sup>  
<sup>1</sup> Tokyo University of Pharmacy and Life Sciences, Hachioji, Japan  
<sup>2</sup> Tokyo University of Pharmacy and Life Sciences, Tokyo, Japan  
<sup>3</sup> Teikyo University, Sagamihara, Japan
- P2-5 Inhibition of melanoma metastasis by dendritic cell-based cancer immunotherapy utilized liposomal bubbles and ultrasound**  
Otake S.<sup>1</sup>, Oda Y.<sup>2</sup>, Suzuki R.<sup>1</sup>, Utoguchi N.<sup>1</sup>, Taira Y.<sup>1</sup>, Maruyama K.<sup>1</sup>  
<sup>1</sup> School of Pharmaceutical Sciences, Teikyo University, Kanagawa, Japan  
<sup>2</sup> School of Pharmaceutical Sciences, Teikyo University, Sagamihara, Japan
- P2-6 Dose comparison of ultrasonic transdermal insulin delivery to subcutaneous insulin injection?**  
Smith N.<sup>1</sup>, Park E.<sup>2</sup>, Dodds J.<sup>1</sup>  
<sup>1</sup> The Pennsylvania State University, University Park, USA  
<sup>2</sup> The Pennsylvania State University, State College, USA
- P2-7 The effect of magnetite nanoparticle agglomerates on ultrasound induced inertial cavitation**  
Smith M.<sup>1</sup>, Darton N.<sup>1</sup>, Slater N.<sup>1</sup>  
<sup>1</sup> Cambridge University, Cambridge, UK
- P2-8 Synergistic inhibition of malignant melanoma proliferation by combined ultrasound-induced cavitations and Melphalan**  
Yamaguchi K.<sup>1</sup>, Feril Jr L.<sup>1</sup>, Matsuo M.<sup>1</sup>, Takahashi A.<sup>1</sup>, Tachibana K.<sup>1</sup>, Nakayama J.<sup>1</sup>  
<sup>1</sup> Fukuoka University, Fukuoka, Japan

## P3 - Gene therapy, sonodynamic therapy, chemotherapy, sonoporation

- P3-1 Regulating ultrasound cavitation in order to induce reproducible sonoporation**  
Mestas J. <sup>1</sup>, Alberti L.<sup>2</sup>, El Maalouf J.<sup>2</sup>, Béra J.<sup>2</sup>, Gilles B.<sup>2</sup>, Angel Y.<sup>2</sup>  
<sup>1</sup>INSERM, Lyon, France  
<sup>2</sup>Centre Léon Bérard, Lyon, France
- P3-2 Transfection of cells in suspension by ultrasound cavitation**  
Reslan L. <sup>1</sup>, Herveau S.<sup>1</sup>, Mestas J.<sup>1</sup>, Dumontet C.<sup>1</sup>  
<sup>1</sup>Université Lyon 1, Lyon, France
- P3-3 Micro-bubble enhanced sonoporation**  
Tachibana R. <sup>1</sup>, Okamoto A.<sup>1</sup>, Yoshinaka K.<sup>1</sup>, Takagi S.<sup>1</sup>, Matsumoto Y.<sup>1</sup>  
<sup>1</sup>The University of Tokyo, Tokyo, Japan
- P3-4 The effect of cell killing by ultrasound**  
Tachibana K. <sup>1</sup>, Harada Y.<sup>1</sup>, Feril L.<sup>1</sup>, Endo H.<sup>1</sup>, Ogawa K.<sup>1</sup>, Irie Y.<sup>1</sup>  
<sup>1</sup>Fukuoka University School of Medicine, Fukuoka, Japan
- P3-5 Measurements of blood clot displacements induced by pulsed focused ultrasound**  
Wright C.<sup>1</sup>, Hynynen K.<sup>1</sup>, Goertz D.<sup>1</sup>  
<sup>1</sup>Sunnybrook Health Sciences Centre, Toronto, Canada

## P4 - HIFU devices

- P4-1 Characterisation and application of a custom-made HIFU transducer for robotic manipulation**  
Corner G. <sup>1</sup>, Cochran S.<sup>2</sup>, Gourlay T.<sup>3</sup>, Huang Z.<sup>2</sup>, Mayne K.<sup>4</sup>, Melzer A.<sup>2</sup>  
<sup>1</sup>NHS Tayside, Dundee, Scotland  
<sup>2</sup>University of Dundee, Dundee, Scotland  
<sup>3</sup>University of Strathclyde, Glasgow, Scotland  
<sup>4</sup>Piezo-Composite Transducers, Aberdeen, Scotland
- P4-2 Hydrophone arrays for instantaneous measurement of high-pressure acoustic fields**  
Ketterling J. <sup>1</sup>, Lee P.<sup>1</sup>, Kreider W.<sup>2</sup>, Bailey M.<sup>2</sup>, Cleveland R.<sup>3</sup>  
<sup>1</sup>Riverside Research Institute, New York, USA  
<sup>2</sup>Applied Physics Laboratory, Seattle, USA  
<sup>3</sup>Boston University, Boston, USA
- P4-3 Ex vivo experiments by a non-invasive ultrasound theragnostic system**  
Koizumi N. <sup>1</sup>, Seo J.<sup>2</sup>, Suzuki Y.<sup>2</sup>, Yoshinaka K.<sup>2</sup>, Matsumoto Y.<sup>2</sup>, Mitsuishi M.<sup>2</sup>  
<sup>1</sup>The University of Tokyo, Tokyo, Japan  
<sup>2</sup>School of Engineering, The University of Tokyo, Tokyo, Japan
- P4-4 Pocket-sized ultrasonic surgical and rehabilitation solutions: from the lab bench to clinical trials**  
Lewis Jr. G. <sup>1</sup>, Olbricht W.<sup>1</sup>, Henderson P.<sup>2</sup>  
<sup>1</sup>Cornell University, Ithaca, USA  
<sup>2</sup>Weill Cornell Medical College, Ithaca, USA
- P4-5 Investigation of parameters affecting treatment time in MRI-guided transurethral ultrasound therapy**  
N'Djin WA. <sup>1</sup>, Burtnyk M.<sup>1</sup>, Chopra R.<sup>1</sup>, Bronskill M.<sup>1</sup>  
<sup>1</sup>Medical Biophysics, University of Toronto, Toronto, Canada
- P4-6 Development of noninvasive vascular occlusion method with HIFU**  
Senoo N. <sup>1</sup>, Suzuki J.<sup>1</sup>, Deguchi J.<sup>1</sup>, Takagi S.<sup>1</sup>, Miyata T.<sup>1</sup>, Matsumoto Y.<sup>1</sup>  
<sup>1</sup>The University of Tokyo, Tokyo, Japan

**P4-7 In vivo evaluations of a phased ultrasound array for transesophageal cardiac ablation**

Smith N. <sup>1</sup>, Werner J.<sup>2</sup>, Park E.<sup>1</sup>, Jaiswal D.<sup>1</sup>, Hattel A.<sup>1</sup>, Francischelli D.<sup>3</sup>

<sup>1</sup> The Pennsylvania State University, University Park, USA

<sup>2</sup> The Pennsylvania State University, State College, USA

<sup>3</sup> Medtronic Inc, Minneapolis, USA

**P4-8 Ultrasound strain imaging towards verification and guidance of prostate thermal therapy with catheter-based ultrasound applicators**

Sridhar-Keralapura M. <sup>1</sup>, Chubb N.<sup>1</sup>, Scott S.<sup>2</sup>, Juang T.<sup>2</sup>, Prakash P.<sup>2</sup>, Diederich C.<sup>2</sup>

<sup>1</sup> San Jose State University, San Jose, USA

<sup>2</sup> University of California, San Francisco, USA

## **P5 - Quality assurance of HIFU**

**P5-1 A test-bed to calibrate MR thermometry**

Cunitz B. <sup>1</sup>, Marro K.<sup>1</sup>, Lee D.<sup>1</sup>, Bailey M.<sup>1</sup>

<sup>1</sup> University of Washington, Seattle, USA

**P5-2 Noninvasive characterization of HIFU transducers using infrared thermography and a mathematical inverse method**

Giridhar D. <sup>1</sup>, Robinson R.<sup>1</sup>, Zderic V.<sup>2</sup>, Sliwa J.<sup>3</sup>, Myers M.<sup>1</sup>

<sup>1</sup> Food and Drug Administration, Silver Spring, USA

<sup>2</sup> Georges Washington University, Washington, USA

<sup>3</sup> Epicor, Sunnyvale, USA

**P5-3 A novel device for total acoustic output measurement of high power transducers**

Howard S. <sup>1</sup>, Twomey R.<sup>2</sup>, Morris H.<sup>1</sup>, Zanelli C.<sup>1</sup>

<sup>1</sup> Onda Corporation, Sunnyvale, USA

<sup>2</sup> NTR Systems Inc., Seattle, USA

**P5-4 A study relating thermal dose estimates from RF ultrasound backscatter data and measures of visible tissue discoloration**

Kaczkowski P. <sup>1</sup>, Speyer G.<sup>1</sup>, Kargl S.<sup>1</sup>, Brayman A.<sup>1</sup>, Crum L.<sup>1</sup>

<sup>1</sup> University of Washington, Seattle, USA

**P5-5 Multiple cavitation detection methods for evaluating tissue mimicking materials during HIFU exposure**

Maruvada S. <sup>1</sup>, Liu Y.<sup>1</sup>, Herman B.<sup>1</sup>, Harris G.<sup>1</sup>

<sup>1</sup> Food and Drug Administration, Silver Spring, USA

**P5-6 Metrology research for external beam cancer therapy: a European initiative**

Shaw A. <sup>1</sup>, Koch C.<sup>2</sup>, Durando G.<sup>3</sup>, Karaböce B.<sup>4</sup>

<sup>1</sup> National Physical Laboratory, Teddington, UK

<sup>2</sup> Physikalisches-Technische Bundesanstalt, Braunschweig, Germany

<sup>3</sup> Istituto Nazionale di Ricerca Metrologica, Turin, Italy

<sup>4</sup> Ulusal Metroloji Enstitüsü, Gebze/Kocaeli, Turkey

**P5-7 Temperature dependence of the susceptibility of fat leads to significant temperature errors in PRFS based MR thermometry**

Sprinkhuizen S. <sup>1</sup>, Konings M.<sup>2</sup>, Bakker C.<sup>2</sup>, Bartels W.<sup>2</sup>

<sup>1</sup> Image Sciences Institute, Utrecht, The Netherlands

<sup>2</sup> University Medical Center Utrecht, Utrecht, The Netherlands

## P6 - Ultrasound contrast media

- P6-1 Uniformly sized microbubbles with distinct physical and acoustical properties**  
Borrelli M. <sup>1</sup>, O'Brien Jr. W.<sup>2</sup>, Bernock L.<sup>1</sup>, Tung S.<sup>3</sup>, Oelze M.<sup>2</sup>, Culp W.<sup>1</sup>  
<sup>1</sup>University of Arkansas for Medical Sciences, Little Rock, USA  
<sup>2</sup>University of Illinois, Urbana-Champaign, USA  
<sup>3</sup>University of Arkansas, Fayetteville, USA

## P7 - Ultrasound hyperthermia

- P7-1 Physical therapy system for children with hemiplegia**  
Genis V. <sup>1</sup>  
<sup>1</sup>Goodwin College, Drexel University, Philadelphia, USA
- P7-2 Temperature fields in soft tissue during hyperthermia treatment: numerical predictions and experimental results**  
Kujawska T. <sup>1</sup>, Wójcik J.<sup>1</sup>, Nowicki A.<sup>1</sup>  
<sup>1</sup>IFTR PAS, Warsaw, Poland
- P7-3 In-vivo study of monitoring thermal ablation by ultrasound imaging**  
Winkler I. <sup>1</sup>, Adam D.<sup>1</sup>  
<sup>1</sup>Technion - Israel Institute of Technology, Haifa, Israel
- P7-4 Endocavity ultrasound array integrated within a HDR brachytherapy ring applicator for targeted hyperthermia to the uterine cervix: patient-specific modeling**  
Wootton J. <sup>1</sup>, Prakash P.<sup>1</sup>, Juang T.<sup>1</sup>, Diederich C.<sup>1</sup>  
<sup>1</sup>UCSF, San Francisco, USA

## P8 - HIFU physics

- P8-1 Extension of the angular spectrum method to curved transducer surfaces**  
Christensen D. <sup>1</sup>, Vyas U.<sup>1</sup>  
<sup>1</sup>University of Utah, Salt Lake City, USA
- P8-2 Bandwidth limitations in characterization of high intensity focused ultrasound fields in the presence of shocks**  
Khokhlova V. <sup>1</sup>, Bessonova O.<sup>2</sup>, Canney M.<sup>1</sup>, Bailey M.<sup>1</sup>, Sonesson J.<sup>3</sup>, Crum L.<sup>1</sup>  
<sup>1</sup>University of Washington, Seattle, USA  
<sup>2</sup>Faculty of Physics, Moscow State University, Moscow, Russia  
<sup>3</sup>Food and Drug Administration, Silver Spring, USA
- P8-3 Potential temperature limitations of bubble-enhanced heating during HIFU**  
Kreider W. <sup>1</sup>, Bailey M.<sup>1</sup>, Sapozhnikov O.<sup>1</sup>, Crum L.<sup>1</sup>  
<sup>1</sup>University of Washington, Seattle, USA
- P8-4 Numerical simulation of high intensity focused ultrasound therapy with volume model of human body**  
Okita K. <sup>1</sup>, Sugiyama K.<sup>2</sup>, Ono K.<sup>1</sup>, Takagi S.<sup>1</sup>, Matsumoto Y.<sup>2</sup>  
<sup>1</sup>RIKEN, Saitama, JAPAN  
<sup>2</sup>The University of Tokyo, Tokyo, Japan
- P8-5 Combining thermal and ultrasound modeling techniques for improved monitoring of MR guided HIFU treatments**  
Todd N. <sup>1</sup>, Vyas U.<sup>1</sup>, Payne A.<sup>1</sup>, Christensen D.<sup>1</sup>, Parker D.<sup>1</sup>  
<sup>1</sup>University of Utah, Salt Lake City, USA

## P9 - Ultrasound surgery

- P9-1 Correlation between color flow Doppler study around uterine myomas and nonperfused ratio immediately after magnetic resonance-guided focused ultrasound**  
Funaki K.<sup>1</sup>, Fukunishi H.<sup>1</sup>  
<sup>1</sup>Shinsuma General Hospital, Kobe, Japan
- P9-2 Salvage HIFU: factors influencing the outcome in low or intermediate risk patients with local recurrence after external beam radiation therapy (EBRT)**  
Gelet A.<sup>1</sup>, Murat F.<sup>1</sup>, Cherasse A.<sup>1</sup>, Poissonnier L.<sup>1</sup>, Chapelon JY.<sup>2</sup>, Martin X.<sup>1</sup>  
<sup>1</sup>Hôpital Edouard Herriot, Lyon, France  
<sup>2</sup>INSERM, Lyon, France
- P9-3 Evaluation of an acoustic reflector to protect large abdominal wall scars during MR-guided focused ultrasound ablation (MRgFUS) of uterine fibroids**  
Gorny K.<sup>1</sup>, Chen S.<sup>1</sup>, Hesley G.<sup>1</sup>, Brown D.<sup>1</sup>, Hangiandreou N.<sup>1</sup>, Felmlee J.<sup>1</sup>  
<sup>1</sup>Mayo Clinic College of Medicine, Rochester, USA
- P9-4 Hand-held Ultrasound elastography for guiding liver ablations produced using a toroidal HIFU transducer. Results of animal experiments**  
Chenot J.<sup>1</sup>, Melodelima D.<sup>1</sup>, Souchon R.<sup>1</sup>, Chapelon JY.<sup>1</sup>  
<sup>1</sup>INSERM, Lyon, France
- P9-5 The effect of the rat skull on temperature deposition in the brain**  
King R.<sup>1</sup>, Rieke V.<sup>2</sup>, Butts Pauly K.<sup>1</sup>  
<sup>1</sup>Stanford University, Stanford, USA  
<sup>2</sup>Stanford University, Palo Alto, USA
- P9-6 Harmonic Motion Imaging (HMI) for Focused Ultrasound (HMIFU): Initial in vivo results**  
Maleke C.<sup>1</sup>, Hou Y.<sup>1</sup>, Konofagou E.<sup>1</sup>  
<sup>1</sup>Columbia University, New York, USA
- P9-7 Clinical application of a novel graphical user interface for high intensity focused ultrasound ablation of uterine fibroids**  
Venkatesan A.<sup>1</sup>, Stratton P.<sup>2</sup>, Segars J.<sup>2</sup>, Merino M.<sup>3</sup>, Sokka S.<sup>4</sup>, Wood B.<sup>1</sup>  
<sup>1</sup>National Institutes of Health, Bethesda, USA  
<sup>2</sup>National Institute of Child Health and Human Development, Bethesda, USA  
<sup>3</sup>National Cancer Institute, Bethesda, USA  
<sup>4</sup>Philips Medical Systems, Boston, USA

## P10 - HIFU treatment planning

- P10-1 HIFU dose delivery time reduction through focal zone size and path and transducer power optimization**  
Coon J.<sup>1</sup>, Vyas U.<sup>1</sup>, Payne A.<sup>1</sup>, Christensen D.<sup>1</sup>, Roemer R.<sup>1</sup>  
<sup>1</sup>University of Utah, Salt Lake City, USA
- P10-2 Real-time tissue thermometry using an acoustic neural network method during HIFU treatment**  
Fan L.<sup>1</sup>, Sekins K.<sup>1</sup>  
<sup>1</sup>Siemens Healthcare, Issaquah, USA
- P10-3 Patient specific modeling platform for transurethral and interstitial ultrasound thermal therapy**  
Prakash P.<sup>1</sup>, Diederich C.<sup>1</sup>  
<sup>1</sup>University of California, San Francisco, USA
- P10-4 Development of computer controlled three dimensional HIFU focus model scanning system**  
Seo J.<sup>1</sup>, Koizumi N.<sup>1</sup>, Yugo S.<sup>1</sup>, Akira N.<sup>1</sup>, Yoichiro M.<sup>1</sup>, Mamoru M.<sup>1</sup>  
<sup>1</sup>School of Engineering, The University of Tokyo., Tokyo, Japan



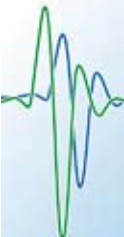
# Oral Communications Thursday, September 24

[www.istu2009.org](http://www.istu2009.org)

Thursday,  
September 24



IMASONIC



CUSTOM-DESIGNED  
ULTRASONIC TRANSDUCERS  
For Therapeutic Applications

IMASONIC SAS • ZA Rue des Savoirs  
70190 Verzy-sur-Fognon • FRANCE  
Phone : +33 (0)3 81 40 31 30  
Fax : +33 (0)3 81 40 31 39  
Email : [imasonic@imasonic.com](mailto:imasonic@imasonic.com)  
Web : [www.imasonic.com](http://www.imasonic.com)



## HIFU

- From Single Element to Phased Array Transducer
- MRI compatible or Ultrasonic Guided Solutions

- The unequalled performance of the IMASONIC Piezocomposite High Power Technology







## Global clinical vision of the role of HIFU therapy

Invited speaker: **Wu F.**<sup>1</sup>

<sup>1</sup>The Churchill Hospital, Oxford, UK

Institute of Ultrasonic Engineering in Medicine, Chongqing Medical University, China & HIFU Unit, Nuffield Department of Surgery, University of Oxford, UK. In the past two decades, technological advances have initiated a change from open surgery towards less invasive techniques including laparoscopic surgery and minimally invasive techniques in local treatment of tumours. The concept of high intensity focused ultrasound (HIFU) as a noninvasive tool for local destruction of diseased tissue dates back more than 60 years. Current improvements in medical imaging modalities have led to great progress in HIFU technique, and clinical applications have dramatically changed scientific attitude from a theoretic assumption to a real clinical feasibility. Recently, this noninvasive in situ tumour ablation with ultrasound energy has received increasing interest in clinical application. European Community has approved two ultrasound-guided transrectal HIFU devices for prostate cancer, and an ultrasound-guided extracorporeal HIFU device for solid tumours, including those of liver, pancreas, breast, kidney, uterus, soft tissue and bone. A MRI-guided HIFU device has been also approved by both FDA and European Community for the treatment of uterine fibroid. HIFU is being performed clinically to treat both malignant and benign tumours. This has only been the case in the past, but recently five-year survival rate has emerged in patients with prostate cancer, hepatocellular carcinoma, breast cancer and osteosarcoma. These data are very encouraging, and the role of HIFU in the local ablation of solid tumours will expand as the devices become more widely available in clinics. This presentation is to review global clinical application of HIFU therapy, and to discuss the challenge and future of this noninvasive tool. It will introduce the first HIFU Clinical Guidelines worldwide, promulgated by Chinese Medical Association in 2005, and the current situation of HIFU clinical applications in China, where the largest population of patients has been treated with HIFU in the world.



## Optimal transthoracic targeting of liver tumors using dual-mode ultrasound arrays: a numerical and experimental study

**Casper A.**<sup>1</sup>, Ballard J.<sup>1</sup>, Ebbini E.<sup>1</sup>

<sup>1</sup>University of Minnesota, Minneapolis, USA

The targets of therapeutic ultrasound are often located behind strongly scattering objects and layered tissue. These inhomogeneities can degrade the intended foci and misdirect acoustic energy causing unwanted hot spots or failure to meet the therapeutic endpoint at the target. We have previously shown the capabilities of dual-mode ultrasound arrays (DMUAs) in imaging strongly scattering objects in the path of the HIFU beam and, consequently, refocusing the beam to optimize the power deposition at the target while minimizing direct exposure to the obstacles. This capability may be a key to successful transthoracic targeting of abdominal tumors. We have experimentally verified the efficacy of this approach in improving the quality of the therapeutic focus and minimizing collateral damage to critical tissue structures in the path of the HIFU beam. In order to study the phenomena associated with transthoracic focusing more thoroughly, we have developed a finite-difference time-domain simulation capable of characterizing the transient propagation of the therapeutic beam through inhomogeneous, attenuating media. This simulation is shown to provide the necessary information for aberration correction of deep seated foci as well as control over the acoustic field at select points. In addition, the FDTD simulation allows for computation of the temperature rise throughout the therapeutic region as governed by the transient bioheat transfer equation. We have validated the predictive abilities of our simulation with hydrophone measurements as well as thermocouple readings from within tissue mimicking phantoms. The experimental validation of the simulation model allows for its use as a key component in treatment planning of thermal therapy using HIFU. Experimental and simulation results demonstrating the role of the advantages of incorporation of the computational model in optimizing the quality of HIFU beams will be presented and discussed.



### Segmental liver resection assisted by HIFU: tissue precauterization using a toroidal-shaped HIFU transducer

**N'Djin WA.**<sup>1</sup>, Melodelima D.<sup>1</sup>, Schenone F.<sup>2</sup>, Rivoire M.<sup>2</sup>, Chapelon JY.<sup>1</sup>

<sup>1</sup>Inserm, Lyon, France

<sup>2</sup>Centre Leon Berard, Lyon, France

The development of new cauterization techniques for hepatic resection is critical for improving the safety of the procedure. Previous studies showed the feasibility of using HIFU or radiofrequency pre-coagulation to limit blood loss during dissection of the organ. Here we report a new therapeutic modality using high intensity focused ultrasound (HIFU) to perform a bloodless hepatic resection that could represent a promising alternative. A comparative study was performed to evaluate the interest of using this complementary tool to improve surgical resection in the liver. This study used a 3 MHz HIFU toroidal-shaped phased array transducer which allows the generation of a single conical lesion of 7 cm<sup>3</sup> in 40 seconds (I<sub>focal</sub> = 100 W.cm<sup>-2</sup>). In order to minimize blood loss and dissection time, a barrier of coagulative necrosis was generated with the HIFU device before hepatectomy, by juxtaposing single conical lesions on the line of dissection. Resection assisted by HIFU (RA-HIFU) was compared with classical dissections with clamping (RC) and without clamping (Control). For each technique 14 partial liver resections were performed in seven pigs. The parameters examined were vascular control and times of treatment. Precoagulation allowed the vascular isolation of small vessels and surgical clips were mainly used for the control of vessels > 5 mm in diameter. The number of clips used per unit of liver surface dissected in RA-HIFU (0.8 ± 0.2 cm<sup>-2</sup>) was significantly lower than in the other groups (50%, p < 0.01). In addition, blood loss was lower in RA-HIFU (7.4 ± 3.3 ml.cm<sup>-2</sup>) than in RC (34%) and Control (47%). The time of dissection in RA-HIFU (13 ± 3 min) was significantly shorter than in RC (44%, p < 0.01). The feasibility and the efficiency of RA-HIFU using a toroidal-shaped HIFU transducer without additional devices were demonstrated. This technique enhances the resection procedure and will be able to be tested in clinic.



### Efficacy and safety of focused ultrasound ablation for small hepatocellular carcinoma

**Fukuda H.**<sup>1</sup>, Ohto M.<sup>1</sup>, Ito R.<sup>1</sup>, Sakamoto A.<sup>1</sup>, Zhu H.<sup>2</sup>, Wang Z.<sup>2</sup>

<sup>1</sup>Naruto General Hospital, Chiba, Japan

<sup>2</sup>Chongqing University, Chongqing, China

**PURPOSE:** To evaluate the therapeutic efficacy of focused ultrasound ablation for patients with small hepatocellular carcinoma (HCC).

**MATERIALS AND METHODS:** 12 patients with HCC were enrolled in this clinical study. The maximum diameter of the tumors measured on sonography were smaller than 20 mm. The tumor therapy system (Chongqing Haifu Tech Co., Ltd, Chongqing, China) used in this study was guided by means of real-time ultrasonographic imaging.

**RESULTS:** Complete ablations were obtained in all patients on the evaluation of CT scan and contrast-enhanced ultrasonography 1 month after the treatment. Local recurrence was occurred in one case 18 months after the treatment. Epidural anesthesia could provide sufficient pain suppression during the procedure. Serum alanine aminotransferase (ALT), serum aspartate aminotransferase (AST), total-bilirubin, albumin levels and CRP showed statistically significant increases over baseline 1 day after the treatment, and they recovered 7 days after the treatment. There was no treatment-related deaths, and no severe complications.

**CONCLUSION:** Focused ultrasound ablation is considered a reliable treatment for small HCC in terms of safety and efficacy.



### MR guided focused ultrasound surgery for early breast cancer

**Furusawa H.**<sup>1</sup>, Yasuda Y.<sup>1</sup>, Nakahara H.<sup>1</sup>, Machida E.<sup>1</sup>, Maeda Y.<sup>1</sup>, Komaki K.<sup>1</sup>

<sup>1</sup> Breastopia Namba Hospital, Miyazaki, Japan

**BACKGROUND:** The prognosis of the breast cancer patient doesn't depend on the local treatment, but on the systemic treatment. Breast conserving therapy, lumpectomy following radiotherapy, has been proved to be good enough as compared to mastectomy in several clinical trials. Focused ultrasound beams develop thermal energy and coagulate the protein. MRI is the best modality in spatial resolution of breast cancer spread. Two phase II clinical studies (excision study) to investigate pathological efficacy and clinical safety of MR guided focused ultrasound surgery (MRgFUS) have been published.

**PURPOSE:** The purpose of this study is to inspect of efficacy and safety of excisionless MRgFUS with radiotherapy of breast cancer in phase III study.

**METHODS:** The inclusion criteria is made of 1) the tumor was diagnosed by bore needle biopsy 2) HER-2,HR status were checked 3) the tumor size is less than 15mm in diameter, 4) well demarcated mass in contrast enhance MRI. The exclusion criteria is made of 1) pure type mucinous carcinoma, 2) dimple ,dimpling sign and previous surgical scar of the skin above the tumor, 3) the location of the tumor needed high angle of sonication.

**RESULTS:** Forty lesions were treated from April 2005 to March 2009. The average age was 56.5 years old (37 - 72). The average tumor size was 11.0mm (6 - 15). The average follow up period was 16 months (4 - 46). The following radiotherapy is whole breast and boost. Thirty two cases were followed up for more than 12 months. There were no severe adverse events and no local recurrent case.

**CONCLUSIONS:** However the number of cases was too small and the follow-up period was too short, MRgFUS has potentiality to take the place of usual breast conserving surgery. It is the most important that the case is strictly selected.



### Can extracorporeal HIFU adequately ablate small renal tumours?

**Ritchie R.**<sup>1</sup>, Leslie T.<sup>1</sup>, Phillips R.<sup>1</sup>, Protheroe A.<sup>1</sup>, Cranston D.<sup>1</sup>

<sup>1</sup> Churchill Hospital, Oxford, UK

**INTRODUCTION:** Extirpative surgery currently remains the gold standard treatment for localized renal cell carcinoma. Partial nephrectomy is indicated for T1a (<4cm) renal cancer. However, complication rates with partial nephrectomy are 20-25%. HIFU has been proposed as an alternative, minimally-invasive therapy but its development has been hindered by lack of efficacy.

**MATERIALS & METHODS:** 17 patients with localised renal tumours <4cm maximum diameter (mean 3.5cm) were treated with HIFU (0.8MHz, focal length 12-15cm) using the Model-JC System (Chongqing HAIFU™, China). Real-time diagnostic ultrasound was used for targeting and monitoring. Patients were followed with contrast MRI.

**RESULTS:** 14 patients completed six months radiological follow-up; two treatments were abandoned due to intervening bowel in the target field. One patient underwent surgery prior to six month follow-up due to an area of residual enhancement. Radiological evidence of ablation was seen in seven out of 15 patients (47%) at day 12 imaging. Eight (53%) showed no clear radiological ablation – four underwent surgery at a mean of 11 months post HIFU and one underwent radiofrequency ablation. Ten patients remain under surveillance at a mean of 36 months post treatment (range 24-51). The targeted lesion shows central loss of enhancement; a rim of peripheral enhancement was seen in all patients. There has been no increase in tumour dimension over the mean 3 year follow-up.

**CONCLUSION:** This is the first medium term follow-up study of extracorporeal HIFU for renal cancer demonstrating that two-thirds of patients have stable lesions. However, definite evidence of ablation was absent in over half of patients. Central loss of enhancement suggests successful ablation but the significance of the peripheral enhancing ring is uncertain. Extracorporeal HIFU may yet have a role in the primary management of small renal cancers but the technique and treatment parameters need further refinement.



### **Preliminary results: MR guided volumetric HIFU ablation of uterine fibroids with binary feedback control**

**Mougenot C.**<sup>2</sup>, Enholm J.<sup>1</sup>, Soini J.<sup>1</sup>, Köhler M.<sup>1</sup>, Trillaud H.<sup>3</sup>

<sup>1</sup> Philips Healthcare, Vantaa, Finland  
<sup>2</sup> Philips Healthcare, Bordeaux, France

<sup>3</sup> Hôpital St André, Bordeaux, France

**OBJECTIVES:** MR guided HIFU with feedback control has been improved for regulation of the heating in an extended volume. This study describes the preliminary results obtained using a volumetric binary feedback control method for the ablation of uterine fibroids.

**MATERIALS AND METHODS:** In compliance with the local ethics committee and regulatory authorities, five patients with anterior fibroids underwent HIFU treatment with light sedation. Series of volumetric ablations were performed by electronically steering the focal point along concentric outwards-moving circles (diam. 4mm and 8mm). A total of 18 ablations without temperature control and 38 ablations with feedback control were performed inside the fibroids. The therapeutic power level (60-140Wac) was chosen by the user based on low power test sonications. The feedback algorithm adjusted the sonication duration by an online comparison of the mean temperature and/or thermal dose in the treated area to predefined limits. Specifically, the algorithm determined when to switch to the next circle and when to stop the sonication.

**RESULTS:** The non-feedback sonications with a predefined duration of 27s induced an average ablation volume of  $269 \pm 122 \text{ cm}^3/\text{J}$  with a mean maximum temperature of  $68.8 \pm 4.5^\circ\text{C}$ . Using feedback control the sonication durations ranged from 19s to 40s, thereby producing an average ablation volume of  $353 \pm 102 \text{ cm}^3/\text{J}$  with a mean maximum temperature of  $66.1 \pm 1.7^\circ\text{C}$ . No complications occurred during or after the procedure. Patients returned to normal activity 1-4 days after treatment.

**CONCLUSION:** Using binary feedback control for guiding the HIFU ablations improved the treatment safety and efficiency since it limited the maximum temperature and reduced the amount of required energy per ablated volume unit. In addition, abnormal heating behavior and thermal map artefacts were automatically detected. To further evaluate feedback control the study will be extended to a larger population.



### **Focused ultrasound to move kidney stones**

**Bailey M.**<sup>1</sup>, Cunitz B.<sup>1</sup>, Shah A.<sup>1</sup>, Paun M.<sup>1</sup>, Kaczkowski P.<sup>1</sup>, Sapozhnikov O.<sup>1</sup>

<sup>1</sup> University of Washington, Seattle, USA

**INTRODUCTION:** Residual kidney stone fragments often remain after extracorporeal shockwave lithotripsy, ureteroscopic laser lithotripsy, or percutaneous nephrolithotomy. There is a 50% recurrence within 5 years of new stones from these fragments. Here, radiation pressure and streaming created by transcutaneous focused ultrasound are used to manipulate the location of stone fragments within the collecting system in order to facilitate their passage.

**METHODS:** Natural and artificial stones were placed in a transparent kidney phantom consisting of gel surrounding a water-filled space and in cadaveric porcine kidneys. Stone motion was observed visually in the kidney phantom and using diagnostic ultrasound in the porcine kidneys. The imaging probe was placed within and oriented down the axis of the focused ultrasound probe, which consisted of an 8-element annular array of 2.75 MHz elements with an outer diameter of 6 cm. The array allowed focused at depths ranging from 4.5-8.5 cm. Longer bursts of higher amplitude ultrasound were applied than are applied in diagnostic ultrasound (30-ms, 10-MPa bursts repeated at 10 Hz).

**RESULTS:** Stones in kidney phantom were seen to move. Stone velocities were on the order of 1 cm/s and quickly moved out of the ultrasound focus. Operators could generally control the direction of stone movement. A sonographer using Doppler ultrasound and what is known as "twinkling artifact" visualized stones as small as 1 mm in the kidney. When focused ultrasound was applied these stones jumped at ~1 cm/s before falling back down. No evidence of thermal necrosis of kidney tissue was observed on gross examination.

**CONCLUSION:** Focused ultrasound can be used to move stones within the collecting system. Further studies are required to assess minimum ultrasound exposures necessary to move stones, bio-effects caused by the ultrasound, and whether passage of fragments is facilitated. Work supported by NIH DK43881 and NSBRI SMST001601.



## Histotripsy for pediatric cardiac applications: in vivo piglet model

Miller R.<sup>1</sup>, Owens G.<sup>1</sup>, Ensing G.<sup>1</sup>, Ludomirsky A.<sup>2</sup>, Cain C.<sup>1</sup>, Xu Z.<sup>1</sup>

<sup>1</sup> University of Michigan, Ann Arbor, USA

<sup>2</sup> New York University School of Medicine, New York, USA

**OBJECTIVE:** This study investigated the feasibility of using non-invasive histotripsy to create a ventricular septum defect (VSD) in an in vivo piglet model. Histotripsy can mechanically erode tissue at fluid interfaces by ultrasonically inducing controlled cavitation events. The overall goal is to develop a non-invasive procedure to aid in treatment of complex congenital heart diseases such as Hypoplastic Left Heart Syndrome (HLHS).

**MATERIAL AND METHODS:** Approximately 3-4 kg piglets were anesthetized and seated in a water bath. Treatments were delivered by a spherically focused 1MHz transducer positioned in the water outside the piglet's chest wall. Histotripsy treatment was applied using 5-cycle ultrasound pulses at 1 kHz pulse repetition frequency with 12-18 MPa peak negative pressure. The treatment was guided and monitored with an 8 MHz imaging transducer inserted in the center hole of the therapy transducer. At the conclusion of the treatment, the heart was collected for gross morphology and histology.

**RESULTS:** In all four subjects treated, histotripsy pulses generated a targeted bubble cloud through the piglet's chest wall. The hyperechoic cloud was positioned on the ventricular septum under ultrasound guidance. After 4-12 minutes of treatment, a VSD was created in two separate piglets and confirmed by B-mode imaging and color flow Doppler. Gross morphology and histology on all hearts showed demarcated damage to the target location on the ventricular septum with complete perforations found in the two hearts where a VSD was identified by Doppler.

**DISCUSSION AND CONCLUSIONS:** We have shown that a VSD can be created transcatheterously in a neonatal animal model using histotripsy under real-time ultrasound guidance. Even with the bone obstruction and constant heart motion, cavitation could be induced precisely on the ventricular septum. To further increase the treatment accuracy and efficiency we may investigate phase aberration correction and motion tracking.

---





**S2A-1**

**Advances in sonothrombolysis**

**Invited speaker: Meairs S.<sup>1</sup>**

<sup>1</sup> Universitätsmedizin Mannheim, Mannheim, Germany

Improved treatment of acute ischemic stroke with ultrasound and microbubbles in combination with thrombolytic drugs shows great promise, but the optimal techniques, indications, and contraindications have not yet been well defined. Details such as microbubble dosage, delivery, required thrombolytic drug dosage, and optimal ultrasound characteristics remain uncertain. In vitro results suggesting that stable cavitation may be more effective than inertial cavitation for clot lysis have recently found support in a new mouse ischemic stroke model employing focused ultrasound at low acoustic pressure in combination with novel therapeutic microbubbles and t-PA. Application of ultrasound and microbubbles without lytic drugs potentially could be suited for hyperacute stroke treatment, since it appears that ultrasound may activate endogenous t-PA. Moreover, targeting thrombus with specific immunobubbles may improve the efficacy of sonothrombolysis. Another recent approach for clot lysis utilizes high intensity focused ultrasound in combination with MRI (MRgFU) for targeting and monitoring of therapy. First results demonstrate rapid lysis without thrombolytic drugs. Interestingly, this technology may have application for treatment of intracerebral hemorrhage, i.e. removal of coagulated blood. Clinical outcome following sonothrombolysis also may be related to other ultrasound bioeffects including BBB disruption, drug transport, perfusion alteration, and angiogenesis. Safety remains a major concern in the further development of ultrasound-enhanced thrombolysis and further animal work is required to define the most promising methods for translation into a human application.

---



**S2A-2**

**Acoustic fields involved in clinical trials of sonothrombolysis: investigation of the TRUMBI device**

**Aubry J.F.<sup>1</sup>, Gateau J.<sup>1</sup>, Tanter M.<sup>1</sup>, Fink M.<sup>1</sup>, Meairs S.<sup>2</sup>**

<sup>1</sup> ESPCI, Paris, France

<sup>2</sup> Universität Heidelberg, Mannheim, Germany

**OBJECTIVES:** Several clinical trials have used ultrasound to improve tPA thrombolysis in patients with acute ischemic stroke. The TRUMBI trial was discontinued prematurely because of an increased number of secondary hemorrhages, possibly related to the use of low frequency 300-kHz ultrasound. It has long been hypothesized that given the TRUMBI ultrasonic parameters, a mechanical index (MI) as high as 1.2 was involved, and not less than 0.2 as stated by the TRUMBI team. The purpose of our work is to identify the pressure levels involved in TRUMBI with two approaches: first a simulation tool is used to estimate the pressure distribution in the brain and second pressure levels are measured in vitro through a human skull with a TRUMBI device.

**MATERIAL & METHODS:** A simulation software based on a finite difference time domain 3D scheme has been developed. This tool numerically models the wave propagation through the skull and reproduces the protocol of the TRUMBI study for analysis of the distribution of acoustic pressure in the brain during treatment. In parallel, we managed to get hold of a TRUMBI device in order to measure experimentally the pressure levels through human skulls. Pressure levels are measured with a calibrated 400- $\mu$ m-diameter hydrophone.

**RESULTS:** The spatial peak temporal average intensity has been measured experimentally in water with the TRUMBI device in the absence of skull: it is equal to 0.035 W/cm<sup>2</sup>. This is in contradiction with the value given by the TRUMBI team, but it confirms the 0.2 MI stated by the TRUMBI team. Given those acoustical parameters, simulated mean peak rarefactional pressures in the brain are 0.06 $\pm$ 0.05 MPa, with maximal local values as high as 0.27 MPa for the configurations modelled in this study.

**CONCLUSION:** The pressure levels involved in the TRUMBI study are lower than previously suspected. Simulations could prove useful in the initial design and optimization of future protocols for ischemic stroke therapy.



### An investigation of the use of pulsed high intensity focused ultrasound for thrombolysis

**Goertz D.**<sup>1</sup>, Wright C.<sup>1</sup>, Hynynen K.<sup>1</sup>

<sup>1</sup> Sunnybrook Health Sciences Centre, Toronto, Canada

The majority of sonothrombolysis work to date has used ultrasound to enhance the action of thrombolytic agents, or by cavitating contrast agents. In stroke applications, it would be desirable to avoid the serious side effects of tPA, and it may also be useful to not employ contrast agents. High intensity ultrasound approaches may be viable for use in peripheral blood vessels and, with recent advances in techniques for transcranial ultrasound delivery, and may also be possible in the context of stroke therapy. The objective of this work is to investigate the conditions under which HIFU induces thrombolysis in vitro and in vivo. In vitro experiments were conducted on rabbit blood clots contained within 2mm diameter polyethylene tubing. In vivo experiments were conducted using a rabbit femoral artery clot model initiated by the injection of thrombin. A single element focused transducer (f-number 0.8; -3dB with 0.8mm) was employed operating at a frequency of 1.51 MHz with a pulse duration of 1 ms and a repetition rate of 1 Hz. A high frequency (30MHz) ultrasound system was used to provide information about clot size, clot lysis, and the presence or absence of flow. A passive cavitation detection transducer was also employed (0.52 MHz). In vitro experiments were observed to produce effective clot lysis only in the presence of cavitation signals (>100 acoustic W). The width of the clot lysis zone, as measured by quantitative volumetric analysis of the imaging data, was found to be dependant upon the insonation power and exposure time. With a 5s exposure for example the lysis zone width was 1.8 and 2.7 mm at 125 and 150W respectively. In vivo experiments were found to produce consistent lysis effects at power levels of 150-200W. These results support the hypothesis that clot lysis with HIFU in the absence of thrombolytic agents is linked to the effects of cavitation, and that the spatial extent of effects are highly dependent upon insonation parameters.



### Enhancement of purely ultrasound thrombolysis efficiency using a bifrequency excitation

**Saletes I.**<sup>1</sup>, Gilles B.<sup>2</sup>, Bera J.<sup>2</sup>

<sup>1</sup> INSERM, Lyon, France

<sup>2</sup> Université Lyon 1, Lyon, France

**OBJECTIVES:** It has been shown that high-intensity focused ultrasound can be an efficient method to induce thrombolysis, but the choice of the pulsed-wave parameters is critical and the risk of thermal lesions in neighbouring tissues is still an important issue. The present work aims at using a bifrequency excitation combining two neighbouring frequencies to reduce the intensity needed to achieve thrombolysis without any pharmacological agent.

**MATERIEL & METHODS:** In vitro clots of human blood are inserted in small tubes filled with physiological saline, and placed at the focus of a piezoelectric transducer. The typical clot weight before sonication is 700 mg. Ultrasound excitation consists in monofrequency (resp. bifrequency) pulsed wave at 550 kHz (resp. 535 kHz and 565 kHz), with a pulse length of 27 ms and a duty cycle of 1:10, emitted during 5 min. Efficiency of the thrombolysis is obtained weighting each clot after filtration on a 20 µm filter before and after sonication. The efficiency of mono- and bifrequency excitations is compared for intensities ranging from  $I_{sppa} = 200 \text{ W/cm}^2$  ( $I_{spta} = 20 \text{ W/cm}^2$ ) to  $I_{sppa} = 2000 \text{ W/cm}^2$  ( $I_{spta} = 200 \text{ W/cm}^2$ ). For each set of experiments, a control group of 3 clots not sonicated is used.

**RESULTS:** In the conditions of the experiment, an intensity of  $I_{sppa} = 1400 \text{ W/cm}^2$  ( $I_{spta} = 140 \text{ W/cm}^2$ ) is needed to achieve a complete thrombolysis when monofrequency emission is used. With a bifrequency excitation, this intensity is reduced by 40%, and a complete thrombolysis is achieved with intensities of  $I_{sppa} = 800 \text{ W/cm}^2$  ( $I_{spta} = 80 \text{ W/cm}^2$ ).

**CONCLUSION:** The use of a bifrequency excitation enables, with a single transducer, to largely reduce the intensities needed to achieve thrombolysis without any thrombolytic agent. Further optimization of the bifrequency emission parameters could lead to more important reduction of the intensity needed to achieve purely ultrasound thrombolysis.



**S2A-5**

**The effects of microbubble size, physical properties, and acoustical properties on the efficacy of microbubble-ultrasound mediated sonothrombolysis**

**Borrelli M.**<sup>1</sup>, Bernock L.<sup>1</sup>, O'Brien Jr. W.<sup>2</sup>, Tung S.<sup>1</sup>, Oelze M.<sup>2</sup>, Culp W.<sup>1</sup>

<sup>1</sup> University of Arkansas for Medical Sciences, Little Rock, USA

<sup>2</sup> University of Illinois, Urbana-Champaign, USA

**OBJECTIVES:** Quantify the influence of microbubble size, Young's modulus, microbubble concentration, and microbubble collapse threshold on clot sonothrombolysis.

**MATERIALS AND METHODS:** Uniformly sized microbubbles were produced from serum albumin and dextrose with the mean diameter for different preparations ranging from 0.1  $\mu\text{m}$  to 10  $\mu\text{m}$ . Clots formed from fresh rabbit blood (3 h, 24 h, or 72 h old) were insonated (1 MHz, 2 MHz, or 3 MHz) in a my-lar chamber into which microbubbles were infused at a constant rate (chamber positioned vertically in a water-filled tank). Different acoustic intensities from 0.1 W/cm<sup>2</sup> to 2.5 W/cm<sup>2</sup> were tested using either continuous or pulsed wave ultrasound. Sonothrombolysis efficacy was measured as the loss in clot mass per minute of insonation.

**RESULTS:** Microbubble diameter had the biggest effect on sonothrombolysis efficacy. Preparations with mean diameters in the range of 3.0  $\mu\text{m}$  to 6.0  $\mu\text{m}$  yielded the highest sonothrombolysis rates, which were three times higher than with 1.0  $\mu\text{m}$  or 10  $\mu\text{m}$  diameter microbubbles. For microbubbles with the same diameter, sonothrombolysis efficacy was greater for preparations with higher Young's modulus and collapse threshold values, ostensibly because these were more resilient to ultrasonic lysis. Microbubble-mediated sonothrombolysis rates were two times greater on fresh clot (3 h) than on aged clot (72 h) regardless of microbubble diameter or ul-trasonic parameters used.

**CONCLUSIONS:** Microbubble size, Young's modulus, and single microbubble collapse threshold all influenced sonothrombolysis efficacy regardless of ultrasonic frequency or clot age. The most influential microbubble parameter on sonothrombolysis efficacy was diameter. Microbubbles with higher Young's modulus and collapse threshold values were more effective for sonothrombolysis, but it is suspected that using a constant microbubble flow rate mitigated their influence on sonothrombolysis efficacy.

---



**S2A-6**

**Transcranial clot lysis using high intensity focused ultrasound**

**Hoelscher T.**<sup>1</sup>

<sup>1</sup> University of California, San Diego, USA

Stroke is the third common cause of death worldwide. The majority of strokes are caused by sudden vessel occlusion, due to a blood clot. Vessel recanalization is the primary goal of all acute stroke treatment strategies. Initial data using ultrasound in combination with a therapeutic agent for clot lysis in stroke are promising. However, sound absorption and defocusing of the ultrasound beam occur during transskull insonation, limiting the efficiency of this approach to high extent. Using a transskull High Intensity Focused Ultrasound (HIFU) head system we were able to lyse blood clots within seconds and in absence of further lytic agents. We could show that any correction for the distortion might be negligible to focus the ultrasound beam after transskull insonation. The use of transskull HIFU for immediate clot lysis in the human brain without the need of further drugs and disregarding individual skull bone characteristics could become a successful strategy in early stroke treatment. Using magnetic resonance tomography for neuronavigation MRI Guided High Intensity Focused Ultrasound has the potential to open new avenues for therapeutic applications in the brain including Stroke, Intracranial Hemorrhages, Braintumors, Neurodegenerative Diseases, Thalamic Pain, BBB opening, and local drug delivery. First results in transcranial clot lysis will be presented in this paper.



## Penetration and diffusion of tissue plasminogen activator into whole blood clots following pulsed-high intensity focused ultrasound exposures

**Jones G.**<sup>1</sup>, Kapoor A.<sup>1</sup>, Dreher M.<sup>1</sup>, Stone M.<sup>2</sup>, Wood B.<sup>1</sup>, Frenkel V.<sup>1</sup>

<sup>1</sup> National Institutes of Health Clinical Center, Bethesda, USA

<sup>2</sup> Massachusetts General Hospital, Boston, USA

**OBJECTIVE:** Acute and chronic vascular thrombosis remains challenging to treat, limited by the time required for lysis and the penetration of drugs into clot. Anticoagulation therapy slows the propagation of clot, but often fails to eliminate the occlusion or lyse existing organized clot, even with physical intervention. Our studies have demonstrated that pulsed high intensity focused ultrasound (pulsed-HIFU) significantly enhanced tissue plasminogen activator (tPA) mediated thrombolysis both in vitro and in vivo. We hypothesized that pulsed-HIFU improved thrombolysis by enhancing penetration of tPA, thereby improving clot lysis.

**MATERIALS AND METHODS:** Penetration into clots following pulsed-HIFU was investigated using multiple techniques including scanning electron microscopy (SEM), immunohistochemistry with fluorescent antibodies to tPA, and fluorescence recovery after photobleaching (FRAP) to elucidate the mechanism of improved thrombolysis. FRAP was performed using dextrans (MW = 3-2000kDa) in water, agarose gels and fresh clot.

**RESULTS:** SEM of the surface of clots demonstrated that HIFU exposures increased exposed fibrin and the number of openings to more interior or deeper regions within clot. These openings may have facilitated improved tPA binding to the surface, increased exposed binding sites, and penetration into clot as detected by fluorescence microscopy. Diffusion in the more structurally complex clots was spatially heterogeneous and much slower than in 2% agarose gels. Following HIFU exposures, diffusion of 70kDa dextran (similar to tPA in size) increased 6.3-fold.

**CONCLUSION:** Penetration and diffusion of thrombolytic drugs into clot is improved following pulsed-HIFU exposures, supporting our previous results showing they significantly enhance clot lysis with tPA. Understanding the manner by which pulsed-HIFU increased the effectiveness of thrombolytics may facilitate optimization of exposures and translation of this work to the clinic.

---







S2B-1

## Feasibility of HIFU tissue ablation in the presence of ribs using a 2D random phased array

**Bobkova S.**<sup>1</sup>, Shaw A.<sup>2</sup>, Gavrilov L.<sup>3</sup>, Khokhlova V.<sup>1</sup>, Hand J.<sup>4</sup>

<sup>1</sup> Moscow State University, Faculty of Physics, Moscow, Russia <sup>2</sup> N.N. Andreev Acoustics Institute, Moscow, Russia  
<sup>3</sup> National Physical Laboratory, London, UK <sup>4</sup> Imperial College Healthcare NHS Trust, London, UK

**OBJECTIVES:** The goal of this work was to demonstrate feasibility of HIFU tissue ablation through the rib cage using a high power 2D random phased array.

**MATERIAL & METHODS:** A method to minimize heating ribs while maintaining high intensities at the focus of a 2D phased array was proposed and tested theoretically and experimentally. The concept is to switch off array elements located opposite the ribs whilst maintaining the total acoustic power by increasing output from the other elements. The piezocomposite 1 MHz array consisted of 254 circular 7 mm size elements, distributed randomly on a spherical surface (130 mm radius of curvature; 170 mm diameter). Acoustic power was in the range of 5-150 W. The ribs were modelled as strongly absorbing infinitely thin parallel strips. Tissue mimicking phantom and pork rib cages were used as experimental models. Spatial distributions of intensity in the rib plane and in the focal plane were calculated and measured using an infra-red camera. Temperature in tissues near and between the ribs was measured using 5 thermocouples.

**RESULTS:** Modeling and measurements showed that it was possible to produce an adequate focusing through the ribs for a single focus and several (3-4) foci, including steering the focus (foci) 10-15 mm off the array axis and at least  $\pm 20$  mm along the axis. Focus splitting due to the regularity of ribs was demonstrated both in simulations and experiments. Thermal lesions were produced in the pork chops placed beyond the rib phantom. Temperature measurements confirmed the absence of dangerous overheating of ribs and overlaying tissue.

**CONCLUSION:** Theoretical and experimental data demonstrated the feasibility of the proposed approach of minimizing the field on ribs while maintaining high focal intensities sufficient to produce tissue ablations. The work was supported in parts by INTAS-05-1000008-7841, Cancer Research UK-C18509/A78, NIHR BRC, RFBR 09-02-00066, and NIH R01EB007643 grants.



S2B-2

## A tissue phantom for evaluation of mechanical damage caused by cavitation

**Maxwell A.**<sup>1</sup>, Wang TY.<sup>1</sup>, Yuan L.<sup>1</sup>, Duryea A.<sup>1</sup>, Xu Z.<sup>1</sup>, Cain C.<sup>1</sup>

<sup>1</sup> University of Michigan, Ann Arbor, USA

**OBJECTIVES:** We have developed a phantom which acts as an indicator of mechanical tissue damage caused by cavitation in therapeutic ultrasound, such as histotripsy. The phantom is an optically-transparent gel, allowing real-time visualization of cavitation. Lesions are visible as a change in transparency, giving immediate feedback of the damage. The phantom has tissue-mimicking acoustic properties and appears similar to tissue on ultrasound imaging.

**METHODS:** The phantom was formed in 3 layers of agarose gel, with the center layer containing 5% porcine red blood cells. High-speed imaging was used to correlate cavitation activity with the formation of lesions. To compare lesions induced in the phantom and tissue, phantoms and ex-vivo liver and kidney were treated using a focused 1-MHz transducer applying 15 cycle pulses at a rate of 100 Hz and peak negative pressure of 14 MPa. Doses from 1 – 3000 pulses were applied. Acoustic properties and B-mode ultrasound images were recorded.

**RESULTS:** During ultrasound exposure, cavitation clouds were observed in the phantom by high-speed optical imaging. Cavitation caused lysis of red blood cells, which changed the affected area from translucent red to transparent. Lesions in the gel only formed when and where cavitation was observed. Lesion morphology of the phantom was similar to tissue, with no cellular structures remaining inside the lesion and sharp boundaries between the transparent and translucent zones. The phantom had a sound speed of 1505 m/s and density of 1030 kg/m<sup>3</sup>. B-Mode ultrasound images displayed hypochoic regions where lesions were formed, commonly observed in tissue treated by histotripsy.

**CONCLUSIONS:** The tissue phantom allows immediate visualization of cavitation and cavitation tissue damage providing a useful research tool for cavitation ultrasound therapy studies. This may be useful for cavitation ultrasound therapy development through testing acoustic parameters or scanning algorithms.



### Tissue erosion using shock wave heating and millisecond boiling in high intensity focused ultrasound fields

**Canney M.**<sup>1</sup>, Khokhlova V.<sup>1</sup>, Hwang JH.<sup>1</sup>, Khokhlova T.1, Bailey M.<sup>1</sup>, Crum L.<sup>1</sup>

<sup>1</sup> University of Washington, Seattle, USA

**OBJECTIVES:** In recent studies using high intensity focused ultrasound (HIFU), there has been significant interest in generating purely mechanical damage in tissue and such effects have been attained using low duty cycle pulsing with high pulse average intensities of greater than 20 kW/cm<sup>2</sup>. Shocks can form in such acoustic fields and lead to rapid temperature increases to 100°C and boiling after only several thousand cycles of HIFU exposure. The goal of this work is to demonstrate that such rapid heating and millisecond boiling using shock waves can be used to generate purely mechanical erosion of tissue with little or no evident thermal coagulation.

**MATERIAL & METHODS:** Experiments were performed using a 1 and 2 MHz single-element sources as well as using a 1 MHz clinical array in tissue phantoms and ex vivo liver. The transducers were operated using treatment protocols with equal average intensity levels and duty cycles ranging from 1% to 100%. Bubble activity was monitored during exposures using three separate detection systems: a 20 MHz passive cavitation detector, a high voltage probe in parallel with the HIFU source, and with an ultrasound imaging system. In situ acoustic fields and heating rates were determined for exposures using a novel derating approach for nonlinear HIFU fields.

**RESULTS AND CONCLUSION:** In experiments with tissue phantoms, no thermal denaturing was observed when millisecond boiling was initiated, even though temperatures reached 100°C. Experiments in liver tissue showed that varying types of lesions were induced that ranged from purely thermal to purely mechanical depending on the pulsing protocol used. Significant mechanical effects were only observed in tissue when boiling activity was first initiated. Therefore, shock wave heating and millisecond boiling may be an effective method for reliably generating significant tissue erosion effects in vivo. Work supported by NIH EB007643, NSBRI SMST01601, and RFBR 09-02-01530.



### Tissue ablation using cavitating bubbles triggered by high intensity ultrasound pulse

**Yoshizawa S.**<sup>1</sup>, Takagi R.<sup>1</sup>, Umemura S.<sup>1</sup>

<sup>1</sup> Tohoku University, Sendai, Japan

It has been investigated that oscillating microbubbles can enhance tissue heating in HIFU applications. In this study, a HIFU sequence to efficiently ablate tissue using microbubbles is investigated. High intensity ultrasound pulse is used to trigger cavitating bubbles. Relatively low intensity ultrasound burst wave follows just after the triggering pulse to ablate tissue. The tissue ablation with the high and low intensity ultrasound is investigated in vitro. The intensity of the ultrasound for cavitation triggering (triggering ultrasound) is from 0.5 to 2.0 kW/cm<sup>2</sup>, and that for tissue ablation (heating ultrasound) is from 100 to 200 W/cm<sup>2</sup>. The intensity is estimated with assuming quadratic relation between the input voltage to the transducer and the intensity. The duration time of the triggering ultrasound is 200  $\mu$ s, and that of the heating ultrasound is 5 s. The frequency of the both ultrasound is 1.08 MHz. Chicken filets are used for the target tissue. The fillet is located in deionized and degassed water. A hydrophone is set in water to detect acoustic pressure from the cavitating bubbles. Before ablating chicken fillet, the triggering ultrasound is focused to the target and acoustic pressure is measured with the hydrophone to detect cavitation inception by subharmonic signal. When the fillet was coagulated, the lesion shape was not like cigar but spherical. When the cavitation inception with the triggering ultrasound was not detected, the fillet was not coagulated. The intensity of the heating ultrasound was so low that the ultrasound energy absorption in the fillet without cavitation was not sufficient for the coagulation. Once the cavitating bubbles were generated at the focus, they oscillated with the heating ultrasound and greatly enhanced tissue heating. The results show that the combination of high and low intensity ultrasound is effective for thermal therapy due to cavitating bubbles.



S2B-5

**Why are short pulses more efficient in tissue erosion using pulsed cavitation ultrasound (histotripsy)?**

**Wang TY.**<sup>1</sup>, Maxwell A.<sup>1</sup>, Xu Z.<sup>1</sup>, Fowlkes B.<sup>1</sup>, Cain C.<sup>1</sup>

<sup>1</sup> University of Michigan, Ann Arbor, USA

**OBJECTIVES:** Histotripsy uses high intensity short duration ultrasound pulses to induce mechanical tissue fractionation or erosion. Extremely short pulses ( $\leq 10$  cycles) result in higher tissue erosion efficiency. The cavitating bubble clouds have been shown to play an important role in tissue erosion. This study provides insight into this dependence of erosion efficiency on pulse duration by investigating bubble dynamics within a pulse using various pulse durations.

**MATERIAL & METHODS:** Bubble clouds were generated at a gel-water interface using 10-, 30-, or 50-cycle, 1-MHz pulses at  $>19$ MPa peak negative pressure and 1-kHz pulse repetition frequency. An ultrahigh speed camera was used to image the overall clouds and individual bubbles over three time periods- 1) within the first 3 cycles of a pulse, 2) over the entire pulse, and 3) during a 220- $\mu$ s interval after the pulse ended. The total cross-sectional area of the bubble clouds and the radii of individual bubbles were analyzed as a functional of time.

**RESULTS:** 1) Within the first 7-10 cycles, the overall cloud grew to the maximal size for all three pulse durations. The individual bubbles underwent violent expansion and collapse, and grew in size with each cycle of ultrasound. 2) Between the 10th cycle and the end of the pulse, the overall cloud size did not change even if further cycles of ultrasound were delivered. During this time, the individual bubbles no longer underwent violent collapse. 3) After the pulse, the overall cloud gradually dissolved. The individual bubbles continued expanding for 0-30 $\mu$ s depending on the bubble size, and then gradually dissolved.

**CONCLUSIONS:** Violent bubble growth and collapse likely occur only within the first few cycles of a pulse. We believe it is this violent bubble activity that causes the majority of tissue damage. This may explain why shorter pulse durations induce more efficient tissue erosion.



S2B-6

**Evaluation of the contrast between tissues in rabbit in vivo and thermal lesions produced by HIFU using fast spin echo MRI sequences**

**Damianou C.**<sup>1</sup>, Mylonas N.<sup>1</sup>, Hadjisavas V.<sup>1</sup>, Couppis A.<sup>1</sup>, Iosif D.<sup>1</sup>, Ioannides K.<sup>2</sup>

<sup>1</sup> Frederick University Cyprus, Nicosia, Cyprus

<sup>2</sup> Poliklinik Ygia, Limassol, Cyprus

**INTRODUCTION:** In this paper the goal was to measure the contrast to noise ratio (CNR) of fast spin echo (FSE) magnetic resonance imaging (MRI) sequences in detecting thermal lesions created by high intensity focused ultrasound (HIFU) in rabbit kidney, liver, heart, and brain and lamb pancreas.

**MATERIALS AND METHODS:** A spherically focused transducer was used which is navigated inside MRI by a custom made positioning device. A simple simulation model was developed which predicts the CNR for the two FSE MRI sequences.

**CONCLUSIONS:** The maximum contrast measured with T1-W FSE ranges from 10 to 25. For all 5 tissues of interest if one uses TR between 400 and 500 ms the contrast is maximized. The T1 value of lesion depends strongly on the host tissue and is always lower than the host tissue. The greater the difference in T1 value, the greater the CNR. The trend of CNR vs. repetition time (TR) and CNR vs. echo time (TE) in all 5 tissues starts to increase then it becomes flat and then at high TRs or TEs it starts to decrease again. The CNR measured with T2-W FSE varies between 12 and 15 for all 5 tissues. With T2-W FSE if one uses TE between 40 and 50 ms, the contrast is maximized. The T2 value of lesion also depends strongly on the host tissue, and was concluded that the T2 of lesion is always lower than the T2 of the host tissue. We use the simulation model in order to study the effect of varying T2 for T2-W FSE with the T2 of liver fixed.



## Adaptive volumetric MR-guided high-intensity focused ultrasound ablations in moving organs

**Hey S.**<sup>1</sup>, De Senneville B.<sup>1</sup>, Köhler M.<sup>2</sup>, Quesson B.<sup>1</sup>, Moonen C.<sup>1</sup>, Ries M.<sup>1</sup>

<sup>1</sup> CNRS/Université Victor Segalen Bordeaux 2, Bordeaux, France

<sup>2</sup> Philips Healthcare, Helsinki, Finland

**OBJECTIVE:** An adaptive method for volumetric focused ultrasound (HIFU) ablations of moving targets is presented which is based on on-line MR thermal dose measurements.

**MATERIAL AND METHODS:** For the volume ablation control algorithm, the cumulative thermal dose is calculated from real-time 2D motion stabilized MR-thermometry (10Hz refresh time) and continuously compared to the desired target value. The required dose correction is calculated and translated into the necessary energy (E) to be deposited into the tissue. This defines the updated trajectory and the required acoustic power for the current sonication cycle (25ms per point, four points). The trajectory is multiplexed with the current target position derived from MR imaging and subsequently sonicated. The efficiency of the proposed motion compensated adaptive ablation of a predefined volume is demonstrated with phantom experiments (Philips 1.5T MRI with integrated 256-channel HIFU platform) simulating respiratory motion (1cm ptp, 0.45Hz). For MR-imaging echo-planar imaging (TE=41ms, TR=100ms, voxel size: 2.4x2.4x6mm<sup>3</sup>) was used.

**RESULTS:** A detailed evaluation of the thermal dose profile after the treatment (50W acoustic power, 80s duration) reveals that all points in the designated target area (1cm circular ablation, N=13 voxels) reached the desired lethal thermal dose, while adjacent tissue was preserved. The effect of the continuous 2D target displacement during the ablation was found to be fully compensated.

**CONCLUSIONS:** The proposed method enables precise volume ablations in the presence of motion with amplitudes similar to those due to respiratory motion. This method ensures a uniform dose deposition within a predefined region, without requiring precise knowledge of the thermal characteristics of the target tissue.

---







**S3A-1**

**Ultrasound guided HIFU: strengths and weaknesses**

**Invited speaker: Ter Haar G.**<sup>1</sup>

<sup>1</sup>Institute of Cancer Research, Royal Marsden Hospital, Surrey, UK

The successful guidance and monitoring of High Intensity Focused Ultrasound (HIFU) treatments, whether by ultrasound (US), magnetic resonance (MR) or other imaging techniques has a number of requirements: i. accurate targeting for placement of the focus; ii. Monitoring of physical events in tissue that correlate with required tissue damage (eg. temperature or bubble activity), and/or changes in tissue properties that indicate successful cell destruction (eg. stiffness or changes in attenuation); and iii. Monitoring of sensitive tissue regions outside the target volume for the avoidance of adverse events.

For the purposes of guiding HIFU treatments, US has a number of important advantages. These include its low cost, high spatial and temporal resolution, ability to monitor acoustic cavitation, changes in local blood flow and tissue stiffness. Diagnostic ultrasound's inability to penetrate bone and gas has advantages and disadvantages for HIFU treatments. While it may be a problem that tissue structures lying, for example, behind the ribs cannot readily be visualised, it is also true that a HIFU beam can generally not expose these regions without use of sophisticated delivery techniques such as time reversal. The creation of gas body collections in tissue (for example, from tissue water boiling) is readily visible on a diagnostic ultrasound image.

It seems clear that HIFU will find its place in cancer therapy, and that both US and MR guidance will find their own, complementary, niches in this area.

---



**S3A-2**

**Validating ultrasound-based HIFU lesion-size monitoring technique with MR thermometry and histology**

**Zhou S.**<sup>1</sup>, Petruzzello J.<sup>1</sup>, Anand A.<sup>1</sup>, Sethuraman S.<sup>1</sup>, Azevedo J.<sup>1</sup>

<sup>1</sup>Philips Research North America, Briarcliff Manor, USA

In order to control and monitor HIFU lesions accurately and cost-effectively in real-time, we have developed an ultrasound-based therapy monitoring technique using acoustic radiation force to track the change in tissue mechanical properties. We validate our method with concurrent MR thermometry and histology. Comparison studies have been completed on in-vitro bovine liver samples. A single-element 1.1MHz focused transducer was used to deliver HIFU, and to produce acoustic radiation force for the ultrasound monitoring. A 5MHz single-element transducer was placed co-axially with the HIFU transducer to acquire the RF data. During therapy, the monitoring procedure was interleaved with HIFU. MR thermometry (Philips Panorama 1T system) and ultrasound monitoring were applied simultaneously. The tissue temperature and thermal dose (CEM43=240mins) were computed from the MR thermometry data. The tissue displacement induced by the acoustic radiation force was calculated from the ultrasound RF data in real-time using a cross-correlation based method. A normalized displacement difference (NDD) parameter was developed and calibrated to estimate the lesion size. The lesion size estimated by the NDD was compared with both MR thermometry and the histology analysis. Our ultrasound monitoring technique showed very similar results to MR thermometry on multiple lesions of different sizes in liver tissue. Lesion formation times were predicted within <10% of each other and the estimated lesion sizes agreed with histology analysis within  $\pm 2$ mm. The study demonstrates the potential of our ultrasound based technique to achieve precise HIFU lesion control through real-time monitoring. The results compare well with histology and an established technique like MR Thermometry. This approach provides feedback control in real-time to terminate therapy when a pre-determined lesion size was achieved, and can be extended to 2D and implemented on commercial ultrasound scanner systems.



### Real-time two-dimensional temperature imaging using ultrasound

**Liu D.**<sup>1</sup>, Ebbini E.<sup>1</sup>

<sup>1</sup> University of Minnesota, Saint Paul, USA

An integrated system capable of performing high frame-rate two-dimensional temperature imaging in real-time is being developed. The system consists of a SonixRP ultrasound scanner and a custom build data processing unit connected with Gigabit Ethernet (GbE). The SonixRP scanner which serves as the frontend of the integrated system allows us to have flexibilities of controlling the beam sequence and accessing the radio frequency (RF) data in real-time through its research interface. The RF data is then streamlined to the backend of the system through GbE, where the data is processed using a two-dimensional temperature estimation algorithm running in a general purpose graphics processing unit (GPU), the combination of massive amount of computation power and re-designed parallel processing implementation make it capable of processing the data in a fraction of the acquisition time. The estimated temperature is visualized in real-time and also ready to be further processed and used as feedback for HIFU control. The system has been verified with elastography tissue mimicking phantom and shows excellent repeatability and sensitivity. In vitro experiment was also performed which measures the temperature rise under sub-therapeutic level HIFU application before and after lesion formation, results consistently show the changes of tissue thermal properties due to lesion formation.



### Ultrasound-based mapping of elasticity and temperature during HIFU therapy: an ex vivo feasibility study

**Sapin E.**<sup>1</sup>, Arnal B.<sup>1</sup>, Gennisson J.<sup>1</sup>, Pernot M.<sup>1</sup>, Fink M.<sup>1</sup>, Tanter M.<sup>1</sup>

<sup>1</sup> Institut Langevin, ESPCI ParisTech, CNRS UMR 7587, INSERM, Paris, France

**OBJECTIVES:** The use of High Intensity Focused Ultrasound (HIFU) for non invasive therapy requires improving real-time monitoring of the lesion formation during treatment, to avoid damage of the surrounding healthy tissues. The goal of this study is to show the feasibility of a full ultrasound approach that relies on the assessment of the changes in both tissue elasticity and temperature.

**MATERIALS AND METHODS:** HIFU treatment was performed using a 2.25MHz single element probe focused at 38mm in ex vivo bovine muscle samples. Two-dimensional temperature estimation from pulse echo diagnostic ultrasound imaging was combined with Supersonic Shear Imaging (SSI) on the same device (SuperSonic Imagine). To lower the thermo-acoustic lens effect, the ultrasound thermometry was performed using sub-aperture plane wave emissions steered at 11 angles (-10 to 10 degrees, 4 sub-apertures). Local elasticity was assessed using a conventional ultrasonic probe (L7-4, 5MHz). The SSI sequence consisted in 4 successive shear waves at different lateral positions. Each wave was created thanks to 4 pushing beams for 200µs at 4 depths. The shear wave propagation was acquired with 30 images at 5000 frames/s, from which the elasticity map was recovered.

**RESULTS:** A full elasticity and temperature mapping was achieved every second during the treatment. Temperature increase was measured up to 65°C in the focal zone. After the lesion formation, a strong increase of the elastic modulus was found in the focal zone (up to hundreds kPa). A good correlation between the temperature threshold and the elasticity change was established. Finally, the robustness of the technique was shown on tissue samples under motion.

**CONCLUSION:** A full ultrasound-based monitoring technique was developed to achieve at the same time elasticity and temperature mapping of soft tissues under HIFU treatment. It demonstrated the feasibility of monitoring and detecting the thermal lesion during HIFU therapy.



S3A-5

**Monitoring high intensity focused ultrasound therapy with backscattered ultrasound with a parametric treatment model**

**Speyer G.**<sup>1</sup>, Kaczkowski P.<sup>1</sup>, Brayman A.<sup>1</sup>, Crum L.<sup>1</sup>

<sup>1</sup> University of Washington, Seattle, USA

**OBJECTIVE:** Formulate estimates of the heating delivered by high intensity focused ultrasound (HIFU) by using frames of backscattered pulse-echo diagnostic ultrasound (DU).

**MATERIALS AND METHODS:** Displacement tracking of scatterers between two backscattered frames of DU, one preceding and one following ablative therapy, provides an effective method for non-parametric temperature estimates. The relative displacements observed between backscattered ultrasound frames also provide a means for estimating the applied heating over the course of therapy, by utilizing a model for the beam and heat diffusion, and ascribing all changes in treatment delivery to a time-varying modulation of the beam. Heat estimation is made parametric by using a functional expansion for the time-varying modulation, with the functions in the expansion corresponding to the modes of a Fisher information matrix (FIM) derived from a statistical measurement model for the DU and the physics of ultrasound propagation and heat diffusion. An expansion in terms of these modes provides the lower bound on the variance of coefficient estimates as the diagonal components of the inverse FIM.

**RESULTS:** We show through approximation, simulation, and experiment that the modal functions attain the Cramer-Rao bound for heating estimates independent of the specific heating applied and particular realization of backscattering. The accuracy of heat estimation is thus determined by the material properties, including spatial correlation, and the protocol employed.

**CONCLUSIONS:** Temperature estimates well below 1 degree Celsius are possible, and the estimation algorithm can be implemented to enable near real time monitoring.

---



S3A-6

**Monitoring of thermal ablation during HIFU exposure using passive cavitation mapping**

**Gyöngy M.**<sup>1</sup>, Ritchie R.<sup>2</sup>, Arora M.<sup>1</sup>, Leslie T.<sup>2</sup>, Coussios C.<sup>1</sup>

<sup>1</sup> University of Oxford, Oxford, UK

<sup>2</sup> Churchill Hospital, Oxford, UK

Inertial cavitation during HIFU exposure creates broadband acoustic emissions at frequencies well above that of the primary HIFU signal, enhancing the local rate of heat deposition in tissue due to frequency-dependent ultrasound absorption. By using a linear array on receive only, acoustic emissions can be received during HIFU exposure and used to form passive maps of cavitation activity. In order to demonstrate the usefulness of passive cavitation mapping as a means of monitoring lesion formation in real-time, fresh samples of ox liver were degassed and exposed to 0.5 MHz and 1.1 MHz continuous-wave HIFU at various acoustic intensities. Passive cavitation maps and active B-mode images were generated using a 5–10 MHz linear array placed through a rectangular opening of the HIFU transducer, and connected to an ultrasound imaging system (z.one, Zonare Medical Systems Inc., Mountain View, CA). The cavitation maps were compared to hyperechogenicity on the B-mode images. After HIFU exposure, the tissue samples were fixed and examined for macroscopic changes (denaturation) and microscopic changes (cell viability). The experiments clearly show that inertial cavitation occurs at acoustic intensities well below those required to achieve hyperechogenicity on B-mode images. Furthermore, while passive cavitation maps correlate well with tissue death, B-mode hyperechogenicity is found to be a less reliable indicator of tissue death. In conclusion, passive cavitation mapping provides a novel way of monitoring HIFU treatment. Like B-mode hyperechogenicity, the monitoring system is low-cost and can provide images in real-time. However, unlike B-mode hyperechogenicity, passive cavitation mapping provides a more reliable indicator of lesion formation, produces interference-free images during HIFU insonation, and does not rely on the creation of boiling bubbles, thus preventing overtreatment.



**HIFU induced displacement estimation (HIDE) maps for monitoring the creation of thermal lesions.**

**Haw C.**<sup>1</sup>, Noble A<sup>1</sup>, Arora M<sup>1</sup>, Coussios C<sup>1</sup>

<sup>1</sup> University of Oxford, Oxford, UK

The widespread use of Focused Ultrasound Surgery (FUS) remains hindered by a lack of accurate monitoring, both during each exposure and in the overall evaluation of the ablated area of tissue. Elastographic techniques, that harness the use of the acoustic radiation force to induce tissue movement, are a promising solution to the monitoring problem. Using a novel experimental rig that combines a linear element diagnostic ultrasound transducer unilaterally aligned with a HIFU probe we have investigated the potential for monitoring the HIFU induced displacement change that occurs during the formation of a thermally induced lesion. Contrary to other researchers in this area, the results indicate that a displacement increase occurs during lesion formation which is believed to be caused by an increase in the attenuation coefficient of the denatured tissue. This increase is a promising way to determine the optimal exposure time for operating procedures which may reduce the operation time by up to 80% whilst also providing information about the size and location of the ablated region.



**Real time motion correction for transcostal liver therapy: in vitro experiments**

**Marquet F.**<sup>1</sup>, Aubry JF.<sup>1</sup>, Pernot M.<sup>1</sup>, Tanter M.<sup>1</sup>, Fink M.<sup>1</sup>

<sup>1</sup> ESPCI, Paris, France

**OBJECTIVES:** Two factors limit transcostal HIFU ablation of liver tumors: the energy deposition at focus is decreased by respiratory movements of the liver and the energy deposition on the skin is strongly increased by the presence of highly absorbing and reflecting bone structures. Compensating the liver motion would have an impact on both effects: beside the fact that treatment accuracy would be enhanced, it would indeed enable decreasing the amount of emitted energy required to induce a necrosis at the targeted location and thus have an impact on skin preservation. In this study, experiments have been conducted to estimate transcostally liver motion and produce real time motion-corrected lesions.

**MATERIAL & METHODS:** A chest phantom made of three human ribs immersed in water was placed in front of a 200 elements array working at 1MHz. Ex-vivo liver samples were fixed to 3D motor controllers and moved behind the ribs along a 3D curve acquired previously in vivo on ventilated pigs. These realistic but yet deterministic movements enabled evaluating the errors on the motion estimation. Motion detection was achieved by cross correlating the backscattered signals received on sub-apertures of the array, according to a previously introduced method.

**RESULTS:** The maximum error on the transcostal motion detection was measured to be on the anterior-posterior axis (0,09mm error on average with a 0,097mm variance). Thanks to motion correction and beam steering, lesions as large as 1cm have been produced at focus whereas no necrosis could be obtained without correction.

**CONCLUSION:** These experiments correspond to a first attempt to combine adaptive transcostal focusing and real time motion tracking and correction. 3D motion correction can be performed transcostally and has been used to induce large lesions with optimized emission power and without ribs overheating. Such ultrasonic sequences could open the way to safe transcostal liver treatment.



**An automated dosing method for a HIFU device containing multiple phased arrays**

**Zeng X.**<sup>1</sup>, Barnes S.<sup>2</sup>, Sekins K.<sup>1</sup>

<sup>1</sup> Siemens Healthcare, Issaquah, USA

<sup>2</sup> Siemens Corporate Research Inc., Princeton, USA

A device containing multiple therapeutic ultrasound 2D phased arrays is proposed for tumor ablation or acoustic hemostasis applications. An automated dosing algorithm selects the optimal combination of arrays and calculates the acoustic power required of each array. Simulations demonstrate that therapeutic temperatures ( $70 < T < 95^{\circ}\text{C}$ ) are achieved over a tissue depth range with highly localized heating minimizing damage to surrounding tissue. The device has the 2D arrays mounted in panels that embody a cuff, patch or blanket type device. Using array and tissue target positions, an algorithm automatically estimates the available power at the target using depth, beam steering angles, directivity and the tissue properties. The individual array powers are then assigned using a power balance (equalization) algorithm that adjusts the size and shape of the heated target region. The treatment volume is adjusted by dynamically scanning the individual foci through patterns in the target zone. The temperature elevation was simulated using 3D finite element models. Numerical simulations were performed on the therapeutic performance of the device. The surface acoustic intensity of the arrays was maintained below a threshold associated with avoidance of skin burning. The total absorbed power producing therapeutic temperatures within an 8 mm diameter target was 4 to 5W for 30 second continuous dosing times. The spatial-peak-time-averaged intensity in the target focal zone was  $>600\text{W}/\text{cm}^2$ , below the inertial cavitation threshold for these conditions. An automated algorithm was developed to select the optimal combination of therapy arrays, power and scanning to control dosimetry. Using acoustic and thermal simulations, the proposed ultrasound device yielded a relatively uniform temperature distribution in the target volume. The multiple-array therapy device may be well suited for HIFU therapy. This research sponsored by United States DARPA contract HR0011-08-3-0004.



**Ultrasound-based monitoring technique to control lesion size during HIFU therapy**

**Anand A.**<sup>1</sup>, Petruzzello J.<sup>1</sup>, Zhou S.<sup>1</sup>, Sethuraman S.<sup>1</sup>, Azevedo J.<sup>1</sup>

<sup>1</sup> Philips Research North America, Briarcliff Manor, USA

**OBJECTIVE:** The lack of accurate and low-cost techniques for real-time monitoring and feedback during ablative therapies such as HIFU has limited its widespread clinical adoption. A good ultrasound solution would enable a much more widespread usage of HIFU therapy. We have developed an acoustic radiation force (ARF) based technique for controlling the lesion size and its placement during HIFU therapy.

**METHODS:** A series of experiments were performed in excised bovine liver tissue to evaluate the proposed technique. A single element therapy transducer was used to deliver HIFU therapy with a duty cycle of 98%. During a brief interruption of HIFU, ARF pulses were delivered by the same transducer. The therapy transducer excitation was synchronized with a Philips iE-33 ultrasound scanner to acquire 2-D beam summed RF data from a S5-1 diagnostic probe (placed confocally with the therapy transducer). RF data was processed to estimate the ARF induced displacements. The change due to therapy at each spatial location was quantified by a unitless parameter, normalized displacement difference (NDD), defined as the difference between normalized displacement at the therapy endpoint and a reference determined from the data.

**RESULTS:** The 2-D displacement map (normalized to the value before therapy commenced) illustrated that displacements initially increased due to the temperature rise, reached a maximum, and then decreased with continuing therapy. Strong correlation was observed between the NDD parametric map and the lesion size independently determined by histological examination. The lesion dimensions estimated with this noninvasive approach matched histology to within  $\pm 2$  mm. Moreover, it was observed that the NDD parameter was independent of treatment time and power.

**CONCLUSIONS:** This study demonstrates potential for use of this ultrasound-based technique in real-time monitoring and feedback of HIFU therapy to determine therapeutic endpoint and improve treatment efficacy.



**Ultrasound guided high intensity focused ultrasounds (US-gFUS) therapy for uterine fibroids. Initial experience in our center**

**Isern Quintilet J.**<sup>1</sup>, Pessarrodona A.<sup>1</sup>, Muchart J.<sup>1</sup>, Cassadó J.<sup>1</sup>, Canales L.<sup>1</sup>, Rodríguez J.<sup>1</sup>

<sup>1</sup>Hospital Universitari Mutua de Terrassa, Terrassa, Spain

**INTRODUCTION:** HIFU is an emerging technology for thermal ablation of solid tumors, truly non-invasive, that is developing very quickly. Since recent CE approval of this Chinese devices they are now also available for Western countries.

**OBJECTIVES:** We want to present our experience with the USgFUS technology for the non-invasive treatment of uterine fibroids, report our study and treatment protocol, and the safety issues of the procedure. Finally we give some preliminary data about the imaging results and symptom improvement.

**DESIGN AND METHODS:** In the study we have included the first 60 patients treated with the HAIFU JC System from February 2008 until now. All the patients had symptomatic uterine fibroids, according to the UFS-QOL questionnaire. Each patient was diagnosed by US and contrast enhanced MRI and all of them followed a standard protocol with close follow-up. The follow-up was made clinically with a specially designed questionnaire regarding immediate postoperative pain, discomfort and recovery, about the possible discomfort in the first week after treatment, and one month after, this time together with a new UFS-QOL questionnaire, contrast-enhanced MRI and blood analysis.

**RESULTS AND DISCUSSION:** There were no clinically relevant complications during or immediately after treatment. There was three grade I skin burn, fully recovered one week after, four postablation febrile syndrome and one watery discharge menses. All treatments were performed at high power with an average of 274 W.. From the one month follow-up MRI (n=12) the treatment area covered more than 80% of the uterine fibroid in most cases and some of the patients already show improvement in the UFS-QOL scores. No complications were found at the follow-up.

**CONCLUSIONS:** We didn't find any clinically significant complications related to the procedure neither immediately after the treatment nor in the one month follow-up. The patients recovered very soon after the procedure.

---





S3B-1

**Development of a cannulated vessel model for the study of cell sonoporation in the presence of contrast agents**

**Tokarczyk A.**<sup>1</sup>, Rivens I.<sup>1</sup>, Ter Haar G.<sup>1</sup>

<sup>1</sup>The Institute of Cancer Research, Sutton, UK

Sonoporation is considered to be an effective way of enhancing gene and/or drug delivery. The presence of ultrasound contrast agents (UCAs) has been found to increase the efficiency of cell monolayer gene transfection while the cells' viability remained unaffected (Rahim et al. 2006). The intention of this study is to investigate the effects of ultrasound exposure of UCAs on the blood vessels in order to assess the spatial distribution of sonoporation and other cellular effects. An experimental model using a cannulated artery (~200µm diameter) has been developed. The laboratory system, which allows real time imaging of the artery and its contents during US exposure, comprises several components: a fluorescence microscope, US sources at different frequencies (0.9–2MHz) and power capabilities (0.5–4MPa peak negative pressure) and a chamber designed to allow vessel attachment to micropipettes, perfusion with a feeding buffer and infusion with UCAs. Fluorescent dyes such as propidium iodide and fluorescein isothiocyanate(FITC)-dextran have been chosen to reveal cell death and sonoporation. High intensity focused ultrasound and diagnostic ultrasound exposures will be tested in order to find the US conditions which promote sonoporation with no decrease in cell viability. The problems of imaging a submerged artery and US alignment have been successfully overcome, and preliminary microscopy images have been obtained. This novel system will now allow microscopic visualisation of the effect of US-exposed contrast microbubbles on endothelial and smooth muscle cells of arteries. The perfused artery provides a more biologically relevant model than cell monolayers as smooth muscle and collagen are present. These may affect the efficiency of cell membrane permeabilisation by increasing the resistance to US. Rahim et al. 2006, Physical parameters affecting ultrasound/microbubble mediated gene delivery efficiency in vitro, *Ultrasound in Med.&Biol.*32:1269-79.

S3B-2

**Validation of an acoustic cavitation dose in pulsed mode by the terephthalate dosimeter for in vitro drug delivery application**

**Somaglino L.**<sup>1</sup>, Bouchoux G.<sup>1</sup>, Mestas J.<sup>1</sup>, Matias A.<sup>1</sup>, Chapelon JY.<sup>1</sup>, Lafon C.<sup>1</sup>

<sup>1</sup>INSERM U556, Lyon, France

**OBJECTIVE:** Chemotherapy encapsulated in nanoparticles such as liposomes can be triggered by ultrasound by means of inertial cavitation. Generated with a focused transducer operating at 1 MHz in pulse mode, cavitation can be very irregular. Hence, the quantity of cavitation applied is not proportional to sonication time. Consequently, there is a need to assess the dose applied to the media so as to control drug release from liposomes.

**MATERIAL & METHODS:** The chosen indicator was broadband noise emitted by bubble collapse during inertial cavitation. It was measured with a wide-band needle hydrophone, bandpass filtered, and then integrated over experiment time to create a Cavitation Dose (CD). To validate this CD, another indicator was used: the generation of hydroxyl radicals ( $\cdot\text{OH}$ ) induced by water sonolysis during inertial cavitation. Terephthalate(TA) solution allows dosing precisely  $\cdot\text{OH}$  radicals: TA anions react with them to form fluorescent anions. Experiments were performed on TA samples sonicated using distinct ultrasound parameters (Ispta= 560-1605W/cm<sup>2</sup>, PRF: 10Hz-10KHz, duty cycle: 3% to 25%) and measuring the CD. Then, the release extent of doxorubicin from 85nm liposomes was determined as a CD function.

**RESULTS:** For TA tests, results showed a good correlation between the CD and fluorescence but the data set was disperse. However, a very good correlation and less dispersion were obtained performing experiments with fixed PRF and duty cycle, with varying amplitude. For three sets of parameters curves were statistically different: this can stem from cavitation itself or from the analog filter. For various liposome formulations, an excellent correlation was found between drug release and CD using one set of parameters.

**CONCLUSION:** The CD was validated chemically for different set of ultrasound parameters. It allows controlling drug release from diverse liposome formulations Work grant: Nanomat(Norwegian Research Council). Liposomes supply: Epitarget AS, Norway.



### Cavitation-enhanced momentum transfer for drug delivery

**Rifai B.**<sup>1</sup>, Arvanitis C.<sup>1</sup>, Bazan-Peregrino M.<sup>1</sup>, Ventikos Y.<sup>1</sup>, Coussios C.<sup>1</sup>

<sup>1</sup> University of Oxford, Oxford, UK

**OBJECTIVES:** Our aim is to use ultrasound-instigated cavitation micromixing, promoted by the use of cavitation nucleation agents, to enhance the delivery of therapeutic agents into an obstructed (»blunt-end«) vessel within an experimental model of a solid tumour. The role of various treatment parameters on the momentum imparted upon the treated volume, and the relationship between momentum transfer and drug delivery, is investigated.

**METHODS:** We used a 0.483MHz HIFU transducer driven continuously for 2 seconds to deliver peak rarefactional focal pressures up to 2MPa. A 15MHz broadband cavitation detector was used to monitor emissions. Image analysis permitted quantitative measurement of the distribution of a dye-labeled therapeutic macromolecule. Experiments were performed with and without cavitation-nucleating microparticles. Experimental results were compared qualitatively and quantitatively to numerical simulations of cavitation microstreaming.

**RESULTS:** The presence of microparticles resulted in an up to seven-fold increase in overall inertial cavitation activity, as measured by broadband noise emissions. In this regime, acoustic excitation resulted in delivery of therapeutic up to 17mm into the blunt-end vessel - more than twice the convective length-scale observed in the absence of microparticles. Additionally, there was a very strong correlation ( $r > 0.97$ ) between broadband emissions and total therapeutic delivered into the blunt-end vessel.

**CONCLUSIONS:** We have developed an experimental model to simulate certain attributes of solid tumor vasculature, and demonstrated both experimentally and computationally that inertial cavitation enhances momentum transfer to the surrounding fluid, and thus convective mass transport of therapeutic agents within the tumor model. Further validation of the model will enable optimization of treatment parameters for successful drug delivery across a broad range of applications.



### Correlation of ultrasound-mediated drug delivery with acoustical properties of the transducer by macroscopic fluorescence imaging

**Lepetit-Coiffe M.**<sup>1</sup>, Yudina A.<sup>1</sup>, Lourenco de Oliveira P.<sup>1</sup>, Deckers R.<sup>1</sup>, Couillaud F.<sup>1</sup>, Moonen C.<sup>1</sup>

<sup>1</sup> CNRS UMR 5231 / Université Bordeaux 2, Bordeaux, France

**OBJECTIVE(S):** To visualise and quantify the ultrasound-mediated (US) internalization of a 'smart' model drug by means of macro- and microscopic imaging and correlate it with acoustical properties of the transducer

**MATERIAL&METHOD(S):** US pressure field of a 5.8mm diameter mono-element transducer working at 1.5MHz was measured by a calibrated needle hydrophone. A 0.88MPa p-p (at 1.0W electrical power) maximum was found at 8mm from the active surface. Spatial profile was radially concentric decreasing from the centre (diameters at -3dB, at -6dB and -12dB were 3, 7 and 13mm). C6 rat glioblastoma cells were cultured in Opticell chambers up to confluence. 2µM Sytox Green, a cell-impermeable cyanine dye that exhibits a 1000-fold increase upon binding to nucleic acids was co-injected with 3x10<sup>8</sup> SONOVUE microbubbles into the Opticell positioned 8mm from the active surface. US exposure duration was varied from 10sec to 3min, electrical power from 0.5 to 2.0W. After 15 min of recovery, the Opticell was viewed under epifluorescence Leica DM R microscope and Leica Z 16 APO (Macroflu). For quantitation, amount of nuclei with Sytox Green was reported as uptake percentage of the total amount of Hoechst 33258 stained nuclei in the same area (Metamorph processing).

**RESULT(S):** At macroscopic imaging, the spatial profile of the cell internalized model drug by means of US closely matched with the acoustical field. The maximum internalization diameter at 1W was 9,7,6 and 3mm for 3min, 1.5min, 45s and 10s respectively suggesting a cumulative effect of acoustical-pressure with exposure duration. Inside these zones, the uptake percentage was the same and close-to-25%. A rim of less intense internalization (3-4%) was visible around the main areas. At 2W, uptake increased up-to-35%.

**CONCLUSION(S):** The correlation of US-mediated drug delivery with acoustical properties of the transducer is demonstrated with fluorescence imaging using a fluorescent 'smart' dye Sytox Green as a model drug.



S3B-5

Ultrasound-inducible fluorescent particles for internal tattooing

**Couture O.**<sup>1</sup>, Pannacci N.<sup>1</sup>, Tabelaing P.<sup>1</sup>, Fink M.<sup>1</sup>, Servois V.<sup>2</sup>, Tanter M.<sup>1</sup>

<sup>1</sup> ESPCI, Paris, France

<sup>2</sup> Institut Curie, Paris, France

**OBJECTIVES:** Despite registration methods such as guiding wires, resecting diseased tissue previously detected with medical imaging remains challenging for surgeons. Our objective is to selectively and non-invasively deposit markers under image guidance for internal tattooing. This study describes the production of ultrasound-inducible particles carrying large payloads of fluorescent markers.

**METHODS:** Our particles are double-emulsions. The primary emulsion consists of nanoparticles of fluorescein-saturated water encapsulated in perfluorohexane. This emulsion is then encapsulated in aqueous Pluronic (1%) using a flow-focusing microfluidic system. The vaporization threshold of these particles is measured with a 2.25 MHz transducer (f: 38 mm, #1) focused in the exit channel of the microfluidic system. The release of fluorescein is observed under an inverted fluorescence microscope.

**RESULTS:** The composite particles are monodisperse with a diameter of 5 microns. The fluorescein-containing water represents about 70% of the particles' content. They last for several weeks with minimal loss of fluorescein into the medium. When submitted to 2.25 MHz pulses (20 kHz PRF), the particles vaporize at 6 MPa peak-negative pressure. A violent increase in volume is observed. While the original composite particles are dark orange, the surrounding liquid becomes brightly fluorescent after ultrasound-induced release.

**CONCLUSIONS:** Two third of the composite particles consists of payload that can be released at the focal spot of the transducer. Such a large amount of fluorescein could be observed under fluorescence endoscopy. This payload can also contain other hydrophilic markers and chemotherapy. The combined effect of the vaporization of these particles and sonoporation is now being tested in the vascular-bed of fertilized chicken eggs and mice.



S3B-6

Real-time monitoring of drug delivery with MRgHIFU and image-able low temperature sensitive liposomes

**Partanen A.**<sup>1</sup>, Negussie A.<sup>2</sup>, Yarmolenko P.<sup>3</sup>, Frenkel V.<sup>2</sup>, Wood B.<sup>2</sup>, Dreher M.<sup>2</sup>

<sup>1</sup> Philips Healthcare, Bethesda, USA

<sup>3</sup> Duke University Medical Center, Durham, USA

<sup>2</sup> National Institutes of Health, Bethesda, USA

**OBJECTIVE:** The combination of magnetic resonance guided high intensity focused ultrasound (MRgHIFU) and low temperature sensitive liposomes (LTSLs) may deliver therapeutics to targeted tissues with accuracy and precision not currently available. However, spatial and temporal control of drug delivery may require the ability to image drug release as the treatment progresses. The objective of this study was to develop image-able LTSLs and demonstrate the ability to induce and monitor drug release in real-time with non-ablative MRgHIFU in phantoms.

**MATERIALS & METHODS:** LTSLs were prepared containing both doxorubicin (dox) and Gd. An integrated Philips MRgHIFU platform was used for sonications and MR guidance. Low power sonications were performed on an agar-silica gel tissue-mimicking phantom with cavities containing the image-able LTSLs. Temperature maps and T1-weighted images were acquired in real-time during and after HIFU.

**RESULTS:** Relaxivity and MRI signal intensity of an LTSL solution increased ~2-fold when heated above the phase transition temperature (T<sub>t</sub>) of the LTSL using a hot water bath. Release of dox was confirmed at temperatures above T<sub>t</sub>. Sonications in an agar-silica phantom resulted in temperatures greater than the T<sub>t</sub> of the LTSL (41°C), reaching as high as 45°C, which is still well below the threshold for tissue damage. Control regions without LTSLs had no signal change during sonications but regions containing the image-able LTSLs demonstrated a signal increase in T1-weighted images both during and after the sonications. The signal increased only after the temperature rose above the T<sub>t</sub> of the LTSLs. Most importantly, the signal increase corresponded spatially to locations of the sonications.

**CONCLUSION:** MRgHIFU combined with image-able LTSLs can release contrast agents from LTSLs with precise spatial control and real-time noninvasive monitoring of contrast release, temperature, and potentially drug levels in the future.



## Ultrasonic activation of thermally sensitive liposomes

**Mylonopoulou E.**<sup>1</sup>, Arvanitis C.<sup>1</sup>, Bazan-Peregrino M.<sup>1</sup>, Arora M.<sup>1</sup>, Coussios C.<sup>1</sup>

<sup>1</sup>Institute of Biomedical Engineering, University of Oxford, Oxford, UK

Cancerous cells are known to be more vulnerable to mild hyperthermia than healthy cells, which can survive temperatures above 43°C for brief periods of time. Currently in phase III clinical trials for liver cancer, ThermoDox®(Celsion Corporation) is a drug delivery system containing doxorubicin, a common anti-cancer agent, encapsulated within thermally sensitive liposomes designed to release their contents above 39.5°C. Activation of doxorubicin with the use of HIFU, which can generate localized heating non-invasively, would combine the benefits of targeted chemotherapy and hyperthermia. The resolution and reliability with which HIFU-induced hyperthermia can achieve ThermoDox release was investigated using a novel agar-based gel embedding a uniform distribution of human cancer cells and liposomes at clinically relevant concentrations (0.02 mg/ml). Attenuation of the gel was quantified using both a through-transmission method and an embedded hydrophone (Onda HNA) technique to ensure relevance of the observed heating rates to human tissues. The gel was exposed to 1.15 MHz HIFU (Sonic Concepts H102) using a range of clinically relevant pressure amplitudes (0-6 MPa peak rarefactional), duty cycles (10-100%) and exposure durations to identify optimal insonation conditions for complete doxorubicin release. The corresponding temperature profiles were mapped and drug release was quantified using fluorimetry. Complete release over the HIFU focal area was obtained for 6-s continuous wave exposure at 5.2 MPa peak rarefactional pressure, i.e. under exposure conditions for which the temperature exceeded 43°C throughout the focal volume. Both the final temperature reached and the rate of heating were found to affect release significantly. ThermoDox release was achieved only due to thermal effects of HIFU, and not by other ultrasound effects, like cavitation without heating, showing robustness of HIFU-induced hyperthermia as a release mechanism.

---







## Future clinical role of HIFU in the brain and the mission of the Focused Ultrasound Surgery Foundation

Invited Speaker: **Kassel N.**<sup>1</sup>

<sup>1</sup> University of Virginia, Charlottesville, USA

The Focused Ultrasound Surgery Foundation was founded in October 2006 to advance the field of MR guided focused ultrasound. Its mission is to facilitate the development of new applications and accelerate the worldwide adoption of this technology.

The foundation operates by complementing, supplementing, and integrating the activities of the other traditional organizations involved in the development of the technology.

The foundation funds research and fellowships, sponsors symposia and workshops, publishes a website and newsletter, facilitates the development of new centers of excellence, and is developing a collaborative network of research sites. The research program concentrates on supporting the application rather than the development of MR guided focused ultrasound.

An area of emphasis for the foundation is its Brain Program with dedicated personnel and financial resources. Brain is arguably the most important application of MR guided focused ultrasound and represents the ultimate «killer application». It is recognized that the brain is the most difficult organ to treat safely and effectively and the ability to accomplish this will be interpreted as the ability to treat all other organs. Treatment of the brain will garner disproportionate media attention and increase awareness amongst the lay, medical and scientific communities which will facilitate funding the development and adoption of other applications.

The accumulated data regarding the use of focused ultrasound to treat brain diseases is encouraging and will be reviewed. Also, the foundation's roadmap for the development of brain applications will be presented.



## Experience in brain tissue necrosis using real time magnetic resonance-guided laser interstitial thermal treatment (MRgLITT)

Invited speaker: **Carpentier A.**<sup>1 & 2</sup>, Itzcovitz J.<sup>2</sup>, Mc Nichols R.<sup>4</sup>, Guichard J.<sup>3</sup>, Reizine D.<sup>3</sup>, Stafford J.<sup>5</sup>, Gowda A.<sup>4</sup>, George B.<sup>3</sup>

<sup>1</sup> Hôpital Pitié Salpêtrière, AP-HP, Université Paris VI, Paris, Fr

<sup>2</sup> Hôpital Pitié Salpêtrière, Paris, Fr

<sup>3</sup> Hôpital Lariboisière, AP-HP, Université Paris VII, Paris, Fr

<sup>4</sup> Biotex Inc, Houston, USA

<sup>5</sup> University of Texas M.D. Anderson Cancer Center, Houston, USA

**OBJECTIVES:** We report the first pilot safety clinical trial exploring real-time MRgLITT of focal cerebral metastasis tumours resistant to chemotherapy, whole-brain radiation and radiosurgery.

**MATERIAL AND METHODS:** Patients eligible for this trial presented breast or pulmonary adenocarcinomas (mean Age 54 y.o., median KPS 70%, and mean cerebral metastasis per patient 3.3). Before MRgLITT, median Recursive Partitioning Analysis class was 2, and median Score Index for Radiosurgery was 6.5, with a median patient survival prediction of 7 months. Under local anaesthesia, a 17Ga laser applicator was placed inside the target lesion under Leksell stereotactic guidance. Laser energy was delivered to the tumour while continuous imaging was performed in a 1.5T MRI scanner. The computerized system extracted temperature-sensitive information and displayed real-time thermal maps and estimates of thermal necrosis while simultaneously providing feedback control over the laser output. Clinical and imaging follow-up were scheduled up to M12.

**RESULTS:** 15 treatments on 6 patients have been performed: 9 total treatments and 6 partial treatments due to complex tumour geometry. Metastasis diameters were 10-20 mm (n=10) and 20-30 mm (n=5). Adverse events were 1 blood suffusion, 1 probe misplacement, 1 transient cerebellum syndrome, 1 transient aphasic deficit. Thermal necrosis induced a transient volume progression for 2 weeks. No severe adverse event related to MRgLITT occurred. Improved neurological status occurred in 2 cases. The procedure was painless and well tolerated. All patients were discharged within 24 hours of treatment. Median/mean patient survival is 19.8/17.4 months. Among the 6 partial treatments, the non-treated portion of lesions continued to grow with a median/mean tumour progression free of 6/6.6 months. Among the 9 complete treatments, median/mean tumour progression free is 15/12.6 months so far. 8 had no recurrence with a mean follow-up of 14.2 months.

**CONCLUSIONS:** MRgLITT allows safe thermal treatment by providing real-time feedback, necrosis prediction and control over the ablated volume. MRgLITT seems effective in treating <25mm diameter focal spherical metastasis when the entire volume is thermally necrosed. A larger series is needed to define the future indications of this technology.



### MR-guided ultrasonic brain therapy : high frequency approach

**Aubry JF.**<sup>1</sup>, Marsac L.<sup>2</sup>, Pernot M.<sup>1</sup>, Robert B.<sup>2</sup>, Tanter M.<sup>1</sup>, Fink M.<sup>1</sup>

<sup>1</sup> ESPCI, Paris, France

<sup>2</sup> SuperSonic Imagine, Aix-en-Provence, France

**OBJECTIVES:** Brain therapy with transcranial focused ultrasound is a scientific and technological challenge. The choice of the working frequency has important outcomes on the treatment precision and safety. A novel prototype is presented here, working at the highest frequency envisioned for transcranial brain treatment (1MHz). Increasing the frequency optimizes the focusing precision and the antenna gain. However the aberrations induced by the skull are increasing with frequency, so that a precise adaptive focusing correction is mandatory. A non invasive time-reversal focusing technique based on CT scans is performed for that purpose.

**MATERIAL & METHODS:** An MR-compatible high power prototype made of 512 transducers able to deliver up to 20 W/cm<sup>2</sup> has been constructed and installed in a 1.5T Philips Achieva scanner. Temperature rise has been mapped every 1s with a proton resonance frequency shift MR sequence in two orthogonal planes. The total acoustical power has been measured with a radiation force balance. 3D finite difference time domain simulations were used to compute the propagation of the wave field through human skulls. The simulated phase distortions were used as inputs for transcranial correction and the corresponding pressure fields were scanned in the focal plane.

**RESULTS:** For a total electrical power ranging from 200W to 5kW, the efficiency of the transducers was equal to 57% +/- 2.6%. At maximum power, the peak negative and peak positive pressure at focus were respectively 5.0 MPa and 9.2 MPa. At half of the maximum power, necroses were induced 2cm deep in turkey breasts placed behind a human skull. In vitro experiments on human skulls show that simulations restore more than 85% of the pressure level through the skull bone when compared to a control correction performed with an implanted hydrophone.

**CONCLUSION:** Such a brain therapy device operating at 1MHz should be particularly suited for well defined targets such as metastasis and essential tremors.



### Nonlinear ultrasound propagation through the skull

**Pinton G.**<sup>1</sup>, Aubry JF.<sup>1</sup>, Tanter M.<sup>1</sup>, Fink M.<sup>1</sup>

<sup>1</sup> ESPCI, Paris, France

**OBJECTIVES:** As an ultrasound wave propagates nonlinearly energy is transferred to higher frequencies where it is more strongly attenuated. Compared to soft tissue the skull has a strongly heterogeneous material parameters. We characterize with experiments and establish a numerical method that can describe the effects of the skull on the nonlinear components of ultrasonic wave propagation for application to high intensity focused ultrasound (HIFU) therapy in the brain.

**METHODS:** A degassed desiccated human skull was placed in a water tank and insonified with a single 0.7 mm 1 MHz circular transducer from a custom array designed for HIFU treatment. Two dimensional scans were performed preceding and following propagation through the skull with a calibrated hydrophone. Data from the scan preceding the skull were used as an input to a three dimensional finite difference time domain (FDTD) simulation that calculates the effects of diffraction, density, attenuation with linear dependence on frequency via relaxation mechanisms, and second order nonlinearity. A previously established equation was then used to transform a computed tomography scan to a set of registered maps of these four material properties.

**RESULTS:** Prior to propagation through the skull the second harmonic component was 19 dB lower than the fundamental, and the third harmonic component was 37 dB lower. Following the skull the second harmonic component was 35 dB lower and the third harmonic was 55 dB lower. The simulation is in agreement with the measurements to within 0.5 dB across the considered frequency range and shows good agreement across the 2d scan.

**CONCLUSIONS:** We have established a three dimensional FDTD simulation that accurately models the effects of nonlinearity and attenuation for propagation through the skull. Experimental validation shows good agreement across a broad frequency range and spatial extent. These results will be used to improve treatment planning.

S4A-5

Large-scale analysis of focused ultrasound in heterogeneous media

**Uebayashi J.**<sup>1</sup>, Tamura Y.<sup>1</sup>, Matsumoto Y.<sup>2</sup>

<sup>1</sup>Toyo University, Kawagoe, Japan

<sup>2</sup>University of Tokyo, Tokyo, Japan

Focused ultrasound is less invasive but is not applicable to deep body or a heterogeneous medium because an ultrasound would travel with reflections, refractions and attenuations. In the previous research[1], three dimensional simulation of transkull focused ultrasound was carried out with the assumption of no attenuation. In this research, the attenuation term is added to the governing equation and large-scale analysis of focused ultrasound in heterogeneous media is preformed. Firstly two dimensional analysis in homogeneous media is conducted. The governing equation is derived from the equation of continuity and Navier–Stokes equations, and is discretized with second-order accurate central difference in space and second-order accurate explicit difference in time. Computed result shows the same wave pattern of the sound pressure. Next, large-sale analysis of transkull focused ultrasound in heterogeneous media is preformed. The governing equation and discretization method are the same as those for two dimensions. The skull model is created from CT images. The skull has three-layered structure of compact bone layers and spongy bonein in between. The focused ultrasound is irradiated from the piezotransducer placed above the skull bone. The brain is an absorbing material and the attenuation property is given inside the skull. The present method will be applicable to the tarseffing of the transkull focused ultrasound for practical therapy. [1] Yoshiaki Tamura, Yusuke Nakajima, Yoichiro Matsumoto, “Evaluation and Application of Large-Scale Ultrasound Propagation Simulation in Heterogeneous Media”, WCCM8-ECCOMAS2008, Venice, Italy, 2008.6.30-7.4.

S4A-6

Transcranial MR-guided high intensity focused ultrasound for non-invasive functional neurosurgery

**Werner B.**<sup>1</sup>, Morel A.<sup>2</sup>, Zadicario E.<sup>3</sup>, Jeanmonod D.<sup>2</sup>, Martin E.<sup>1</sup>

<sup>1</sup>University Children's Hospital Zurich, Zurich, Switzerland

<sup>2</sup>University of Zurich, Zurich, Switzerland

<sup>3</sup>InSightec Ltd., Tirat Carmel, Israel

**OBJECTIVE:** Based on our long-term clinical experience in functional neurosurgery with stereotactic interventions in the thalamus, subthalamus and pallidum, we have developed intervention processes to access ablation targets in the brain non-invasively using Transcranial MR-guided High Intensity Focused Ultrasound (TcMRgHIFU). The aim of this phase I study was to demonstrate the ability of our clinical setup for non-invasive TcMRgHIFU surgery to safely, precisely, reproducibly and efficiently conduct these new treatment processes, exemplified on our clinical implementation of the selective regulatory central lateral thalamotomy (CLT) against chronic therapy-resistant neuropathic pain.

**MATERIAL & METHODS:** Ten patients scheduled for CLT were enrolled after obtaining fully informed written consent. The treatments were conducted on a clinical prototype system for transcranial MRgHIFU with a phased array of 1024 elements, operating at 650kHz (ExAblate 4000) integrated into our clinical 3Tesla MR-system. The stereotactic targets were located using the multiarchitectonic Morel atlas of the human thalamus and basal ganglia. Assessment of ablation dynamics, treatment results and patient outcome were done by MR-imaging, MR-thermometry, stereotactic lesion reconstruction and clinical/neurological patient follow up.

**RESULTS:** All treatments were well tolerated without neurological deficits. Peak focal temperatures ranged from 51 °C to 59 °C and two-days postoperative MRI revealed ablations of up to 5 mm in diameter located in the central lateral thalamic nucleus of the patients. Being not limited by trajectory restrictions individual treatment planning could fully exploit the ability of TcMRgHIFU to shape lesion patterns according to local target anatomy.

**CONCLUSIONS:** Our findings demonstrate for the first time that transcranial MRgHIFU can be used safely and reliably for non-invasive functional neurosurgery in the human thalamus.



### MR guidance, monitoring and control of brain HIFU therapy in small animals: In vivo demonstration in rats at 7T

**Larrat B.**<sup>1</sup>, Pernot M.<sup>1</sup>, Souilah A.<sup>1</sup>, Aubry JF.<sup>1</sup>, Fink M.<sup>1</sup>, Tanter M.<sup>1</sup>

<sup>1</sup> Université Paris VII - CNRS UMR 7587, Paris, France

**OBJECTIVES:** In the framework of HIFU transcranial brain therapy it is mandatory to develop techniques capable of assessing the focusing quality and location before the treatment. Monitoring heat deposition in real time and verifying the extension of the treated area are also important steps. The objective of this study was to develop a non invasive protocol to: -locate the US radiation force induced displacement in tissues and quantify the acoustical pressure at focus prior to HIFU; -monitor the temperature rise during HIFU; -assess the changes in elasticity in the treated area.

**MATERIAL & METHODS:** A 7T MRI scanner was equipped with a home-made stereotactic frame for rats and a US focused transducer working at 1.5MHz. A motion sensitized sequence was able to measure the radiation force induced displacement in brain. Once localized, the maximum displacement was measured and linked to the acoustical pressure at focus. An MR-Thermometry sequence allowed mapping the temperature rise every 500ms in the focal plane. MR-Elastography datasets were acquired before and after HIFU. Wave propagation and bioheat equation were simulated using 3D finite differences schemes in order to maximize heat deposit at focus while minimizing skull heating.

**RESULTS:** The proposed protocol was successfully evaluated on 10 rats. The accurate localization of the focal point prior to HIFU was demonstrated in vivo. Furthermore, the pressure estimation in situ allowed to accurately simulate the heat deposition at focus and to plan the treatment (electrical power, duration). The temperature measurements were in good accordance with the predicted curves. The elasticity maps showed significant changes after treatment.

**CONCLUSION:** Radiation force, temperature and elasticity MR-imaging were combined and implemented in a small animal MR-guided HIFU setup. In the perspective of human therapy at 1MHz, this protocol seems adequate and all sequences should be transposable at lower field.



### Real-time magnetic resonance temperature mapping in the brain

**Kickhefel A.**<sup>1</sup>, Roland J.<sup>1</sup>, Weiß C.<sup>1</sup>, Schick F.<sup>2</sup>

<sup>1</sup> Siemens Healthcare, Erlange, Germany

<sup>2</sup> University Tübingen, Tübingen, Germany

**PURPOSE:** Quality assessment of magnetic resonance (MR) thermometry in the human brain in vivo and in an ex-vivo swine skeletal muscle model using three pulse sequences based on the proton resonance frequency (PRF) method at 1.5T and 3T.

**MATERIAL AND METHODS:** Repetitive MR thermometry was performed on the brain of six volunteers using gradient recalled echo (GRE), segmented echoplanar imaging (segEPI), and single shot echoplanar imaging (ssEPI) sequences on whole-body 1.5T and 3T clinical systems using comparable acquisition parameters. Phase stability and temperature data precision in the human head was determined over 12 minutes for the three sequences at both field. Accuracy of the ssEPI sequence was compared to the GRE sequence in an ex-vivo swine skeletal muscle model during heating by high intensity focused ultrasound (HIFU). strengths.

**RESULTS:** In vivo examinations of brain revealed an average temperature precision of 0.4°C/0.4°C/0.2°C at 3T for the GRE/segEPI/ssEPI sequences. At 1.5T, a precision of 0.7°C/0.8°C/0.4°C was achieved. In the in ex vivo swine model a strong correlation of temperature data derived using ssEPI and GRE sequences was found with an average temperature difference of 2°C.

**CONCLUSION:** The ssEPI sequence was the fastest (time per measurement: 100ms) and the most precise for thermometry, with accuracy similar to the GRE sequence. Both EPI sequences were more sensitive to motion and image distortions than the GRE sequence. Since interventions in the brain are typically performed within a stereotactic frame to limit motion, the ssEPI sequence may be the 'sequence of choice' for MR thermometry of the brain.







S4B-1

**Enhancement of antitumor effect by the combination of therapeutic ultrasound and immunotherapy**

**Nishiie N.**<sup>1</sup>, Suzuki R.<sup>1</sup>, Oda Y.<sup>1</sup>, Taira Y.<sup>1</sup>, Utoguchi N.<sup>1</sup>, Maruyama K.<sup>1</sup>

<sup>1</sup> School of Pharmaceutical Sciences, Teikyo University, Kanagawa, Japan

**OBJECTIVES:** Recently, we developed novel liposomal bubbles (Bubble liposomes (BLs)) containing ultrasound (US) imaging gas, perfluoropropane. Additionally, we have established novel gene delivery system with collapse (cavitation) that was induced by US exposure to BLs. In this system, there was a low risk for cytotoxicity because of low intensity US. On the other hand, if intensity higher than this condition is utilized, there will be serious damages to adjacent cells by high temperature and strong shock waves caused by cavitation. Thus, we examined about antitumor effects using high intensity US. In this cancer therapy, it's thought that antigens from damaged tumor cells were released and inflammatory cytokines were secreted in tumor tissue. It's expected that strong tumor-specific immunity by intratumoral injection of dendritic cells (DCs), which are the most potent antigen-presenting cells, after US therapy. In this study, we examined about enhancement of anti-tumor effects by the combination of US therapy and DC-based immunotherapy.

**MATERIAL & METHODS:** Colon 26 cells (mouse colon carcinoma) were inoculated into the backs of mice. After 8 days, BLs were intratumorally injected and US was transdermally exposed toward tumor tissue (1 MHz, 4 W/cm<sup>2</sup>, 120 sec). DCs were intratumorally immunized on days 9, 10, 11, and 13 after tumor inoculation. The anti-tumor effect was evaluated by measuring tumor volume.

**RESULTS:** In either US therapy with BLs or DC-based immunotherapy, we obtained only slight anti-tumor effects. On the other hand, the combination of US therapy with BLs and DC-based immunotherapy efficiently suppressed tumor growth.

**CONCLUSIONS:** It seems that US therapy with BLs support induction of effective antitumor immunity. Therefore, the combination of US therapy with BLs and DC-based immunotherapy might be a useful cancer therapy strategy. Acknowledgements: This work was supported by MEXT KAKENHI (21700511)



S4B-2

**Sonoporation of cervical carcinoma cells affected with E6-oncoprotein for the treatment of uterine cancer**

**Curriel L.**<sup>1</sup>, Pichardo S.<sup>1</sup>, Lee K.<sup>1</sup>, Zehbe I.<sup>1</sup>

<sup>1</sup>Thunder Bay Regional Research Institute, Thunder Bay, Canada

**OBJECTIVES:** Cervical cancer development is strongly associated with human papillomavirus (HPV) infection. The viral protein E6 is instrumental for transformation and tumour growth maintenance. Existing vaccines against the variants HPV16 and 18 do not have therapeutic effects against pre-existing HPV infections. We propose to target the E6-oncoprotein in new treatments since healthy, non-infected cells would be spared while targeted tumour cells would be driven into apoptosis. However, the delivery of antibodies against E6 is limited by membrane permeability. We propose the combination of ultrasound exposures and microbubbles to induce the required cell permeability to allow the passage of antibodies specific to the E6-oncoprotein.

**METHODS:** This study shows our first results of achieving successful sonoporation in SiHa cervical carcinoma cells (E6+) that were seeded into Opticell(tm) chambers. Activated Definity (using recommended dose for diagnostic use) and EX-EGFP-M02 vector were mixed and injected into the chamber. A focused transducer with diameter of 6 cm and F-number of 1.25 was used to expose the cells during 30s with 30 pulses at 930 kHz and a repetition-frequency of 1.5 kHz. Thirty-six randomized experiments were done for pressure values of 0, 125, 250, 500, 750 and 1000 kPa (6 experiments per pressure value). Immunofluorescence was used to determine the levels of intracellular proteins.

**RESULTS:** A ratio of gene delivery ranging from 82 to 96% was observed for pressure values greater or equal to 125 kPa. Verification of the viability of cells was confirmed by observation of cell morphology under microscope.

**CONCLUSIONS:** Results suggest that cells affected with E6+ are an excellent target for drug delivery for cancer treatment using sonoporation. The delivery of antibody against E6 will be next tested and confirmed that apoptosis can be induced into HPV16 cells while sparing non-infected cells.



### Sonoporation outcome correlated with time-resolved measurements of microbubble dynamics

**Fan Z.**<sup>1</sup>, Park J.<sup>1</sup>, Kumon R.<sup>1</sup>, Deng C.<sup>1</sup>

<sup>1</sup> University Of Michigan, Ann Arbor, USA

**BACKGROUND:** Ultrasound application in the presence of microbubbles has been demonstrated as a promising method to facilitate drug and gene delivery into cells. However, the mechanism has not been fully understood due to the difficulty of investigating the complex microscopic, dynamic processes of ultrasound interaction with bubbles. Understanding the detail mechanisms of sonoporation can help to select ultrasound parameters to optimize technique for in vivo application. Objective: To investigate the microbubble dynamics driven by various ultrasound parameters such as the duration and pulse repetition frequency using time-resolved optical imaging, and to correlate the bubble dynamics with intracellular molecular uptake and cell viability in individual cells.

**MATERIAL & METHODS:** Human Umbilical Vein Endothelial Cells (HUVEC) were cultured on the ceiling of 400 micron height microchannel (ibidi,  $\mu$ -Slide I 0.4 Luer) under 5dyne/cm<sup>2</sup> shear stress. Propidium iodide was used as an intracellular delivery marker. Calcein AM was perfused into the microchannel to assess cell viability after ultrasound application. High-speed optical imaging (Photron FASTCAM SA1 and Specialized Imaging SIM 802) was used to capture time-resolved microbubble dynamics under ultrasound exposure.

**RESULT:** Various complex bubble dynamics were observed for different ultrasound parameters. Translational movement, microstreaming, coalescence and repeated responses of bubbles were observed in addition to bubble oscillation and collapse. The different microbubble dynamics were correlated with different delivery outcome in terms of intracellular uptake and cell viability.

**CONCLUSION:** Interaction of bubbles with ultrasound demonstrated wide range of different behaviors depending on ultrasound parameters include acoustic pressure, pulse duration, and pulse repetition frequency. Sonoporation outcome is determined by microbubble dynamics driven by ultrasound.



### Short-duration focused ultrasound stimulation of Hsp70 expression in vivo

**Kruse D.**<sup>1</sup>, Mackanos M.<sup>2</sup>, O'Connell-Rodwell C.<sup>2</sup>, Contag C.<sup>2</sup>, Ferrara K.<sup>1</sup>

<sup>1</sup> University of California, Davis, USA

<sup>2</sup> Stanford University, Palo Alto, USA

**OBJECTIVES:** The development of transgenic reporter mice and advances in in vivo bioluminescent imaging (BLI) have created unique opportunities to assess and analyze biological responses to thermal therapy directly in living tissues. Reporter mice incorporating firefly luciferase (luc) linked to a gene of interest can be used as a reporter to non-invasively reveal gene activation in living tissues. The objective of this study is to quantify the ability of measured short-duration high intensity focused ultrasound (HIFU) exposures to stimulate gene expression in vivo in a localized and controlled manner.

**MATERIALS & METHODS:** A transgenic (Tg) reporter mouse where expression of luciferase is controlled by the regulatory region of the inducible 70 kDa Hsp (Hsp70) was used to analyze its up-regulation related to thermal stress. The Tg mouse expressed the Hsp70-luciferase reporter only in the skin. Hsp70 expression was tracked for 96 hours following the application of 1 second-duration, 1.5 MHz continuous wave ultrasound pulses with spatial peak intensities ranging from 53 to 352 W/cm<sup>2</sup>. A finite element model was developed to predict the temperature rise in the skin assuming both a thermally conductive and a non-conductive condition at the skin surface.

**RESULTS:** Peak Hsp70 expression was observed 6-48 hours post-heating, with a significant elevation remaining at 96 hours. Exposure durations were simulated using a finite-element model, and the predicted temperatures and thermal doses were consistent with the observed spatial patterns of Hsp70 expression. Histological evaluation revealed that the thermal damage starts at the stratum corneum and extends deeper with increasing intensity.

**CONCLUSION:** Short-duration HIFU successfully induced statistically significant Hsp70 expression when the estimated peak temperature exceeded approximately 45-48°C with a CEM43 dose below 0.5 min; and repeated expression is expected when the period between treatments is greater than 96 hours.



S4B-5

### Ultrasound-enhanced nanotherapy of pancreatic cancer

**Rapoport N.**<sup>1</sup>, Nam K.<sup>1</sup>, Kennedy A.<sup>1</sup>, Shea J.<sup>1</sup>, Scaife C.<sup>1</sup>

<sup>1</sup> University of Utah, Salt Lake City, USA

Phase-shift paclitaxel (PTX)-loaded perfluoropentane (PFP) nanoemulsions combined with tumor-directed ultrasound have been used with a considerable success for tumor-targeted chemotherapy of gemcitabine (GEM)-refractory pancreatic cancer that is the fourth leading cause of the cancer deaths in the USA. Due to increased permeability of tumor blood vessels, drug-loaded nanodroplets accumulated in the tumor via passive targeting, which was confirmed by ultrasound imaging. Nanodroplets converted into microbubbles in situ under the action of tumor-directed 1-MHz or 3-MHz therapeutic ultrasound. The GEM-resistant pancreatic cancer proved sensitive to treatment by a micellar encapsulated PTX formulation Genexol PM (GEN). This formulation served as a starting point for manufacturing PTX-loaded phase-shift PFP nanoemulsions (ndGEN). The effect of combination therapy by drug loaded phase-shift nanodroplets and ultrasound (i.e. ndGEN+ultrasound) was stronger than that observed for therapy by GEN alone or GEN + ultrasound. Combination therapy ndGEN+US resulted in a spectacular tumor regression and in some cases complete tumor resolution. Moreover, formation of metastases was dramatically decreased and ascites generation was completely suppressed. However for all animal groups, local tumor recurrence was observed after the completion of the treatment indicating that some cancer cells survived the treatment. The recurrent tumors proved more resistant to the repeated therapy than initial tumors. Ultrasound imaging revealed non-uniform distribution of nanodroplets and microbubbles inside the tumor volume, which most probably presents the major reason of tumor recurrence and developed resistance. Approached to prevention of tumor recurrence will be discussed. Elucidation of mechanisms involved in suppression of tumor metastases by combined microbubble/ultrasound therapy is currently in progress.



S4B-6

### Cancer gene therapy by the combination of liposomal bubbles and ultrasound

**Suzuki R.**<sup>1</sup>, Oda Y.<sup>1</sup>, Nishiie N.<sup>1</sup>, Utoguchi N.<sup>1</sup>, Negishi Y.<sup>2</sup>, Maruyama K.<sup>1</sup>

<sup>1</sup> School of Pharmaceutical Sciences, Teikyo University, Kanagawa, Japan

<sup>2</sup> University of Pharmacy and Life Sciences, Tokyo, Japan

**OBJECTIVES:** Recently, we developed novel liposomal bubbles (Bubble liposomes (BLs)) containing ultrasound (US) imaging gas, perfluoropropane. Additionally, we have established novel gene delivery system with collapse (cavitation) that was induced by US exposure to BLs. Interleukin-12 (IL-12) has potent anti-tumor activities through the activation of natural killer cells and CD8+ T cells. Gene therapy by the intratumoral injection of the IL-12 gene expect as an effective tumor therapy because of IL-12 locally release in tumor. Non-viral vector system has many advantages over gene therapy, including ease of plasmid DNA production and lower toxicity compared to viral vector system. In this study, we assessed a feasibility of BLs and US as non-viral vector system in cancer gene therapy using IL-12 gene.

**MATERIAL & METHODS:** B6C3F1 mice were intradermally inoculated with mouse ovarian cancer cells (OV-HM cells) into flank. After 7, 9, 12, 14, 16, 19 days, BLs (2.5 µg) and mouse IL-12 coding plasmid DNA (10 µg) were injected into tumor, and ultrasound (1 MHz, 0.7 W/cm<sup>2</sup>, 60 sec.) was transdermally exposed toward tumor. Anti-tumor effects were evaluated by measuring tumor volume. We also examined about migration of CD8+ T cells which were mainly effector cells for anti-tumor effect.

**RESULTS:** IL-12 gene delivery with BLs and US was dramatically suppressed tumor growth and complete regression occurred in 80 % of the tumor bearing mice. In the tumor tissues delivered IL-12 gene with BLs and US, migration of CD8+ T cells were observed.

**CONCLUSIONS:** The combination of BLs and US would be a good non-viral vector system in cancer gene immunotherapy. Acknowledgements: We are grateful to Dr. Shinsaku Nakagawa (Graduate school of Pharmaceutical Sciences, Osaka University). This work was supported by JSPS KAKENHI (20240053) and Health and Labour Sciences Research Grants.



### Investigations in to the influence of pulsed high intensity focused ultrasound on metastasis in a murine model

Hancock H. <sup>1</sup>, Dreher M.<sup>1</sup>, Crawford N.<sup>1</sup>, Wood B.<sup>1</sup>, Hunter K.<sup>1</sup>, Frenkel V.<sup>1</sup>

<sup>1</sup> National Institutes of Health, Bethesda, USA

Pulsed-high intensity focused ultrasound (HIFU) exposures may enhance the permeability of tissue for improved delivery of drugs and genes, for example, by opening up gaps between cells in the vasculature and parenchyma. These effects may improve local targeting of therapeutic agents however; concerns exist that they could also facilitate dissemination of tumor cells and exacerbate metastasis. We describe development of a metastatic murine model for investigating alterations in metastatic potential. A breast cancer cell line producing metastases specific to lung was used. A series of factors were investigated including optimal timing for treatment of primary tumors and growth of metastases, as well as influence of pulsed HIFU exposures on metastatic burden. Primary tumors were grown, treated, and tumor bearing limbs were amputated 24 hours later. After a specific metastatic grow out period, mice were euthanized, tissues harvested and images were captured from whole-lung histological sections. A novel quantitative technique was developed using image processing to quantitate metastatic burden. In the HIFU-treated group 47% (7/15) of the mice had lungs that were overgrown with metastases (where individual lesions could not easily be distinguished), whereas only 13% (2/15) of control mice presented similar overgrowth. Furthermore, area fraction of metastatic burden (area of metastases/area of lungs) was 30% greater in HIFU treated mice compared to sham treatment. Although not statistically significant, this trend could be clinically relevant and merits further investigation. Presently, studies are being carried out investigating potential changes in gene expression occurring through the process of mechanical transduction in primary tumors, as well as direct mechanical effects that could enhance dissemination of tumor cells. This research tool could potentially be used to optimize ablative therapies while minimizing risk of inducing metastases.



### Pulsed-HIFU enhanced delivery and therapy using radiolabeled monoclonal antibodies

Razjouyan F. <sup>1</sup>, Shin I.<sup>1</sup>, Jang B.<sup>1</sup>, Dreher M.<sup>1</sup>, Frenkel V.<sup>1</sup>, Paik C.<sup>1</sup>

<sup>1</sup> National Institute of Health, Bethesda, USA

**OBJECTIVE:** Cytotoxic radioisotopes can be used to enhance therapeutic efficacy when coupled with monoclonal antibodies for the treatment of cancer. However, the current use of antibodies suffers from poor tumor uptake and penetration. Previous studies demonstrated that pulsed high intensity focused ultrasound (HIFU) improved the tumor uptake of antibodies. The objective of this study was to investigate the therapeutic efficacy of pulsed-HIFU combined with radiolabeled antibodies and distribution of fluorescently labeled antibodies in tumor tissue following HIFU exposures.

**MATERIALS AND METHODS:** The ability of pulsed-HIFU to improve the therapeutic efficacy of Y-90-labeled B3 mAb, directed against the Ley antigen, in the treatment of the Ley-positive A431 tumors was examined. Antibody penetration following HIFU exposures was investigated with fluorescently labeled B3 mAb in frozen sections of tumor tissue.

**RESULTS:** The tumors in the control mice grew rapidly with a median survival time of 5 days while Y-90-labeled B3 mAb treated tumors had a median survival time of 18 days. Pulse-HIFU exposures prolonged the median survival time to 26 days. Control tumors had limited penetration of antibody from the tumor surface. In addition to antibody accumulation at the tumor surface, pulsed-HIFU treated tumors demonstrated isolated regions of antibody accumulation in the tumor center, mostly around vascular structures that was not found in control tumors.

**CONCLUSION:** The improved growth delay demonstrated by the combination of radiolabeled antibodies and pulsed-HIFU exposures are encouraging. These results suggest that the improved therapy may be not only due to a greater accumulation of radiolabeled antibody but also due to more favorable distribution.



S4B-9

### Therapeutic benefits of ultrasound delivery of anti-A $\beta$ antibody in an Alzheimer's mouse model

**Jordao J.**<sup>1</sup>, Ayala-Grosso C.<sup>2</sup>, Huang Y.<sup>1</sup>, McLaurin J.<sup>3</sup>, Aubert I.<sup>1</sup>, Hynynen K.<sup>1</sup>

<sup>1</sup> Sunnybrook Research Institute, Toronto, Canada

<sup>3</sup> University of Toronto, Toronto, Canada

<sup>2</sup> Universidad Central de Venezuela, Caracas, Venezuela

Several therapeutic approaches in Alzheimer's disease (AD) aim to reduce the toxicity of amyloid-beta (A $\beta$ ) peptides in the brain. Clinical trials using anti-A $\beta$  antibodies successfully cleared A $\beta$ -plaques from AD brains, but raised safety concerns due to the high levels of antibodies required.

**HYPOTHESIS:** Magnetic resonance imaging-guided FUS (MRlgFUS) can deliver anti-A $\beta$  antibodies, administered at a low dose intravenously, to the brain of TgCRND8 mice and reduce A $\beta$  loads in targeted cortical areas.

**OBJECTIVES:** (1) Evaluate the spatio-temporal distribution of anti-A $\beta$  antibodies in the brain after FUS treatments; (2) Reduce A $\beta$  pathology with MRlgFUS and anti-A $\beta$  antibodies; (3) Evaluate the influence of FUS on glial cells.

**METHODS:** TgCRND8 mice were treated intravenously with the anti-A $\beta$  antibody BAM-10 and Definity microbubbles. MRlgFUS was applied along the right hemisphere. At different time-points post-treatment, TgCRND8 mice were sacrificed and their brains processed for biochemical analyses and quantitative imaging, including design-based stereology to estimate the number and size of cortical A $\beta$ -plaques.

**RESULTS:** We confirmed that MRlgFUS delivered anti-A $\beta$  antibodies from the bloodstream to the brain. BAM-10 antibodies entered the brain in vivo where they colocalized with other anti-A $\beta$  antibodies applied ex vivo, on the right hemisphere of the brain. Within days, MRlgFUS-delivered anti-A $\beta$  antibody significantly reduced A $\beta$  plaque number and size. Preliminary data suggests that MRlgFUS did not cause reactive astrogliosis, or an apparent change in the levels of microglia/macrophages.

**CONCLUSIONS:** The use of MRlgFUS shows promise as a therapeutic strategy for delivery of anti-A $\beta$  agents to AD brains; reducing A $\beta$  toxicity while potentially avoiding detrimental side effects currently associated with the use of high doses of anti-A $\beta$  antibodies. MRlgFUS had no apparent effect on gliosis, suggesting non-damaging properties of FUS under these conditions.



S4B-10

### Virus loaded microbubbles as a tool for targeted gene delivery

**Geers B.**<sup>1</sup>, Lentacker I.<sup>1</sup>, Demeester J.<sup>1</sup>, Desmedt S.<sup>1</sup>, Sanders N.<sup>1</sup>

<sup>1</sup> Ghent University, Ghent, Belgium

**OBJECTIVES:** Adeno-associated virus is a promising gene therapy vector because of its high transfection efficiency. However, the use of AAVs in humans is limited by their high toxicity and their risk of infecting non-target cells. For safe use, the immunogenic capsid of the AAV should be shielded from the immune system and the vector should be targeted to specific tissues. The objective of this study is to shield the immunologic properties of the AAV capsid by pegylation and to couple AAVs with avidin-biotin chemistry to lipid microbubbles to obtain an ultrasound targeted release and transfection. This study will evaluate whether lipid microbubbles release PEG-biotinylated AAVs upon ultrasound exposure and evaluate the transfection efficiency of AAV loaded microbubbles in vitro. Hence AAV-loaded microbubbles may provide a solution to obtain ultrasound targeted viral gene delivery.

**METHODS:** PEGylation of EGFP expressing AAV2 (kindly provided by the German Cancer Research Centre) was done using NHS-PEG-Biotin (Iris Biotech GmbH, Marktredwitz, Germany). Lipid microbubbles containing 85 mol% DPPC and 15 mol% of DSPE-PEG-Biotin were prepared. In vitro experiments were performed on BLM melanoma cells in Opticell plates and EGFP expression was measured with an FC500 Flow Cytometer. Ultrasound experiments were performed using a Sonitron sonoprotator with an ultrasound frequency of 1MHz, 2W/cm<sup>2</sup> intensity and a 10% duty cycle.

**RESULTS:** Zeta-potential measurements confirmed AAV pegylation using NHS chemistry. Flow cytometry revealed that PEGylation of the AAV surface lowers their biological activity. We could prove microbubble coupling of AAVs through NHS-PEG-Biotin chemistry, by confocal microscopy. Flow cytometry analysis showed that melanoma cells can be infected by AAV loaded microbubbles and ultrasound, provided that the AAVs are not too strongly PEGylated.



# Oral Communications Friday, September 25

[www.istu2009.org](http://www.istu2009.org)

Friday,  
September 25

## InSightec welcomes you to ISTU 2009

**We invite you to learn more about Magnetic Resonance guided Focused Ultrasound Surgery, and our ongoing research in:**

- » Uterine fibroids
- » Pain palliation of bone metastases
- » Breast cancer
- » Prostate cancer
- » Neurosurgery applications

For more information: [www.insightec.com](http://www.insightec.com), [info@insightec.com](mailto:info@insightec.com)

**InSightec**  
*Bringing therapy into focus*





## HIFU dosimetry

**Invited speaker: O'Brien Jr. W.**<sup>1</sup>

<sup>1</sup> University of Illinois at Urbana-Champaign, Urbana, USA

Dosimetry is the determination of a dose, or similar type of physical quantity, that characterizes the physical agent as to its potential or actual interaction with the biological material of interest. The objective of ultrasonic dosimetry is to relate magnitudes of specific quantities, such as intensity, acoustic pressure, particle displacement, etc., or perhaps some quantity yet to be developed, to the likelihood of occurrence of a biological alteration. As the biological alteration goal becomes more defined, such as thermal ablation in the case of HIFU, the dosimetric goal can likewise become more defined. Here thermal ablation refers to the removal of tissue or the destruction of the tissue function using heat. Dosimetric concepts related to thermal ablation have been proposed some four decades ago with the ophthalmic "cataract-producing unit" and then three decades ago with the brain tissue "energy absorbed per unit volume". Later, the Arrhenius activation energy concept was introduced, leading to an isothermal dose concept. It is thus suggested that the formalism may exist to develop an appropriate HIFU dose unit. It is argued that contemporary delivered dose and temperature-time data are needed to validate a potential dose unit. This research is supported by NIH Grant R37EB002641.



## Non invasive transcostal focusing based on the decomposition of the time reversal operator: in vitro validation

**Cohard E.**<sup>1</sup>, Aubry JF.<sup>1</sup>, Prada C.<sup>1</sup>, Fink M.<sup>1</sup>

<sup>1</sup> ESPCI, Paris, France

**OBJECTIVES:** Thermal ablation induced with high intensity focused ultrasound has produced promising clinical results to treat hepatocarcinoma and other liver tumors; however skin burns have been reported in many clinical studies. The energy deposition on the skin is indeed enhanced by the presence of the ribs. This study proposes a signal processing method to produce an acoustic field focusing on a chosen target while avoiding the ribs, using the decomposition of the time-reversal operator.

**MATERIAL & METHODS:** A chest phantom made of three human ribs immersed in water is placed in front of a 128 elements array working at 1.5MHz. In order to avoid focusing on the ribs, an excitation weight vector is applied to the transducers array: the transducers is first used in pulse echo mode (synthetic aperture imaging) to measure the time reversal operator. The set of singular vectors associated to the time reversal operator are then calculated. Usually, such vectors are used to focus on a reflective target. Here a weight vector is calculated to be orthogonal to the subspace of emissions focusing on the ribs. The resulting propagating fields are measured both in the focal plane and in the plane of the ribs, using a needle-hydrophone and the specific absorption rate (SAR) gain ratio of the energies absorbed at the focal point and on the ribs are measured when using this none invasive ribs sparing technique and with a non-corrected beam (spherical beam).

**RESULTS:** Depending on the intercostal space (set to vary between 10mm and 15mm), the SAR gain ratio was 25 to 100 fold better with the non invasive ribs sparing method compared to the non corrected beam. The pressure field at the bone location was on average 23dB lower with the proposed correction.

**CONCLUSION:** A novel non invasive ribs sparing technique enabled to decrease energy deposition on the ribs. Such a technique should benefit to transcostal ultrasonic ablation of the liver by reducing the risk of skin burns.



**An analytical comparison of the thermal dose equation and the intensity-time product,  $I t^m$ , for predicting tissue damage thresholds**

**Harris G.**<sup>1</sup>, Herman B.<sup>1</sup>, Myers M.<sup>1</sup>

<sup>1</sup> Food and Drug Administration, Silver Spring, USA

**OBJECTIVE:** For the successful application of ablative therapies such as high intensity focused ultrasound (HIFU), it is important to establish well-defined thresholds for tissue necrosis. A method based on thermal dose is most generally accepted, but another approach based on the intensity-time product of the form  $D = I t^m$  has been used, where  $D$  is a tissue-dependent damage threshold,  $I$  is the spatial-peak, temporal-average intensity,  $t$  is time, and  $m$  is an exponent less than one. The most commonly reported value for  $m$  is 0.5. In this study these two relationships are compared analytically.

**METHODS:** The thermal dose is expressed as  $t_{43} = \int 2^{T(t)-43} dt$  for  $T > 43^\circ\text{C}$ , where the integration is performed over the period in which the temperature is thermally significant. Using the generally accepted value for  $t_{43}$  of 240 minutes as a thermal dose threshold for necrosis, an expression containing intensity and time was derived from the thermal dose equation by substituting a well-known soft tissue solution for temperature vs. time (DR Bacon and A Shaw, Phys. Med. Biol. 38, 1647-59, 1993.) Then power law fits were found for  $I$  vs.  $t$  for various frequencies and beam diameters using published values for tissue acoustic and thermal properties.

**RESULTS:** Using soft tissue thermal conductivity and diffusivity values of  $6 \text{ mWcm}^{-1}\text{C}^{-1}$  and  $0.15 \text{ mm}^2\text{s}^{-1}$ , respectively, and a pressure attenuation coefficient of  $0.05 \text{ cm}^{-1}$ ,  $m$  was found to vary from approximately 0.4 to 0.8 for frequencies from 1-4 MHz, Gaussian beam diameters (at the  $e^{-1}$  level) of 0.5-3 mm, and times from 1 s to 20-30 s. For example, at a frequency of 1.5 MHz and a beam diameter of 1.5 mm,  $m$  is about 0.6. The value for  $m$  increased with increasing diameter but was relatively independent of frequency.

**CONCLUSION:** Thresholds of the form  $D = I t^m$  can be derived from the thermal dose equation over certain ranges of exposure duration, making either relationship potentially useful in predicting tissue damage thresholds.



**Energy based adaptive focusing: optimal ultrasonic focusing using radiation force MR guidance**

**Larrat B.**<sup>1</sup>, Pernot M.<sup>1</sup>, Montaldo G.<sup>1</sup>, Fink M.<sup>1</sup>, Tanter M.<sup>1</sup>

<sup>1</sup> Université Paris VII - CNRS UMR 7587, Paris, France

**OBJECTIVES:** The non invasive correction of phase aberrations is mandatory in the framework of human brain HIFU therapy at relatively high frequency (> 500 kHz). The aim of the study was to propose an adaptive focusing technique based on the use of acoustic radiation force MR imaging.

**MATERIAL & METHODS:** A 64-element linear phased array operating at 6MHz was used inside a 7T MRI scanner. In a first experiment, an aberrating law with strong phase shifts was added numerically to the transmitted US beam. In a second experiment a physical aberrator was placed between the array and the phantom. The technique consists in the emission of ultrasonic coded excitations and the indirect measurement of the resulting acoustic intensity at the focus. This intensity is estimated while recording tissue displacements induced by the radiation force of 400 $\mu$ s US bursts. The displacement field is mapped in a tissue mimicking gelatin based phantom via motion sensitized MR sequences. The set of time delays and amplitudes to be applied on each element of the US array for the optimal focusing is recovered by a direct inversion.

**RESULTS:** MR imaging allowed accurate estimation of the acoustical power at the focus of the array. After the complete 256 transmit experiment, the proposed method was able to recover the spatial distribution of phase aberrations up to 2 $\pi$  radians for both numerical and physical phase aberrating layers. A relatively low error was found on the non invasive phase aberration estimation (standard deviation of 0.3 radians). Moreover, the acoustical power at the focus was doubled after phase correction.

**CONCLUSION:** An adaptive focusing technique based on the single knowledge of the acoustic intensity at desired focus is here demonstrated to perform optimal focusing through strongly aberrating layers using MR motion sensitive sequences. This corresponds to a first experimental evidence of extremely efficient MR guidance for US aberration correction.



### The effect of electronically steering a phased-array transducer on proximal tissue heating

**Payne A.**<sup>1</sup>, Vyas U.<sup>1</sup>, de Bever J.<sup>1</sup>, Todd N.<sup>1</sup>, Christensen D.<sup>1</sup>, Parker D.<sup>1</sup>

<sup>1</sup> University of Illinois at Urbana-Champaign, Urbana, USA

Dosimetry is the determination of a dose, or similar type of physical quantity, that characterizes the physical agent as to its potential or actual interaction with the biological material of interest. The objective of ultrasonic dosimetry is to relate magnitudes of specific quantities, such as intensity, acoustic pressure, particle displacement, etc., or perhaps some quantity yet to be developed, to the likelihood of occurrence of a biological alteration. As the biological alteration goal becomes more defined, such as thermal ablation in the case of HIFU, the dosimetric goal can likewise become more defined. Here thermal ablation refers to the removal of tissue or the destruction of the tissue function using heat. Dosimetric concepts related to thermal ablation have been proposed some four decades ago with the ophthalmic "cataract-producing unit" and then three decades ago with the brain tissue "energy absorbed per unit volume". Later, the Arrhenius activation energy concept was introduced, leading to an isothermal dose concept. It is thus suggested that the formalism may exist to develop an appropriate HIFU dose unit. It is argued that contemporary delivered dose and temperature-time data are needed to validate a potential dose unit. This research is supported by NIH Grant R37EB002641.



### On the mathematical model of ultrasound propagation in liver

**Vilenskiy G.**<sup>1</sup>, Saffari N.<sup>1</sup>, Ter Haar G.<sup>2</sup>, Woodford S.<sup>2</sup>

<sup>1</sup> University College London, London, UK

<sup>2</sup> Institute of Cancer Research, Sutton, UK

Presently, there is no universally accepted system of partial differential equations for modelling of ultrasound propagation in biological tissues. A variety of approaches exists in the literature. All sets of equations proposed so far involve a certain amount of phenomenological considerations introduced due to the uncertainties about the tissue properties. The current work examines possible formulations of the problem of nonlinear ultrasound wave propagation in soft biological tissue from the standpoint of high intensity focused ultrasound applications for medical treatment. The human liver is taken as a prototype of the propagation medium. Visco-elastic Voigt model previously successfully used in the literature to analyze sound wave propagation in soft tissue is employed to obtain accurate assessment of the range of validity of the fluid dynamics approach and to justify its applicability in the limit of ultrasound frequencies. A number of phenomenological approaches towards the construction of non-equilibrium thermodynamics have been documented in the literature for fluid media. Owing to the differences in the physical assumptions, these theories do not necessarily give the same results in the context of ultrasound absorption in bio tissue. In the present work the existing phenomenological models of irreversible thermodynamics and the nonlinear fluid dynamics transport equations which follow are studied in terms of their suitability for the description of ultrasound propagation in the soft tissue. Special emphasis is placed on the analysis of the mechanisms of ultrasound absorption. Relative efficiencies of different energy dissipation mechanisms are assessed on the basis of the available experimental data for mechanical and thermodynamical properties of the liver tissue. The approaches to the construction of relaxation models of energy dissipation based on the related non-equilibrium thermodynamic theories are analyzed.



## The effect of visco-elasticity on the stability of inertial cavitation

**Sinden D.**<sup>1</sup>, Stride E.<sup>1</sup>, Saffari N.<sup>1</sup>

<sup>1</sup> University College London, London, UK

The accurate prediction in the variation of attenuation and wave-speed due to cavitation activity is of importance in the delivery of high intensity focussed ultrasound, and for potential cavitation enhanced heating. However, many threshold measures neglect the influence of the surrounding tissue. By modelling liver tissue as a visco-elastic material, we investigate the effects of visco-elasticity on the stability of inertial cavitation. Specific attention is paid to how stability thresholds change due to small-amplitude axisymmetric shape oscillations, either through a Rayleigh-Taylor or a parametric instability. If the shape oscillations become too extreme bubbles could break-up, leading to a growth of the bubble cloud and the increased likelihood of nucleation sites appearing, defocussing the beam and leading to unwanted thermal effects. An extended Rayleigh-Plesset equation incorporating the coupled effects of visco-elasticity and shape instability with physically realistic parameters was derived. The system was then investigated both analytically and numerically. Shape oscillations destroyed the spherical symmetry of the system, enhancing the complexity of the problem. Static, single- and multi-cycle stability thresholds were re-derived. It was found that fluid elasticity may actually retard bubble collapse and enhance bubble growth, increasing the likelihood of unpredictable inertial cavitation. Visco-elasticity may inhibit translational bubble motion, reducing energy interchange between modes and the overall magnitude of the shape oscillation, thus, reducing the likelihood of shape instability. In conclusion, the effect of visco-elasticity plays a significant role on the stability of inertial cavitation, through either radial and shape oscillations, which if unaccounted for may lead to errors in accurate prediction of HIFU treatment.



## Perfusion models for steep thermal gradients

**Woodford S.**<sup>1</sup>, Vilensky G.<sup>2</sup>, Ter Haar G.<sup>1</sup>, Saffari N.<sup>2</sup>

<sup>1</sup> Institute of Cancer Research, Sutton, UK

<sup>2</sup> University College London, London, UK

**OBJECTIVE:** We have investigated the validity of perfusion models at HIFU-relevant heating profiles, for the purpose of improving treatment planning.

**MATERIAL AND METHODS:** We have used both numerical and analytical solutions of the heat equation to undertake this theoretical study.

**RESULTS:** The accuracy and reliability of different perfusion models have been evaluated. We provide guidelines for the maximum diameter and flow-rate of blood vessels that can be incorporated into a continuum description instead of being modelled discretely.

**CONCLUSIONS:** Perfusion models known from hyperthermia studies have been brought into a HIFU context. Their range of applicability has been evaluated and their accuracy estimated.



### Fast ultrasound beam simulation in inhomogeneous tissue geometries for MRI-guided HIFU

**Vyas U.**<sup>1</sup>, Roemer R.<sup>1</sup>, Parker D.<sup>1</sup>, Christensen D.<sup>1</sup>

<sup>1</sup> University of Utah, Salt Lake City, USA

**OBJECTIVE:** Develop a fast and accurate numerical method for simulating the propagation of an ultrasound beam in inhomogeneous tissue regions for increased clinical efficacy, treatment reliability and patient safety in MRI-guided HIFU.

**METHODS:** Ultrasound beam propagation in complex tissue geometries is calculated in two steps: The beam is first propagated in a homogeneous medium (water or other coupling medium) from the phased-array transducer surface to the beginning of the inhomogeneous model using the element response function array (ERFA) technique. ERFA pre-calculates (once for a given transducer) and stores the response from each element of the phased-array transducer in a 3D array. At runtime, each element's response is multiplied by a phase function for the desired focus and summed to produce the overall input pressure pattern at the front plane of the inhomogeneous model. For calculation of the beam propagation in the inhomogeneous tissue region, the hybrid angular spectrum (HAS) method has been developed. The inhomogeneous tissue is segmented into voxels, each voxel having a unique speed of sound, absorption coefficient and density. The final 3D pressure pattern is calculated by alternating between the space domain and spatial-frequency domain for each layer of voxels in the inhomogeneous tissue model.

**RESULTS:** The beam propagation software was verified in homogeneous tissue models by comparing it with the Rayleigh-Sommerfeld integral technique. It results in an order of magnitude decrease in calculation times for a 201x201x201 model.

**CONCLUSIONS:** This beam simulation software can make accurate and fast predictions of the effects of inhomogeneities in tissue acoustic properties that cause absorption, refraction and diffraction of the ultrasound beam, which can result in reduced intensity and misalignment of the ultrasound focus.



### HIFU thermometry and acoustic calibration using a fibre-optic hydrophone

**Civale J.**<sup>1</sup>, Morris P.<sup>2</sup>, Rivens I.<sup>1</sup>, Ter Haar G.<sup>1</sup>, Beard P.<sup>2</sup>

<sup>1</sup>Institute of Cancer Research, Sutton, UK

<sup>2</sup> University College London, London, UK

HIFU clinicians and researchers need to perform regular quality assurance of their transducers to ensure their correct operation. We report on the potential use of a novel fibreoptic hydrophone system which may be used for acoustic field characterisation and simultaneous acoustic and temperature measurements when implanted in HIFU exposed tissue or phantom materials. The fibre-optic hydrophone (Precision Acoustics Ltd. UK) was originally developed in the UCL Medical Physics and Bioengineering department. It is based upon the interferometric detection of acoustically and thermally induced changes in the optical thickness of a thin (10µm) polymer film deposited at the tip of a single mode optical fibre. Both plane and tapered tipped sensors were tested, the latter designed to have a smoother frequency response. Acoustic characterisation of the output of a HIFU transducer (15cm focal length, 1.7MHz) was made with both fibre-optic and membrane hydrophones (0.4mm active sensor). Simultaneous temperature and acoustic measurements were performed with the fibreoptic hydrophone inserted into ex-vivo bovine liver tissue exposed to non-ablative 10s HIFU exposures. Free-field calibrations showed excellent fibreoptic hydrophone sensitivity (150-300mV/MPa), immunity to RF pickup and good correlation with the membrane hydrophone measurements. Temperature measurements made with the fibre-optic hydrophone in tissue showed good repeatability between similar exposures (within ±10%) and agreed with thermocouple measurements. In conclusion, the fibreoptic hydrophone system is a new device suitable for the quality assurance of HIFU transducers. The size of the sensor offers excellent spatial resolution combined with excellent acoustic sensitivity. A key advantage of the system over other devices is the ability to simultaneously measure temperature and acoustic pressure when the sensor tip is implanted in tissue or phantom materials.





## Cavitation and HIFU

Invited speaker: Crum L.<sup>1</sup>

<sup>1</sup> University of Washington, Seattle, USA

The very nature of high intensity focused ultrasound (high negative pressure amplitudes) suggests that cavitation may be induced during HIFU operation. Even though mammalian tissues tend to lack cavitation nuclei, the cavitation threshold is normally exceeded by most HIFU applications. In most cases, the inception of cavitation is unwanted, as the presence of bubbles at the focus can efficiently scatter the incident sound, thus distorting the desirable thermal lesion. In other cases, its presence is desirable in that the interaction of the cavitation bubbles with the incident sound can increase the rate of heat production. It is likely that in many applications of HIFU, cavitation is undetected and inconsequential. Cavitation can be detected by measuring the sound scattered from the incipient bubbles, but in most clinical machines, this option is not readily available. More often, one looks for artifacts in the imaging as an indication of the presence of cavitation. In ultrasound-guided HIFU, the presence of hyperechogenicity is often interpreted as evidence of cavitation, although recent research suggests that this hyperechogenicity is more likely due to boiling, which is more likely to not be inconsequential. In this presentation, a general overview of the role of cavitation (and boiling) in HIFU will be discussed with references to recent research on this topic. [Research supported in part by NIH GM077318, CA109557, DK43881, and NASA NCC9-58-50.]



## Characterization of HIFU-induced cavitation activity and heating in porcine subcutaneous fat

Kyriakou ZM.<sup>1</sup>, Ignasi Corral-Baques M.<sup>2</sup>, Amat A.<sup>2</sup>, Coussios C.<sup>1</sup>

<sup>1</sup> University of Oxford, Oxford, UK

<sup>2</sup> SOR Internacional SA, Barcelona, Spain

**OBJECTIVES:** The objective of this research is to investigate, optimize and establish a practical, effective and safe ultrasound-based technique for the non-invasive destruction of subcutaneous fat tissue. Factors that motivated this research include the fact that (i) the mechanisms for ultrasound-based optimal fat destruction remain poorly understood, (ii) there are no published studies of cavitation thresholds and ultrasound-induced heating in fat tissue and (iii) there is currently no non-invasive method for monitoring successful treatment delivery.

**MATERIALS AND METHODS:** HIFU exposures were performed in excised porcine fat at four different frequencies (0.483, 1.150, 1.641 and 3.355 MHz) over a range of pressure amplitudes and exposure durations. A coaxially aligned 15-MHz Passive Cavitation Detector (PCD) was used to capture acoustic emissions emanating from tissue during HIFU exposure, while the focal temperature rise was measured using minimally invasive needle thermocouples. The transmission loss arising from reflection at the skin interface and attenuation through fat tissue was quantified at all four frequencies using an embedded needle hydrophone (Onda HNA). Haematoxylin & Eosin staining was used to assess the resulting histological damage.

**RESULTS:** Cavitation activity was readily instigated at 0.483MHz for peak rarefactional pressures in excess of 1.5 MPa and was found to greatly enhance focal heat deposition. Cavitation was difficult to instigate at higher frequencies. Very repeatable temperature rises of 15°C could be readily induced at 1.641 MHz with peak rarefactional pressures as low as 1.1. MPa.

**CONCLUSIONS:** Optimal frequency ranges to generate reliable cavitation activity and heating in subcutaneous fat using realistic pressure amplitudes and exposure durations have been identified. At 0.483 MHz, the use of passive cavitation detection during HIFU exposure shows great promise as a technique for non-invasive monitoring of successful treatment delivery.



### **S6A-3** On cellular response to low intensity ultrasound

**Mizrahi N.**<sup>1</sup>, Kimmel E.<sup>1</sup>, Fredberg J.<sup>2</sup>, Weihs D.<sup>1</sup>

<sup>1</sup> Technion, Haifa, Israel

<sup>2</sup> Harvard School of Public Health, Boston, USA

The mechanism through which low intensity ultrasound (LIUS) affects cells is still unknown. Several mechanisms were suggested, but they do not tell the whole story; for instance radiation pressures are much too small when LIUS acts in physiological conditions. Another mechanism, linear in nature, was suggested recently by us for vibrations of particles of different density than the surrounding medium (Or and Kimmel, 2009). In this study, we subject adherent cells to LIUS irradiation with 1.0 MHz frequency while allowing real time microscopy. This provides the mechanical properties of cells at nanometer scale; and of remodeling dynamics in real time. Two microrheology approaches were used. Spontaneous bead motion of fluorescent 200nm cell-internalize probes or externally anchored to the cytoskeleton 4µm beads were used to evaluate mean square displacement (MSD). The MSD measurements can be attributed to time-dependent response of the cytoskeleton dynamics. The MSD profiles for different time intervals were measured by tracking the centroid position of each bead during spontaneous bead motion. Both methods demonstrate the immediate softening of cells induced by LIUS irradiation. Additionally, the fluctuating motion of cytoskeleton-attached microbeads, during the relaxation phase, follows LIUS irradiation show dynamic reorganization of the cytoskeleton, and recovery to the initial baseline position. Moreover, the effect of cell softening is directly proportional to the level of the applied ultrasonic energy. Our findings suggest a possible regulatory mechanism coupling between mechanical stimulation and biochemical response initiated by LIUS. It seems that when LIUS is applied to mechanosensitive cellular structures, alterations in the molecular level such as conformation changes of proteins might follow. Note that in all those examples heating, or cavitation effects were not present or had minor influence.



### **S6A-4** Analysis of the microbubble dynamics under the ultrasound exposure

**Nakamura Y.**<sup>1</sup>

<sup>1</sup> School of Engineering, Tokyo, Japan

Microbubble contrast agents are used in the configuration which is not invasive for the human body in the diagnosis, but ultrasound parameters used are not physically analyzed. That means we do not have the enough data about the parameters to explain something unexpected in the diagnostics. The purpose of this study is to have enough knowledge about the parameters concerning with the ultrasound diagnosis using the microbubble contrast agents and analyze the microbubble dynamics under the ultrasound exposure. To have the data concerned with the parameters, we constructed the experimental setup consisted of the transducer, the medical ultrasound equipment, the hydrophone and the super high-speed camera. By changing the transducer, we had the knowledge according to the ultrasound frequency. We used the super high-speed camera to capture the cavitation. The camera we used is IMACON200, which can take photos with maximum frame rate 200Mfps. The order of the ultrasound frequency we used is several MHz, so IMACON200 has enough performance to capture the cavitation. Using this setup, we fixed the microbubble at the focal point of the ultrasound and measured acoustic pressures and took diagnostic images and sequential photographs. We can have those results in synchronization. We used Sonazoid® as a microbubble. The range of the ultrasound frequency is from 500 KHz to 5 MHz. Under this condition, we measured the acoustic pressure and the wave profile exposed to the microbubble and the echo from the microbubble. We also took the diagnostic image of the microbubble and had the sequential photographs of the cavitation and also the propagation of the shock wave.



S6A-5

**A real-time controller for sustaining thermally relevant cavitation during HIFU exposure**

**Hockham N.**<sup>1</sup>, Arora M.<sup>1</sup>, Coussios C.<sup>1</sup>

<sup>1</sup> University of Oxford, Oxford, UK

Cavitation activity during HIFU exposure has been previously shown to enhance focal heating whilst providing unique opportunities for real-time treatment monitoring. However, the unstable and stochastic nature of cavitation makes it difficult to confine and sustain focal cavitation activity. Previous open-loop control systems have employed low duty cycles that result in significant heat loss due to conduction, thus preventing the achievement of ablative temperature rises. The present work presents the design, validation and testing of a real-time closed-loop controller for sustaining thermally-relevant cavitation within the HIFU focal region at duty cycles in excess of 95%. Agar-based tissue-mimicking materials were manufactured and exposed to 1.067 MHz HIFU (Sonic Concepts H102) using a broad range of amplitudes and duty cycles. Cavitation activity was quantified for using a co-axial passive cavitation detector (PCD) and resulting temperature rises were measured using embedded fine-needle thermocouples. Spectral analysis of the PCD data was used to identify cavitation-enhanced heating regimes and optimal parameter ranges for sustaining cavitation. The location of the cavitation activity was quantified throughout the exposures using time-of-flight information from the PCD data. A closed-loop feedback controller implemented in Labview to modulate the HIFU amplitude in real-time in response to the received cavitation signal at a fixed duty cycle (97.5%). In the absence of any cavitation control, cavitation activity decays significantly after a few seconds of exposure and heating rates drop sharply. By contrast, the cavitation controller succeeded in maintaining temperature rises in excess of 30C in the focal region for more than 25 seconds, using significantly less HIFU energy. The technique shows great promise as a means of achieving cavitation-enhanced, cavitation-controlled, cavitation-monitored thermal ablation at lower intensities than in current clinical use.

---



S6A-6

**Characterization of perfluorocarbon droplets for focused ultrasound therapy**

**Schad K.**<sup>1</sup>, Hynynen K.<sup>1</sup>

<sup>1</sup> Sunnybrook Health Sciences Centre, Toronto, Canada

**OBJECTIVE:** Focused ultrasound therapy can be enhanced with microbubbles and the spatial control of gas bubbles can be achieved with acoustic vaporization of perfluorocarbon droplets. This study was undertaken to determine the acoustic parameters for droplet vaporization and how it depends on the acoustic conditions and droplet physical parameters.

**MATERIALS & METHODS:** Lipid encapsulated droplets containing dodecafluoropentane were manufactured with sizes ranging from 1.9 to 7.2  $\mu\text{m}$  and diluted to concentrations of 8 x 106 droplets/mL. The droplets were sonicated with a single focused transducer under flow conditions through an acoustically transparent vessel. The sonications were 10 ms in duration at frequencies of 0.6, 1.7 and 2.8 MHz with varying pressure. The vaporization threshold was measured with an active transducer operating in pulse echo mode and simultaneously the inertial cavitation (IC) threshold was measured with passive acoustic detection.

**RESULTS:** The mean IC threshold of the droplets was 2.9 $\pm$ 0.2 MPa, 4.4 $\pm$ 0.2 MPa, 5.3 $\pm$ 0.2 MPa, for sonications at 0.6, 1.7 and 2.8 MHz, respectively. The vaporization threshold increased with decreasing frequency and no droplet vaporization was detected at 0.6 MHz. The IC threshold did not depend on droplet size, however the vaporization threshold decreased with increasing droplet size. Pressure-time vaporization curves were obtained for several droplet batches. The results showed a decrease in pressure threshold for increased sonication duration.

**CONCLUSIONS:** We have demonstrated that droplet vaporization is feasible for clinically-relevant sized droplets and acoustic exposures. The vaporization threshold depends on the length and frequency of the sonication and also on the droplet diameter. The study shows that droplets cannot be vaporized at low frequencies without IC occurring. Further investigations are required to determine the optimal physical and acoustic parameters to achieve droplet vaporizations in vivo.



## Temperature distribution heating experiment using HIFU and microbubble

**Utashiro H.**<sup>1</sup>, Kajiyama K.<sup>1</sup>, Yoshinaka K.<sup>1</sup>, Takagi S.<sup>1</sup>, Matsumoto Y.<sup>1</sup>

<sup>1</sup>University of Tokyo, Tokyo, Japan

HIFU treatment with microbubbles enhancing heating effect has been investigated for less-invasive and rapid tumor therapy. It is important to examine the bubble's effect to ultrasound exposure. So we need to check the heat distribution. In our experiment, heat distribution is visualized by temperature-sensitive crystalline liquid sheet. When exposing ultrasound in the tissue filled with gas, the gas shuts out the ultrasound, and the focus point's temperature doesn't rise. This is because the heat up region broadened toward the radial direction of the transducer as the void fraction increased. So, we thought the elimination method of bubbles in front of the focus position by exposing intensive ultrasound in very short time. By this method, we could heat up around the target position effectively. In this research, we also use 6ch multiphase piezoelectric transducer, and confirm moving the focus point. Our future work is to combine the two methods, and try to master how to treat tumor therapy.



## Modelling oscillations of a microbubble in an elastic vessel

**Martynov S.**<sup>1</sup>, Kostson E.<sup>1</sup>, Saffari N.<sup>1</sup>, Stride E.<sup>1</sup>

<sup>1</sup>University College London, London, UK

**OBJECTIVE:** Encapsulated microbubbles have been extensively investigated as contrast agents for diagnostic ultrasound imaging and more recently for therapeutic applications such as drug delivery. Currently, however, theoretical models for microbubble dynamics only exist for either encapsulated bubbles in an infinite volume of liquid, or for unencapsulated bubbles in a confined volume. The aim of the present study is to quantify the effects of both encapsulation and confinement in a blood vessel upon a microbubble's response to ultrasound excitation.

**MATERIALS & METHODS:** A model for the dynamics of a bubble in a narrow blood vessel has been developed for uncoated and also coated bubbles located on the axis of an elastic vessel filled with a viscous Newtonian liquid. The effect of encapsulation has been examined for both polymeric and surfactant coatings and elastic deformations of the vessel wall were described using a lumped-parameter model, considering the wall as a thin membrane. The governing equations were solved in the time domain using the finite element method.

**RESULTS:** The results show that even at low acoustic pressures, microbubble oscillations can be significantly modified as a result of both encapsulation and confinement. The unforced oscillations of a confined bubble are characterised by two frequencies and that the natural frequency of a bubble confined in an elastic vessel can be higher than that for unconfined bubble. Similarly, the deformation modes of the vessel wall, including wave motion and local vibrations are sensitive to both the material properties and excitation frequency and this will be discussed in the context of assessing the potential for tissue damage and therapeutic applications.

**CONCLUSIONS:** These findings have important implications for the accurate interpretation of contrast enhanced ultrasound backscattered signals, contrast agent safety and therapeutic applications of microbubbles.







S6B-1

**In vivo and ex vivo assessment of pulsed HIFU-enhanced penetration of small molecules**

**Hwang JH.**<sup>1</sup>, Wang Y.<sup>1</sup>, Zhou Y.<sup>1</sup>, Jung J.<sup>1</sup>

<sup>1</sup> University of Washington, Seattle, USA

**BACKGROUND/AIM:** Pulsed HIFU (pHIFU) has been demonstrated to increase concentration of drugs and small molecules in a targeted fashion in vivo; however, the mechanisms and parameter space are still poorly understood. Potential mechanisms that have been suggested include increased vascular permeability due to intravascular cavitation or thermal effects, and enhanced penetration due to mechanical effects. The aim of this study is to investigate the role of pHIFU specifically in enhancing penetration of small molecules into ex vivo and in vivo liver tissue.

**METHODS:** All experiments were performed with a HIFU transducer operated at 1.1 MHz. Pulsing parameters (duty factor and PRF) and acoustic intensity were varied in all studies. Three sets of experiments were performed: 1) ex vivo study where a solution of fluorescein isothiocyanate-dextran (FITC-dextran, molecular weights of 20 and 500 kDa), placed on the surface of liver tissue, was exposed to pHIFU to qualitatively evaluate depth of penetration of FITC-dextran using fluorescence microscopy; 2) ex vivo study where a solution of Evans blue dye (EB) was placed on the surface of liver tissue and exposed to pHIFU for a quantitative assessment of penetration; and 3) an in vivo study in swine where a solution of EB was administered intravenously followed by exposure of the liver to pHIFU for a quantitative assessment of delivery into tissue.

**RESULTS:** A qualitative increase in FITC-dextran penetration and a quantitative increase in EB concentration was observed in ex vivo samples exposed to pHIFU compared to controls. In vivo test results demonstrate that pHIFU (ISAPA=2500 W/cm<sup>2</sup>, P=-7 MPa, PRF=2 Hz, DF=4%) significantly increased the mean [SD] EB concentration compared to control (0.37 [0.013] vs. 0.24 [0.006] µg EB/mg tissue, p=0.001). Overall, enhanced penetration appears to be a function of ISAPA and exposure duration as long as thermal damage and/or mechanical tissue erosion is avoided.

---



S6B-2

**Closed-loop controlled noninvasive ultrasonic glucose sensing and insulin delivery**

**Smith N.**<sup>1</sup>, Park E.<sup>1</sup>, Werner J.<sup>1</sup>, Jaiswal D.<sup>1</sup>

<sup>1</sup> The Pennsylvania State University, University Park, USA

To prevent complications in diabetes, the proper management of blood glucose levels is essential. Previously, ultrasonic transdermal methods using a light-weight cymbal transducer array has been studied for noninvasive methods of insulin delivery for Type-1 diabetes and glucose level monitoring. In this study, the ultrasound systems of insulin delivery and glucose sensing have been combined by a feedback controller. This study was designed to show the feasibility of the feedback controlled ultrasound system for the noninvasive glucose control. For perspective human application, in vivo experiments were performed on large animals that have a similar size to humans. Four in vivo experiments were performed using about 200 lbs pigs. The cymbal array of 3x3 pattern has been used for insulin delivery at 30 kHz with the special-peak temporal-peak intensity (Isptp) of 100 mW/cm<sup>2</sup>. For glucose sensing, a 2x2 array was operated at 20 kHz with Isptp = 100 mW/cm<sup>2</sup>. Based on the glucose level determined by biosensors after the ultrasound exposure, the ultrasound system for the insulin delivery was automatically operated. The glucose level of 115 mg/dl was set as a reference value for operating the insulin delivery system. For comparison, the glucose levels of blood samples collected from the ear vein were measured by a commercial glucose meter. Using the ultrasound system operated by the close-loop, feed-back controller, the glucose levels of four pigs were determined every 20 minutes and continuously controlled for 120 minutes. In comparison to the commercial glucose meter, the glucose levels determined by the biosensor were slightly higher. The results of in vivo experiments indicate the feasibility of the feedback controlled ultrasound system using the cymbal array for noninvasive glucose sensing and insulin delivery. Further studies on the extension of the glucose control will be continued for the effective method of glucose control.



### Ultrasonic drug delivery in phase-shift nanoemulsions

**Rapoport N.**<sup>1</sup>, Nam K.<sup>1</sup>, Christensen D.<sup>1</sup>, Efras A.<sup>1</sup>

<sup>1</sup> University of Utah, Salt Lake City, USA

Therapeutic implications of droplet-to-bubble transition in drug loaded perfluoropentane nanoemulsions, bubble coalescence, catalysis of ultrasound-induced droplet-to-bubble transition by pre-existing bubbles, and bubble formation in systemically injected nanoemulsions are discussed. Clinically relevant physical factors that trigger droplet-to-bubble transition in liquid nanoemulsions and gels have been evaluated, namely heat, ultrasound, and injections through fine-gauge needles. Among those listed, ultrasound irradiation was found to be the most efficient factor. The dependence of droplet-to-bubble transition on droplet size is discussed. Ovarian and breast cancerous tumors were treated by systemic injections of paclitaxel-loaded nanoemulsions that converted into microbubbles locally in tumor tissue under the action of tumor-directed therapeutic ultrasound. Tumor accumulation of nanoemulsions was confirmed by ultrasound imaging. Significant tumor regression was observed signifying efficient ultrasound-triggered drug release from tumor-accumulated nanodroplets. No therapeutic effect of nanodroplets and ultrasound was observed without drug indicating that therapeutic effect was caused by ultrasound-enhanced chemotherapeutic action of tumor-targeted drug rather than mechanical or thermal action of ultrasound itself. Mechanism of drug release in the process of droplet-to-bubble conversion is discussed. In gel matrices, ultrasound-induced droplet-to-bubble transition was catalyzed by large pre-existing microbubbles irradiated by low frequency (hundred kilohertz) ultrasound, which allowed suggesting a novel tumor treatment protocol based on ultrasound-mediated chemotherapy.



### Enhancement of doxorubicin effect on cancer cell mortality with ultrasound and microbubbles

**Piron J.**<sup>1</sup>, Kaddur K.<sup>1</sup>, Bouakaz A.<sup>1</sup>

<sup>1</sup>INSERM U930-CNRS ERL 3106, Tours, France

Potential use of clinical ultrasound (US) in enhancing the anti-cancer drugs effects in the treatment of cancers has been recently reported. Moreover US in combination with microbubbles have proven its efficiency in improving molecule uptake into cells through sonoporation mechanism. In this study, we evaluate the benefit of sonoporation in enhancing cell mortality using anti-cancer drug doxorubicin and U87MG cells (human glioma cells). Experiments were conducted in five groups: non treated, doxorubicin treated, US-microbubble treated, doxorubicin + US, and doxorubicin + US-microbubble. Cells were exposed to 5 $\mu$ M doxorubicin and sonicated at 1 MHz (with 40% duty cycle for 30s and acoustic pressures from 0.4 to 0.8 MPa). Six and 24h after treatment, cell mortality was evaluated by Trypan blue dye exclusion test. Three experimental microbubble types were investigated: BR14, BG6437 and polylactide shelled microbubbles. The results showed that for all microbubble types, a significant enhancement in doxorubicin effect was achieved when it was co-administrated with microbubbles in comparison to the drug alone. The highest effect was obtained at 800 kPa BG6437 microbubbles which doubled the cell mortality. Cell mortality in doxorubicin + US group was comparable to doxorubicin alone (25.3  $\pm$  5.6 % versus 22.2  $\pm$  4.9 % at 6h and 20.5  $\pm$  4.1 % versus 29.8  $\pm$  4.7 % at 24h). When BG6437 were co-administrated with doxorubicin, cell mortality percentage reached 45.8  $\pm$  4.6 % and 51.0  $\pm$  4.5 % at 6h and 24h respectively. Using polylactide shelled microbubbles and BR14 microbubbles, cell mortality at 24h reached respectively 42.8  $\pm$  2.4 % and 57.6  $\pm$  8.8 %. Our results demonstrate that low intensity US and microbubbles could enhance anti-cancer drug effect, suggesting that this combination might be a useful tool for the cancers therapy. In vivo validation is underway.



S6B-5

**Qualitative and quantitative evaluation of nanoparticles delivery into tumor tissue enhanced by focused ultrasound with microbubbles**

**Lin C.Y.**<sup>1</sup>, Chen C.<sup>1</sup>, Liu T.<sup>1</sup>, Chang F.<sup>1</sup>, Lin W.<sup>1</sup>

<sup>1</sup> National Taiwan University, Taipei, Taiwan

**OBJECTIVES:** In this study, we used lipid-coated cadmium-selenide (CdSe) nanoparticles to study drug delivery in the tumor region, and its enhancement caused by focused ultrasound in the presence of microbubbles.

**MATERIALS AND METHODS:** Lipid nanoparticles with CdSe inside were synthesized and conjugated through lipid mixtures, cationic lipid GEC-Chol, cholesterol and DOPE-PEG2000, and resulted four different sizes from 30 nm to 180 nm. 1.0 MHz pulsed-wave focused ultrasound was sonicated on tumor regions at 1.2 MPa pressure, 1% duty cycle, 10 ms burst length, 1 Hz repetition frequency, and 2 min duration. Microbubbles (30 ug/Kg, SonoVue) were injected into each mouse intravenously, then focused ultrasound was sonicated immediately on the tumor region, and finally 50 ul nanoparticles were injected. The mice were sacrificed about 24 h after the injection of nanoparticles, and atomic absorption spectroscopy (AAS), photoluminescence (PL), and three-harmonic generation (THG) were used to determine the presence of nanoparticles in the tumor tissues, and immunoblotting was used to understand the mechanism for vascular permeability.

**RESULTS:** The quantitative result from AAS has shown that the amount of Cd delivery into the tumor region is inversely proportional to nanoparticle size. Smaller sizes of nanoparticles were enabled to extravasate to tumors more effectively (4.47, 2.27, 0.99, 0.82 ug/g tissue of Cd for 30, 80, 130, and 180 nm nanoparticles, respectively). The imaging of PL was displayed a strong signal intensity after sonication. The THG imaging indicated that the enhancement of nanoparticle extravasation into tumor tissue was caused by microbubble cavitation, and the disruption of vasculature by immunoblotting.

**CONCLUSION:** Ultrasound with microbubbles is able to disrupt the blood vessels to enhance the permeability of nanoparticles through the vessels into the tumor tissue. It is a very promising modality to effectively deliver nanodrug to tumors.



S6B-6

**Modelling oscillations of a microbubble in an elastic vessel**

**Lafon C.**<sup>1</sup>, Somaglino L.<sup>1</sup>, Bouchoux G.<sup>1</sup>, Chesnais S.<sup>1</sup>, Mestas J.<sup>1</sup>, Fossheim S.<sup>2</sup>

<sup>1</sup> INSERM, Lyon, France

<sup>2</sup> Epitarget AS, Oslo, Norway

The ability of ultrasound (US) to permeabilize liposomes has opened the potential of using US to enhance delivery of chemotherapeutic drugs to tumor cells. A 1MHz spherical transducer, 50mm diameter and focal depth, was used. A hydrophone recorded the broadband noise emitted by collapsing bubbles to define a cavitation index. Exposure conditions were set in vitro to 200Hz PRF, 100W peak power and 25% DC. The dose of cavitation varied with exposure time. The %doxorubicin release from liposomes correlated well with the dose of cavitation, demonstrating that inertial cavitation contributed to drug release. A dose corresponding to 25% release in vitro was selected for the therapy studies. In vivo experiments were performed on rats implanted with AT2 Dunning tumors. In the pharmacokinetic study, 36 rats received an intravenous injection of liposomal doxorubicin (3 and 6mg/kg) 10 days after tumor implantation (D10). The rats were sacrificed sequentially post injection, tumors excised and digested for doxorubicin quantification. A maximum tumor uptake of doxorubicin was evidenced between D11 and D12. The efficacy of a combined treatment of liposomal doxorubicin and US on tumor growth was investigated. 63 rats were dispatched into 7 groups: US, free doxorubicin 3 and 6mg/kg, liposomal doxorubicin 3 and 6mg/kg and liposomal doxorubicin 3 and 6mg/kg +US. Injections and US were done at D10 and D12 respectively. Tumors were monitored until D38. Liposomal doxorubicin showed to be more efficient than free doxorubicin in retarding tumor growth. Doses of 6mg/kg masked the effect of US. However, at D24 and 31, the rats receiving both 3mg/kg liposomal doxorubicin and US showed a lower tumor growth than rats receiving 3mg/kg liposomes. This work is promising given the fact that the liposomes used were weakly sonosensitive and are considered prototype. Work funded by the Norwegian Research Council. Liposomes provided by Epitarget AS, Norway.



## Inertial cavitation enhances the extravasation and therapy of an oncolytic adenovirus for breast cancer treatment

**Bazan-Peregrino M.**<sup>1</sup>, Arvanitis C.<sup>1</sup>, Rifai B.<sup>1</sup>, Seymour L.<sup>1</sup>, Coussios C.<sup>1</sup>

<sup>1</sup>University of Oxford, Oxford, UK

Irregular tumour vasculature acts as a barrier to extravasation of anti-cancer agents, making it difficult to deliver drugs away from blood vessels.

**OBJECTIVE:** We employed a potent oncolytic adenovirus, AdEHE2F, which kills breast cancer cells selectively. We evaluated whether ultrasound-induced stable or inertial cavitation can overcome the barrier of extravasating AdEHE2F to regions that are remote from vessels and whether this adenoviral transgene expression is due to enhanced extravasation or sonoporation.

**MATERIAL & METHODS:** We developed a novel in vitro tumour model made of cancer cells (BT474-GFP) within a porous gel (agarose) traversed by a 1.6mm channel with flowing AdEHE2F. A 0.5MHz HIFU transducer (SonicConcepts-H107SN96) was used to instigate acoustic cavitation in the presence or absence of microbubbles (Sonovue, Bracco). While delivering the same amount of energy, maximum ultraharmonic emissions (stable cavitation) were seen at Peak Rarefactional Focal Pressures (PRFP) of 360kPa, a Duty Cycle (DC) of 90%, and a Pulse Repetition Frequency (PRF) of 10Hz; maximum broadband emissions (inertial cavitation) were seen at PRFP 2400kPa, DC 2%, PRF 10Hz.

**RESULTS:** None of the ultrasound settings used affected cell viability in the absence of adenovirus. Virus transgene expression increased by a factor of 2 in the presence of stable cavitation, and by up to 100 times with inertial cavitation, but did not occur in the absence of Coxsackie and Adenovirus Receptor cell expression. AdEHE2F distribution after inertial cavitation spanned several millimetres from the vessel, particularly in the direction of the HIFU beam. AdEHE2F killed up to 80% of all cancer cells at the cavitation site.

**CONCLUSIONS:** Inertial cavitation promotes AdEHE2F delivery, distribution and therapeutic activity in the in vitro tumour model not through sonoporation, but through increased mass transfer that makes it possible to deliver active AdEHE2F to large distances from the vessel.

---







S7A-1

HIFU and regulatory challenges in the U.S.A

Invited speaker: Harris G.<sup>1</sup>

<sup>1</sup> Food and Drug Administration, Silver Spring, USA

The U.S. Food and Drug Administration (FDA) has the responsibility for assuring the safety, effectiveness, and truthful labeling of medical devices intended for human use in the United States. Before a medical device can be marketed legally, the sponsor desiring to distribute the device must secure permission from the FDA. The formal process is defined in the Medical Device Amendments to the U.S. Food, Drug, and Cosmetic Act, enacted on May 28, 1976. Several regulatory paths are defined, depending on the complexity of the device, device safety, and indications for use. In the case of new or emerging technologies such as high intensity focused ultrasound (HIFU), the regulatory process typically includes the evaluation of both pre-clinical and clinical device testing. No guidance or standards documents have been developed for HIFU to date for use in the regulatory review process, but the development of voluntary standards is underway within the International Electrotechnical Commission. Pre-clinical testing generally includes ultrasound power and intensity measurements, in vitro and in vivo temperature measurements, thermal computational modeling, and, where applicable, a demonstration of the accuracy for targeting the region of interest and monitoring treatment progress. The design and conduct of clinical trials are developed by the device sponsor in coordination with FDA medical and scientific staff. In this presentation some general highlights of the regulatory review process for HIFU devices in the U.S. will be described, including examples of the regulatory paths to market that have been taken. Also, pre-clinical testing procedures and basic clinical study concepts will be discussed. Lastly, current activities in standards development relevant for regulatory reviews of HIFU devices will be addressed.

---



S7A-2

Realtime acousto-optical QA methods for high intensity fields

Butterworth I.<sup>1</sup>, Shaw A.<sup>1</sup>

<sup>1</sup> National Physical Laboratory, Teddington, UK

**OBJECTIVES:** When used clinically, HIFU transducers and systems may be driven very close to their operating limits and it might be expected that their performance will change with time either over the relatively short time of an individual treatment or gradually over weeks and months. Similarly bioeffects studies require confidence that the exposure levels are consistent. There is therefore a need for Quality Assurance methods which can reveal changes to the beam characteristics: these methods should ideally be usable during an exposure so that short term changes can be seen. Schlieren imaging is able to reveal many useful characteristics of ultrasound fields, but it is expensive to implement for large aperture fields and is not a convenient technique for general use.

**MATERIAL & METHOD:** Two related techniques have been developed which, like Schlieren imaging, are based on optical diffraction caused by the acousto-optic interaction and provide a line-of-sight transmission representation of the ultrasound field. They allow for either the whole field to be visualised or any small region to be examined in more detail. Unlike Schlieren, they are easy and cheap to implement and can be readily used in a research, commercial, or clinical environment.

**RESULT:** Early testing spanning the range from below 10W/cm<sup>2</sup> to more than 1400W/cm<sup>2</sup> has shown that the focal location, and changes in output level can be easily identified by eye or with simple digital image analysis techniques. Distortions, for instance caused by air bubbles or reflecting objects in the beam, can also be clearly seen.

**CONCLUSION:** We have developed the principles of two optical methods which give useful qualitative information about HIFU fields. We believe that these methods can be further enhanced to provide more information and to monitor the stability of output of HIFU systems.



### Effects of thermal dose-dependent absorption on temperature rise and lesion volume in HITU applications

**Soneson J.**<sup>1</sup>

<sup>1</sup> Food and Drug Administration, Silver Spring, USA

**OBJECTIVE:** In order to accurately determine high intensity therapeutic ultrasound (HITU) treatment protocols, it is important to understand the effect that changing tissue characteristics have on heat generation and thermal dose accumulation. One tissue characteristic which changes dramatically during treatment is absorption. In this study the effects of dynamic absorption are examined in silico.

**METHODS:** A parabolic approximation of the acoustic wave (Kuznetsov's) equation is coupled to the bioheat transfer (Pennes') equation through the absorption parameter, which is allowed to vary according to spatial position and accumulated thermal dose. The HITU system modeled is a 5 cm diameter, 8 cm focal length single-element transducer radiating a continuous wave of 50 W acoustic power at 1.5 MHz into dog muscle, whose absorption has been reported to approximately double when cooked. Under these conditions, cavitation and higher harmonic generation are negligible and the influence of dynamic absorption may be observed.

**RESULTS:** Peak temperature rise, lesion volume, and the volume of tissue which reaches boiling temperature (boiled volume) are compared with models including and neglecting dynamic absorption for sonication times ranging from 1 to 30 seconds. This study shows that neglecting changes in tissue absorption can result in underpredicted peak temperature rise by as much as 40%, lesion volume by approximately 30%, and indicated boiled volume is only half its true size. Furthermore, the simulations indicate that changes in absorption in the prefocal region do not significantly reduce focal intensity.

**CONCLUSION:** Incorporating strong effects such as dynamic absorption in propagation and heating models results in more accurate prediction of the bioeffects of treatment protocols using non-cavitation inducing ultrasound beams.



### Spatially and temporally-controlled mild hyperthermia using a linear array

**Lai CY.**<sup>1</sup>, Kruse D.<sup>1</sup>, Stephens D.<sup>1</sup>, Sutcliffe P.<sup>1</sup>, Ferrara K.<sup>1</sup>

<sup>1</sup> University of California, Davis, USA

**OBJECTIVES/METHODS:** Previous studies have shown that image-guided single-beam heating can maintain mild hyperthermia in a small region of interest (ROI). The object of this study was to develop methods for creating and maintaining ultrasound-induced mild hyperthermia in an extended ROI using a linear array in vitro and in vivo. This system consists of a SIEMENS Antares ultrasound scanner, a custom-designed co-linear array transducer, and a real-time temperature feedback controller. The co-linear array transducer provides the dual functions of imaging and heating at 5.5MHz and 1.54MHz, respectively. A color-mode ROI was used to guide heating, with periodic B-mode image updates during the therapy. A needle-type thermocouple was inserted into a phantom/tumor, with the measured temperature fed to a proportional-integral-derivative (PID) controller embedded in a LabVIEW program with an Internet-based diagnostic user interface (DUI). Duty cycle and pressure can be scaled; however, the primary PID control parameter is the duty cycle via the pulse repetition frequency (PRF). A 74% (w/w) syrup-based polyacrylamide phantom was used for in vitro experiments and five thermocouples were placed in the phantom for temperature distribution examination. Single-beam and scanned-beam heating were compared in the same phantom. For in vivo heating, a 10-mm Met-1 tumor was tested, and the heating response was compared for the two heating modes.

**RESULTS/CONCLUSIONS:** In the in vitro tests with a 2W total acoustic power, single-beam and scanned-beam heating achieved a 5°C temperature increase in 45 and 165 seconds, respectively. With scanned-beam heating, the spatial variation in temperature within the ROI was less than 6%. In in vivo tests, orthotopic breast tumors reached 42±0.2°C within 2-6 minutes with scanned-beam heating. In this presentation, we will explore weighting scanned-beam profiles in order to achieve more uniform heating. Acknowledgement: NIH CA 103828



S7A-5

**Contrast agent ultrasonography before and after HIFU treatment of parathyroid glands**

**Lacoste F.**<sup>1</sup>, Arnaud F.<sup>1</sup>, Kovacheva R.<sup>2</sup>

<sup>1</sup> Paris Santé Cochin, Paris, France

<sup>2</sup> University Hospital of Endocrinology, Sofia, Bulgaria

**OBJECTIVES:** To observe changes in the parathyroid tissue treated by extracorporeal HIFU

**MATERIAL AND METHODS:** 10 patients were treated for primary and secondary hyperparathyroidism by thermally ablating enlarged parathyroid glands using an external HIFU applicator. The treated glands were visualised with contrast injected ultrasonography (CAUS) and Doppler US before and 7 to 28 days post HIFU. Serum iPTH, calcium, and phosphorus levels were monitored before and after the treatment.

**RESULTS:** The initial results showed a correlation between contrast agent uptake of treated parathyroid tissue and the decrease of iPTH levels, particularly in the patients treated for primary hyperparathyroidism where elevated iPTH is due to only one gland.

**CONCLUSIONS:** These results indicate the possibility of using CAUS to monitor the thermal ablation of parathyroid gland.

---



S7A-6

**Tumor-specific immune response induced by HIFU therapy: a study in a mouse model**

**Khokhlova T.**<sup>1</sup>, Bailey M.<sup>1</sup>, Canney M.<sup>1</sup>, Hwang JH.<sup>1</sup>, Yee C.<sup>2</sup>, Crum L.<sup>1</sup>

<sup>1</sup> Applied Physics Laboratory, University of Washington, Seattle, USA

<sup>2</sup> Fred Hutchinson Cancer Research Center, Seattle, USA

**OBJECTIVES:** High intensity focused ultrasound (HIFU) therapy has been applied extensively and successfully to ablation of cancerous tumors. In addition, several clinical case reports describe the regression of metastases throughout the body following HIFU treatment of the primary tumor. Animal studies have provided evidence that HIFU does induce non-specific immune response. The goal of this work was to develop a relevant animal model and ultrasound exposure protocol to determine if HIFU can induce a tumor-specific immune response.

**MATERIALS & METHODS:** B16 melanoma was inoculated in a hind limb of B6 wild type mice and the tumor was treated with HIFU when it reached the diameter of 1 cm. The animals were then sacrificed at specific time points to measure the time course of immune response and evaluate the number of metastases. The HIFU source was a 1.1 MHz focused transducer; the exposure was optimized so that it would result in tissue emulsification without noticeable thermal coagulation. The first pulse of very high amplitude caused the tissue to reach its boiling temperature and, therefore, large bubbles appeared in several milliseconds. Lower amplitude pulses that followed maintained bubble activity and lead to tissue erosion.

**RESULTS & CONCLUSION:** Normally, in wild-type mice the number of any antigen-specific T lymphocytes is too low to quantify a tumor-specific immune response. To increase this number we performed a T cell transplant from a transgenic p-mel mouse that was bred to have a large number of gp100-specific naive T cells. The tumor-specific immune response was then quantified by the number of circulating activated gp100-specific T cells. The T cells were collected from the spleens of the sacrificed animals and counted using flow cytometry. Our most recent results will be presented and implications for potential use of HIFU to treat tumor metastases will be discussed. Work supported by NIH EB007643, NSBRI SMST01601, RFBR 09-02-01530.





**S7B-1**

**Mechanism and safety at the threshold of BBB opening in vivo**

**Konofagou E.**<sup>1</sup>, Choi J.<sup>1</sup>, Baseri B.<sup>1</sup>, Tung YS.<sup>1</sup>

<sup>1</sup> Columbia University, New York, USA

Current treatments of neurological and neurodegenerative diseases are limited due to the blood-brain barrier (BBB). In this paper, the threshold of BBB opening and its dependence on the microbubble diameter as well as the associated mechanism and safety are identified in vivo. In vivo BBB opening in mice (n=13) was achieved by systemically injecting microbubbles (1-2 and 4-5  $\mu\text{m}$  lipid-shelled, gas-filled) and applying pulsed FUS (frequency: 1.525 MHz, peak-rarefactional pressure: 150-600 kPa) to the left hippocampus through the intact skin and skull. Systemically administered, BBB-impermeable, fluorescent-tagged dextrans at 3 kDa were injected to confirm BBB opening. H&E histology was also performed to determine any associated vascular or neuronal damage. Detection of stable and inertial cavitation was performed using a passive cavitation device (PCD) in a blood vessel phantom at the same pressure amplitudes as those used in vivo. Larger microbubbles (4-5  $\mu\text{m}$ ) resulted in a larger region of BBB opening at a lower peak rarefactional pressure (300 kPa) compared to 1-2  $\mu\text{m}$  (450 kPa). Histological studies indicated that, at the BBB opening threshold, no red-blood cell extravasation or neuronal damage was noted. Cavitation studies confirmed that stable cavitation occurs at the threshold of BBB opening and inertial cavitation follows at larger pressure amplitudes. FUS coupled with microbubbles was shown to open the BBB in mice, noninvasively, safely and sufficiently to allow passage of nanoparticles into the brain and permit subsequent fluorescence imaging of the brain parenchyma in vivo. Larger microbubbles resulted to higher fluorescence intensities at pressure thresholds than smaller microbubbles. The mechanism of BBB opening at the threshold was identified to be mainly related to stable cavitation. This study was supported by NSF CAREER 0644713, NIH R21 EY018505 and NIH R01 EB009041.



**S7B-2**

**Focused ultrasound induced blood-brain barrier to enhance chemotherapeutic drugs (BCNU) delivery for glioblastoma treatment**

**Liu HL.**<sup>1</sup>, Hua M.<sup>1</sup>, Chen P.<sup>2</sup>, Huang C.<sup>2</sup>, Wang J.<sup>1</sup>, Wei K.<sup>2</sup>

<sup>1</sup> Chang-Gung University, Taoyuan, Taiwan

<sup>2</sup> Chang-Gung Memorial Hospital, Taoyuan, Taiwan

Focused ultrasound has been recently found to capable of temporally and reversibly disrupt local blood-brain barrier (BBB) and opens new frontier in delivering various type of drugs into brain for central nerve system (CNS) disorder treatment. In this study, we aim to investigate the feasibility of delivering 1, 3-bits (2-chloroethyl) -1-nitrosourea (BCNU) to treat glioblastoma in animal models and evaluate whether this approach would gain treatment efficacy. Under the presence of microbubbles administration, a 400-kHz focused ultrasound was employed to deliver burst-tone ultrasonic energy stimulation to disrupt BBB in animal brains transcranially, and in-vivo monitored by magnetic-resonance imaging (MRI). C6-glioma cells were cultured and implanted into Sprague-Dawley rats as the brain-tumor model. BCNU deposited in brain was quantified by using high-performance liquid chromatography (HPLC), and brain tissues were examined histologically. MRI was employed to longitudinal evaluate the brain tumor treatment including the analysis of tumor progression and animal survival. We confirmed that the focused ultrasound, under the secure ultrasonic energy level, can significantly enhance the BCNU penetration through BBB over 300% than control without cause hemorrhage. Apparent improvement of treatment efficacy achieved by combining focused ultrasound with BCNU delivery, including significant suppression of tumor growth and a prolonged animal survival. This study highly support that this treatment strategy could be clinically-relevant and may help to provide another potential strategy in increasing local chemotherapeutic drugs for brain-tumor treatment.



### Dual photon investigation of ultrasound induced BBB disruption – a threshold and dynamics study

**Drazic J.**<sup>1</sup>, Hynynen K.<sup>1</sup>

<sup>1</sup> University of Toronto, Toronto, Canada

**OBJECTIVE:** Using low frequency ultrasound (~0.8MHz) in combination with Definity microbubbles, blood brain barrier disruption (BBBD) was induced and observed on in vivo rats. A scanning dual photon microscope captured these dynamics with a temporal resolution on the order of seconds. The threshold sonication pressure for vasculature response as well as dye extravasation dynamics were quantified for the first time with 4D data of microscopic resolution.

**MATERIAL AND METHODS:** (i)Ultrasound The 0.8MHz therapeutic transducer was fabricated from a PZT4 crystal ring (10ms pulse, PRF 1Hz, for 30-45s). It was calibrated for pressure with a laser vibrometer. (ii)Optical Imaging The images were obtained with an Olympus FV1000 scanning dual photon microscope as 3D stacks in time. ROIs were selected over the area where dye extravasation occurred. (iii)Animal Preparation A 5mm diameter cranial window was closed with a #1.5 coverslip on anesthetized rats. The transducer was coupled to the skull. Texas Red dextran and Definity microbubbles were intravenously injected prior to imaging and sonication.

**RESULTS:** The pressure required for BBBD was 0.455MPa +/- 0.027MPa. There are 3 time constants for leakage: (i)Fast response, fast time to peak, (ii)Fast response, slower time to peak, and (iii)Slow response, slow time to peak. The fast response manifested itself during sonication, while the slow one occurred minutes after the end of sonication. Category (i) signal peaked within the first minute post sonication. Category (ii) signal peaked within minutes post sonication. Category (iii) signal took over 40min to peak. Bifurcated vessels and small vessels (diameter < 10µm) showed the fast response. Most large vessels (diameter ~ 40µm) with no bifurcations exhibited the slow response.

**CONCLUSIONS:** Three time constants were found to exist in ultrasound and microbubble induced BBBD.



### The dynamic of FUS-induced BBB opening in mouse brain assessed by contrast enhanced MRI

**Jenne JW.**<sup>1</sup>, Kraff A.<sup>1</sup>, Maier F.<sup>1</sup>, Krause N.<sup>1</sup>, Huber P.<sup>1</sup>, Bock M.<sup>1</sup>

<sup>1</sup> German Cancer Research Center, Heidelberg, Germany

Focused ultrasound (FUS) in combination with the administration of gas-filled micro-bubbles (MB), can induce a localized and reversible opening of the blood brain barrier (BBB). MRI has been demonstrated as a precise tool to monitor such a local BBB disruption. However, the opening/closing mechanisms of the BBB with FUS are still largely unknown. In this ongoing project, we study the BBB opening dynamics in mouse brain comparing an interstitial and an intravascular MR contrast agent (CA). FUS in mouse brain was performed with an MRI compatible treatment setup (1.7 MHz fix-focus transducer,  $f^* = 68$  mm, NA = 0.44) in a 1.5 T whole body MRI system. For BBB opening, forty 10 ms-long FUS-pulses were applied at a repetition rate of 1 Hz at 1 MPa. The i.v. administration of the MBs (50 µl SonoVue®; Bracco) was started simultaneously with FUS exposure. To analyze the BBB opening process short- and long-term signal dynamics of the interstitial MR CA Magnevist® and the intravascular CA Vasovist (Bayer-Schering) were acquired using T1w inversion recovery turbo FLASH (1s) and 3D FLASH (90s) MRI images, respectively. The short-term MRI signal enhancements showed comparable time constants for both types of MR CAs: 1.1±0.2min (interstitial) vs. 0.8±0.3min (intravascular). This may serve as a time constant of the BBB opening process with the given FUS exposure parameters. For the long-term signal dynamics the intravascular CA (62±10 min) showed a five times greater time constant as the interstitial CA (12±10 min). This might be explained by the high molecular weight (~60 kDa) of the intravascular CA due to its reversible binding to blood serum albumin resulting in a prolonged half-life in the blood. As the intravascular CA offers a much longer time window for therapy assessment, it might be favorable for FUS-BBB therapy control. In the next step, we are going to study the BBB opening dynamics by analyzing MRI signal enhancements at different FUS exposure times.



### Identifying the inertial cavitation threshold of monodispersed microbubbles and skull effects in a vessel phantom using focused ultrasound

Tung YS.<sup>1</sup>, Choi J.<sup>1</sup>, Konofagou E.<sup>1</sup>

<sup>1</sup> Columbia University, New York, USA

Using Focused Ultrasound (FUS) and microbubbles to open the blood-brain barrier (BBB) has been shown promising for brain drug delivery. Here, the effects of the murine skull, vessel diameter and bubble diameter on the threshold of inertial cavitation were investigated. Cylindrical channels with 360 and 610  $\mu\text{m}$  diameter were generated within a polyacrylamide gel to simulate large blood vessels. Microbubbles were injected into each channel before sonication (frequency: 1.525 MHz; peak-negative pressure: 0.15–0.90MPa; pulse length: 100-cycles; PRF: 10Hz; pulse duration: 2s). Definity® (Lantheus Medical Imaging, USA) microbubbles at  $2.5 \times 10^7$  bubbles/mL were first used to determine the skull and vessel effects. To investigate the dependence of inertial cavitation on the microbubble size, monodispersed lipid-shelled microbubbles at 1-2 or 4-5- $\mu\text{m}$ -diameter were used. A cylindrically focused hydrophone, confocal with the FUS transducer, acted as a passive cavitation detector (PCD) to identify the threshold. A 7.5 MHz linear array with the field-of-view perpendicular to the axial length of the FUS beam was also used to image the occurrence of bubble fragmentation. The threshold using Definity® was found to be at the peak-negative pressure of 0.45 MPa, with or without the skull present. However, the skull induced 10–50% lower inertial cavitation dose. The threshold using 1-2 and 4-5- $\mu\text{m}$  microbubbles was respectively equal to 0.60 and 0.45 MPa. The threshold was identical at both blood vessel diameters studied. In conclusion, the murine skull presence or blood vessel size did not affect the threshold of inertial cavitation but the skull presence caused a lower inertial cavitation dose. The threshold at 1-2- $\mu\text{m}$  microbubbles was higher than that at 4-5- $\mu\text{m}$ . The B-mode images confirmed the detection of inertial cavitation with PCD. Acknowledgements: Supported by NIH grant R21EY018505, R01 EB009041 and NSF CAREER 0644713. The authors thank Mark Borden's group for their microbubbles.



### Time reversal ultrasound system for enhanced drug delivery in rat brain

Fillinger L.<sup>1</sup>, Kurtenoks V.<sup>1</sup>, Lewis Jr G.<sup>2</sup>, Sutin A.<sup>1</sup>, Sarvazyan A.<sup>1</sup>

<sup>1</sup> Artann Laboratories, Trenton, USA

<sup>2</sup> Cornell University, Ithaca, USA

**OBJECTIVE:** Therapeutic ultrasounds have been shown in vitro to improve convection enhanced drug delivery in mammalian brain tissue. The goal of this study is to develop a clinically translatable therapeutic ultrasonic system for in vivo experiments of combined ultrasound and convection enhanced drug delivery in rat brain. Ultrasound will be focused on the injection needle using time reversal acoustics.

**MATERIAL & METHOD:** The time reversal ultrasound focusing system under development is constituted of several components. A programmable time reversal electronic allows recording of the hydrophone signal and simultaneous emission of 10 independent signals. Each emitted signal is supplied to a binary power amplifier with ultra low output impedance. These amplified signals are supplied to a multi-element transducer designed for coupling with a rat head. Acoustic signals are measured and focused on a needle instrumented into a hydrophone.

**RESULTS:** Two time reversal based composite transducers designed for coupling on rat skull were tested at the time of writing of this abstract. One is constituted of piezoelectric disks glued on the surface of an aluminum block that is to be coupled to the focusing medium. The other transducer is a three dimensional arrangement of piezoelectric disks embedded into a non conductive medium. Focusing was tested in a water tank of dimensions similar to a rat skull, demonstrating the ability to produce focused ultrasonic field of characteristic size of 1 mm, at central frequency 1.7 MHz and of acoustic pressure of 5 MPa. A method for producing continuous exposure with time reversal ultrasound focusing has been developed and will be implemented in the rat brain sonication experiments.

**CONCLUSION:** The system under development proved its ability to generate focused ultrasound of 1 mm focal spot size in a small complex medium similar to a rat skull and with amplitude in a range sufficient to achieve therapeutic effects.



**A high precision MR-compatible three-axis positioning system for focused ultrasound drug delivery in small animal models**

Waspe A. <sup>1</sup>, Chau A.<sup>1</sup>, Kukic A.<sup>1</sup>, **Chopra R.**<sup>1</sup>, Hynynen K.<sup>1</sup>

<sup>1</sup> Sunnybrook Health Sciences Centre, Toronto, Canada

**OBJECTIVE:** Small animal models of disease are increasingly being employed for the evaluation of novel pharmaceuticals during focused-ultrasound-enhanced drug delivery studies. The objective of this work was to develop an MR-compatible positioning system that is capable of manipulating an ultrasound transducer in 3D with high precision within any closed-bore clinical MRI.

**METHODS:** A three-axis positioning system was developed using ceramic actuators and linear encoders to position a focused ultrasound transducer precisely, under MR guidance, to target tissue in small animals. The actuators and encoders are RF-shielded from the drive electronics by transmitting the cabling through a grounded and low-pass filtered waveguide-insert penetration panel. Registration between ultrasound and MRI coordinates involves insinuating a Zerdine ultrasound phantom and measuring the centroid of the thermal focal zone in 3D. A focused ultrasound transducer is attached to the positioning system by a rigid arm and is submerged in a closed water tank. The arm passes into the tank through flexible bellows to ensure that the system remains sealed. An RF coil acquires high-resolution images in the vicinity of the target tissue. An aperture on the water tank, centered with the RF coil provides an access point for insinuating the target.

**RESULTS:** Linear distances of 5 cm with a positioning resolution of 0.05 mm were achieved for each axis. The entire system was constructed with non-magnetic components including aluminum, plastics, glass, copper, stainless steel, ceramics, and brass. Operation of the positioning system within the bore of clinical MRI scanners of different manufacturers was feasible and simultaneous motion during MR imaging did not result in any mutual interference or image artifacts.

**CONCLUSION:** An MR-compatible positioning system has been developed that can be used for high-throughput small-animal experiments to study the efficacy of ultrasound-enhanced drug delivery.

---







## HIFU transducers – a vision for the future

Invited speaker: Khuri-Yakub P.<sup>1</sup>

<sup>1</sup> Stanford University, Stanford, USA

High intensity focused ultrasound (HIFU) is fast becoming a very important tool treating tissue in a number of different benign and malignant conditions. The generation of HIFU has been mainly the domain of piezoelectric transducers. Also recently, capacitive micromachined ultrasonic transducers (CMUT) are coming of age, and becoming in their own right, a competitor technology in HIFU applications. With proper implementation, CMUTs present the following advantages: dual use (imaging and HIFU), flexible configuration (single element, 1D array, 2D array, annular array, etc...), efficiency, weak internal loss mechanism (minimal self heating), uniformity, ease and control of manufacture, ease of electronic integration (3D integration), flexible conformable arrays, broad frequency of operation (kHz-MHz), and MR compatibility (MR guided HIFU).

This talk will present the principle of operation of the CMUT and its potential for use in HIFU applications. Next, we will present a novel technology for implementing CMUTs and show sample results.



## High power low impedance therapeutic intracavitary phased array

Kukic A.<sup>1</sup>, Hynynen K.<sup>1</sup>

<sup>1</sup> Sunnybrook Research Institute, Toronto, Canada

**OBJECTIVE:** Therapeutic phased arrays have high electrical impedance due to elements of small width-thickness ratio. Lateral mode coupling reduces the electrical impedance of small cylindrical elements for high power phased arrays for therapeutic purposes such as tumor coagulation[1]. We propose lateral mode coupling use in therapeutic intracavitary linear phased arrays. [1]Hynynen et al "Lateral Mode Coupling to Reduce the Electrical Impedance of Small Elements Required for High Power Ultrasound Therapy Phased Arrays", IEEE Trans. on UFFC, vol. 56, no.3, Mar 2009

**MATERIAL & METHODS:** A linear composite array was built using thickness poled PZT4. Pairs of elements (.155x1.4x14.5mm) were stacked in a linear array; each element had its electrodes on its sides. The elements were driven at frequency corresponding to their height, emitting sound laterally. Electrical impedance of elements was measured using a network analyzer (4195A Hewlett-Packard Palo Alto CA). Acoustic surface displacements of a matched element pair were measured using scanning laser vibrometer (PSV-400-M2-20 20 MHz Polytec Tustin CA).

**RESULTS:** The electrical impedance at lateral mode coupling resonant frequency of 1.3 MHz (height of 1.4 mm) was 149 ohms at minimum phase peak of -33 deg. An element of similar dimensions (.3x1.1x15 mm) and resonant frequency of 1.5 MHz exhibited an electrical impedance of 1.4 kohms at -22 deg. A matched pair of elements was able to achieve therapeutically significant spatially averaged acoustic intensity of 15 W/cm<sup>2</sup> (std 5). The maximum displacement at each input power level varied spatially by 20% (std .9).

**CONCLUSION:** Lateral mode coupling combined with element pairing allows for smaller distance between the electrodes, and an increase in electrode area, resulting in significant electrical impedance decrease. Paired elements provide at least 50% larger acoustic power output than has been reported with current arrays for the purposes of intracavitary thermal therapy.



### Dual-mode 64-element array for interstitial ultrasound imaging and thermal ablation

**Owen N.**<sup>1</sup>, Bouchoux G.<sup>1</sup>, Ambroise L.<sup>1</sup>, Berriet R.<sup>2</sup>, Lafon C.<sup>1</sup>

<sup>1</sup> Inserm, Lyon, France

<sup>2</sup> Imasonic, Voray sur l'Ognon, France

Minimally invasive devices are often used to treat unresectable tumors or other pathological tissues that are deep-seated or adjacent to critical structures. Here we present the evaluation of an experimental dual-mode array transducer and its integration with a research ultrasound imager and a multichannel amplifier. The piezocomposite linear array had 64-elements with 0.280 mm pitch and 3.0 mm height in elevation. Standard measurements were performed to characterize its electroacoustic conversion efficiency, imaging resolution, and sensitivity. As a therapy applicator, efficiency was above 40% for frequencies between 4.0 MHz and 5.0 MHz, and for surface intensities up to 20 W/cm<sup>2</sup>. The average pulse-echo impulse response length was 1.36  $\mu$ s at -20 dB, and fractional bandwidth was 38.4% centered at 4.5 MHz. Pulse echo insertion loss for a single element was less than 35 dB for frequencies between 4 MHz and 5 MHz. A custom circuit board was built to integrate the array with a research ultrasound interface, which collected RF data for offline processing, and a multi-channel amplifier, for which frequency, phase, and power could be specified for each channel and adjusted under software control. This system was evaluated using tissue response simulations and in vitro using porcine liver. Imaging depth was 30 mm, transmit and receive apertures were 8 elements, and echo data were sampled at 40 MHz. These data were taken at a rate of 8 frames per second, and the duty factor for therapy was 92%. The therapeutic beam was steered to discrete foci during sequential therapy periods. Data indicate that array can denature a clinically-relevant volume of tissue within 5 min. This evaluation demonstrates that the dual-mode array and integrated system could be used for real-time image-guided interstitial ultrasound therapy. [Supported by ANT 05 RNTS 01101 and Inserm Post-doctoral Fellowship]



### Development of a new HIFU device for treating glaucoma: Preliminary results

**Charrel T.**<sup>1</sup>, Aptel F.<sup>2</sup>, Birer A.<sup>1</sup>, Chavrier F.<sup>1</sup>, Chapelon JY.<sup>1</sup>, Lafon C.<sup>1</sup>

<sup>1</sup> Inserm, Lyon, France

<sup>2</sup> Hôpital Edouard Herriot, Lyon, France

In order to treat glaucoma using high intensity focused ultrasound (HIFU), a compact and easy to use device is developed. In the 80's, Lizzi et al. clinically demonstrated the feasibility of HIFU treatment. Despite hopeful clinical results, lasers and surgery were preferred because less cumbersome than this ultrasonic device. In case of glaucoma, the reduced quantity of aqueous humor drained by trabecular meshwork causes an increase of the intra-ocular pressure (IOP). This new device will immediately fit to the geometry of ciliary bodies (CB) to treat the eye. Its geometry was first defined from anatomical criteria. Six cylindrical transducers (focused at about 10mm) were set like petals with a central hole for alignment on the pupil and the periphery of the cornea. Numerical simulations allow to define a large range of frequency (from 14 to 28 MHz) and exposure conditions. In theory, when HIFU are emitted sequentially on each transducer at 21MHz and 6W/cm<sup>2</sup> for 3s, thermal lesions cover 45% of CB with no other undesired damage. This device is built and characterized by acoustic power measurements and pressure maps. The transducers radiate up to 7.5W/cm<sup>2</sup> at a frequency of 21MHz. Pressure maps are consistent with theoretical results. The device has been tested in vivo on the eye of four rabbits. An intensity of 6W/cm<sup>2</sup> is applied sequentially on 1, 3 or 6 transducers (3s duration / 20s pause between exposures). The last experiment on the fourth rabbit has no pause between the 6 consecutive exposures. IOP has been tracked during one week. Histology demonstrates thermal damages confined to the CB without side effects. These first results should be confirmed by other in vivo experiences. With this new HIFU therapeutic device, treatment will be easy and achieved in less than one minute. Work funded by EyeTechCare SA.



### Design of a high intensity focused ultrasound multi-element phased array for transcatheter treatment of liver tumours

Gélat P.<sup>1</sup>, Rivens I.<sup>2</sup>, Saffari N.<sup>3</sup>, Ter Haar G.<sup>2</sup>

<sup>1</sup> National Physical Laboratory, Teddington, UK

<sup>3</sup> University College London, London, UK

<sup>2</sup> Institute of Cancer Research, London, UK

The efficacy of high intensity focused ultrasound (HIFU) for the non-invasive treatment of cancer has been clearly demonstrated for a range of different cancers including those of the liver, prostate and breast. As a non-invasive focused therapy, HIFU offers considerable advantages over other techniques such as chemotherapy and surgical resection, in terms of invasiveness and risk of harmful side effects. Despite its advantages, however, there are a number of significant challenges currently hindering its widespread clinical application. One of these challenges is the need to transmit sufficient energy through the rib cage to induce tissue necrosis at the required foci whilst minimising the formation of side lobes. This study involved the design and modelling of a randomly distributed 256-element bowl-shaped phased array transducer. Each individual element consisted of a PZT ceramic modelled using the finite element method. The full piezoelectric properties are included in the model. A sensitivity analysis on the array design parameters was carried out and the ultrasonic field computed using boundary element techniques at required field positions. Shadowing was imposed on the pressure field at selected locations, and the field forward propagated to locations close to the geometric focus using the angular spectrum approach. Optimisation was then used to determine the values of the magnitude and phase of the voltage across each element electrodes to achieve a local maximum at the required treatment region. This analysis shows that, using a random multi-element phased array transducer, it is possible to achieve a focused beam through a shadowed array representing the ribs and to electronically steer the beam within centimetres of the geometric focus without generation of substantial side lobes. It represents a useful design tool for drawing up the specifications of a prototype device that will enable transcatheter HIFU therapy for liver tumours.



### Thermal ablation of liver tumors by high intensity focused ultrasound using a toroid transducer. Results of animal experiments

Melodelima D.<sup>1</sup>, Battais A.<sup>1</sup>, N'Djin WA.<sup>1</sup>, Rivoire M.<sup>2</sup>, Chapelon JY.<sup>1</sup>

<sup>1</sup> Inserm, Lyon, France

<sup>2</sup> Centre Leon Berard, Lyon, France

**OBJECTIVES:** To demonstrate in a rabbit liver tumor model that high intensity focused ultrasound (HIFU) produced with toroid-shaped emitters may have a role in treating colorectal liver metastases.

**MATERIAL AND METHODS:** A 256 elements toroidal piezocomposite transducer with a diameter of 70 mm and a radius of curvature of 70 mm was used. The operating frequency was 3 MHz. Using this transducer, single lesions of 7 cm<sup>3</sup> can be created in 40 seconds. Juxtaposition of single lesions was performed under ultrasound guidance using a 7.5 MHz ultrasound imaging probe placed in the centre of the HIFU transducer. VX2 tumor segments (25 mg) were implanted into livers of 45 New Zealand rabbits. Fifteen rabbits were treated with toroidal HIFU ablation (Group 1). Fifteen rabbits were resected (Group 2). Fifteen rabbits were not treated and formed a control group (Group 3). Group 1 and 3 were compared to evaluate treatment efficacy. Group 1 and 2 were compared to evaluate if the toroidal HIFU treatment increases the risk of tumor dissemination. The therapeutic response was evaluated 11 days after treatment with gross pathology and the corresponding histology.

**RESULTS:** HIFU ablation produced using the toroidal transducer allowed fast and homogeneous tumor treatments. The VX2 tumors were completely coagulated and were surrounded by ablated liver tissue without secondary thermal lesions in surrounding organs. In the control group Tumor volume was 225% higher at the time of autopsy when compared to the volume at the day of the treatment. Tumor dissemination was lower in the HIFU group (25%) compared with resected (67%) and control (38%) groups. Findings of ultrasound imaging, gross pathology and histology supported these outcomes.

**CONCLUSIONS:** Successful rabbit liver tumor ablation can be achieved using a toroidal HIFU transducer under ultrasound imaging guidance and therefore could be an effective treatment of localized tumors. Its clinical usefulness has to be further proven.



S8-7

### Effects of respiratory motion on in-vivo HIFU treatments: a comparative study in the liver

**N'Djin WA.**<sup>1</sup>, Miller N.<sup>2</sup>, Bamber J.<sup>2</sup>, Chapelon JY.<sup>1</sup>, Melodelima D.<sup>1</sup>

<sup>1</sup>Inserm, Lyon, France

<sup>2</sup>Royal Marsden NHS trust and Institute of Cancer Research, London, UK

Current development of HIFU strategies for the treatment of localized abdominal tumors are limited by organ motion during respiration. In preliminary studies, a numerical model simulated the effects of in-vivo movements on HIFU treatments in the liver. It was shown that a HIFU treatment performed during respiration with juxtaposition of millimetric lesions is modified in shape and homogeneity. Here, we report recent results from a comparative study which evaluated in simulation and in in-vivo experiments, the interest of using, during respiratory, a toroidal-shaped HIFU device developed for the treatment of Liver Metastases from Colorectal Cancer. These experiments were performed during an open procedure, on 9 pigs divided into 3 groups. On the first group, a spherical HIFU transducer was used to juxtapose 49 millimetric lesions in the liver during respiration. The second group was treated during respiration with a 3 MHz toroidal-shaped HIFU transducer. The last group (control) was treated during apnea. For each animal, sequences of ultrasound images were acquired in the liver. Then, a combined method of modeling based on ultrasound speckle tracking and BHTe equation resolution, was used to quantify liver motion and to simulate HIFU treatments during breathing. Liver motions were mainly encountered in the cranial-caudal direction with a frequency comparable to the respiratory frequency ( $f = 0.2$  Hz). Magnitude of the motion was 8.2-10.0 mm. Results of the modeling were well fitted to the observations made on in-vivo gross samples. In vivo lesions created with the spherical device were stretched by 64% and then were split in the tissues. The toroidal-shaped HIFU strategy allowed the generation of homogeneous lesions (12% stretching). These results provide a preliminary validation of the method for modeling liver motion effects. This method was used to demonstrate the effectiveness of a new HIFU device which shows promise for HIFU therapy during respiration.



S8-8

### Criteria for modelling the capabilities of a 48 element phased array HIFU transducer

**Rivens L.**<sup>1</sup>, Woodford S.<sup>1</sup>, Civale J.<sup>1</sup>, Ter Haar G.<sup>1</sup>

<sup>1</sup>Institute of Cancer Research : Royal Marsden NHSF Trust, Sutton, UK

Phased array transducer technology is increasingly being used to deliver non-invasive therapeutic ultrasound for the treatment of both malignant and benign disease. We have designed a simple, but steerable, transducer consisting of 48 elements uniformly arranged in 6 annuli and 8 sectors. A central imaging aperture allows for diagnostic ultrasound guidance. The axial and lateral steering capabilities of this transducer were explored using a linear acoustic-propagation model. Steering was investigated using two methods: (i) a requirement of phase coherence at the focal point, and (ii) intensity maximisation at the focal point with additional minimisation at all other points. As a result of this study, criteria for determining the maximum extent of electronic steering were identified: (i) Spatial Precision - the steered point of maximum intensity must lie at the centre of the intended volume contained by the contours defined by the 50% of the full width half maximum pressure (centred on the steered beam axis) in each direction (ii) Cost (intensity loss) - focal peak intensity  $\geq 50\%$  of the unsteered value (iii) Side effects – the second highest peak intensity  $\leq 15\%$  of the focal value ( $\leq 10\%$  if incident on skin) Axial steering could be achieved using phase variation across 6 rings of elements. The greatest peak intensity occurred closer to the transducer than the geometric focus. Steering towards the source narrowed and shortened the focus, but was effective over a greater distance (3.0 cm) than steering away from it (1.8 cm). Using the criteria defined for effective steering, lateral steering was most effective when using 48 separate elements, but with the achievable range limited to  $\pm 1.8$  mm this will not be of significant clinical use. A drive system is being constructed to allow testing of these results using a high-precision membrane hydrophone beam-plotting system prior to ex-vivo tissue and pre-clinical safety studies.



### Direct methods for free field characterization of HIFU transducers using acoustic streaming

**Hariharan P.**<sup>1</sup>, Myers M.<sup>1</sup>, Banerjee R.<sup>2</sup>

<sup>1</sup> Food and Drug Administration, Silver Spring, USA

<sup>2</sup> University of Cincinnati, Cincinnati, USA

**OBJECTIVE:** Free-field estimation of the HIFU intensity field can be difficult due to the possibility of hydrophone damage or of sensor interference with the focused beam. In our previous work, we showed that acoustic streaming can be employed to characterize HIFU transducers without perturbing the acoustic field. We measured the streaming velocity experimentally and then determined the acoustic intensity through an iterative computational procedure. A drawback of the iterative streaming technique is the extensive computation time required to repeatedly solve the governing equations. This talk introduces two alternative techniques ("direct methods") which circumvent the iterative procedure and determine the intensity field with far less computation time.

**METHODS:** The streaming field generated by the absorption of acoustic energy within the medium is measured using digital particle image velocimetry (DPIV). The acoustic intensity distribution giving rise to the streaming field is then computed by inserting the velocity field directly in to the equations governing the streaming motion (Navier-Stokes). Two different methods, namely i) Gaussian Curve fitting (GCF) and ii) Finite differencing (FD) are adopted for estimating derivatives in the Navier-Stokes equation. In the FD method, derivatives are evaluated by numerical differentiation of the experimental data. In GCF method, the intensity field is obtained by fitting the streaming velocity field to a Gaussian function and its antiderivatives.

**RESULTS:** Comparisons performed in the range of 100–1000 W/cm<sup>2</sup> focal intensity showed differences between the direct methods and the iterative technique to be less than 20%. Similar differences were observed in low-power comparisons (of focal intensities and beam widths) with hydrophone measurements.

**CONCLUSION:** This noninvasive technique allows characterization of HIFU transducers to be performed in an intensity range that may be harmful to conventional hydrophones.



### Measurement of the total acoustic output power of HITU transducers

**Jenderka KV.**<sup>1</sup>, Beissner K.<sup>1</sup>

<sup>1</sup> Physikalisch-Technische Bundesanstalt, Braunschweig, Germany

**OBJECTIVE:** High Intensity Therapeutic Ultrasound (HITU) is a non-invasive technique for the treatment of various types of cancer, as well as non-malignant pathologies by inducing localized necrosis of the tissue. Even though HITU is already in clinical use, the metrology of the applied high power ultrasound fields is still a challenge.

**MATERIAL & METHOD:** A crucial step for the prediction of the desired temperature rise in a HITU-treated region and in terms of treatment planning is the measurement of the total ultrasound output power. While ultrasound fields are well-investigated for output powers smaller than 20 W, this paper describes preliminary results of measurements in much stronger, highly focused fields (> 400 W ultrasound power at 1.5 MHz) by means of the radiation force. For this purpose, a radiation force balance setup (arrangement A in accordance with IEC 61161, variable distance between the transducer and the absorbing target) was adapted for the determination of large acoustic output powers.

**RESULTS:** The relationship between the total acoustic output power and the applied net electrical power was measured for a close transducer-target distance. Up to an acoustic power of 420 W the transducer under investigation showed a stable efficiency of 78.4 %. In a second attempt, the dependence of the measured electro-acoustic radiation conductance on the distance of the absorbing target from the transducer was investigated at reduced power level. The radiation conductance declined with increasing distance, which is typical for radiation force measurements, and exhibited no focal anomaly.

**CONCLUSION:** The maximum power achieved with this setup was more than 400 W total acoustic output power. Considering all uncertainty contributions, the estimation of the uncertainty budget yields a total uncertainty of 4.3 % (coverage factor k=2) for measurements in the high power range.



## Feasibility of a PVDF receiver for monitoring of transcranial therapy

O'Reilly M.<sup>1</sup>, Hynynen K.<sup>1</sup>

<sup>1</sup> Sunnybrook Research Institute, Toronto, Canada

**OBJECTIVE:** Non-invasive transcranial therapy can be conducted using large scale, phased arrays. Currently, such arrays lack diagnostic capabilities and depend on MRI technology to monitor treatment. We hypothesize that monitoring of therapy is possible using ultrasound receivers. This study examines the feasibility of incorporating PVDF receivers into a transcranial array.

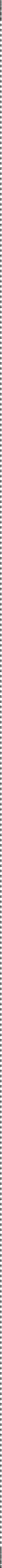
**MATERIALS & METHODS:** 110 $\mu$ m thick PVDF film with an active area »17.8mm<sup>2</sup> was air-backed by clamping it across brass tubing. A preamplifier was enclosed within the tubing. The receiver was mounted inside a ring element (h=6mm;  $\phi_{in}$ =7mm;  $\phi_{ex}$ =10mm; f=306kHz) from an existing array (1372 elements). The receiver performance was compared with a 0.5mm needle hydrophone (Precision Acoustics). The transmit/receive pair was used to sonicate degassed water in a thin-walled tube both directly and through a fragment of human skull. Definity contrast agent was injected into the tube and the waveforms were compared.

**RESULTS:** The sensitivity of the receiver (1.616V/MPa@306kHz; 1.377V/MPa@830kHz) was much higher than that of the hydrophone (0.250V/MPa@306kHz; 0.352V/MPa@830kHz). On their own, both the PVDF and the hydrophone had high SNR (93; 152). In combination with the transmit element, the hydrophone performed poorly (SNR=0.41) compared to the PVDF (SNR=16.43). Microbubble detection was confirmed by the presence of higher harmonics and an increase in waveform amplitude when the Definity was injected. Through-skull SNR was 1.6 for the single element, but could be improved to 10.3 using post-acquisition analysis.

**CONCLUSIONS:** A low cost receiver with high sensitivity and superior performance to a commercial hydrophone was constructed. The receiver is able to function in combination with transmit elements to sonicate a transcranial target and detect the returning sound waves. Future work will focus on developing a multi-element receiver array and its testing for brain treatment monitoring.

---

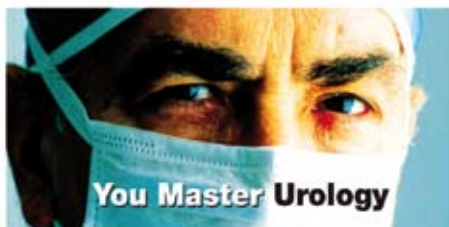




# Oral Communications Saturday, September 26

[www.istu2009.org](http://www.istu2009.org)

Saturday,  
September 26



**We Master  
Therapeutic Ultrasound**

[www.edap-tms.com](http://www.edap-tms.com)



**HIFU**  
Prostate Cancer

Ablatherm<sup>®</sup>  
Robotic HIFU<sup>®</sup>

**ESWL**  
Stone Management

Sonolith<sup>®</sup>  
i-eyes  
Sonolith<sup>®</sup>  
Praxis



S9-1

## How HIFU has mediated the change from whole gland therapy to focal therapy

Invited speaker: **Emberton M.**<sup>1</sup>

<sup>1</sup> UCLH/UCL Comprehensive Biomedical Centre, London, UK

**INTRODUCTION:** Prostate cancer has traditionally been managed by treating the whole gland, whether the approach is radio-therapeutic or surgical. The reasons for this are largely technical in that neither surgery nor radiotherapy in its traditional form can do anything other than this. Most prostate cancers at the time of presentation occupy less than 5% of the prostate volume. This means that in most cases that are treated a considerable amount of tissue is sacrificed.

**METHODS:** Several NCRI badged Phase I studies were initiated to assess the feasibility and utility of treating only the cancer and leaving non-cancerous tissue untreated. All patients were treated with the Sonablate 500TM device. These studies took the form of prostate hemi-ablation, prostate focal therapy and index lesion control. Functional outcomes were collected at 3, 6 and 12 months post therapy and included IPSS, IIEF and FACT-P self-reported questionnaires. Oncological outcomes were derived from PSA at 3, 6 and 12 months and protocol-mandated biopsies of the treated tissue at 6 months.

**RESULTS:** Pad free urinary continence and preservation of erectile function sufficient for penetration returned to baseline between 3 and 6 months post treatment. In the most mature study of the three the proportion of patients free of any clinically important disease (Gleason 3+3 or less and maximum cancer core length of 2mm or less) was 100%. The proportion of patients free of any cancer was 90%.

**CONCLUSIONS:** Focal therapy for men with localised prostate cancer undertaken in a number of formats using the Sonablate 500TM device has resulted in a return to baseline in the key aspects of genito-urinary function and high levels of disease control.

S9-2

## Primary prostate HIFU: local control and biochemical survival of 966 patients tracked with the @-registry

**Gelet A.**<sup>1</sup>, Chaussy C.<sup>1</sup>, Conti G.<sup>1</sup>, Rebillard X.<sup>1</sup>, Robertson C.<sup>1</sup>, Blana A.<sup>1</sup>

<sup>1</sup> Hôpital Edouard Herriot, Lyon, France

**INTRODUCTION & OBJECTIVES:** The use of High Intensity Focused Ultrasound (HIFU) as a primary therapy for localized prostate cancer has increased. The objective of this study is to report the outcome of patients who have undergone HIFU in 10 centers participating at the @-Registry. This is the largest prostate HIFU series of patients ever reported.

**MATERIAL & METHODS:** The @-Registry is a secure on-line database consisting of case report forms which collect relevant de-identified pre and post treatment information for patients undergoing prostate HIFU. Data collected from 1993 were reviewed. Only those who had localized disease (T1-2, NX, M0) treated with curative intent (whole gland ablation) and presenting at least a two-year follow-up were considered in this study. Previously irradiated patients were excluded from this analysis. All patients were stratified according to D'Amico's 2003 risk group definitions. Kaplan-Meier analysis was performed to determine biochemical survival with failure defined according to the 2006 Phoenix definition (nadir+2).

**RESULTS:** A total of 966 patients met the inclusion criteria. The average age was 69.3 ± 6.2 years. Pre treatment PSA was 9.3 ± 9.3 ng/ml, the median Gleason sum was 5.9±1.3 and the clinical stages were T1 (50.3%) and T2 (49.7%). Patients were followed for 55.2 ± 23.8 months. The mean PSA nadir was 0.45 ± 1.0 ng/ml which was reached 14 ± 11 weeks after HIFU. Stratification according to D'Amico's 2003 was: low risk 42%, intermediate risk 46% and high risk 12%. 79% of the 966 patients underwent control biopsies and 85% presented negative biopsies. The 5 year biochemical survival rates were 85%, 82% and 76% for low, intermediate and high risks patients, respectively.

**CONCLUSIONS:** The data of this large cohort allowed by the central collection of data from several centers thanks to @-registry demonstrates that HIFU provides a good local control of the localized prostate cancer and encouraging biochemical control of the disease.



S9-3

### Ten-year experience of high intensity focused ultrasound (HIFU) for localized prostate cancer

**Uchida T.**<sup>1</sup>, Nakano M.<sup>1</sup>, Shoji S.<sup>1</sup>, Nagata Y.<sup>1</sup>, Usui Y.<sup>2</sup>, Terachi T.<sup>2</sup>

<sup>1</sup> Tokai University Hachioji Hospital, Tokyo, Japan

<sup>2</sup> Tokai University, Kanagawa, Japan

**INTRODUCTION:** The purpose of the study was to assess the long-term outcome of HIFU for prostate cancer. **METHODS:** From January 1999, a total of 662 patients were treated with three different types of Sonablate® (Focus surgery, IN, USA) devices. Thirty-two patients were treated with Sonablate® 200 (S200) from 1999 to 2001, 406 patients with Sonablate® 500 (S500) from 2001 to 2005 and 224 patients with Sonablate® 500 version 4 (V4) from 2005-2008. Biochemical failure was defined according to the criteria recommended by the revised American Society for Therapeutic Radiology and Oncology consensus panel.

**RESULTS:** The mean age, PSA and Gleason score in S200, S500, and V4 groups were 71, 68, and 67 years, 15.4, 12.3, and 10.2 ng/ml, and 5.6, 6.3, and 6.6, respectively. The mean operation time in S200, S500, and V4 groups were 174 min, 123 min, and 68 min, respectively. The mean operation time was shortened in V4 group ( $p < 0.0001$ ). The mean follow-up months in S200, S500, and V4 groups were 46, 34, and 21 months, respectively. The biochemical disease-free survival rate (BDFR) in all patients was 57% in 8 years. The BDFR in 8 years in patients with S200 and S500 groups were 56% and 53%, and BDFR in 3 years in patients with V4 group was 83%. The BDFR in the low, intermediate, and high risk groups were 100%, 53%, and 30% in S200, 69%, 48%, and 46% in S500, and 95%, 88%, and 65% in V4 group, respectively. The negative prostate biopsy rate after HIFU was 100% in S200, 79% in S500 and 93% in V4 group.

**CONCLUSION:** HIFU is indicated as the primary therapy for prostate cancer for with low-and intermediate-risk patients. The clinical outcome has significantly improved over the years due to technical improvements in the device.



S9-4

### Analysis of acoustic access to the prostate through the abdomen and perineum for extracorporeal ablation

**Hall T.**<sup>1</sup>, Wheat J.<sup>1</sup>, Hempel C.<sup>1</sup>, Roberts W.<sup>1</sup>

<sup>1</sup> University of Michigan, Ann Arbor, USA

As part of the development of a noninvasive treatment for BPH using histotripsy, this study aimed to measure acoustic access for extracorporeal ablation of the prostate. Both transabdominal and transperineal approaches were considered. The objective was to measure the size and shape of a transducer aperture that could target the prostate without obstruction. CT images obtained from 17 subjects >56 years of age were used to create 3D reconstructions of the lower abdomen and pelvis. Target locations on the urethra at the base, veru, and apex in the prostate were marked along with a transrectal imaging probe. 1001 evenly space rays spanning a 120° solid angle (equivalent to  $\# = 0.6$ ) were traced from each target location towards the perineum and separately towards the abdomen with the maximum xray density encountered along each path recorded. Those exceeding a soft tissue threshold were assumed blocked by bone. The remaining rays comprised the total available transducer aperture. The fraction of unblocked rays reaching an optimally placed  $\# = 1$  transducer was recorded. The overall free aperture through the perineum was a triangular shaped region bounded by the lower bones of the pelvis and the transrectal probe varying significantly in size between subjects. The free aperture through the abdomen was wedge shaped limited by the pubis also with great subject to subject variability. Average unblocked fractions of the  $\# = 1$  transducer to target base, veru, and apex through the perineum were 77.0%, 94.4%, and 99.6%, respectively. Averages targeting through the abdomen were 86.1%, 52.3%, and 11.0%. Target locations in the center and lower part of the prostate for most subjects were found to be very accessible from the perineum with the top somewhat less. Access from the abdomen was good for the top of the prostate, but likely inadequate for the center and bottom for many subjects. Acoustic access to the prostate for histotripsy through the perineum should be feasible.



S9-5

### Histological evaluation of conformal 3D MRI-guided transurethral ultrasound therapy in the prostate

**Vedula S.**<sup>1</sup>, Boyes A.<sup>1</sup>, Chopra R.<sup>2</sup>, Bronskill M.<sup>2</sup>

<sup>1</sup> Sunnybrook Health Sciences Centre, Toronto, Canada

<sup>2</sup> Medical Biophysics, University of Toronto, Toronto, Canada

**OBJECTIVES:** MRI-guided transurethral ultrasound therapy can treat a targeted region in the prostate gland with high spatial accuracy. We have extended this treatment to a 3D targeted volume within the prostate, using a multi-element transducer and temperature feedback from multiple imaging planes. The objective of this study was to use histological comparison to evaluate the spatial accuracy of heating in the canine prostate gland.

**MATERIALS & METHODS:** Animals (n=8) were placed supine in a 1.5T clinical MRI, and the transurethral heating device was positioned with image guidance. A four-element transducer (each 5mm long, operating at ~8MHz) was rotated to treat a targeted volume around the device. Temperature maps transverse to each element were acquired during heating and used to control appropriate acoustic powers from each element and the rate of rotation for the device. T2-weighted and contrast-enhanced (CE) MR images were obtained before and after treatment. Following treatment, prostates were removed and fixed, axially sliced, stained with H&E and digitally imaged at high-resolution to outline boundaries of cell death. Slice alignment and image registration techniques were developed to enable quantitative comparison of the axial MRI images and matching histological sections.

**RESULTS:** Prostate sections showed clear regions of coagulative necrosis, extending ~20mm along the urethra, which correlated well with CE MRI data and transducer length. After registration, the outer border of coagulative necrosis on H&E conformed well to the target isotherm, similar to results from earlier (single element) acute studies.

**CONCLUSIONS:** These results confirm that our previous analysis technique for a single transducer applies to multiple elements with similar precision. Multi-planar analysis of the treated volume is guiding improvements to the controller, consequently leading to greater 3D treatment accuracy.

---



S9-6

### Ultrasound-activated microbubble enhancement of radiation response

**Czarnota G.**<sup>1</sup>, Karshafian R.<sup>2</sup>, Giles A.<sup>1</sup>, Al Mahrouki A.<sup>1</sup>

<sup>1</sup> Sunnybrook Health Sciences Centre, Toronto, Canada

<sup>2</sup> Ryerson University, Toronto, Canada

It is now appreciated that radiation not only damages the DNA inside tumour cells in vivo but may act by damaging the endothelial cells of the vasculature. In this study we tested the hypothesis that microbubble agents in vivo may be used a priori to cause endothelial cell perturbations thus causing »radiosensitization« of tumours. Human prostate cancer xenograft-bearing mice (120 animals) were exposed to combinations of ultrasound, activated-microbubbles, and radiation (8 animals per group). For ultrasound treatments, animals were exposed to 16 cycles tone burst at 500kHz center frequency 570kPa peak negative pressure with a 3kHz pulse repetition frequency for 5 minutes. For treatments involving bubbles, Definity bubbles (Bristol Myers-Squibb) were first administered and for radiation treatments 160 kVp X-rays were used at doses of 2 and 8 Gy. Representative tumour sections were examined using immunohistochemistry. Clonogenic assays and growth delay studies were also carried out. Separate experiments were carried out using endothelial cells in vitro to identify the biochemical mechanism of cell death activation due to microbubbles. Analyses indicated a synergistic increase in tumour cell kill due to vascular disruption caused by the combined therapies that increased when microbubbles were used in conjunction with radiation with increases of cell kill from 5% to over 50% with combined single treatments. Immunohistochemistry indicated endothelial cell apoptosis and activation of the ceramide cell-death pathway to be caused by microbubbles. gene expression analyses using gene-profiling and RT-PCR were confirmatory for ceramide pathway component increased activity and apoptosis induction. Radiation effects were synergistically enhanced by using microbubbles to perturb tumour vasculature prior to the administration of radiotherapy. This works forms the basis for ultrasound-induced spatial targeting of radiotherapy enhancement.



S9-7

## Ultrasound properties of human tissues

Retat L.<sup>1</sup>, Zahur S.<sup>2</sup>, Civale J.<sup>1</sup>, Ter Haar G.<sup>1</sup>, Rivens I.<sup>1</sup>

<sup>1</sup> Institute of Cancer Research, Sutton, UK

<sup>2</sup> Institute of Cancer Research/Royal Marsden Hospital, London, UK

**INTRODUCTION:** Differences in ultrasound (US) properties of human tissues may, provide a basis for US monitoring of US thermal therapies such as high intensity focused ultrasound (HIFU). In this study different fresh human tissues will be characterised using techniques being established initially in prostatectomy samples.

**METHODS:** Cancer bearing human prostate samples were obtained within one hour of prostatectomy and cut into approximately 4 mm thick slices by the pathologist for histological analysis. One slice per specimen (n=5) was characterised using a pair of weakly focused 2.5 MHz transducers (Imasonic, France). A transmission insertion method based on a fixed-path measurement of attenuation and sound speed was used to avoid problems due to diffraction losses. Attenuation was measured over the transducer's bandwidth (1.5 to 3.5 MHz) at body temperature (37±30C) at a number of positions within each slice. In order to calculate attenuation coefficients, the thickness of each slice was measured using both pulse-echo US and digital calipers. Then the slice was fixed, stained with haematoxylin and eosin, and the histological status of tissue at the measurement positions established.

**RESULTS:** A systematic thickness difference of 20 ±10 %, was observed between pulse-echo and caliper measurements. Within a single prostate, the attenuation coefficients measured in normal tissue varied by 10±2% with a 13±3% difference between benign & malignant regions. The inter-prostate mean (and standard deviation) of the attenuation coefficients for normal and malignant tissues at 2.80 MHz (37°C) were 1.56 ±0.21 dB/cm (n=5) and 1.91 ±0.81 dB/cm (n=2). The corresponding frequency (f) dependencies of attenuation were 0.41x f1.33 dB/cm/MHz and 0.69x f0.99 dB/cm/MHz.

**CONCLUSION:** The measured variation in tissue properties within prostates may have clinically significant impact on the delivery of HIFU treatment.



S9-8

## Practical measures for evaluation of ultrasound therapies of the prostate

Kobelevskiy I.<sup>1</sup>, Burtnyk M.<sup>2</sup>, Bronskill M.<sup>2</sup>, Chopra R.<sup>2</sup>

<sup>1</sup> Sunnybrook Health Sciences Centre, Toronto, Canada

<sup>2</sup> University of Toronto, Toronto, Canada

**OBJECTIVES:** 1.To derive measures for quantitative evaluation of the effectiveness and safety of ultrasound prostate therapies. 2.To determine the effects of device parameters and MRI factors in MRI-guided transurethral ultrasound therapy using these measures.

**MATERIAL & METHODS:** Our group has previously reported on MRI-guided transurethral ultrasound therapy. Improvements of this technique and comparison to other techniques have led to development of quantitative measures for treatment evaluation. These new measures are described and their utility is illustrated by analyzing MRI factors and device parameters for 3D multi-element transurethral prostate treatments. Parameters considered included MRI factors such as in-plane resolution, slice thickness, SNR and acquisition time and device parameters such as element size, operating frequencies and maximum element power. All simulations were performed on 10 prostate boundaries segmented from MR images of prostate cancer patients.

**RESULTS:** Treatment effectiveness and safety can be evaluated using three fundamental measures: volume treatment accuracy, heating of adjacent structures, and treatment time. 1.Volume treatment accuracy was measured by computing undertreated volume >1mm inside the target boundary plus overtreated volume >1mm outside the target boundary. Tissue within a 1mm margin of the target boundary was considered to lie within the accuracy of the controlling MR imaging. 2.Heating of surrounding structures was measured by computing the volume of tissue with thermal dose above thresholds for possible damage determined from the literature. 3.Treatment time was defined as the time during which the treatment device emitted acoustic power.

**CONCLUSION:** These measures provide a quantitative framework for evaluating ultrasound prostate thermal therapies. When used with treatment simulations, these measures enable quantitative comparison of device configurations and enhancement of control algorithms.

S9-9

Salvage therapy of high-intensity focused ultrasound (HIFU)

Shoji S.<sup>1</sup>, Uchida T.<sup>1</sup>, Nakano M.<sup>1</sup>, Nagata Y.<sup>1</sup>, Terachi T.<sup>2</sup>

<sup>1</sup> Tokai University Hachioji Hospital, Tokyo, Japan

<sup>2</sup> Tokai University School of Medicine, Kanagawa, Japan

**OBJECTIVE:** To investigate the usefulness of salvage therapy of high-intensity focused ultrasound for recurrence prostate cancer after radiotherapy.

**PATIENTS AND METHODS:** Between January 2002 and March 2009, 19 patients were treated the recurrence of prostate cancer after radiotherapy with HIFU using the Sonablate 500. The Sonablate system consists of a rectal probe with an operating frequency of 4MHz to optimize the combined imaging and therapy role of the transducer. We classified the patients three groups of low risk group (Low), intermediate risk group (Inter), and high risk groups (High) by D' Amico criteria. And we investigate the therapeutic effectiveness of HIFU for the three groups by Phenix ASTRO criteria.

**RESULT:** The mean (range) age of the patients was 68.5 (58-85) years old. The mean (range) PSA levels of pre-radiotherapy and pre-HIFU were 24.7 (5.7-118) ng/ml and 6.65 (0.8-30.1) ng/ml. The contents of radiotherapy were external beam radiotherapy (9 patients), brachy therapy (2 patients), proton therapy (3 patients), brachy therapy + external beam radiotherapy (4 patients), and cryotherapy + proton therapy (1 patient). The patient's number of Low, Inter, and High were 2, 6, and 11. The biochemical disease free rates of Low, Inter, and High after HIFU were 100%, 100%, and 45%. Side-effects included urethral stricture (2 patients, 11%), urinary incontinence (2 patients, 11%), and recto-urethral fistula (1 patients, 5%)

**DISCUSSION AND CONCLUSION:** Our data showed that salvage therapy of HIFU for prostate cancer in Low- and Intermediate risk groups after radiotherapy is effective. The patients with biochemical recurrence of prostate cancer after radiotherapy have local recurrence, metastatic disease, or both. Salvage therapy of HIFU is useful to treat the local recurrence of prostate cancer after radiotherapy.

S9-10

HIFU partial treatment of localized prostate cancer: influence on erectile dysfunction (ED)

Gelet A.<sup>1</sup>, Murat F.<sup>1</sup>, Poissonnier L.<sup>1</sup>, Kulisa M.<sup>1</sup>, Chapelon JY.<sup>2</sup>, Martin X.<sup>1</sup>

<sup>1</sup> Hôpital Edouard Herriot, Lyon, France

<sup>2</sup> Inserm, Lyon, France

**INTRODUCTION & OBJECTIVES:** We evaluated the benefit of HIFU sub total prostate ablation on ED using a 5-item version of the International Index of Erectile Function (IIEF-5) score and defined the oncological efficacy of such a partial gland ablation.

**MATERIAL & METHODS:** 56 patients (Pts) with prostate cancer (PCa) biopsy-proven exclusively in one prostate lobe (mean positive core number: 1.55), mean age 65±5 years, mean PSA 7.2±3.6 and clinical stages T1 (39 Pts), T2 (17 Pts) were selected. They were stratified according to D'Amico's 2003 risk group definitions as low (33 Pts) and intermediate risks (23 Pts). They received a HIFU sub total ablation of prostate: in the biopsies negative lobe, a 6 mm safety margin was defined between the closest shot from the prostate capsule and the actual prostate capsule, whereas in the biopsies positive lobe a complete treatment was performed. ED was evaluated using a pre and post HIFU IIEF-5 score. The combined Phoenix criteria (pathological + biochemical) was used for disease free survival rate (DFSR) calculation.

**RESULTS:** Over the 56 Pts, 52 had a pre-HIFU IIEF-5 score over 17 (no ED: 29 Pts, mild ED: 23 Pts). Among the 56 Pts, 19 required 2 HIFU sessions. Mean PSA nadir after the first and second HIFU session was 0.5ng/ml and 0.47ng/ml, respectively; with a median follow-up of 42 months. DFSR were 76% and 60% at 3 and 5 years, respectively. The overall IIEF-5 scores significantly decreased after each session (Wilcoxon test, p=0.0027). After the first HIFU session among the 52 Pts with a pre-HIFU IIEF-5>17, 54% had a post- HIFU IIEF-5 score>17. After the second HIFU session, only 20% of retreated Pts remained in the same group i.e. Pts with an IIEF-5>17.

**CONCLUSIONS:** HIFU partial ablation of prostate allows a better preservation of sexual function without compromising the oncological efficacy. HIFU focal therapy is an exciting area of research that can hold promise for low or intermediate risk PCa.





S10-1

**Rapid and volumetric MRI thermometry for monitoring HIFU ablation in the liver during breathing**

**Quesson B.**<sup>1</sup>, Laurent C.<sup>1</sup>, Maclair G.<sup>1</sup>, Denis de Senneville B.<sup>1</sup>, Ries M.1, Moonen C.<sup>1</sup>

<sup>1</sup>CNRS/Université Victor Segalen Bordeaux 2, Bordeaux, France

**OBJECTIVE:** Magnetic Resonance (MR) thermometry of the liver remains difficult because of the presence of motion. HIFU ablation requires important energy deposition to compensate blood cooling effects, increasing the risks of damaging adjacent tissues. The objectives of this study were to perform precise, rapid and volumetric temperature monitoring of HIFU ablations in the liver and surrounding tissues (skin) during breathing.

**MATERIAL AND METHODS:** MR-HIFU was evaluated at 1.5Tesla (Philips HIFU prototype) in vivo in the liver of 5 pigs under general anesthesia. Eight HIFU sonications were performed during breathing, varying the sonication power (80-300W) and duration (10-27sec). Rapid and volumetric MRI thermometry (PRF method) was performed at a frequency of 2.5Hz, using a multi-slice (3 coronal and 1 sagittal slice located in the liver and 1 coronal slice located on the skin) single shot echo planar imaging sequence (TE/TR=34/80ms, flip angle=30°, FOV=210x300mm, matrix=96x112). The motion artifacts on temperature maps were compensated with multi-baseline reference images. The thermal dose maps were computed (Sapareto equation) and compared to histological analysis of the liver and the skin after sacrifice of the animals.

**RESULTS:** Each HIFU sonication could be identified on temperature images. The standard deviation of temperature was 0.9°C in the liver and 2.5°C on the skin. The maximal temperature rise was 30°C for a sonication performed at 300W during 15sec. The lethal thermal dose (equiv. to 240 minutes at 43°C) was reached in 4/8 sonications in the liver (minimal energy deposition of 2.7kJ) but never on the skin. Histological analysis confirmed the presence of lesions in the liver and the absence of skin alterations

**CONCLUSION:** Rapid and volumetric MRI thermometry during HIFU ablation is feasible in presence of motion in the liver and in surrounding tissues. It opens perspectives for the development of sophisticated temperature control algorithms on mobile organs.

---



S10-2

**Real time MR for in vivo monitoring of HIFU of the liver**

**Holbrook A.**<sup>1</sup>, Santos J.<sup>1</sup>, Kaye E.<sup>1</sup>, Rieke V.<sup>1</sup>, Butts Pauly K.<sup>1</sup>

<sup>1</sup>Stanford University, Stanford, USA

At ISTU2008, we demonstrated the capability of real-time MR temperature imaging of HIFU in a moving phantom. Since then, we have tailored the sequence for in vivo temperature imaging of the liver. More specifically, the spatial saturation time has been lengthened to better saturate in the presence of varying T1 and B1 inhomogeneity, and the readout trajectory is a flow compensated multishot flyback readout segmented EPI (RS-EPI) trajectory. Additionally, our referenceless thermometry reconstruction engine has been incorporated into RTHawk, a real time pulse sequence control environment. Upon acquisition, images are immediately displayed with temperature overlays showing the heated spot. Phantom experiments were performed to assess the sequence's motion performance. A polyacrylamide gel phantom was sonicated (62.4 acoustic W, 50 second duration, 550 kHz center frequency) while both stationary and moving. Additionally, in vivo abdominal imaging of healthy volunteers was performed to test the sequence and reconstruction's ability to acquire high-resolution images (1.4 x 1.4 x 4.7 mm<sup>3</sup>) of the liver and to assess its statistics. Heating spots and the corresponding temperature plots matched each other very well, and the mean measured temperature in the in vivo studies was -0.01°C. For the HIFU experiments, the two manually moved sonications had temperature standard deviations of 0.28°C and 0.43°C, compared to a value of 0.15°C for the stationary sonication. For the volunteers, the standard deviation was 1.72°C. These standard deviations are all sufficiently small for sonications on the order of 15-30°C, suggesting real time imaging of moving HIFU sonications is clinically feasible.

## S10-3

### Three dimensional motion compensation for real-time MRI guided focused ultrasound treatment of abdominal organs

**Ries M.**<sup>1</sup>, Denis de Senneville B.<sup>1</sup>, Maclair G.<sup>1</sup>, Köhler M.<sup>2</sup>, Quesson B.<sup>1</sup>, Monnen C.<sup>1</sup>

<sup>1</sup> CNRS/Université Victor Segalen Bordeaux 2, Bordeaux, France  
<sup>2</sup> Philips Healthcare, Vantaa, Finland

**OBJECTIVE:** MR-guided High Intensity Focused Ultrasound (HIFU) for the ablation of tumors in abdominal organs under free-breathing conditions poses two challenges: 1)The current organ position in 3D-space must be continuously tracked in order to reposition the focal point of the HIFU-device to avoid undesired tissue damage. 2)Phase variations due to the organ displacement must be corrected in real-time to prevent temperature artifacts. The presented work addresses both problems in three dimensions and in real-time. The feasibility of the proposed method is demonstrated with phantom experiments and in-vivo with an ablation of a pig kidney.

**MATERIAL AND METHODS:** This is achieved by tracking the target position on the MR-images with 2D-optical flow based image registration, while out-of-plane motion is compensated by slice tracking based on 2D selective navigator data. This allows real-time 3D positioning of the HIFU beam onto the moving target with an update frequency of up to 15Hz and sub-millimeter precision. The temperature evolution during the intervention is monitored by 3D motion compensated PRF-based MR-thermometry. For this, phase variations are pre-recorded during the respiratory cycle according to the navigator tracking position and subsequently eliminated in real-time from the thermometry data.

**RESULTS:** For both, phantom and in-vivo experimentation, real-time MR-thermometry (precision  $\pm 1^\circ\text{C}$ ) revealed that 3D tracking coupled with dynamic beam steering was able to fully compensate the continuous displacement of the target (1.5cm ptp), resulting in a well focused energy deposition in the preselected target area.

**CONCLUSIONS:** MR-guided HIFU-ablations of abdominal organs require a robust motion compensation of both, MR-thermometry and target position. The presented in-vivo data shows that real-time MR-thermometry coupled with dynamic beam steering are promising candidates for this role.

## S10-4

### Inter-costal liver ablation under real-time MR-thermometry with partial activation of a HIFU phased array transducer

**Quesson B.**<sup>1</sup>, Merle M.<sup>1</sup>, Roujol S.<sup>1</sup>, Köhler M.<sup>2</sup>, Denis de Senneville B.<sup>1</sup>, Moonen C.<sup>1</sup>

<sup>1</sup> CNRS/Université Victor Segalen Bordeaux 2, Bordeaux, France  
<sup>2</sup> Philips Healthcare, Vantaa, Finland

**OBJECTIVE:** HIFU ablation of liver tissue is hampered by the rib cage, which partially obstructs the beam path. This study presents a method for selectively deactivating transducer elements causing undesired temperature increases near the bones. The effectiveness of the method for HIFU ablations is demonstrated ex vivo and in vivo (pig liver) with real-time MR thermometry.

**MATERIAL AND METHODS:** Ex vivo: A porcine rib bone and liver sample was sonicated with a MR (1.5T) compatible Philips HIFU platform (256 elements transducer). 3D anatomical MR-imaging (TE/TR=4.6/8.6 ms, 1.8x1.8x3 mm voxel size) and manual segmentation of the bones was performed to identify the beam obstruction. The resulting mask was projected (ray tracing starting from the focal point) on the transducer and elements with more than 50% obstruction of their active surface were deactivated. Liver sonications (with/without deactivation) were monitored with real-time MR thermometry (EPI, TE/TR=22/200 ms, 1.5x2.5x6 mm voxel size, one slice observing the target, the other the bone obstruction). In vivo: Two liver sonications (250W acoustic power, 20 seconds duration) were performed on an anesthetized pig while breathing and motion related MR-thermometry artifacts were compensated with a multi-baseline phase correction.

**RESULTS:** Ex-vivo: With all elements active, a temperature increase of 15°C near the bones was observed, while deactivation of the 126 obstructed elements resulted in a 4°C increase only. Although this effectively halves the emitted power, the temperature increase (24°C) at the focal point was identical for both experiments. In vivo: Similarly, the temperature increase near the bones (12°C) was significantly reduced (5°C) when the obstructed elements were deactivated. The temperature increase at the focal point was found similar (16°C and 17°C) in both cases.

**CONCLUSION:** The proposed method is promising for inter-costal MR guided HIFU ablations, without requirement of partial rib resection.



**S10-5**

**The optical sensing and imaging of HIFU lesions**

**Roy R.**<sup>1</sup>, Lai P.<sup>1</sup>, Draudt A.<sup>1</sup>, Cleveland R.<sup>1</sup>, Murray T.<sup>1</sup>

<sup>1</sup> Boston University, Boston, USA

High intensity focused ultrasound (HIFU) is a powerful noninvasive tool for targeted tissue ablation. Effective and efficient utilization calls for monitoring techniques that can non-invasively image bubble-free lesions and/or detect the onset of lesion formation in real time. Tissue necrosis can lead to changes in both the optical scattering and absorption. We therefore propose a hybrid technique using light and sound, acousto-optic (AO) imaging, to sense and/or image changes in optical contrast at depth. The tissue to be treated is illuminated with diffuse near-infrared light that interacts nonlinearly with a focused ultrasound beam, resulting in an outgoing flux of phase modulated photons emanating from volume where both light and sound coexist. Both the photon flux and the average phase shift depend on the tissue optical properties. By using B-Mode ultrasound to pump the interaction, one can generate conventional ultrasound images with a color overlay indicating spatially-dependent optical properties. By using the HIFU beam to pump the AO response, one can monitor continuously and sense the initial stages of lesion formation in real time. We describe a method for both sensing and imaging lesion formation and present results obtained ex vivo in chicken breast. [Work supported by the Dept. of the Army (award No. DAMD17-02-2-0014) and the Center for Subsurface Sensing and Imaging Systems (NSF ERC Award No. EEC-9986821).]

---



**S10-6**

**Rapid MR-ARFI method for focal spot localization during focused ultrasound treatments**

**Kaye E.**<sup>1</sup>, Chen J.<sup>2</sup>, Butts Pauly K.<sup>1</sup>

<sup>1</sup> Stanford University, Stanford, USA

<sup>2</sup> Chinese Academy of Sciences, Beijing, China

**OBJECTIVES:** In MRgFUS, visualization of the focal spot has relied on “test spots” of a small temperature rise. MR acoustic radiation force imaging (MR-ARFI) could be used instead for visualization, without the need for a temperature rise. Previously, MR-ARFI has relied on relatively lengthy MR acquisition times of several minutes with the line scan acquisition [N.McDannold, 2008; J.Chen, 2008]. The goal of this study was to develop a method for rapid focal spot displacement mapping, based on MR-ARFI.

**MATERIALS AND METHODS:** A single shot MR-ARFI sequence was developed based on EPI with a reduced FOV. The MRI pulse sequence triggered the HIFU system to emit 6.1ms ultrasound pulses ( $f = 550$  kHz,  $P_a = 40$ W) during the encoding gradients, both applied along the y axis. Imaging was done in x-z plane with 1.56 mm x 2.1 mm resolution. A pair of MR images were obtained with identical imaging and sonication parameters, but with opposite polarity of the gradients. From these images, a phase difference image was calculated and converted to displacement. The imaging sequence was tested in a gel phantom and porcine tissue on a 3T GE MRI Scanner equipped with an InSightec ExAblate 2000 HIFU system with a 1000 element transducer.

**RESULTS:** The focal spot is well depicted in the displacement maps. A shortened the echo time of 50 ms and reduced b-value of 35 s/mm<sup>2</sup> gave improved SNR. For the same ultrasound power level, the maximum displacement was 3.14 $\mu$ m +/- 0.06 $\mu$ m in porcine tissue and 0.52 $\mu$ m +/- 0.13 $\mu$ m in the gel phantom.

**CONCLUSION:** The results of this study show that with the rapid MR-ARFI sequence the focal spot can be localized in 3 seconds with only two ultrasound pulses of < 10 ms each.



**Thermal analysis of the surrounding anatomy during 3D MRI-guided transurethral ultrasound prostate therapy**

**Burtnyk M.**<sup>1</sup>, Chopra R.<sup>1</sup>, Bronskill M.<sup>1</sup>

<sup>1</sup> University of Toronto, Toronto, Canada

Previous numerical simulations have shown that MRI-guided transurethral ultrasound therapy can generate highly accurate volumes of thermal coagulation conforming to 3D human prostate geometries. The goal of this work is to simulate, quantify and evaluate the thermal impact of these treatments on the rectum, pelvic bone, neurovascular bundles (NVB) and urinary sphincters, because damage to these structures can lead to complications. This study used twenty 3D anatomical models of prostate cancer patients and detailed bio-acoustic simulations incorporating an active feedback algorithm which controlled a rotating, planar ultrasound transducer (17-4x3mm elements, 4.7/9.7MHz, 10W/cm<sup>2</sup>). Heating of the adjacent surrounding anatomy was evaluated using thermal tolerances reported in the literature. Heating of the rectum poses the most important safety concern and is influenced largely by the water temperature flowing through an endorectal cooling device; temperatures of 7-37°C are required to limit potential damage to less than 10mm<sup>3</sup> on the outer 1mm layer of rectum. Significant heating of the pelvic bone occurred in 30% of the patient models in the absence of "treatment planning"; setting the frequency to 9.7MHz where the bone is less than 10mm away from the prostate reduced heating in all cases to below the threshold for irreversible damage. Heating of the NVB was significant in 80% of the patient models in the absence of treatment planning; this proportion was reduced to 5% by using treatment margins of up to 4mm. To avoid damaging the urinary sphincters, margins from the transducer of 1-4mm were used, depending on the transurethral cooling temperature. Simulations show that MRI-guided transurethral therapy can treat the prostate accurately. In the absence of treatment planning, however, significant thermal impact can be predicted for surrounding anatomy. Strategies have been developed which can be used to avoid causing thermal injury to the surrounding anatomy.



**Temperature mapping near the surface of ultrasound transducers using susceptibility-compensated magnetic resonance imaging**

**Webb A.**<sup>1</sup>, Neuberger T.<sup>2</sup>, Park E.<sup>2</sup>, Smith N.<sup>2</sup>

<sup>1</sup> Leiden University Medical Center, Leiden, The Netherlands

<sup>2</sup> The Pennsylvania State University, University Park, USA

MRI-based temperature mapping very close to the surface of an ultrasound transducer is not possible due to the large magnetic susceptibility-induced image artifacts which arise from the materials used in transducer construction. Here, it is shown in phantoms that the use of "susceptibility-compensated" MRI sequences can be used to measure thermal increases ~ 1 mm from the surface of a four-element cymbal array transducer, which has been used widely for non-invasive transdermal drug delivery. The estimated temperatures agree well with those measured using thermocouples.



## S10-9 Alternative focal spot geometry for more efficient HIFU treatment assessment

**Kaye E.**<sup>1</sup>, Chen J.<sup>2</sup>, Prus O.<sup>3</sup>, Medan Y.<sup>3</sup>, Butts Pauly K.<sup>1</sup>

<sup>1</sup> Stanford University, Stanford, USA

<sup>3</sup> InSightec Ltd., Tirat Carmel, Israel

<sup>2</sup> Institute of Biophysics, Beijing, China

**OBJECTIVES:** During MRI-guided HIFU treatments, assessment of the therapy is commonly performed with a gadolinium injection that delineates the non-perfused tissue. However, not all patients are candidates for this injection and those that are can only be assessed once at the end of the treatment. Another possibility is to obtain "stiffness-weighted" images with MR-ARFI by rastering the ultrasound focal spot through the tissue of interest and acquiring the image with a line scan acquisition [N.McDannold, 2008]. The goal of this work was to develop a more efficient MR-ARFI stiffness imaging method by focusing the ultrasound beam to a line focus, imaging with a rapid reduced FOV single shot EPI sequence, and repeating the acquisition while rastering the focal spot through one direction only.

**MATERIALS AND METHODS:** The imaging method was tested in gel phantom and porcine tissue on a 3T GE MRI Scanner equipped with an InSightec ExAblate 2000 HIFU system (550kHz) with a 1000 element transducer, focused to a line. Ultrasound pulses and displacement encoding gradients were 6.1ms long and applied along the y axis. Imaging was done in x-z plane. From pairs of images with opposite polarity of the encoding gradients, a phase difference image was calculated and converted to a displacement map.

**RESULTS:** A line focus can be seen in the magnitude images obtained after continuous HIFU heating in both gel phantom and porcine muscle. In the displacement maps, the shape of the focal spot appears more like two adjacent ovals rather than one line, with a total area approximately 6 times greater than the area of the point focal spot.

**CONCLUSION:** The combination of a line-shaped US focal spot and a reduced FOV single shot EPI acquisition can enhance the efficiency of "stiffness-weighted" MR imaging and serve as an alternative MRI-based technique for HIFU treatment assessment.

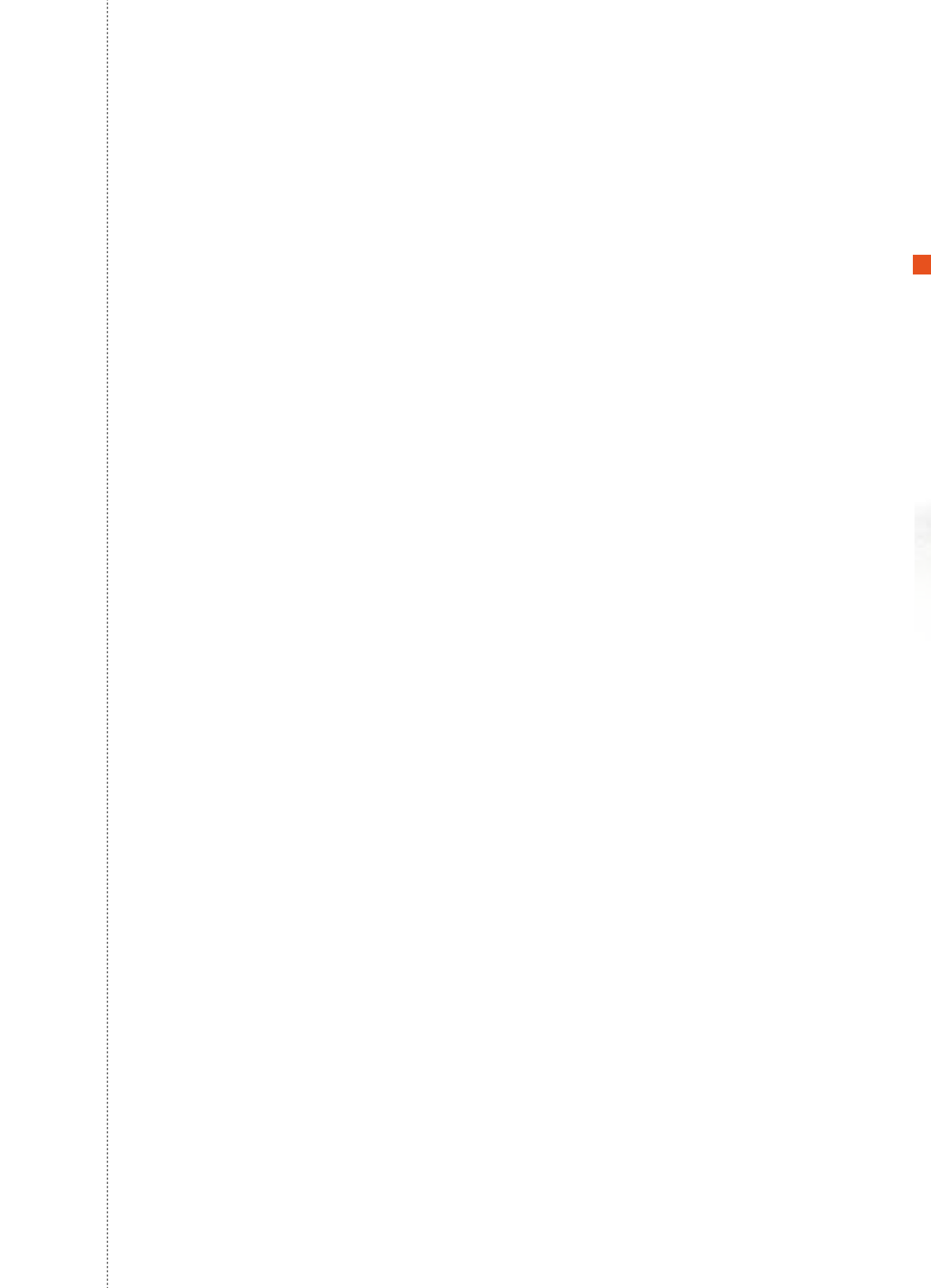


## S10-10 Robotically assisted MRgFUS system

**Jenne JW.**<sup>1</sup>, Kraff A.<sup>1</sup>, Maier F.<sup>1</sup>, Rauschenberg J.<sup>1</sup>, Huber P.<sup>1</sup>, Bock M.<sup>1</sup>

<sup>1</sup> German Cancer Research Center, Heidelberg, Germany

Magnetic resonance imaging guided focus ultrasound surgery (MRgFUS) is a highly precise method to ablate tissue non-invasively. The objective of this ongoing work is to establish an MRgFUS therapy unit consisting of a specially designed FUS applicator as an add-on to a commercial robotic assistance system originally designed for percutaneous needle interventions in whole-body MRI systems. The fully MR compatible robotic assistance system Innomotion™ (Innomedic, Germany) offers six degrees of freedom. The developed "add-on" FUS treatment applicator is directly connected to the head of the robotic system and features a ultrasound transducer ( $f = 1.7$  MHz;  $f = 68$  mm,  $NA = 0.44$ ) embedded in a water-filled flexible bellow. A polyester foil is used as acoustic window encompassed by a dedicated MRI loop coil. The treatment region is targeted from above. Newly in-house developed software modifications allow a complete remote control of the MRgFUS-robot system and online analysis of MRI thermometry data. The system's ability for therapeutic relevant focal spot scanning was tested in a closed-bore clinical 1.5 T MR scanner (Siemens) in animal experiments with pigs. The FUS therapy procedure was performed entirely under MRI guidance including initial therapy planning, on-line MR-thermometry, and final contrast enhanced imaging for lesion detection. In vivo trials proved the MRgFUS-robot system as highly MR compatible. MR-guided focal spot scanning experiments were performed and a well-defined pattern of thermal tissue lesions was created. A total in vivo positioning accuracy of the US focus better than 2mm was estimated which is comparable to existing MRgFUS systems. The newly developed FUS-robotic system offers an accurate, highly flexible focus positioning. With its access to the patient from above, it provides a wide range of flexibility for acoustic target access. In the next step, a motion correction unit should be integrated.



# Posters

[www.istu2009.org](http://www.istu2009.org)



## FOCUSED ULTRASOUND SURGERY FOUNDATION

### The Focused Ultrasound Surgery Foundation Congratulates ISTU on the Success of their 9th International Symposium

The Focused Ultrasound Surgery Foundation (FUSF) would like to recognize GE, InSightec, Philips, Siemens and Supersonic Imagine in establishing its Collaborative Research Network for MR-guided focused ultrasound.

Scientists and clinicians interested in MR-guided focused ultrasound are invited to speak with Heather Huff-Simonin, FUSF Director of Collaborative Research, regarding future funding opportunities and participation in the FUSF Research Network. Visit us at stand #7. We look forward to supporting your research.



**Save the Date** October 17 - 20, 2010 —————  
2<sup>nd</sup> **INTERNATIONAL MRgFUS SYMPOSIUM** - Washington, DC

Join our email list to receive research, funding and symposium updates at [www.fusfoundation.org](http://www.fusfoundation.org)





### **A photoacoustic sensor for monitoring in situ temperature during HIFU exposures**

**Chitnis P.**<sup>1</sup>, McLaughlan J.<sup>2</sup>, Mamou J.<sup>1</sup>, Murray T.<sup>2</sup>, Roy R.<sup>2</sup>

<sup>1</sup>Riverside Research Institute, New York, USA

<sup>2</sup>Boston University, Boston, USA

**OBJECTIVE:** To investigate the feasibility of using a photoacoustic (PA) sensor to monitor in situ temperature and cavitation during high intensity focused ultrasound (HIFU) exposures.

**MATERIAL & METHODS:** PolyAcrylamide phantoms (40X40X27mm) with a cylindrical inclusion (3X20mm) of graphite (0.01g/ml) were heated using 30s exposures from a HIFU transducer (center frequency 2MHz, focal distance 60mm, aperture 70mm). The focus was aligned to the tip of a wire thermocouple (diameter 0.13mm), that was embedded in the inclusion for monitoring the temperature. A pulsed laser (wavelength 532nm, pulse duration 10ns) was used to illuminate the inclusion. A 15MHz transducer (focal distance 19mm, aperture 9mm) was employed as a passive receiver (PR) to simultaneously detect (1) the PA response (an ultrasonic pulse emanating from the inclusion due to thermoelastic expansion induced by optical absorption) and (2) the HIFU-induced, inertial cavitation noise. The temperature and the PR signals were recorded pre-, during-, and post-HIFU exposure. Singular-value-decomposition (SVD) analysis of the received PR signals was performed to separate the contributions from temperature change and cavitation.

**RESULTS:** Thermocouple measurements indicated a temperature increase from 22°C to between 45 and 60°C for different HIFU intensities. The SVD-deduced temperature curves obtained from the real-time PA signals correlated well with the thermocouple measurements (root mean squared error <4°C). Net increase in temperature corresponded to a 20-30% increase in PA amplitude. The SVD-deduced cavitation data extracted from the PR signals showed that cavitation onset was immediate and higher HIFU intensities resulted in larger cavitation signals followed by the "shielding" phenomenon.

**CONCLUSIONS:** The PA temperature-measurement technique was able to track both heating and cooling phases over temperatures characteristic of HIFU treatment. The PR also provided quantifiable measure of inertial cavitation.



### **Ultrasound temperature monitoring in the scalp**

**Garapon P.**<sup>1</sup>, Couture O.<sup>1</sup>, Tanter M.<sup>1</sup>

<sup>1</sup>ESPCI, CNRS, Paris, France

**OBJECTIVES:** Intracranial high intensity focused ultrasound can induce dose-limiting cavitation and temperature elevation within the scalp. Heating at the focus of a HIFU array has been previously monitored with ultrasound speckle decorrelation. Our objective is to measure the temperature increase within the scalp using the elements of the HIFU array in pulse-echo mode.

**METHODS:** A thermocouple (type J) was attached to a human skull and covered with a 5 mm thick layer of tissue mimicking gel (agar 3%, cellulose 1.5%). The skull was placed in a water tank and its surface was aligned within the focus of a 2.25 MHz transducer (f: 38 mm, #1). Heating was induced by pulses of 0.2 to 3 seconds in length at 0.5 to 3 MPa peak-negative pressure. 15 microseconds later, a series of 450 one-arch pulses were generated to follow the cooling of the skull. The echoes from the surface of the gel and the skull were collected by the electronic of the HIFU array. The apparent thickness change of the scalp, due to a modification in the speed of sound, was measured by cross-correlation with the echo of the first pulse.

**RESULTS:** Following a 2 seconds 3 MPa pulse, a 6.2oC temperature increase was measured at the thermocouple. Such heating lead to a 900 ns shift in the main echo of the cranium. This shift gradually decreased with thermal diffusion until reaching the noise floor after several minutes. The speckle behind the skull surface (within the bone) displayed important decorrelation during heating. The shift of the main skull echo was compared to the thermocouple as an estimator for temperature change. A variation of 1.5oC could be detected with pulse-echo (n=10).

**CONCLUSIONS:** Small temperature variations, below the threshold for thermal damage of healthy tissue, can be detected in the scalp using the electronics of a HIFU array. Lower temperature-resolution are expected at 1 MHz, but could be compensated by using, as an estimator, the complex speckle within the skull bone.



**P1-3**

**Effect of low intensity pulsed ultrasound on transcriptional gene expression of calvarial bone**

**Gleizal A.**<sup>1</sup>, Li S.<sup>2</sup>, Pialat J.<sup>2</sup>, Béra J.<sup>1</sup>, Lavandier B.<sup>2</sup>, Beziat J.<sup>1</sup>

<sup>1</sup>Hopitaux Nord, Lyon, France

<sup>2</sup>INSERM, Lyon, France

The capacity to re-ossify a calvarial bone defect is very small in mature animals and in humans older than two years of age. The use of low intensity pulsed ultrasound offers a possible treatment of injured tissue sites of bones. The biological mechanisms implicated are not well known. The present work investigated the expression of osteogenesis-associated genes after sonication in adult mouse osteoblasts from the parietal calvaria using real-time polymerase chain reaction. Three intensities of pulsed ultrasound (1MHz, 100 Hz pulse repetition frequency and 20% duty cycle): 100, 300 and 500 mW/cm<sup>2</sup> SATA were investigated. Ultrasound was applied 5 minutes per day. Results on proliferation rate show an increase in osteoblast proliferation rate induced by ultrasound. The gene associated with the Runx2 pathway had notably higher levels after 1, 2 and 3 days of stimulation. Results show that 100 mW/cm<sup>2</sup> was the most efficient of the three investigated intensities, particularly after one day.



**P1-4**

**Detailed histological assessment of in vivo tissue exposed to high intensity focused ultrasound (HIFU)**

**Jayadewa C.**<sup>1</sup>, Rivens I.<sup>1</sup>, Ter Haar G.<sup>1</sup>

<sup>1</sup>Institute of Cancer Research, Sutton, UK

HIFU is used clinically for the treatment of soft tissue tumours. Long treatment times are one of the main limitations of HIFU therapy and ways of overcoming this are being sought. A more comprehensive understanding of the biological effects that occur during and following HIFU exposure may aid treatment optimisation. The aim of this study is to investigate the biological response to HIFU exposure histologically over a period of up to 3 weeks. The study was performed on rat liver in vivo using a highly-focused (f-number 1.2) transducer driven at 1.7 MHz (Siemens Germany). Single lesions (4 per liver) were created at a focal depth of 5 mm below the liver surface using a free-field spatial-peak intensity of 2753±192 Wcm<sup>-2</sup> for 4 s (Boiling) or 1751±119 Wcm<sup>-2</sup> for 6s (Acoustic Cavitation). The resulting lesions were investigated using an array of histological stains, chosen to assess both morphological (tinctorial stains) and functional changes (immunohistochemistry). The stains included Haematoxylin and Eosin for basic morphology, Picrosirius Red-Millers for collagen and elastin, Ki67 for cellular proliferation, cleaved Caspase 3 for apoptotic cells and CD68 for macrophages. The preliminary results at 1 and 2 day time points from Ki67 stained tissue show positive cellular staining in the lesion, indicative of proliferating cells within the lesion volume, however, further studies are required to confirm this possibility. Cleaved caspase 3 and CD68 stained tissue show positive staining only at the lesion periphery. Further extended timescale studies should provide better understanding of the spatial and temporal evolution of apoptotic and inflammatory reactions. The band of apoptotic cells at the lesion margin may increase the final volume of damaged tissue. Understanding this effect could help in optimising clinical lesion placement.

P1-5

**Does low intensity pulsed ultrasound accelerate calvarial bone defect reconstruction ? An experimental study in murine model.**

**Lavandier B.**<sup>1</sup>, Gleizal A.<sup>2</sup>, Béra J.<sup>1</sup>

<sup>1</sup> INSERM, Lyon, France

<sup>2</sup> Hôpitaux Nord, Lyon, France

Ultrasound treatment has been proposed by several authors to enhance the repair of long bone injury. The present study investigated in a murine model the treatment by low-intensity pulsed ultrasound (LIPUS) of calvarial flat bone defect. The animals were operated to create bone defect and exposed to ultrasound for 5 min per day, 5 days per week, during two weeks. Two intensities of ultrasound (1MHz, 100 Hz pulse repetition frequency and 20% duty cycle) were investigated: 100 and 300 mW/cm<sup>2</sup> SATA. Re-ossification surface and volume were determined after 30 and 60 days using computerized X-ray tomography in all animals of the control and treated groups. The results showed a significant increase of bone regeneration in the group treated with the higher-intensity ultrasound (mean value of 18% volume reconstruction) whereas quasi-similar low bone reconstruction was observed in the lower-intensity and the control groups (respective mean values of 10 and 12% volume reconstruction). The results showed that bone regeneration occurred during the first month after surgery, no significant increase was observed after 30 days.

P1-6

**Study of parameters affecting the level of ultrasound exposure with in vitro set-ups**

**Leskinen J.**<sup>1</sup>, Hynynen K.<sup>2</sup>

<sup>1</sup> University of Kuopio, Kuopio, Finland

<sup>2</sup> University of Toronto and Sunnybrook Health Sciences Centre, Toronto, Canada

**OBJECTIVES:** Ultrasound (US) exposures are widely used with in vitro cell systems e.g. in stem cell and tissue engineering research. However, without the knowledge of factors affecting the level of US exposure, the outcome of the biological result may vary from test to test or even be misinterpreted. Thereby, several factors affecting in vitro exposures were studied specifically in cases where sound reflecting fluid-air interface is present as this type of set-ups are routinely used with success.

**MATERIAL & METHODS:** Level of US exposure was characterized in cell culturing plates with different methods. These included temperature distributions measurement inside the wells using infrared camera and fine wire thermocouples, and pressure and intensity distributions measurements using laser vibrometer and Schlieren system. The measurements were made at operating frequency of around 1 MHz with varying temporal parameters and powers (up to 2 W of acoustic power).

**RESULTS:** Heat accumulation between the wells may vary up to 40 to 50% according the location of the well on the plate. This well-to-well variation can be linked to the activity of reporter plasmid on osteoblastic cells. Similar level temperature variation within the wells was also found. Small sub-wavelength change of exposure distance or, respectively, liquid volume inside the well was found to alter the acoustic field in both magnitude and shape due the standing wave and liquid movement.

**CONCLUSIONS:** The gathered data reveals the complexity of the acoustic field with many in vitro set-ups and gives new information about the circumstances the cells are experiencing during US in vitro stimulations. This data may be especially useful when US set-ups are designed or characterized e.g. in vitro stem cell differentiation studies where long-duration, repeated exposures are used.



**Dynamic analysis of irradiation of high intensity focused ultrasound (HIFU) to achieve a living tissue perforation**

**Mochizuki T.**<sup>1</sup>, Kitazumi G.<sup>2</sup>, Katsuike Y.<sup>2</sup>, Hotta S.<sup>2</sup>, Maruyama H.<sup>3</sup>, Chiba T.<sup>2</sup>

<sup>1</sup> Aloka Co. Ltd., Tokyo, Japan

<sup>2</sup> National Center for Child Health and Development, Tokyo, Japan

<sup>3</sup> Japan Broadcasting Corporation, Tokyo, Japan

**OBJECTIVE:** As an intrauterine prevention of development of hypoplastic cardiac crisis, we have been investigating feasibility of high intensity focused ultrasound (HIFU) irradiation to perforate the atrial septum within a beating heart. Here, we discuss the HIFU parameters that are potentially most appropriate for this purpose.

**MATERIALS & METHODS:** Experiment 1: Both a piece of chicken meat and an excised rabbit mesenterium were irradiated with HIFU and its focal zone was viewed and recorded in real time using a high speed CCD camera at the rate of 10,000 frames per second (fps). Experiment 2: Cavitations generated by continuous HIFU irradiation in degassed water have been observed for 100 micro seconds by the other ultra-high speed camera at 770,000 fps.

**RESULTS:** Ultrasonic perforations may be caused by three mechanisms; cavitations, irradiation force and thermal destruction. Experiment 1, however, strongly suggests that the cavitations predominantly cause living tissue perforations. HIFU irradiation immediately could push down the surface of the meat with its subsequent cracking. Probably, the irradiation force can also push away the surface, but its power did not seem enough to make a crack. Time for cracking was too short to be caused by the thermal destructive effect on the tissue. In experiment 2, generations of cavitations were definitely observed and the HIFU focal point where bubbles appeared subsequently was clearly recorded.

**CONCLUSIONS:** The mechanism of tissue perforation was based on the shock wave generation. These waves were generated when the cavitation bubbles were intensively pressed and collapsed. To achieve cavitations and to grow the bubbles effectively, a low frequency ultrasound that has greater negative sound pressure with a long burst waveform is needed. Based on these outcomes, in the next stage, best parameter conditions for HIFU irradiation will be studied to accomplish therapeutic tissue perforation.



**Multi-frequency characterization of speed of sound for longitudinal transmission on freshly excised human skulls**

**Pichardo S.**<sup>1</sup>, Hynynen K.<sup>2</sup>

<sup>1</sup> Thunder Bay Regional Research Institute, Thunder Bay, Canada

<sup>2</sup> Sunnybrook Research Institute, Toronto, Canada

The results of measurements of longitudinal speed of sound are presented for seven specimens of human calvaria. The study was done for frequencies between 0.27 and 2.525 MHz. Specimens were obtained from fresh cadavers through a protocol with the Division of Anatomy of the University of Toronto. The specimens were mounted in polycarbonate supports that were marked for stereoscopic positioning. CT scans of the skulls mounted on their supports were performed and a three-dimensional reconstruction of the skull surface was done. A positioning system ensured normal sound incidence of an acoustic signal produced by a focused device with a diameter of 5 cm and a F-number of 2. Speed of sound estimation was done with measurements of time-of-flight using a needle hydrophone (diameter of 0.5mm) and a sound propagation model through layers that takes into account change of speed of sound in function of density. For six of seven specimens, measurements were done on five locations on the calvaria and for the other specimen three measurements were done. In total, measurements were done on thirty-three locations. Results showed that the average ( $\pm$ s.d.) of the speed of sound was 2265( $\pm$ 202), 2360( $\pm$ 207), 2317( $\pm$ 283), 2309( $\pm$ 248) and 2080( $\pm$ 148) m/s for frequencies of 0.27, 0.836, 1.402, 1.965 and 2.525 MHz, respectively. Dispersion effects were observed at individual basis per specimen, which were detected for the six of specimens as an increase in the speed sound when frequency went from 0.27 to 0.836 MHz. However, this increase was only statistically significant ( $p$ -value $\leq$ 0.05) for two specimens, with a maximal increase of +152m/s. A decrease in the speed of sound was also observed for four specimens when the frequency reached the highest values but it was statistically significant only for one of them ( $p$  = 0.03), with a decrease of -229m/s.



**P1-9**

**New dynamical focusing method for HIFU therapeutic applications**

**Rybyanets A.**<sup>1</sup>

<sup>1</sup> South Federal University, Rostov on Don, Russia

New method for direct synthesis of dynamically focused acoustic field suitable for HIFU applications is proposed. The method is based on the continuous cyclic generation of different focal patterns at optimal repetition frequency by simultaneous applying of "M" different frequency signals to "N" sectors of spherically shaped sectorized transducer array. The HIFU transducer arrays comprising a spherical piezoceramic cap with back electrode divided circumferentially into "N" ( $N > 1$ ) regular or specially shaped sectors were designed and tested. The sectors were simultaneously powered by "M" ( $1 < M \leq N$ ) sinus or burst drive signals with different frequencies from 6 dB bandwidth of the transducer array. Calculation and modeling of acoustic field patterns for different array configurations and frequencies sets were performed. Acoustic pressure in focal planes was measured in water using calibrated hydrophone and 3D acoustic scanning system. In vitro experiments on different tissues confirming the advantages of dynamical focusing method were performed. The benefits of dynamical focusing method are creating bigger treated tissue volumes and enhancement of the cavitation, mechanical or thermal influences due to higher pressure gradients, microstreamings and shear deformations. Additional increase of influence is provided by optimal repetition frequency corresponding to a specific resonance/relaxation times for tissues and/or cavitation "clouds". Applications of dynamical focusing method for ultrasonic surgery, hyperthermia, therapy and body aesthetics were considered.



**P1-10**

**Multi-frequency harmonic method for HIFU tissue treatment**

**Rybyanets A.**<sup>1</sup>, Iugovaya M.<sup>1</sup>, Rybyanets A.<sup>1</sup>

<sup>1</sup> South Federal University, Rostov on Don, Russia

New method for enhancing of tissue lysis and enlarging treatment volume during one sonification is proposed. The method consists in simultaneous or alternative (at optimal repetition frequency) excitation of single element HIFU transducer on a number of frequencies corresponding to odd natural harmonics of piezoceramic element. Calculation and modeling of acoustic field patterns for different frequencies sets were performed. Acoustic pressure in focal plane was measured in water using calibrated hydrophone and 3D acoustic scanning system. In vitro experiments on different tissues confirming the advantages of multi-frequency harmonic method were performed. In the experiments the HIFU transducer was excited simultaneously or sequentially on frequencies corresponding to 1st, 3rd and 5th harmonics at ultrasound energy levels sufficient for producing cavitation, thermal or mechanical damage of fat cells at each of aforementioned frequencies. Enhancement of the lysis was reached due to simultaneous or sequential influence of harmonic frequencies providing cavitation or mechanical lysis of tissue, formation of inhomogeneous ultrasound beam patterns with enhanced pressure gradients and shear deformations, and generation of difference and summary frequencies as a result of non linear parametric and radiation pressures interactions of main frequencies. Additional increase in lysis activity is provided by optimal repetition frequencies, bursts lengths and sonification times that correspond to specific resonance/relaxation times of cavitation "clouds" and/or tissues as well as natural body reaction times. Applications of multi-frequency harmonic method for ultrasonic surgery, hyperthermia, therapy and body aesthetics were considered. The multi-frequency harmonic method brings a new approach to accelerate treatment of big volumes of adipose tissue or tumors ablation with HIFU and also provides a miniaturization of the conventional HIFU transducers.



**P1-11** QOL after HIFU for prostate cancer

**Satoh M.**<sup>1</sup>, Kuwahara M.<sup>1</sup>, Nakano O.<sup>1</sup>, Horinouchi T.<sup>1</sup>, Kudo T.<sup>1</sup>, Arai Y.<sup>2</sup>

<sup>1</sup> Sen-en General hospital, Tagajo, Japan

<sup>2</sup> Tohoku University, School of Medicine, Sendai, Japan

**OBJECTIVE:** To determine the effect of high-intensity focused ultrasound (HIFU) on health related quality of life(HRQOL) for organ-confined prostate cancer.

**MATERIALS AND METHODS:** From May 2006 to March 2009, 89 patients were treated using sonoablate-500 (focus Surgery, Indianapolis, IN, USA) and 36 patients were underwent radical prostatectomy (RRP) for T1 or T2, T3 prostate cancer at our institution. We investigated the prostate specific HRQOL by Expanded Prostate Cancer Index Composite (EPIC) and the general HRQOL by the Medical Outcomes Study 8-Item Short Form (SF 8) -1, 0, 6, 12, 18, 24 months after HIFU therapy. Follow-up included prostate specific antigen tests at 1month and then every 3 months after HIFU, and random prostate biopsy at 6 months. Failure was defined according to positive findings on follow-up biopsy and biochemical failure according to the definition decided during a joint American Society for Therapeutic Radiology and Oncology-Radiation Therapy Oncology Group conference in Phoenix (ASTRO criteria).

**RESULTS:** In HIFU group, there was no biochemical evidence of disease in 87% overall. At 6 months the negative biopsy rate was 91 %. Urinary function, bother and irritation score substantially declined just after HIFU therapy and continued to recover to the base line after 3 months. Sexual function score in patients with high base line before HIFU therapy showed good recovery after 1months and recover to near the base line after 3 months. In RRP group, sexual function score decreased just after RRP and remained substantially lower than the base line level. There was no significant difference in general HRQOL scores of HIFU and RRP group.

**CONCLUSION:** Prostate specific and general HRQOL scores were mostly unaffected by HIFU after 3 months after treatment.

---





P2-1

### In vitro models of thrombolysis of arterial bypass grafts with pulsed high-intensity focused ultrasound

**Abi-Jaoudeh N.**<sup>1</sup>, Jones G.<sup>2</sup>, Hancock H.<sup>1</sup>, Razjouyan F.<sup>1</sup>, Frenkel V.<sup>1</sup>, Wood B.<sup>1</sup>

<sup>1</sup> National Institute of Health, Bethesda, USA

<sup>2</sup> National Institute of Health, Rockville Pike, USA

**OBJECTIVES:** Thrombolysis is the accepted treatment of failed arterial and arterio-venous bypass grafts. However thrombolysis can require prolonged time and is associated with increased bleeding risk. The purpose of the study was to determine feasibility and efficiency of pulsed high-intensity focused ultrasound (pHIFU) thrombolysis of typical bypass graft materials using a published in vitro model. The effects of pHIFU mediated thrombolysis on various material compositions and geometries of clinical grafts are unknown.

**MATERIALS & METHODS:** Several types of grafts were tested including Penrose tubing (Sherwood Medical, Mo, USA), woven polyester grafts (Ultramax, Atrium, NH, USA), ePTFE grafts (ePTFE Ultrathin, wrap, Vascutek, Terumo, MI, USA, & Flexine, Atrium, NH, USA). Thrombus was formed by placing 1mL of human blood in sealed 2 inch sections of the graft materials. Penrose tubing served as the control group. Several samples of each material were studied. Half the groups were treated with pHIFU for 30 minutes at a total acoustic power of 60 W, 6x 2 raster points, 60 pulses per raster point. The other half was incubated in a 37° C water bath. All clots were infused with 2mL of thrombolytic solution (t-PA) for 33 minutes in a 37° C water bath. Thrombolysis was measured as the relative reduction in thrombus weight.

**RESULTS:** There was a significant, variable interaction between pHIFU and the various materials. Therefore we did a separate paired t-test for pHIFU with each material; p values were Bonferroni adjusted for multiple comparisons. The increase in the degree of thrombolysis was for the Penrose: 8% (p: 0.54), for the ribbed woven polyester: 1% (p: 1.00), for the ePTFE grafts: 12% (p: 0.042). **CONCLUSIONS:** pHIFU does not enhance t-PA thrombolysis in all types of grafts. In our experiments, the effect of pHIFU was significant only with the ePTFE grafts compared to other materials.

P2-2

### Development of an acoustic droplet vaporization, ultrasound drug delivery emulsion

**Fabiilli M.**<sup>1</sup>, Sebastian I.<sup>2</sup>, Fowlkes J.<sup>1</sup>

<sup>1</sup> University of Michigan, Ann Arbor, USA

<sup>2</sup> University of Michigan, Miyagi, Japan

**OBJECTIVE:** Superheated liquid emulsions that can be vaporized using ultrasound (US), a process called acoustic droplet vaporization (ADV), may be used in US based drug delivery (DD). Compared to gaseous contrast agents, ADV has the added therapeutic capability of spatially-selective vascular occlusion. This work develops micron-sized, superheated emulsions that carry the chemotherapy drug chlorambucil (CHL).

**MATERIAL & METHODS:** Emulsions were prepared using a surfactant (lipid, albumin or Pluronic F68), saline, perfluoropentane (PFP), and soybean oil containing dissolved CHL or a fluorescent dye. Droplets were sized with a Coulter counter (CC). Fluorescence microscopy was used to determine the location of the oil (drug carrying phase) within the droplets. The effect of CHL leakage, without US exposure, was determined in vitro using Chinese hamster ovary (CHO) cells plated in 6-well microtiter plates. The cells were incubated with the injected emulsions for up to 24 hours, washed, and then the medium was replaced. The cells were trypsinized and counted, using a CC, 48 hours post-injection.

**RESULTS:** Lipid-stabilized droplets displayed the most desirable size distributions, with a 3 µm mean diameter and <2% (by number) greater than 10 µm, and the least cytotoxicity due to CHL leakage. The dye-stained oil layer homogeneously surrounded the PFP core. Droplets without CHL or dye showed no significant effect on the CHO cell growth rate at a concentration of 100 droplets/cell for up to a 24 hour exposure. At the same concentration, CHL emulsions caused a 20% and 70% decrease in cell growth rate at 30 minute and 24 hour exposures, respectively. All emulsions were vaporizable using a 10 MHz linear array (GE L9, MI = 0.9).

**CONCLUSIONS:** Stable, micron-sized, superheated emulsions have been formulated and tested for cytotoxicity due to CHL leakage from the droplets. The oil layer location within the droplet may enhance the CHL dispersion upon ADV.



P2-3

**Delivery improvement into brain tissue with ultrasound sonication after blood-brain barrier opened temporarily by focused ultrasound with microbubbles**

**Lee Y.**<sup>1</sup>, Hu S.<sup>2</sup>, Wu X.<sup>1</sup>, Lin W.<sup>1</sup>

<sup>1</sup> National Taiwan University, Taipei, Taiwan

<sup>2</sup> National Chiao Tung University, Hsinchu, Taiwan

**OBJECTIVES:** In this paper, we investigated the effects of ultrasound sonication on the delivery enhancement of Evans Blue (EB) and self-assemble iron oxide nanocarriers (about 60 nm) into rat brain after the blood-brain barrier was opened temporarily by focused ultrasound with microbubbles.

**METHOD AND MATERIALS:** Wistar rats weighing about 380g were used in this study and the hair on their heads was removed thoroughly. 1.0 MHz focused ultrasound was noninvasively sonicated through the skull to the target region at 1.2 MPa pressure, 50ms burst length, 1 Hz repetition frequency, and 60s duration, to disrupt the blood-brain barrier temporarily, after an intravenous injection of microbubbles (200 µl/kg, Artison). A second sonication was exposed at the same location after microbubbles in the blood were cleared and EB and/or iron oxide nanocarrier were injected. All rats were sacrificed about 4 hrs after the second sonication. The brains were removed and sectioned for extraction and detection of EB/nanocarrier extravasation and distribution.

**RESULTS:** The results of EB extraction showed that the density of EB in the half brains with a second sonication is 98.43±35.48 µg/g of brain tissue compared to 9.46±2.94 µg/g for those without a second sonication. The spatial distribution of EB stain and fluorescent dye (Fluorescein isothiocyanate, FITC) for nanocarrier in the sonicated regions showed that a larger and much deeper region was produced for a second sonication.

**CONCLUSION:** A second sonication without the injection of microbubbles can effectively enhance the delivery of molecules (EB) and nanoparticles (iron oxide nanocarrier) into the region with BBB temporarily disrupted. It indicated that this sonication strategy is potentially employed to improve the drug delivery within a limited duration. Note: This research was supported by National Science Council of Taiwan.



P2-4

**Intravenous delivery of pDNA and siRNA into muscle with bubble liposomes and ultrasound**

**Negishi Y.**<sup>1</sup>, Sekine S.<sup>2</sup>, Endo Y.<sup>1</sup>, Suzuki R.<sup>3</sup>, Maruyama K.<sup>3</sup>, Aramaki Y.<sup>1</sup>

<sup>1</sup> Tokyo University of Pharmacy and Life Sciences, Hachioji, Japan

<sup>2</sup> Tokyo University of Pharmacy and Life Sciences, Tokyo, Japan <sup>3</sup> Teikyo University, Sagami-hara, Japan

**BACKGROUND:** Skeletal muscle is an attractive target tissue for numerous gene therapy strategies. Gene delivery for muscle has been extensively studied. Of these, intravascular delivery of naked pDNA is desirable. Muscle has a high density of capillaries that are in close contact with the myofibers. Previously, we have developed the polyethyleneglycol (PEG)-modified liposomes entrapping echo-contrast gas known as Ultrasound (US) imaging gas. We have called the liposomes "Bubble liposomes" (BLs). It has been reported that BLs improve the tissue permeability by cavitation with US exposure. Here, we modified the naked pDNA or siRNA transfer method into hind limb muscle through blood vessels using BLs and US.

**METHODS:** A tourniquet was placed on the upper hind limb to restrict blood flow into and out of the hind limb. pCMV-Luc encoding Luciferase gene and/or its siRNA was injected with BLs into great saphenous vein. Immediately, the muscle was exposed with Ultrasound (Frequency: 1 MHz, Duty: 50 %, time: 120 sec) and subsequently, tourniquet was removed. The limb muscles were harvested and separated at different time point after the gene delivery. The luciferase expressions were measured.

**RESULTS:** Intravenous delivery of pDNA into the muscle can be greatly enhanced when the pDNA was delivered in the combination of BLs and US. In addition, the expression of pDNA was high in the US-focused site. Moreover, the efficient gene delivery can be achieved by intravenous delivery of pDNA into muscle with Bubble liposomes and ultrasound. The expression was also down-regulated by delivering of its siRNA with BLs and US.

**CONCLUSION:** This US-mediated BLs technique through vein may provide an effective method for gene therapy.

**P2-5**

**Inhibition of melanoma metastasis by dendritic cell-based cancer immunotherapy utilized liposomal bubbles and ultrasound**

**Otake S.**<sup>1</sup>, Oda Y.<sup>2</sup>, Suzuki R.<sup>1</sup>, Utoguchi N.<sup>1</sup>, Taira Y.<sup>1</sup>, Maruyama K.<sup>1</sup>

<sup>1</sup> School of Pharmaceutical Sciences, Teikyo University, Kanagawa, Japan

<sup>2</sup> School of Pharmaceutical Sciences, Teikyo University, Sagami-hara, Japan

**OBJECTIVES:** It is necessary to establish an efficient therapy against cancer metastasis because of impairment of prognosis. In this point, dendritic cell (DC) based cancer immunotherapy is expected that a therapeutic strategy preventable tumor metastasis and recurrence. Recently, we developed novel antigen delivery system for DCs by the combination of ultrasound and liposomal bubbles (Bubble liposomes: BLs) entrapping the ultrasound imaging gas, perfluoropropane. Additionally, we succeeded to induce anti-tumor immunity by the immunization of DCs treated with this antigen delivery system. In this study, we examined the effect of lung metastasis by immunization of DCs treated with BLs and US.

**MATERIAL & METHODS:** Mouse bone marrow-derived DCs were exposed with US (2 MHz, 2 W/cm<sup>2</sup>, Duty 10 %, 10 sec. × 3 times) in presence of BLs and mouse melanoma B16BL6 cells derived antigens. After cell washed and 24 hr-incubation, the mice were intradermally immunized DCs twice with 1 week interval. One week later of final immunization, these mice intravenous administrated mouse melanoma B16BL6 cells for the lung metastasis model. The mice were sacrificed on 14 days after tumor administration, and the inhibiting effect of lung metastasis were assessed by the count of lung metastasis colonies. [Results] Lung metastasis was effectively inhibited by the immunization of DCs delivered antigens with BLs and US compared to the immunization of DCs treated with/without antigens.

**CONCLUSIONS:** This result suggested that the immunization of DCs delivered antigen with BLs and ultrasound could induce effective immunity for melanoma. Therefore, the combination of BLs and ultrasound would be a promising antigen delivery system into DCs for prevention of cancer metastasis.

**ACKNOWLEDGEMENT:** We are grateful to Dr. Naoki Okada (Graduate school of Pharmaceutical Sciences, Osaka University) and Dr. Norimitsu Kadowaki (Graduate school of medicine, Kyoto University). This study was supported by NIBIO.

---

**P2-6**

**Dose comparison of ultrasonic transdermal insulin delivery to subcutaneous insulin injection**

**Smith N.**<sup>1</sup>, Park E.<sup>2</sup>, Dodds J.<sup>1</sup>

<sup>1</sup> The Pennsylvania State University, University Park, USA

<sup>2</sup> The Pennsylvania State University, State College, USA

Prior studies have demonstrated the effectiveness of noninvasive transdermal insulin delivery using a cymbal transducer array. In this study the physiologic response to ultrasound mediated transdermal insulin delivery is compared to that of subcutaneously administered insulin. Anesthetized rats (350–550 g) were divided into four groups of four animals; one group representing ultrasound mediated insulin delivery and three representing subcutaneously administered insulin (0.15, 0.20, and 0.25 U/kg). The cymbal array was operated for 60 minutes at 20 kHz with 100 mW/cm<sup>2</sup> spatial-peak temporal-peak intensity and a 20% duty cycle. The blood glucose level was determined at the beginning of the experiment and, following insulin administration, every 15 minutes for 90 minutes for both the ultrasound and injection groups. The change in blood glucose from baseline was compared between groups. When administered by subcutaneous injection at insulin doses of 0.15 and 0.20 U/kg, there was little change in the blood glucose levels over the 90 minute experiment. Following subcutaneous administration of insulin at a dose of 0.25 U/kg, blood glucose decreased by 190 ± 96 mg/dl (mean ± SD) at 90 minutes. The change in blood glucose following ultrasound mediated insulin delivery was -262 ± 40 mg/dl at 90 minutes. As expected, the magnitude of change in blood glucose between the three injection groups was dependant on the dose of insulin administered. The change in blood glucose in the ultrasound group was greater than that observed in the injection groups suggesting that a higher effective dose of insulin was delivered.



P2-7

**The effect of magnetite nanoparticle agglomerates on ultrasound induced inertial cavitation.**

**Smith M.**<sup>1</sup>, Darton N.<sup>1</sup>, Slater N.<sup>1</sup>

<sup>1</sup> Cambridge University, Cambridge, UK

The effect of magnetite nanoparticle agglomerates (MNP) on cavitation induced by high intensity focussed ultrasound (HIFU) was investigated. MNPs are superparamagnetic particles that can be magnetically targeted within the body. HIFU can penetrate non-invasively into the body and can cause therapeutic cavitation. HIFU induced cavitation has been shown to be significantly enhanced with MNPs, and a combined approach to treatment could be used to increase therapeutic benefits. The effects of MNPs on inertial cavitation were investigated in water, blood and tissue mimicking gel. Upon addition of the MNP, inertial cavitation increased in all three media. Further work was conducted to investigate the effect of duty cycle, peak focal pressure and MNP concentration on cavitation, with increasing duty cycle, peak focal pressure and MNP concentration all increasing the degree of inertial cavitation up to a maximum threshold level. The combined approach of using both MNPs and HIFU could provide more accurate targeting of therapies, and increase the therapeutic effects of HIFU. This would ultimately reduce unwanted side effects and give patients a higher quality of life.



P2-8

**Synergistic inhibition of malignant melanoma proliferation by combined ultrasound-induced cavitations and Melphalan**

**Yamaguchi K.**<sup>1</sup>, Feril Jr L.<sup>1</sup>, Matsuo M.<sup>1</sup>, Takahashi A.<sup>1</sup>, Tachibana K.<sup>1</sup>, Nakayama J.<sup>1</sup>

<sup>1</sup> Fukuoka University, Fukuoka, Japan

**OBJECTIVES:** Malignant melanoma is one of the most malignant tumors known to man. The prognosis of patients who have disseminated melanoma is very poor and conventional treatment methods remain unsatisfactory. Newer effective treatment is greatly needed. We have previously shown that ultrasound-mediated cavitation can be optimized in vitro. Melphalan is known to inhibit tumor growth. It was reported that Melphalan has good effect when combines with TNFa. In this study, we investigated ultrasound-mediated cavitation and Melphalan into melanoma cell line.

**MATERIALS AND METHODS:** About 30,000 human melanoma (C32) cells were plated in each well of the 24-well lumox<sup>TM</sup> MULTIWELL with 50  $\mu$ m thin gas-permeable transparent bottom, and incubated overnight. For sonication, lumox MULTIWELL was placed on top of the ultrasound transducer after applying coupling water-based gel. After Melphalan (dissolved in MEM and adjusted to attain final concentrations of 500, 50, 5, 0.5, 0.05, 0.005 and 0.0005  $\mu$ M) and/or 5  $\mu$ l of echo-contrast agent composed of microbubbles were added to 500  $\mu$ l sample, the cells in monolayer and attached to the bottom of the MULTIWELL were sonicated using an ultrasound device (SonoPore KTAC-4000). Using 2-cm circular transducers designed at 1.011 MHz (power: 0.154 W/cm<sup>2</sup>; burst rate: 0.5 Hz; duty factor: 25%; sonication time: 30 sec). After sonication, cells were incubator. Cell growth and viabilities were assayed by MTS assay at 2 and 3 days after the treatments.

**RESULTS:** Significant cell growth inhibitions were observed in sonicated cells in the presence of Melphalan at concentrations 500, 50, 5 and 0.5  $\mu$ M. However, significant growth inhibition was only observed in groups treated with Melphalan at concentrations 500 and 50  $\mu$ M in unsonicated groups.

**CONCLUSIONS:** These results suggest that ultrasound-mediated cavitation and Melphalan could potentially become a non-surgical method in treating skin diseases, such as malignant melanomas.







### **Regulating ultrasound cavitation in order to induce reproducible sonoporation**

**Mestas J.**<sup>1</sup>, Alberti L.<sup>2</sup>, El Maalouf J.<sup>2</sup>, Béra J.<sup>2</sup>, Gilles B.<sup>2</sup>, Angel Y.<sup>2</sup>

<sup>1</sup>INSERM, Lyon, France

<sup>2</sup>Centre Léon Bérard, Lyon, France

Sonoporation would be linked to cavitation, which generally appears to be a non reproducible and unstationary phenomenon. In order to obtain an acceptable trade-off between cell mortality and transfection, a regulated cavitation generator based on an acoustical cavitation measurement was developed and tested. The cell suspension to be insonified is placed in a medium sample tray. This tray is submerged in degassed water and positioned above the face of a flat ultrasonic transducer (frequency: 445.5 kHz; intensity range: 0.08-1.09 W/cm<sup>2</sup>). This technical configuration was admitted to be conducive to standing-wave generation through reflection at the air/medium interface in the well thus enhancing the cavitation phenomenon. Laterally to the transducer, a homemade hydrophone was oriented to receive the acoustical signal from the bubbles. From this spectral signal recorded each 5 ms, a cavitation index was calculated as the mean of the cavitation spectrum integration in a logarithmic scale, and the excitation power is automatically corrected. The device generates stable and reproducible cavitation level for a wide range of cavitation setpoint from stable cavitation condition up to full-developed inertial cavitation. For the ultrasound intensity range used, the time delay of the response is lower than 200 ms. The cavitation regulation device was evaluated in terms of chemical bubble collapse effect. Hydroxyl radical production was measured on terephthalic acid solutions. In open loop, the results present a great variability whatever the excitation power. On the contrary the closed loop allows a great reproducibility. This device was implemented for study of sonodynamic effect. The regulation provides more reproducible results independent of cell medium and experimental conditions (temperature, pressure).



### **Transfection of cells in suspension by ultrasound cavitation**

**Reslan L.**<sup>1</sup>, Herveau S.<sup>1</sup>, Mestas J.<sup>1</sup>, Dumontet C.<sup>1</sup>

<sup>1</sup>Université Lyon 1, Lyon, France

**OBJECTIVES:** We evaluated the transfection efficiency and toxicity of sonoporation in B-cell Chronic Lymphocytic Leukaemia (CLL) and in a human Follicular Lymphoma cell line (RL).  
**MATERIALS AND METHODS:** B-CLL and RL cells were exposed to continuous ultrasound waves (445 kHz) in presence of either plasmid DNA pEGFP or fluorescent siRNA BCL2L1 in order to assess the transfection efficiency and cell viability. Moreover, we have done stable transfection of both pcDNA3 and PGL3 (coding for luciferase) then injected the luminescent cells in vivo in order to examine the evolution of tumorigenesis in mice. Transfection efficiency and cell viability were assessed using confocal laser scanning microscopy and FACS analysis, respectively.  
**RESULTS:** Sonoporation guarantees a high efficient gene transfer whether in stable or transient transfections with a low rate of mortality. The MFI of both siRNA BCL2L1 and pEGFP were statistically significant in comparison with control.  
**CONCLUSION:** Our ultrasound cavitation device holds great promise for gene therapy and represents an advance for transfection of cells in suspension.



**P3-3**

**Micro-bubble enhanced sonoporation**

**Tachibana R.**<sup>1</sup>, Okamoto A.<sup>1</sup>, Yoshinaka K.<sup>1</sup>, Takagi S.<sup>1</sup>, Matsumoto Y.<sup>1</sup>

<sup>1</sup>The University of Tokyo, Tokyo, Japan

Recently, a development of the ultrasound gene transfer system, called Sonoporation has been investigated. It is known that micro-bubbles can help gene transfection. It is thought that genes are inducted into cells by collapses of cavitation-bubble or micro-bubble. However, the mechanism and optimal induction condition have not been clarified in detail. We examined what factors affect gene induction rate. And, it is intended to issue methods for high-efficiency gene induction rate. In vitro, we inducted GFP-plasmid into fibro-blast cell (NIH3T3) by using ultrasound contrast agent (Sonazoid®, or micro-bubble) and piezoelectric transducer. The cells were cultured on 24-well plates. GFP-plasmid (concentration : 15 mg/mL) and Sonazoid® (number density of micro-bubble : 105 count/mm<sup>3</sup>) were mixed with cell culture solution (D-MEM). Ultrasound frequency was 2.0 MHz (burst wave, duty cycle:10 %). ultrasound intensity was changed from 0 W/cm<sup>2</sup> to 11.0 W/cm<sup>2</sup>, and the exposure time were changed from 0 s to 120 s. Gene induction ratio is higher with stronger or longer ultrasound exposure. However, the ratio is less than 1 %. We also measured cell survival ratio, and visualized cells with holes using Propidium iodide. It is showed that about 80 % cells are alive and many cells get holes under the ultrasound exposure. Therefore, it is suggested that less genes enter into cells or few genes expressed. It is a future task to clear the problem.



**P3-4**

**The effect of cell killing by ultrasound**

**Tachibana K.**<sup>1</sup>, Harada Y.<sup>1</sup>, Feril L.<sup>1</sup>, Endo H.<sup>1</sup>, Ogawa K.<sup>1</sup>, Irie Y.<sup>1</sup>

<sup>1</sup>Fukuoka University School of Medicine, Fukuoka, Japan

Stealth liposome, polyethylene glycolylated liposome, avoids uptake by the reticuloendothelial system, thus improving drug delivery to the tumor while decreasing toxicity. PEGylated liposomes containing doxisolubicin, Doxil®, have been used to treat Kaposi's sarcoma and ovarian cancer in clinical. Doxil circulates around the body at a stable state and accumulates in tumor by passive targeting. But it is difficult to release doxorubicin after accumulation into tumor. So, we made a new bubble liposomes from Doxil. We investigated the effect of cell killing by combination of this new Doxil bubble liposome (encapsulating Doxolubicin bubble liposomes; EDBL) and ultrasound in human monohistiocytic leukemia cell (U937) . In the result, the cell killing effect was enhanced by combination of EDBL and ultrasound.



**Measurements of blood clot displacements induced by pulsed focused  
ultrasound**

**Wright C.**<sup>1</sup>, Hynynen K.<sup>1</sup>, Goertz D.<sup>1</sup>

<sup>1</sup> Sunnybrook Health Sciences Centre, Toronto, Canada

Despite a significant body of work establishing the feasibility of ultrasound potentiated thrombolysis, there remains considerable uncertainty about the specific mechanisms involved in this process. These include acoustic streaming, thermal effects, cavitation, and radiation pressure, though the relative roles of each will likely depend upon the acoustic conditions that are employed. Thrombus displacements due to acoustic radiation forces have been hypothesized to improve the penetration and action of lytic agents and induce strains that promote clot degradation. Their role in thrombolysis is however poorly constrained due to an absence of direct experimental data. The objective of this study is to perform displacement measurements of clots in a focused ultrasound beam. A modified high frequency ultrasound imaging system was employed with an imaging transducer (20 MHz) situated with its plane at an angle of 30 degrees to a focused therapy beam (1.5 MHz, f-# 0.8, -3 dB width 0.8mm). The focal regions of both transducers were colocalized in a blood clot that was situated in a 4mm channel within agar. Therapy pulses (1ms duration) were interleaved (0.1ms spacing) with imaging pulses and successive imaging traces were acquired and processed to extract displacement information along a given line of sight. Acoustic powers ranged from 0.1 to 20W. Thrombus displacements were found to vary linearly with acoustic power, as has been observed in other tissues. For example, after a 16 pulse sequence it was found that the peak displacements at 1 and 8 watts were 25 and 200 microns respectively. It was also observed that 'overshoot' occurred after pulse turn-off, consistent with inertial effects. The time for recovery to initial position varied with power, at 8 watts it was 55 ms. Displacements were negligible by 1.5 mm away from the beam axis. These results provide direct evidence of clot displacements, which may be relevant to understanding and exploiting this effect.

---



P4-1

### Characterisation and application of a custom-made HIFU transducer for robotic manipulation

**Corner G.**<sup>1</sup>, Cochran S.<sup>2</sup>, Gourlay T.<sup>3</sup>, Huang Z.<sup>2</sup>, Mayne K.<sup>4</sup>, Melzer A.<sup>2</sup>

<sup>1</sup> NHS Tayside, Dundee, Scotland

<sup>3</sup> University of Strathclyde, Glasgow, Scotland

<sup>2</sup> University of Dundee, Dundee, Scotland

<sup>4</sup> Piezo-Composite Transducers, Aberdeen, Scotland

**OBJECTIVES:** Areas requiring further research in high-intensity focused ultrasound (HIFU) therapy include treatment time and prevention of tissue heating outside the treatment volume. Electronic beamforming is helpful for precision focusing but requires ultrasound propagation through common regions of adjacent tissue, risking excess thermal dosage. Another potentially valuable technique is robot-mounting of the transducer or array. The objective of the present work is to characterise and apply a custom-made transducer for both ultrasound and MRI-guided (HIFU), with particular reference to use as a robot-mounted device.

**MATERIALS & METHODS:** The transducer is a spherically-focused piezocomposite device, diameter 60 mm, focal distance 70 mm. It was designed principally for robotic manipulation but, for flexibility, has 2 confocal elements of equal area. It is very light, with foam backing, a lightweight casing, and remote electrical impedance matching, to allow rapid motion. It is MRI-compatible but also offers the possibility of ultrasound-guided HIFU. Mounting is possible on 2 robots, a high-precision 6 axis industrial machine and a 5 axis MRI-compatible machine.

**RESULTS:** In early exploration, the industrial robot has been used for basic characterisation, demonstrating performance, and to explore alternative spatial / temporal regimes for lesion creation. Thermal and mechanical tissue resulting from damage using various drive parameters calculated from the known transducer behaviour has been examined microscopically. The transducer has also been mounted on the MRI-compatible robot to demonstrate feasibility of transfer of treatment regimes from the industrial robot.

**CONCLUSIONS:** The development of a lightweight HIFU transducer for robotic manipulation indicates this approach offers significant flexibility and potentially allows performance demonstrated with other systems to be replicated with simplified electronic systems and array design.

P4-2

### Hydrophone arrays for instantaneous measurement of high-pressure acoustic fields

**Ketterling J.**<sup>1</sup>, Lee P.<sup>1</sup>, Kreider W.<sup>2</sup>, Bailey M.<sup>2</sup>, Cleveland R.<sup>3</sup>

<sup>1</sup> Riverside Research Institute, New York, USA

<sup>3</sup> Boston University, Boston, USA

<sup>2</sup> Applied Physics Laboratory, Seattle, USA

**OBJECTIVE:** Lithotripter acoustic field characterization is based on single-point hydrophone measurements even though electrohydraulic lithotripters do not have a highly repeatable sound field. The ability to obtain an instantaneous "snapshot" of the sound field would have broad implications for advancing the understanding of how lithotripters fragment stones and damage kidney tissue. Here, we describe and characterize a hydrophone array composed of 20 elements measuring 0.5 by 0.5 mm and spaced 1.25 mm center to center.

**METHODS:** The arrays were fabricated by bonding a 9- $\mu$ m piezopolymer to a flex circuit. The pattern of the array (i.e., elements and connecting trace lines) was formed on the flex circuit. After bonding, the devices were backed with an epoxy plug in order to provide structural support. The final hydrophone array was secured in an acrylic mount and electrically connected to a 24-line ribbon cable and then to an interface box with 20 SMB connectors. The relative sensitivity of each hydrophone element was measured using a 5.25 MHz focused annular transducer (35-mm focal length, 7.1 mm ID, and 9.45 mm OD). A 46-dB preamp was used prior to digitizing the signals. Excitation was with a 14-cycle tone burst and the pressure was calibrated with a hydrophone.

**RESULTS:** The peak voltage was measured for each hydrophone element for a peak excitation pressure of 4.5 kPa. The peak recorded voltages for all elements were on the order of 120 mV and were within  $\pm 6\%$  of the mean value. One element, number 14, had a very weak signal and was considered dead.

**CONCLUSIONS:** The hydrophone array was able to measure acoustic pressures over a span of 2 cm with very uniform sensitivity. Placed in a lithotripter with acoustic pressures on the order of 10 MPa, the hydrophone elements are expected to directly generate voltages on the order of several volts. By digitizing all channels simultaneously, instantaneous measurement of high-pressure acoustic fields will be possible.



**P4-3**

### Ex vivo experiments by a non-invasive ultrasound theragnostic system

**Koizumi N.**<sup>1</sup>, Seo J.<sup>2</sup>, Suzuki Y.<sup>2</sup>, Yoshinaka K.<sup>2</sup>, Matsumoto Y.<sup>2</sup>, Mitsuishi M.<sup>2</sup>

<sup>1</sup>The University of Tokyo, Tokyo, Japan

<sup>2</sup>School of Engineering, The University of Tokyo, Tokyo, Japan

The authors have developed a non-invasive ultrasound theragnostic system to decrease the strain of patients and medical doctors. The system we propose tracks and follows movement in an affected area –kidney stones here– while High Intensity Focused Ultrasound (HIFU) is irradiated onto the area. The concept behind our proposal focuses on destroying stones. Using focused ultrasound directly without damaging healthy tissue while tracking and following the affected area during movement due, for example to the patient's respiration. In general, the visual servoing performance of the target could be difficult in accordance with the ultrasound image quality. Especially, exquisite background tissues and bubbles generated by HIFU irradiation make the image quality worse and this increases image tracking error. To solve this problem, we propose a novel control framework using quasi-periodical kidney movement, focusing on enhancing servoing performance for this special non-invasive ultrasound theragnostic system. Specifically, we proceed by presenting the concepts, required functions and the system configuration, then discuss the required servoing precision and the problems in the visual motion tracking by ultrasound images. We then analyze kidney movement mainly due to respiration, and propose a controller by utilizing quasi-periodical movement in the affected area to enhance servoing performance. We then review the result of the ex vivo stone motion tracking experiments, while HIFU is irradiated onto the moving kidney stone. Here, the real human kidney motion data is input to the model stone. It is confirmed that the proposed servoing system can track and follow the model stone in the extracted swine kidney. The average motion tracking error is within 1mm (0.65mm in an experiment, for example).



**P4-4**

### Pocket-sized ultrasonic surgical and rehabilitation solutions: from the lab bench to clinical trials

**Lewis Jr. G.**<sup>1</sup>, Olbricht W.<sup>1</sup>, Henderson P.<sup>2</sup>

<sup>1</sup>Cornell University, Ithaca, USA

<sup>2</sup>Weill Cornell Medical College, Ithaca, USA

**OBJECTIVES:** Ultrasound has enormous clinical potential but its clinical implementation has been limited by the size, cost and inefficiency of current technology. Our goal was to develop an easily scalable module base ultrasound system that was capable of producing low-high power ultrasounds over clinically relevant frequencies. Devices based from this technology would then be tested in the hands of physicians and researchers.

**MATERIALS AND METHODS:** In accord with the maximum power transfer theorem (MPTT) engineers match their transducers and amplifier impedances. When ultrasound transducers are intrinsically only 70-80% efficient and the amplifier can only deliver 50% of energy according to the MPTT, less than 40% of the input power will be converted into ultrasound. We proposed that by totally removing the internal impedance of the amplifier the MPTT would not hold. In this new way of thinking, maximum power transfer occurs not when your impedances are matched, but when the source has zero impedance.

**RESULTS:** We have constructed a printed circuit board module 3.8 x 7.6 cm in size that uses commercially available components and has a finite impedance around 0.01 Ohms making it about 99% effective. The ultra-low output impedance amplifier operates in scalable arrangements, where each module provides 100 Vpp and greater than 70 Amps at 0-6 MHz drive frequencies. We have developed multiple portable (0.5-1.8 kg), pocket-sized (10 x 5 x 2.5 cm) battery powered therapeutic ultrasound units from single modules that produce acoustic energies for low and high power applications (1-150 W).

**CONCLUSIONS:** The devices have been used to improve convection enhanced drug delivery 10 fold in brain tissue in vitro and in vivo. Our clinical collaborates use our devices at high powers to cauterize liver and kidney tissue before surgical resection to reduce blood loss, and at lower powers for enhanced drug delivery of systemically injected hydrogen sulfide treatment regimes.



P4-5

### Investigation of parameters affecting treatment time in MRI-guided transurethral ultrasound therapy

**N'Djin WA.**<sup>1</sup>, Burtnyk M.<sup>1</sup>, Chopra R.<sup>1</sup>, Bronskill M.<sup>1</sup>

<sup>1</sup>Medical Biophysics, University of Toronto, Toronto, Canada

MRI-guided transurethral ultrasound therapy shows promise for minimally invasive treatment of localized prostate cancer. Real-time MR temperature feedback can enable the 3D control of thermal therapy to define an accurate region within the prostate. Previous in-vivo canine studies showed the feasibility of this method using transurethral planar transducers. The aim of this simulation study was to reduce the procedure time, while maintaining treatment accuracy by investigating new combinations of treatment parameters. A numerical model was used to simulate a multi-element heating applicator rotating inside the urethra in 10 human prostates. Acoustic power and rotation rate were varied based on the feedback of the temperature in the prostate. Several parameters were investigated for improving the treatment time. Maximum acoustic powers and rotation rates were optimized interdependently as a function of prostate radius and transducer operating frequency, while avoiding temperatures  $>90^{\circ}\text{C}$  in the prostate. Other trials were performed on each parameter separately, with the other parameters fixed. The concept of using dual-frequency transducers was studied, using the fundamental frequency or the 3rd harmonic component depending on the prostate radius. The maximum acoustic power which could be used decreased as a function of the prostate radius and the frequency. Decreasing the frequency (9.7-3.0 MHz) or increasing the power (10-20 W.cm<sup>-2</sup>) led to treatment times shorter by up to 50% under appropriate conditions. Dual-frequency configurations, while helpful, tended to have less impact on treatment times. Treatment accuracy was maintained and critical adjacent tissues like the rectal wall remained protected. The interdependence between power and frequency may require integrating multi-parametric functions inside the controller for future optimizations. As a first approach, however, even slight modifications of key parameters can be sufficient to reduce treatment time.



P4-6

### Development of noninvasive vascular occlusion method with HIFU

**Senoo N.**<sup>1</sup>, Suzuki J.<sup>1</sup>, Deguchi J.<sup>1</sup>, Takagi S.<sup>1</sup>, Miyata T.<sup>1</sup>, Matsumoto Y.<sup>1</sup>

<sup>1</sup>The University of Tokyo, Tokyo, Japan

HIFU treatment with microbubbles is investigated in the present study. It's well known that microbubbles have a potential ability to enhance the heating effect in the ultrasound field. In this study, the heat produced by microbubble oscillation is used to occlude varicose veins. The heated area by HIFU irradiation is measured with white-egg gel, which denatures over 70 degrees. The heated area mainly depends on the frequency of the ultrasound, the intensity at focus, and the irradiation time. Attenuation coefficient is measured in order to confirm that the attenuation at skin is so small that HIFU energy can reach the vein. Then, we conduct animal experiment. We remove rabbit's hair completely and wash rabbit's skin with soap and degassed water in order to eliminate bubbles (which interfere the pass of the ultrasound) from boundary face. The frequency of the ultrasound is 1.7 MHz. The intensity at focus is 1800W/cm<sup>2</sup>. And the irradiation time is 20 seconds. We choose the contrast agent Levovist® as microbubbles, and set the void fraction (the ratio of total gas volume to liquid) in the blood vessel to 10-5. Levovist® is dissolved into normal saline and injected into the vein. The vein is clasped on one side with a forceps and compressed in order to avoid thermal dissipation. Furthermore, hypodermic is injected as coolant for skin. Then, the external jugular vein of rabbit is occluded. Thus, the capability of HIFU treatment to occlude the lower extremity varicose veins is shown.



P4-7

### In vivo evaluations of a phased ultrasound array for transesophageal cardiac ablation

**Smith N.**<sup>1</sup>, Werner J.<sup>2</sup>, Park E.<sup>1</sup>, Jaiswal D.<sup>1</sup>, Hattel A.<sup>1</sup>, Francischelli D.<sup>3</sup>

<sup>1</sup>The Pennsylvania State University, University Park, USA    <sup>3</sup>Medtronic Inc, Minneapolis, USA

<sup>2</sup>The Pennsylvania State University, State College, USA

As one effective treatment, cardiac ablation shows a high rate of success in treating paroxysmal atrial fibrillation. A prevailing modality for this treatment is catheter ablation using radiofrequency. However, there is measurable morbidity and significant costs and time associated with this invasive procedure. To address these issues, a transesophageal ultrasound applicator for noninvasive cardiac ablation has been developed and evaluated in this research. Since the esophagus is close to the posterior of the left atrium, its position makes it attractive for the incision-less surgery of the selected area of the heart using ultrasound. The goal of this research is to create electrically isolating lesions in myocardial tissue by effectively delivering ultrasound energy without moving the array. Based on multiple factors from the simulation results of transducer arrays, current transesophageal medical devices, and throat anatomy, a focused ultrasound transducer that can be inserted into the esophagus has been designed. In this research, a two-dimensional sparse phased array with flat tapered elements as a transesophageal ultrasound applicator was fabricated and evaluated in in vivo experiments. With this array, noninvasive cardiac ablation was performed on five pigs. The array was operated at 1.6 MHz for 8 ~ 15 minutes to create single or multiple lesions on atrial and ventricular myocardium. After ultrasound exposure, lesions having the average size of  $5.1 \pm 2.1$  mm in width and  $7.8 \pm 2.5$  mm in length were created. Based on the experimental results, it was demonstrated that the array can focus and steer the beam inside the tissue. Also, the array can deliver sufficient power to the focal point to produce ablation while not damaging nearby tissue outside the target area. The results demonstrate a potential application of the ultrasound applicator to transesophageal cardiac surgery in atrial fibrillation treatment.



P4-8

### Ultrasound strain imaging towards verification and guidance of prostate thermal therapy with catheter-based ultrasound applicators

**Sridhar-Keralapura M.**<sup>1</sup>, Chubb N.<sup>1</sup>, Scott S.<sup>2</sup>, Juang T.<sup>2</sup>, Prakash P.<sup>2</sup>, Diederich C.<sup>2</sup>

<sup>1</sup>San Jose State University, San Jose, USA

<sup>2</sup>University of California, San Francisco, USA

**INTRODUCTION:** Ultrasound based transurethral and interstitial catheters have been developed and tested in vivo to thermally ablate prostate cancers. Treatment validation and accurate control of therapy is currently done using MR thermal imaging ( $\pm 1^\circ\text{C}$ , update: 5-15s). MRTI is effective for real-time monitoring and guidance, but, cost, setup time, and accessibility can be limiting. Ultrasound imaging methods could be a practicable approach to monitoring.

**OBJECTIVE:** We investigated Ultrasound Strain Imaging (USI) as a tool towards verifying and controlling prostate treatments. Objectives were to - (1) develop a novel methodology for tissue compression using ex vivo tissue models that can be applied in vivo, (2) develop quasi real-time strain estimation algorithms for verifying and tracking treatments.

**METHODOLOGY:** The applicator was inserted into ex vivo porcine muscle tissue and a transrectal or abdominal imaging probe (Terason Inc.) was placed externally. Ablation time was set for 10min at 15W to create a well-defined thermal lesion, with 20s power-off intervals. During power off, tissue was compressed either externally (3-5%) using the probe or by deflating/inflating the applicator's coupling balloon internally. Ultrasound RF data was recorded during the compression and USI was computed within 1 min. USI was also computed post ablation for treatment verification and compared with photographs of corresponding excised tissue sections.

**RESULTS:** USI estimated post ablation using balloon and external methods yielded significant contrast that correlated well with measurements of excised tissue sections. USI with balloon compression during treatments displayed lower contrast as expected but clearly indicated the direction of heating.

**CONCLUSIONS:** USI is an effective feasible tool for verification and guidance of ablation regions with these devices. Balloon compressions could potentially allow for USI in clinical treatments for confirmation and boundary control.







### **A test-bed to calibrate MR thermometry**

**Cunitz B.**<sup>1</sup>, Marro K.<sup>1</sup>, Lee D.<sup>1</sup>, Bailey M.<sup>1</sup>

<sup>1</sup> University of Washington, Seattle, USA

**OBJECTIVE:** MR thermometry is the only FDA-approved temperature monitoring method for clinical transcatheter HIFU procedures, and as implemented, it measures proton resonance frequency shift and maps that to temperature using a linear relationship drawn from historic literature. The goal of this work was to build a test chamber to measure the true relationship in current clinical magnets over a full clinically relevant range of temperatures.

**MATERIAL & METHODS:** A water-filled test chamber was designed to be placed within the magnet bore and heat water uniformly to known temperatures while the proton resonance frequency was measured in a heated slice using a gradient echo sequence. A plot of proton resonance frequency versus temperature was then made. Temperatures from about 37C or less to near boiling were measured because clinical treatments span this range. Also, the goal was to be able to make measurements in several different static magnetic field strengths, specifically 1.5 T, 4.7 T and 3 T, the latter of which are used in clinical HIFU.

**RESULTS:** Heating was accomplished by running an alternating-current through a coil of Nickel-Chromium wire in a water-filled 50-mL closed cylindrical test chamber. Type T thermocouples were mounted in both ends of the chamber to determine actual temperature as well as also measure the uniformity of heating. The system worked reliably with temperatures from 25-95C. Problems with increased pressure and out-gassing were also solved. Preliminary experiments in a 4.7T, 30-cm bore magnet showed a nonlinear dependence of PRF on temperature. In this case, utilizing the standard linear relationship of 0.01 ppm/C would result in a 77C reading when the true temperature was 100C.

**CONCLUSIONS:** A device has been built to measure the PRF vs. temperature curve for various magnets, and initial data obtained to indicate that the relation may differ from the line currently used. Work supported by NIH EB007643 and NSBRI SMST01601.



### **Noninvasive characterization of HIFU transducers using infrared thermography and a mathematical inverse method**

**Girdhar D.**<sup>1</sup>, Robinson R.<sup>1</sup>, Zderic V.<sup>2</sup>, Sliwa J.<sup>3</sup>, Myers M.<sup>1</sup>

<sup>1</sup> Food and Drug Administration, Silver Spring, USA    <sup>3</sup> Epicor, Sunnyvale, USA

<sup>2</sup> Georges Washington University, Washington, USA

**OBJECTIVE:** Characterization of HIFU transducers operating at clinical power levels can be difficult owing to the possibility of hydrophone damage or sensor interference with the focused beam. This study presents a noninvasive method for determining the intensity field of a HIFU beam using infrared (IR) imaging.

**MATERIALS AND METHODS:** A vertical configuration was designed that consisted of a HIFU transducer at the bottom of a tank, sonicating upward into a tissue mimicking material (TMM). The top surface of the TMM was exposed to air with the focal region close to the air-TMM interface. The temperature rise on this top surface that was generated by absorption of ultrasound energy was recorded by an IR camera. Since the top of the TMM was exposed to air, the pressure was zero at the interface, and hence the temperature reading at the top of the TMM layer could not be directly related to intensity. A mathematical inverse method involving simulation of HIFU beam propagation (including reflection off of the air interface) and heat transfer within the TMM was employed to relate measured temperatures to beam intensities.

**RESULTS:** Temperature contours at the upper surface of the TMM were recorded for three different HIFU transducers having gains of 33, 34 and 58. Acoustic power levels varied between 3 Watts and 15 Watts. In the vertical configuration, the thermal patterns recorded by the IR camera spread symmetrically in the radial direction, in contrast to horizontal configuration, where thermal convection currents resulted in a asymmetric (and more difficult to analyze) thermal patterns. Application of the mathematical inverse technique resulted in power predictions that agreed with radiation force measurements to within about 10%.

**CONCLUSION:** The inverse IR method is a promising technique for making quantitative intensity measurements for HIFU transducers.



P5-3

**A novel device for total acoustic output measurement of high power transducers**

**Howard S.**<sup>1</sup>, Twomey R.<sup>2</sup>, Morris H.<sup>1</sup>, Zanelli C.<sup>1</sup>

<sup>1</sup> Onda Corporation, Sunnyvale, USA

<sup>2</sup> NTR Systems Inc., Seattle, USA

**OBJECTIVE:** To develop a device for ultrasound power measurement applicable over a broad range of different medical transducer types, orientations and powers, and which supports automatic measurements to simplify use and minimize errors.

**MATERIAL AND METHODS:** An accurate electromagnetic null-balance has been custom-designed for ultrasound power measurements. All the recommendations from standards such as IEC 61161 were considered. The sensing element was placed in the water, to eliminate errors due to surface tension and water evaporation. The motion and detection of force was constrained to one axis, to increase immunity to vibration from the floor, water sloshing and water surface vibration. The transparent tank was designed so it could easily be submerged in a larger tank to accommodate large transducers or side-firing geometries, and can also be turned upside-down for upward-firing transducers. A vacuum lid was added to allow degassing the water just before a measurement. An external control module was designed to operate the sensing/driving loop and to communicate to a local computer for data logging. The sensing algorithm, which incorporates temperature compensation, compares the feedback force needed to cancel the motion with beams in the "on" and "off" states. These two states can be controlled by the control unit or manually by the user, under guidance by a graphical user interface. Software allows calibration to standard weights, or to independently calibrated acoustic sources.

**RESULTS:** The design was implemented and accommodates a variety of targets, including cone, rubber, brush targets and an oil-filled target for power measurement via buoyancy changes. The system presents measured power live during collection. Measurement examples are presented, emphasizing HIFU sources operating at powers from 1 to 100 W.

**CONCLUSIONS:** This device is user friendly, highly flexible and accurate. It can be used over a wide range of powers and applications.



P5-4

**Study relating thermal dose estimates from RF ultrasound backscatter data and measures of visible tissue discoloration**

**Kaczkowski P.**<sup>1</sup>, Speyer G.<sup>1</sup>, Kargl S.<sup>1</sup>, Brayman A.<sup>1</sup>, Crum L.<sup>1</sup>

<sup>1</sup> University of Washington, Seattle, USA

**OBJECTIVE:** To compare the thermal dose (TD) estimates obtained from backscattered pulse-echo diagnostic ultrasound to TD obtained from observed discoloration in liver tissue.

**MATERIALS AND METHODS:** Backscattered pulse-echo diagnostic ultrasound (DU) provides an effective method of estimating temperature from relative distortion between two frames of ultrasound, one preceding and one following treatment from high intensity focused ultrasound (HIFU). Heat deposition estimation is performed using a parametric modeling technique that relies on the heat transfer equation (HTE), and a functional expansion for the spatio-temporal heat source in a modal series, providing spatially variable estimates of thermal dose within the treated volume. The discoloration visually observed in liver tissue exposed to HIFU therapy is an effective proxy for the applied thermal dose. Samples of bovine liver are treated with high intensity focused ultrasound, with a diagnostic ultrasound positioned to capture RF frames in the focal plane of the HIFU transducer. The treated tissue is sliced in 1mm increments and photographed, and these images are registered to the thermal dose estimates obtained from captured DU RF frames.

**RESULTS:** The correlation between thermal dose estimates and observed discoloration provides a performance index for non-invasive therapy monitoring, allowing the theoretical limits on accuracy to be evaluated. Moreover, this association can be observed for different treatment protocols, varying motion of the HIFU transducer, duration of treatment, applied power and post-treatment acquisition time. In addition, thresholding the discoloration data and thermal dose estimates identifies a lesion volume from which the methods can be compared.

**CONCLUSIONS:** This study dovetails with earlier studies which used simulated thermal dose as a treatment variable for observed discoloration, and supports the use of ultrasonic monitoring of HIFU therapy.



### **Multiple cavitation detection methods for evaluating tissue mimicking materials during HIFU exposure**

**Maruvada S.**<sup>1</sup>, Liu Y.<sup>1</sup>, Herman B.<sup>1</sup>, Harris G.<sup>1</sup>

<sup>1</sup> Food and Drug Administration, Silver Spring, USA

**OBJECTIVE:** Temperature rise during HIFU procedures and the possibility of cavitation activity during heating are important to quantify in planning a safe and effective treatment. Therefore, in pre-clinical testing it is essential to characterize clinical HIFU devices using tissue-mimicking materials (TMM) with well known characteristics, including cavitation properties. The purpose of this study was to monitor cavitation behavior and determine its effect on temperature rise in a HIFU TMM containing an embedded thermocouple

**METHODS:** A 50 um thin wire thermocouple was embedded in a hydrogel-based TMM previously developed for HIFU. HIFU at 1.1 MHz was focused at the thermocouple junction. HIFU focal pressures from 1-6 MPa were applied and the temperature rise and decay were recorded. Three hydrophones were used to monitor cavitation activity during sonication. A hydrophone confocal with the HIFU transducer and a cylindrical hydrophone lateral to the HIFU beam were used for spectral analysis of cavitation signals, and a needle hydrophone placed beyond the HIFU focus was used to record changes in the pressure amplitude due to blockage by bubbles at or near the focus. B-mode imaging was employed to visualize bubble presence during sonication. Forward and reverse electrical powers also were measured.

**RESULTS:** Temperature traces obtained at various pressure levels demonstrated a wide range of heating profiles in the TMM due to the occurrence of cavitation. Hydrophone and reflected power signals varied with focal pressure and B-mode images of cavitation field geometry and the signals could be correlated with suspected cavitation-induced anomalies of the temperature profile.

**CONCLUSION:** Of the several methods studied for detecting cavitation, both the needle hydrophone and electrical power measurements were convenient adjuncts to spectral analysis for evaluating cavitation activity in the TMM. Note: Research supported by DARPA IAG #224-05-6016.



### **Metrology research for external beam cancer therapy: a European initiative**

**Shaw A.**<sup>1</sup>, Koch C.<sup>2</sup>, Durando G.<sup>3</sup>, Karaböce B.<sup>4</sup>

<sup>1</sup> National Physical Laboratory, Teddington, UK

<sup>2</sup> Physikalisch-Technische Bundesanstalt, Braunschweig, Germany

<sup>3</sup> Istituto Nazionale di Ricerca Metrologica, Turin, Italy

<sup>4</sup> Ulusal Metroloji Enstitüsü, Gebze/Kocaeli, Turkey

On 1 April 2008, the European Metrology Research Programme project "External Beam Cancer Therapy" (EBCT) was formally launched with the involvement of nine National Metrology Institutes (NMIs). The central objective of this project is to provide reliable measuring techniques for all forms of cancer therapy based on external radiation. As well as established ionizing radiation techniques, like particle therapy and Intensity Modulated Radiation Therapy (IMRT) with high-energy photon radiation, this project includes the emerging technique of High Intensity Therapeutic Ultrasound (HITU). In the HITU work package, the NMIs involved are from UK, Germany, Italy and Turkey. The overall goal of this part of the project is to improve the efficacy, safety and range of applicability of clinical HITU treatments by providing validated methods for ultrasonic field characterization, HITU system performance testing, quality assurance, and patient exposure monitoring. To achieve this aim, the HITU part will address both the basic calibration and specification of equipment, and the repeatable and controllable clinical use of HITU systems. In general, the methodologies used will build on and extend the techniques used for diagnostic and low intensity physiotherapy ultrasound, by sensor development, computational modelling and materials characterization. Four areas were identified: measurement of power (electrical and acoustic) and efficiency; measurement of acoustic pressure distributions; the development of thermal phantoms to allow the measurement of temperature distributions; and the development of phantoms for evaluating cavitation. This presentation will describe the background to the project and summarise progress related to HITU over the first 18 months. Results will be given from across the four main task areas and the plans for the remaining 18 months will be discussed. The outcomes will be important for equipment development, treatment planning, and standardisation.



**Temperature dependence of the susceptibility of fat leads to significant temperature errors in PRFS based MR thermometry**

**Sprinkhuizen S.**<sup>1</sup>, Konings M.<sup>2</sup>, Bakker C.<sup>2</sup>, Bartels W.<sup>2</sup>

<sup>1</sup> Image Sciences Institute, Utrecht, The Netherlands

<sup>2</sup> University Medical Center Utrecht, Utrecht, The Netherlands

**OBJECTIVE:** Proton resonance frequency shift (PRFS)-based MR thermometry is hampered by temporal field changes. Temporal changes in the susceptibility distribution lead to field changes and are therefore a possible source of errors. The susceptibility of fat,  $\chi_{fat}$ , is temperature dependent, in the same order of magnitude as the temperature dependence of the chemical shift of water (0.0094ppm/°C). PRFS-based temperature measurements may therefore be corrupted by non-local field effects due to temperature induced susceptibility changes in fatty tissue. We performed simulations to quantify the influence of  $d\chi_{fat}/dT$  on PRFS-based MR temperature maps during thermal interventions in the breast.

**MATERIAL & METHOD:** Simulations were performed using a high-resolution 3D breast scan. A thermal intervention was modeled by a spherical thermal spot (TS),  $R=10\text{mm}$ , with a stationary Gaussian temperature distribution and a maximum temperature of 57°C. Susceptibility distributions were calculated for the breast-model without TS and with TS, based on the glandular/fat-fraction, local temperature and using  $\chi_{glandular}=-9.05\cdot 10^{-6}$  and  $\chi_{fat}(T)=-7.79\cdot 10^{-6}+0.0094\cdot 10^{-6}\cdot (T-T_{body})$ . Subsequently, the magnetic field B was calculated in Fourier-domain from these susceptibility distributions. Changes in the magnetic field distribution  $\Delta B$  were quantified by subtraction of the pre- and post-heating outcome. The resulting temperature error was determined using  $\Delta T_{err}=\Delta B[\text{ppm}]/0.0098$ .

**RESULTS:** Our simulations show that temperature induced changes of  $\chi_{fat}$  lead to field changes in glandular tissue. The maximum field change within the glandular tissue was 0.13 ppm, corresponding to a PRFS-based MR temperature error of  $\Delta T_{err}=13.3^\circ\text{C}$ .

**CONCLUSION:** The temperature dependence of  $\chi_{fat}$  leads to significant errors in PRFS-based MR temperature measurements in nearby glandular tissue during thermal interventions in the female breast. Important to stress is that fat-suppression is not a solution for this effect.







**Uniformly sized microbubbles with distinct physical and acoustical properties**

**Borrelli M.**<sup>1</sup>, O'Brien Jr. W.<sup>2</sup>, Bernock L.<sup>1</sup>, Tung S.<sup>3</sup>, Oelze M.<sup>2</sup>, Culp W.<sup>1</sup>

<sup>1</sup> University of Arkansas for Medical Sciences, Little Rock, USA

<sup>3</sup> University of Arkansas, Fayetteville, USA

<sup>2</sup> University of Illinois, Urbana-Champaign, USA

**OBJECTIVES:** Produce uniformly sized microbubbles with distinct physical and acoustic properties that can be stored for a protracted period while maintaining their size and performance characteristics.

**MATERIALS AND METHODS:** Uniformly sized microbubbles were produced by sonicating solutions of serum albumin and dextrose. The mean microbubble diameter in each preparation was adjusted by changing serum albumin and dextrose concentrations, and modulating the ultrasonic power used (20 KHz). Size separation was achieved passively via differential buoyancy (standard deviations 10% or less). Size stability and ultrasonic performance quality control (QC) tests were developed to assure successive microbubble preparations performed identically and to distinguish the acoustic properties of identically sized microbubbles produced with different protocol parameters.

**RESULTS:** Uniformly sized microbubble preparations with average diameters from 0.1  $\mu\text{m}$  to 10  $\mu\text{m}$  were produced reliably. Atomic Force Microscopy confirmed that differences in QC test results are indicative of different Young's modulus values. Microbubble concentration can be measured rapidly and accurately by optical density, which facilitates experimentation. Produced microbubbles can be stored at 5°C for protracted periods ranging from one week to several years, depending on microbubble formulation. Treatment with pH 6.0 citrate buffer protracted storage time without affecting ultrasonic performance while using lower pH buffers increases the Young's modulus and markedly affects other acoustic properties.

**CONCLUSIONS:** Developed protocols can be used to reliably produce uniformly sized microbubble preparations with a wide range of mean diameters and physical and acoustical properties. Such production flexibility will arguably permit investigators to produce microbubbles that are optimally suited for different applications, e.g. acoustic contrast, sonothrombolysis, sonophoresis, sonoporation, etc.

---





## Physical therapy system for children with hemiplegia

**Genis V.**<sup>1</sup>

<sup>1</sup> Goodwin College, Drexel University, Philadelphia, USA

This paper describes a therapeutic system and method for rehabilitating disabled or injured limbs of infants and children diagnosed with hemiplegic cerebral palsy (CP). Children diagnosed with hemiplegic cerebral palsy may benefit by self-generated motor activity produced when they are forced to use their affected limb by constraining their unaffected limb and applying a variety of standard reinforcement techniques. Such "Constraint-Induced Movement Therapy" has shown promise when applied to adults with stroke and more recently to children diagnosed with hemiplegia. Under the guidance of a physical therapist, the child is forced to perform structured behavioral reinforcement exercises using his or her disabled arm, which is typically flexed at the elbow and characterized by a clenched fist. These techniques, however, only facilitate grasping skills, which may lead to significant impairment of hand opening. Only older children who have already learned to use their affected limb to manipulate objects are eligible for this type of therapy. The described system will allow the child to receive multimodal feedback (mainly auditory and visual) when he or she self-produces proprioceptive feedback and moves the affected arm or extends the fingers of the affected hand. This manipulation should produce a richer coordinated information feedback from self-produced activity generated by multimodal sources. The developed device would optimize the spatial and temporal dimensions of stimulation and associated packages that can be used on young children from 7 to 25 months old. The piezoelectric device-based system will allow for training children, such as extending the fingers, lifting the affected arm, and clapping. The results of this work will be used for future clinical investigations of the developed device to verify effectiveness and safety for young children with hemiplegic CP consistent with FDA requirements.



## Temperature fields in soft tissue during hyperthermia treatment: numerical predictions and experimental results

**Kujawska T.**<sup>1</sup>, Wójcik J.<sup>1</sup>, Nowicki A.<sup>1</sup>

<sup>1</sup> IFTR PAS, Warsaw, Poland

Increasing of cells immunity against stress can be obtained through the heat shock proteins (Hsp) expression enhancement induced by hyperthermia. The possibility of the Hsp expression enhancement in soft tissues *in vivo* by means of controlled exposure to ultrasound would allow to evaluate the ultrasound-based treatment efficiency. Ultrasonic regimes can be controlled by adjusting the ultrasound intensity, frequency, pulse duration, duty cycle and exposure time. Our objective was to develop the numerical model capable of predicting in space and time the temperature fields induced by circular focused transducer generating tone bursts in multilayer nonlinear attenuating media and next to compare the numerically calculated results with the measurement results *in vitro* and *in vivo*. For the prediction of temperature distributions in multilayer biological media the Pennes' bioheat transfer equation was employed. The measurements of temperature distributions were performed using the experimental facility including the temperature controlled water tank, 8-thermocouple module and tested tissue chamber. Temperature measurements *in vitro* were carried out in a fresh rat liver using a 15 mm diameter, 25 mm focal length and 2 MHz frequency transducer generating 20-cycle tone bursts (duty cycle 20%) with spatial peak temporal average acoustic intensities lying between 0.56 and 3.4 W/cm<sup>2</sup> and various exposure times. Measurements *in vivo* have been done along the acoustic axis at the focal plane. The experimental data were compared with numerical simulations obtained under experimental boundary conditions. Good agreement between the theoretical and measurement results for all cases considered has verified the validity and accuracy of our numerical model. Quantitative analysis of the obtained results enabled to find how the ultrasound-induced temperature rises in the rat liver could be controlled by adjusting both, the acoustic intensity and exposure time.



P7-3

**In-vivo study of monitoring thermal ablation by ultrasound imaging**

**Winkler I.**<sup>1</sup>, Adam D.<sup>1</sup>

<sup>1</sup> Technion - Israel Institute of Technology, Haifa, Israel

Real-time monitoring of thermal therapy of tumors is still a challenge. While MRI provides such capabilities, ultrasound (US) imaging is preferable due to its wide availability. Yet, US provides reliable measure of tissue changes only for 5-8 degrees elevations. Monitoring thermal damage was reported, by measuring the distribution of microbubbles (MB) generated due to the heating, up to high temperatures (Temp). This approach utilizes measurements of US echoes at half the transmitted frequency, based on the assumption of non-linear oscillation of MB by the incident US field. This study was undertaken to assess this technique in in-vivo animal studies, while movements due to blood pulsation and breathing may interfere. The study included 10 anesthetized rabbits. RF ablation was employed in the liver, while monitoring with a modified commercial US imaging system that allowed processing of raw US echoes. The transmit frequency used was 4 MHz of 15 cycles pulses. Each received A-line was segmented, each segment processed by an auto-regressive estimator of the power spectrum density. Total energies at 2 different frequency bands were derived, at low frequency band 1-2.5 MHz (LFB), and at the transmit frequency band 3.5-4.5 MHz (TFB). The results were compared to thermocouples Temp measurements, and to post-treatment visualization of the ablated region. Results show that mean energies at the LFB and TFB increase substantially in areas adjacent to the RF needle. The amount of these energies also fluctuates at high Temp, thus producing large variance of the received energy. A significant increase of at least 3 dB of the LFB was demonstrated for regions reaching Temp of 53±5 and above. Mean energies in areas distant from the RF needle showed little increase or variance. Thus, the in-vivo studies demonstrate the feasibility of monitoring targeted thermal therapy, in spite of blood pulsation and breathing movements.



P7-4

**Endocavity ultrasound array integrated within a HDR brachytherapy ring applicator for targeted hyperthermia to the uterine cervix**

**Wootton J.**<sup>1</sup>, Prakash P.<sup>1</sup>, Juang T.<sup>1</sup>, Diederich C.<sup>1</sup>

<sup>1</sup> UCSF, San Francisco, USA

**OBJECTIVES:** Investigate the feasibility of targeted hyperthermia delivery by an intrauterine ultrasound applicator to patient-specific treatment volumes in conjunction with HDR brachytherapy using theory and experiment.

**METHODS:** 30 HDR brachytherapy treatment plans were inspected to define hyperthermia treatment volumes (HTVs) based on tumor and radiation target volumes. Several typical cases were imported into a patient-specific treatment planning platform that optimized acoustic output power from an endocavity multisectored tubular array to conform temperature and thermal dose to HTVs. Perfusion was varied within a clinical range of 0.5-3 kg/m<sup>3</sup>/s. Applicators were constructed with 1-3 elements at 6.5-8 MHz with 90-360 degree sectoring and 15-35 mm heating length housed in a water-cooled PET catheter. Acoustic output was compared to heating in phantom assessed with implanted thermometry or MR temperature imaging (MRTI). Radiation attenuation through the device was measured in an ionization chamber.

**RESULTS:** The HTV extends 2-4cm in diameter and 2-4cm in length. The bladder and rectum are within 10-12 mm. HTV targets can be covered with temperature clouds >41C and thermal dose >5min with 45-47C maximum temperature and rectal temperature <41.5C. Sectored applicators preferentially direct energy laterally into the parametrium to limit heating of rectum and bladder. Additional ultrasound devices in interstitial brachytherapy catheters can extend therapeutic heating. Temperature distributions in phantom show preferential heating within sectors and align well with acoustic output. Heating control along the device length and in angle is evident with MRTI. A 4-6% reduction in radiation transmission through the transducers was observed, which could likely be compensated for in planning.

**CONCLUSIONS:** Patient-specific modeling and experimental heating demonstrated 3-D conformal heating capabilities of endocavity ultrasound applicators. Support: NIH R01CA122276







## Extension of the angular spectrum method to curved transducer surfaces

**Christensen D.**<sup>1</sup>, Vyas U.<sup>1</sup>

<sup>1</sup> University of Utah, Salt Lake City, USA

**OBJECTIVE:** To extend the angular spectrum (AS) method to calculate pressure from a curved transducer source (surface of rotation around the axis of propagation). The angular spectrum method is a fast, accurate and computationally efficient method to model wave propagation, but it requires that the source field amplitude be specified on a plane, limiting its utility in applications like HIFU where curved transducers are used extensively. The objective of this paper is to propagate the angular spectrum of a curved source to an intermediate plane that is perpendicular to the propagating axis, from where the fields can then be propagated by conventional AS methods.

**MATERIALS AND METHOD:** The new approach, called the Ring-Bessel technique, decomposes the curved source into circular rings of increasing radii, each ring a different distance  $z_i$  from the intermediate plane, and calculates the angular spectrum of each ring using a Fourier transform. Each angular spectrum is then propagated to the intermediate plane where all the propagated angular spectra are summed (complex addition) to obtain the pressure on that plane. The method can be applied to phased arrays as well as solid transducer faces.

**RESULTS:** The accuracy of the Ring-Bessel technique was compared to the Rayleigh-Sommerfeld integral technique and it was found that when using the same sampling points on the source surface the normalized difference for a 10 cm x 10 cm (201 x 201 voxel) transverse plane in the geometric focal zone was 3%. The Ring-Bessel technique reduces calculation times by a factor of approximately 100 compared to the Rayleigh-Sommerfeld method.

**CONCLUSION:** A purely frequency-domain technique using the angular spectrum approach for modeling beams propagated from curved transducers was developed and shown to be fast and accurate.



## Bandwidth limitations in characterization of High Intensity Focused Ultrasound fields in the presence of shocks

**Khokhlova V.**<sup>1</sup>, Bessonova O.<sup>2</sup>, Canney M.<sup>1</sup>, Bailey M.<sup>1</sup>, Sonesson J.<sup>3</sup>, Crum L.<sup>1</sup>

<sup>1</sup> University of Washington, Seattle, USA

<sup>3</sup> Food and Drug Administration, Silver Spring, USA

<sup>2</sup> Faculty of Physics, Moscow State University, Moscow, Russia

**OBJECTIVES:** Nonlinear propagation effects can result in the formation of weak shocks in high intensity focused ultrasound (HIFU) fields. When shocks are present, the spectrum of the wave theoretically consists of hundreds of harmonics. However, in practice, shock waves are modeled using a finite number of harmonics in numerical simulations and measured with hydrophones that have limited bandwidths. The goal of this work was to determine how many harmonics are necessary to model or measure peak pressures, intensity, and heating rates within an accuracy of 10%.

**MATERIAL & METHODS:** Nonlinear simulations of HIFU fields were performed using different algorithms and different numbers of harmonics. Plane wave propagation was simulated first within a wide range of initial amplitudes; the parameters of shock waves were calculated and compared using different number of harmonics. Focal waveforms were then modeled and measured in water and beyond an absorptive (0.7 dB/cm/MHz) tissue phantom. A 2 MHz HIFU source of 44 mm aperture and focal length was operated at various excitation levels at which in situ intensities reached 25 kW/cm<sup>2</sup>. Two fiber-optic hydrophones of 30 and 100 MHz bandwidth were used in measurements. Peak pressures, intensities, and heating rates were determined in the shock waveforms for different numbers of harmonics included in simulations and measurements.

**RESULTS AND CONCLUSION:** Theoretical and experimental data demonstrated that 10 harmonics were sufficient to determine the peak negative pressure and temporal-average intensity with an accuracy of 10% for shock waves up to intensity levels of 25 kW/cm<sup>2</sup>. Shock amplitude, peak positive pressure, and heating rates were much more sensitive to the bandwidth and more than 100 harmonics were necessary to determine these values with a similar accuracy. The work was supported in parts by NIH EB007643, NSBRI SMS00402, and RFBR 09-02-01530 grants.



P8-3

Potential temperature limitations of bubble-enhanced heating during HIFU

**Kreider W.**<sup>1</sup>, Bailey M.<sup>1</sup>, Sapozhnikov O.<sup>1</sup>, Crum L.<sup>1</sup>

<sup>1</sup> University of Washington, Seattle, USA

**OBJECTIVE:** During high-intensity focused ultrasound (HIFU) treatments in the absence of bubbles, tissue is heated by absorption of the incident ultrasound. However, bubbles present at the focus can enhance the rate of heating. One mechanism for such enhanced heating involves inertial bubble collapses that transduce incident ultrasound to higher frequencies that are more readily absorbed. Previously, it has been reported that bubble-enhanced heating diminishes as treatments progress. The objective of this effort is to quantify how inertial bubble collapses are affected as the focal temperature rises during treatment.

**MATERIAL & METHODS:** A model of a single, spherical bubble has been developed to couple the thermodynamic state of a strongly driven spherical bubble with the temperature of the surrounding liquid. This model allows for the dynamic transport of heat, vapor, and non-condensable gases to/from the bubble and has been demonstrated to fit experimental data from the collapses and rebounds of millimeter-sized bubbles over a range of temperature conditions.

**RESULTS:** The responses of micron-sized air bubbles in water were simulated under exposure to MHz/MPa HIFU excitation at various surrounding liquid temperatures. Each bubble response was characterized by the power spectral density of its radiated pressure in order to emulate a hydrophone measurement. Simulations suggest that bubble collapses are significantly attenuated at temperatures above about 70°C. For instance, the acoustically radiated energy at 80°C is an order of magnitude less than that at 20°C.

**CONCLUSIONS:** Simulations that fully include the effect of vapor on bubbles excited during HIFU suggest that the efficacy of bubble-enhanced heating may be limited to temperatures below 70°C. [Work supported by NIH DK43881 and NSBRI SMST01601.]



P8-4

Numerical simulation of high intensity focused ultrasound therapy with volume model of human body

**Okita K.**<sup>1</sup>, Sugiyama K.<sup>2</sup>, Ono K.<sup>1</sup>, Takagi S.<sup>1</sup>, Matsumoto Y.<sup>2</sup>

<sup>1</sup>RIKEN, Saitama, Japan

<sup>2</sup>The University of Tokyo, Tokyo, Japan

The development of HIFU therapy for the deeply placed cancer has been desired. An array transducer is developed to control the displacement of a focal point due to the reflection and refraction of ultrasound. However, it is difficult to estimate the phase delay preoperatively because of the propagation through the inhomogeneous media, i.e. human body. The objectives of the present study are the estimation of the appropriate phase control of the array transducer and the support for the preoperative planning of HIFU therapy by the computational prediction of the treatment region. HIFU therapy with an array transducer in a human body is simulated. The ultrasound focuses on a target inside the body whose media is discretized into cubic elements with the data for a living human body collected by CT/MRI. To represent the ultrasound propagation, the mass and momentum equations for mixture with the equation of state of media are solved. Additionally, the heat equation with viscous dissipation is solved to consider the heat coagulation, which is modeled as a phase transition by the Allen-Cahn equation with a free energy model. Firstly, as a result of the HIFU therapy for the brain cancer, we obtain a clear focal point where the peak pressure is higher than that without phase delay. Secondly, the result for the liver cancer with considering the heat coagulation shows that the increase of acoustic impedance due to the coagulation causes the scattering of ultrasound at the interface of the coagulation region, which then develops toward the transducer. The results conclude that the appropriate arrangement of the phase delay assigns the focal point to the target even if the ultrasound propagates through the inhomogeneous medium, and the influence of the heat coagulation of tissue on the acoustic field should be considered to predict the treatment region precisely.



**Combining thermal and ultrasound modeling techniques for improved monitoring of MR guided HIFU treatments**

**Todd N.**<sup>1</sup>, Vyas U.<sup>1</sup>, Payne A.<sup>1</sup>, Christensen D.<sup>1</sup>, Parker D.<sup>1</sup>

<sup>1</sup> University of Utah, Salt Lake City, USA

**OBJECTIVE:** Develop model predictive filtering (MPF) to use tissue thermal and acoustic properties to improve temperature monitoring of MR guided HIFU procedures.

**METHODS:** A low level pre-treatment heating pulse prior is used to determine the ultrasound power deposition field and the tissue thermal properties. The MPF algorithm uses this information to reconstruct temperature images from highly undersampled 3-D segmented EPI data. The obtains large coverage, high spatial resolution temperature maps with a time step suitable for monitoring HIFU heating. Ex vivo experiments compared 2 implementations of the MPF method to the traditional PRF technique. The first implementation uses retrospectively undersampled k-space data from a 3-D segmented EPI sequence (R factor = 6.5) and the second instance uses prospectively undersampled data from a 3-D GRE sequence (R factor = 12.1). For electronic steering off axis, ultrasound beam propagation software will be used that can rapidly predict the changes in ultrasound power deposition due to effects of electronic steering and tissue inhomogeneities.

**RESULTS:** When compared to fully sampled PRF temperatures, each implementation of the MPF algorithm successfully reconstructed accurate temperature maps. The temperature RMSE was 0.6°C in each case, and the average differences between the 5 hottest voxels in the hottest time frame were  $-0.3 \pm 1.1^\circ\text{C}$  and  $1.1 \pm 0.7^\circ\text{C}$  for the retrospective and prospective cases, respectively. Although not yet incorporated in the MPF algorithm, the ultrasound beam propagation algorithm has been verified to be accurate in homogeneous tissue by comparing it with the Rayleigh-Sommerfeld technique, with results obtained an order of magnitude faster for a 201x201x201 model.

**CONCLUSION:** Model predictive filtering works well for on axis heating. The robustness and efficiency of MPF and the applicability to inhomogeneous tissue regions will be improved by incorporating the ultrasound beam modeling algorithm

---





**Correlation between color flow Doppler study around uterine myomas and nonperfused ratio immediately after magnetic resonance-guided focused ultrasound**

**Funaki K.**<sup>1</sup>, Fukunishi H.<sup>1</sup>

<sup>1</sup> Shinsuma General Hospital, Kobe, Japan

**OBJECTIVE:** To examine the relationship between color flow Doppler study indices and the ablation effect of magnetic resonance-guided focused ultrasound surgery (MRgFUS)

**MATERIALS AND METHODS:** This study included 29 myoma patients who underwent MRgFUS. Of these, 21 patients were treated for single myomas and 8 were treated for two or more myomas simultaneously. The perimyomatous artery of all the patients was assessed by color flow Doppler study immediately before MRgFUS. Peak velocity, pulsatility index (PI), and resistant index (RI) were measured. Nonperfused Ratio (NPR) immediately after MRgFUS was used to judge an ablated area and the relationship between color flow Doppler study indices and NPR was examined. We have previously reported that high-intensity myomas (type 3), classified using pretreatment T2-weighted MR imaging, are less effectively treated by MRgFUS than low- (type 1) and intermediate- (type 2) intensity myomas. Hence, we have ceased treating type 3 myomas with MRgFUS today. We also compared the color flow Doppler study indices based on the myoma type.

**RESULTS:** This study included 12 type 1 and 17 type 2 patients. Peak velocity, PI, and RI were almost the same irrespective of the myoma type. The treated largest myoma volumes and NPR were  $253.7 \pm 191.6$  cm<sup>3</sup> and  $57.8 \pm 16.7\%$  (mean  $\pm$  standard deviation), respectively. Mild correlation was observed between RI and NPR ( $r = 0.29$ ). However, peak velocity and PI showed no correlation with NPR.

**CONCLUSION:** The perimyomatous artery color flow Doppler study correlates weakly with NPR immediately after MRgFUS. Abundant blood flow around myoma is one of the predictive factors of poor ablation after MRgFUS.



**Salvage HIFU: factors influencing the outcome in low or intermediate risk patients with local recurrence after external beam radiation therapy (EBRT)**

**Gelet A.**<sup>1</sup>, Murat F.<sup>1</sup>, Cherasse A.<sup>1</sup>, Poissonnier L.<sup>1</sup>, Chapelon JY.<sup>2</sup>, Martin X.<sup>1</sup>

<sup>1</sup> Hôpital Edouard Herriot, Lyon, France

<sup>2</sup> INSERM, Lyon, France

**INTRODUCTION & OBJECTIVES:** To evaluate the efficacy of salvage HIFU in low or intermediate risk patients with a local-only prostate cancer recurrence after EBRT and to define prognostic factors.

**MATERIAL & METHODS:** 124 patients with biochemical relapse after EBRT received salvage HIFU for a biopsy-proven local-only recurrence. Pre-EBRT groups included low and intermediate risk patients in 53 and 71 patients, respectively. Mean pre-HIFU age, PSA were  $69 \pm 5.4$  years;  $4.94 \pm 4.05$  ng/ml. Pre-HIFU Gleason sum were  $\leq 6$ ,  $=7$ ,  $\geq 8$  in 51, 33 and 39 patients, respectively. HIFU failure was defined using the combined Phoenix criteria (pathological and biochemical criteria). Kaplan-meier analysis was used to calculate the disease-free survival rate (DFSR).

**RESULTS:** Mean follow-up was 24 months. Mean number of HIFU sessions was 1.18 (1 and 2 sessions in 106, 18 patients, respectively). Systematic control biopsies were negative in 67% with a median PSA nadir of 0.07 ng/ml and 72% of patients with a PSA nadir  $< 0.5$  ng/ml. Overall and specific survival rates were 94% and 96% at 5 years, respectively. Metastasis and adjuvant therapy free survival rates were 88% and 37% at 5 years. The overall DFSR was 30% at 5 years. DFSR was adversely affected by the pre-HIFU Gleason score (GS) (48%; 17% and 16% when GS  $\leq 6$ ,  $=7$ ,  $\geq 8$ , respectively;  $p=0.01$ ) and PSA level (46%; 21% and 9% when PSA  $< 4$ , 4-10,  $> 10$  ng/ml, respectively;  $p=0.004$ ). On the opposite, neither the pre-EBRT risk level ( $p=0.58$ ), the use of androgen deprivation with EBRT ( $p=0.69$ ), nor the pre-HIFU number of positive biopsies ( $p=0.5$ ) did influence the DFSR.

**CONCLUSIONS:** Salvage HIFU is a valid and effective treatment option for low Gleason score local recurrence after EBRT. Salvage HIFU is more effective when intended as early as possible, with a PSA value below 4 ng/ml.



P9-3

**Evaluation of an acoustic reflector to protect large abdominal wall scars during MR-guided focused ultrasound ablation (MRgFUS) of uterine fibroids**

**Gorny K.**<sup>1</sup>, Chen S.<sup>1</sup>, Hesley G.<sup>1</sup>, Brown D.<sup>1</sup>, Hangiandreou N.<sup>1</sup>, Felmlee J.<sup>1</sup>

<sup>1</sup>Mayo Clinic College of Medicine, Rochester, USA

**PURPOSE:** Large anterior abdominal wall scars in the acoustic path of the MRgFUS transducer beam have been considered a contraindication for fibroid treatment due to reports of severe skin burns secondary to absorption of acoustic energy in the scar. Here we evaluate thin, flexible, rectangular foam-based acoustic reflectors for their potential application to protect such scars during MRgFUS treatments.

**MATERIALS AND METHODS:** MR-thermometry was used to visualize and evaluate thermal lesions in a gel-based tissue-mimicking phantom resulting from sonications across the 1×20cm foam reflector positioned at the base of the phantom (corresponding to patient skin level during MRgFUS treatment). The sonications were performed using a clinical patient setup (ExAblate 2000, InSightec, Haifa, Israel) for varied prescribed depth of sonication, transducer output power and angle. The distance between the base of the lesion and the reflector, and peak lesion temperatures were measured for sonications across the reflector and compared to those obtained without the reflector in the beam path.

**RESULTS:** For sonications through the reflector, distance from the reflector to the base of the thermal lesion is shifted in comparison to sonications without the reflector by 1cm for shallow sonications (i.e. less than 35mm of prescribed depth from skin). The shift is unaffected by transducer angle and remains constant for angles of up to 23 degrees. Peak lesion temperature is reduced with reflector in the beam path by 10-15°C for shallow sonications. This reduction however can be compensated by increasing acoustic power.

**CONCLUSION:** The 1×20cm rectangular foam reflects incident acoustic power creating a 1cm deep acoustic shadow zone behind it. These reflectors have potential to protect large abdominal scars and enable MRgFUS in patients previously excluded from treatment.



P9-4

**Hand-held ultrasound elastography for guiding liver ablations produced using a toroidal HIFU transducer. Results of animal experiments**

**Chenot J.**<sup>1</sup>, Melodelima D.<sup>1</sup>, Souchon R.<sup>1</sup>, Chapelon JY.<sup>1</sup>

<sup>1</sup>INSERM, Lyon, France

The use of real-time elastography for imaging HIFU ablations produced during surgery in porcine liver by a toroidal HIFU transducer was investigated. A conventional linear 12 MHz real-time ultrasound imaging probe was used to obtain radiofrequency signals from a modified B-K ultrasound scanner. Strain images were calculated and displayed in real-time at 60 frames/s using a correlation-based method. Ablations produced in pigs during in vivo treatments were imaged. The quality of the elastograms corresponding to the elastically inhomogeneous liver (normal and ablated tissues) was assessed by computing the contrast-to-noise ratio (CNRe) and the signal-to-noise ratio (SNRe). In addition, the ablation dimensions measured on sonograms and on elastograms were compared to gross pathology. The contrast observed between sonograms and elastograms was also compared. Sonograms and elastograms allowed observation of ablations with dimensions corresponding well to dimensions measured on gross pathology ( $r=0.82$  and  $0.94$  respectively). The average CNRe and SNRe were  $4.7 \pm 5.1$  ( $0.1 - 24.7$ ) and  $2.7 \pm 1.3$  ( $1.1 - 7.5$ ) for elastograms and sonograms respectively. The contrast between ablated and non-ablated tissue was higher on elastograms ( $-15.6$  dB) when compared with sonograms ( $-9.5$  dB). In two specific cases, elastograms allowed a better evaluation of the ablation extent than sonograms. Hand-held sonography/elastography is straightforward and allows combining the advantages of both modalities used in a highly complementary manner for the guidance of ablations produced in the liver during surgical HIFU therapy.

**P9-5**

**The effect of the rat skull on temperature deposition in the brain**

**King R.**<sup>1</sup>, Rieke V.<sup>2</sup>, Butts Pauly K.<sup>1</sup>

<sup>1</sup> Stanford University, Stanford, USA

<sup>2</sup> Stanford University, Palo Alto, USA

**OBJECTIVES:** MR-guided therapeutic ultrasound is being investigated for a range of brain treatments including localized tumor ablation, pain alleviation, and localized drug delivery. In the development of an appropriate animal model, the influence of the skull on the acoustic field needs evaluation. Wave propagation simulations through the intact skull of the mouse have shown to cause minimal beam distortion, and thermal deposition. While this may be true in the mouse, it may not hold true for the rat. The purpose of this work was to measure the effect of the skull on ultrasound propagation through the rat skull.

**METHODS:** Experiments were performed both ex-vivo and in-vivo with the InSightec Exablate System in a 3T GE MRI scanner, using a 2D PZT array comprised of 1024 elements at 0.55MHz. Three sets of experiments were performed: a) in two gel phantoms, two grid patterns of 41 sonications total were performed, b) in ex-vivo rat skulls, sonications were performed in a grid pattern encompassing the entire skull, 48 locations total across three different skulls, and c) in 1 in-vivo experiment, sonications were performed in 4 locations. In all experiments, the beam was assessed by quantitation of the temperature profile using PRF thermometry 2-3 mm from the inner surface of the skull.

**RESULTS:** Ex-vivo, 11/48 sonications created small single spots showing a temperature rise in phantom material. In all other sonications the heat was diffuse with multiple foci. This is compared to the phantom with no skull where 39/41 sonications created single temperature spots, which were on average within 0.5 mm from the expected location. In-vivo, only 1/4 sonications created a single thermal spot.

**CONCLUSION:** The effect of the rat skull needs to be considered and possibly compensated for, when using it as a model to perform therapeutic ultrasound in the brain.

---

**P9-6**

**Harmonic Motion Imaging (HMI) for Focused Ultrasound (HMIFU): initial in vivo results**

**Maleke C.**<sup>1</sup>, Hou Y.<sup>1</sup>, Konofagou E.<sup>1</sup>

<sup>1</sup> Columbia University, New York, USA

The capability of HMIFU for real-time monitoring of tissue stiffness changes during heating was previously demonstrated in ex vivo bovine livers<sup>1</sup>. Here, initial feasibility of the HMIFU for thermal ablation is shown in a transgenic mouse model of breast cancer in vivo. The mammary tumor sizes were ranging from 3 to 10 mm in diameter. The FUS transducer with a center frequency of 4.5MHz, was driven by an AM signal at 15Hz, to generate an oscillatory radiation force with acoustic intensity of 1050 W/cm<sup>2</sup> at the focal region. A 3.3MHz phased-array imaging transducer was aligned to be confocal with the FUS beam. The imaging transducer was used to image the relative tissue stiffness changes during application of the oscillatory radiation force. A digital low-pass filter was used to remove the spectrum of the higher power beam and its harmonics from the acquired RF-signals prior to displacement estimation. The resulting axial displacement was estimated using cross-correlation with a window size of 1 mm and 85% overlap. The peak-to-peak displacement amplitudes were compared before and after lesion formation to assess whether HMI correctly localized and ablated the tumor. HMI displacements from two mice with 8 lesions formed in each mouse (16 lesions total) showed that the average displacement amplitude before and after lesion formation were equal to 17.34±1.34µm and 10.98±1.82µm, respectively (p-value<0.001). The lesion formation was identified by a 30% decrease in displacement amplitude. Cell death was confirmed by histology (H&E stain). The HMIFU system may offer a cost-efficient and reliable alternative for real-time monitoring thermal ablation. Grayscale B-mode and M-mode images with overlaying color-coded HMI displacements can be used to visualize the targeted region and follow the relative tissue stiffness changes during heating so that the treatment procedure can be performed in a time-efficient manner. 1 Maleke C & Konofagou EE, Phys Med Biol, 53, 1773-1793.



**Clinical application of a novel graphical user interface for high intensity focused ultrasound ablation of uterine fibroids**

**Venkatesan A.**<sup>1</sup>, Stratton P.<sup>2</sup>, Segars J.<sup>2</sup>, Merino M.<sup>3</sup>, Sokka S.<sup>4</sup>, Wood B.<sup>1</sup>

<sup>1</sup> National Institutes of Health, Bethesda, USA

<sup>3</sup> National Cancer Institute, Bethesda, USA

<sup>2</sup> National Institute of Child Health and Human Development,  
Bethesda, USA

<sup>4</sup> Philips Medical Systems, Boston, USA

**OBJECTIVES:** To describe clinical applications and an open clinical trial using an integrated system with a novel graphical user interface (GUI) developed for treatment planning, closed-loop control, cavitation detection, volumetric monitoring and delivery of MR-guided HIFU ablation of uterine fibroids.

**MATERIAL AND METHODS:** The MR-HIFU graphical user interface (GUI) displays real-time temperature data on T2 anatomical images, accumulated thermal dose information and ultrasound parameters such as transmitted output power and treatment time. The operator can select specific volumes to obtain graphical real-time temperature readouts. The temperature display is updated every 3 seconds. Real-time feedback informs the operator of safety parameters, such as undesired temperature elevations in off-focal and focal areas, a significant drop in transmitted power, a significant drop in temperature versus time curve at the focus, and cavitation reaching a critical level. The cavitation monitor detects bubble activity rather than solely monitoring elevations in temperature. The ultrasound system will automatically shut down if the transducer heats to critical temperatures, if the measured output power substantially varies from requested power, if high levels of reflected power are detected in the amplifiers, or if any system control element fails to respond correctly to a control request. Inclusion criteria for this Phase I clinical trial include symptomatic fibroids from 3-16 cm, up to 250cc treatment volume and > 1.5 cm from serosa.

**RESULTS:** Early clinical and histologic results of the Phase I treat and resect clinical trial will be presented, including radiologic-to-pathologic correlation of HIFU therapy plans with ex vivo hysterectomy specimens.

**CONCLUSIONS:** Tightly integrated feedback loops for MR-guided HIFU could enhance the safety profile. A novel GUI with cavitation detection for clinical use has been deployed in a Phase I clinical trial for uterine fibroid ablation.

---







### HIFU dose delivery time reduction through focal zone size and path and transducer power optimization

**Coon J.**<sup>1</sup>, Vyas U.<sup>1</sup>, Payne A.<sup>1</sup>, Christensen D.<sup>1</sup>, Roemer R.<sup>1</sup>

<sup>1</sup> University of Utah, Salt Lake City, USA

**OBJECTIVES:** Our study investigated the hypothesis that an optimal focal zone size can be utilized to significantly reduce dose delivery time for HIFU treatments.

**MATERIALS AND METHODS:** To test our hypothesis, we performed several simulated treatments and compared the dose delivery times of 8 representational paths and 4 focal zone sizes over several transducer power levels and bulk perfusion levels. Large focal zones were created by rapidly switching a maximally focused focal zone in the X-Y plane with constant transducer power. Focal zone paths were created by mechanically steering each focal zone through predetermined treatment sites. The tissue region had constant and homogeneous physical tissue properties. The power on times were iteratively solved to find the optimal heating time (including dose delivered with the power off) to deliver the target dose for each site. Cooling time was imposed after each pulse if starting a new pulse would violate the normal tissue safety constraints.

**RESULTS:** Our results show that the dose delivery time is reduced by using the smallest focal zone possible. Also, paths which start in the middle of the tumor and then treat positions immediately behind and in front of the initial position, repeating this pattern for the whole tumor, also reduce dose delivery time. These results hold over several transducer power and perfusion levels. Finally, high transducer powers always lowered dose delivery time, even with normal tissue cooling effects considered. Physical mechanisms that produce this time reduction are dose and temperature superposition and maximal tumor power delivery.

**CONCLUSIONS:** To reduce dose delivery time 1. Use small focal zones. 2. Start in the middle of the tumor, treat behind and in front of this initial position, and repeat. 3. Use the highest transducer power possible.



### Real-time tissue thermometry using an acoustic neural network method during HIFU treatment

**Fan L.**<sup>1</sup>, Sekins K.<sup>1</sup>

<sup>1</sup> Siemens Healthcare, Issaquah, USA

Investigate a new real-time, non-invasive tissue temperature monitoring method during HIFU therapy using Neural Networks. Experimental setup included ex-vivo porcine livers, a HIFU transducer, an ultrasound imaging system, and a thermocouple. HIFU power administration and raw image data acquisition were interleaved at 3Hz. Multiple features from ultrasonic signals were used in a recurrent neural network to generate a localized target zone real-time temperature estimate. The features included tissue displacement, signal normalized cross-correlation coefficient, backscattered signal power change, and tissue elasticity. The first three features were computed from comparisons of each temporal frame with the baseline frame. The elasticity was estimated at high pulse repetition rate with milliseconds resolution. The experimental data sets were divided into training sets and testing sets. After training the neural network with the dosing training set, temperature estimation was performed on the testing data. On the testing data, the difference between the time-varying temperatures measured by the thermocouple and that estimated by the neural network method was very acceptable (<1C over 400 temporal sampling points). The maximum difference occurred where second derivative of temperature vs. time approached zero. The results demonstrate that the proposed method has the potential to non-invasively estimate tissue temperatures during HIFU power administration. By analyzing the extracted features and the estimated temperatures, during the initial temperature-rise phase, normalized cross-correlation contributes significantly to the estimation, possibly due to the tissue thermal expansion; then speed of sound change may dominate until the temperature rises to a certain level (~55C); after that, tissue stiffness and backscattered signal power contribute more than the other components. Research sponsored by United States DARPA contract HR0011-08-3-0004.



P10-3

**Patient specific modeling platform for transurethral and interstitial ultrasound thermal therapy**

**Prakash P.**<sup>1</sup>, Diederich C.<sup>1</sup>

<sup>1</sup> University of California, San Francisco, USA

**OBJECTIVE:** Develop a comprehensive 3D patient specific acoustic and biothermal modeling platform for ultrasound ablation with multi-sectored tubular arrays, including all tissue properties and dynamic tissue changes critical to accurate modeling.

**METHODS:** Representative patient anatomies were reconstructed from CT/MR images with critical structures delineated and assigned associated physical properties. A 3D finite element solver was used to compute transient temperature profiles. We explored the applicability of assessing tissue thermal effects using critical temperature, thermal dose and Arrhenius thermal damage thresholds. We analyzed the impact of dynamic acoustic attenuation and blood perfusion as functions of these thermal effects. Closed-loop MRTI control was modeled by: modulating power to each transducer to limit peak temperature, monitoring temperature/thermal dose at multiple pilot-points to ensure complete target coverage, and considering MR update times and temperature uncertainty. We designed and assessed strategies to reliably create conformal ablation zones in various targets including prostate BPH, focal prostate cancer, uterine fibroids, liver and GI tract.

**RESULTS:** Extents of the ablation zone assessed by 50-52C, 240 CEM43 and 99% Arrhenius thermal damage thresholds are in excellent agreement for 5-15 min treatments. Using constant acoustic attenuation and blood perfusion, the model predicts up to 56% larger and 36% smaller ablation zones, respectively, than when dynamically adjusting these parameters. Substantial bone heating occurs when treating prostate within 1-2cm of bone, especially when treating the apex. MR update times <15s suffice for reliable control.

**CONCLUSION:** We have developed a comprehensive modeling platform for catheter-based ultrasound ablation to explore site-specific designs and treatment strategies. The feasibility of conformal ablation with MR control in soft tissue targets is demonstrated.



P10-4

**Development of computer controlled three dimensional HIFU focus model scanning system**

**Seo J.**<sup>1</sup>, Koizumi N.<sup>1</sup>, Yugo S.<sup>1</sup>, Akira N.<sup>1</sup>, Yoichiro M.<sup>1</sup>, Mamoru M.<sup>1</sup>

<sup>1</sup> School of Engineering, The University of Tokyo., Tokyo, Japan

To improve one of the important safety issues and as a basic study of a precise HIFU treatment system, it is required to make sure the spatial acoustic pressure distribution and HIFU focal region. In particular, there are many types of HIFU transducers are used such as the phased array type, ordinary extracorporeal transducer but having big centric hole for monitoring ultrasound probe, or some arbitrarily shaped HIFU transducers and so on. In this situation, since the difference between mathematical and a real HIFU irradiation model can deteriorate therapeutic safety, the inspection of the three dimensional shapes of HIFU focal region and irradiation reproducibility of the designed transducer by scanning system is strongly required. In the meanwhile, notwithstanding many reported approaches for scanning, the conventional method based on hydrophone is still often used to estimate HIFU acoustic pressure distributions due to its reliability, reproducibility, and simplicity of the system. Therefore, this research proposes an optimized scanning solutions to build a three dimensional acoustic pressure distribution of HIFU using mechanical system configured by XYZ stage, oscilloscope and control software. We, firstly, introduce an exact and automated HIFU focal position searching algorithm in the specified scanning volume. And from the searched HIFU focus, we scan acoustic pressure distributions on each X-Y, X-Z, and Y-Z planes by traversing scan path based on global coordinate system. Then we combine three planar scan results and extract focal shape by the user specified threshold. Then the extracted focal shape is fitted by primitive geometry to be parameterized. And the parameterized focal shapes under various irradiation parameters are stored to be used later for quantitative analysis of HIFU focus.





# Authors index

[www.istu2009.org](http://www.istu2009.org)



*Silvacane Abbey  
A Jewel of the Cistercian art  
between Provence and Luberon*

*Art Exhibitions  
Guided tours on Sundays  
Tel : +33 (0)4 42 50 41 69*





**A**

Abi-Jaoudeh N	P2-1
Adam D	P7-3
Akira N	P10-4
Al Mahrouki A	S9-6
Alberti L	P3-1
Amat A	S6A-2
Ambroise L	S8-3
Anand A	S3A-10, S3A-2
Angel Y	P3-1
Aptel F	S8-4
Arai Y	P1-11
Aramaki Y	P2-4
Arnal B	S3A-4
Arnaud F	S7A-5
Arora M	S3A-6, S3A-7, S3B-7, S6A-5
Arvanitis C	S3B-3, S3B-7, S6B-7
Aubert I	S4B-9
Aubry JF	S5-1, S2A-2, S3A-8, S4A-3, S4A-4, S4A-7
Ayala-Grosso C	S4B-9
Azevedo J	S3A-10, S3A-2

**B**

Bailey M	S1-8, S2B-3, S7A-6, P4-2, P5-1, P8-2, P8-3
Bakker C	P5-7
Ballard J	S1-2
Bamber J	S8-7
Banerjee R	S8-9
Barnes S	S3A-9
Bartels W	P5-7
Baseri B	S7B-1
Battais A	S8-6
Bazan-Peregrino M	S3B-3, S3B-7, S6B-7
Beard P	S5-10
Beissner K	S8-10
Bera J	S2A-4, P1-3, P1-5, P3-1
Bernock L	S2A-5, P6-1
Berriet R	S8-3
Bessonova O	P8-2
Beziat J	P1-3
Birer A	S8-4
Blana A	S9-2
Bobkova S	S2B-1

Bock M	S10-10, S7B-4
Borrelli M	S2A-5, P6-1
Bouakaz A	S6B-4
Bouchoux G	S8-3, S3B-2, S6B-6
Boyes A	S9-5
Brayman A	S3A-5, P5-4
Bronskill M	S9-5, S9-8, S10-7, P4-5
Brown D	P9-3
Burtnyk M	S9-8, S10-7, P4-5
Butterworth I	S7A-2
Butts Pauly K	S10-2, S10-6, S10-9, P9-5

**C**

Cain C	S1-9, S2B-2, S2B-5
Canales L	S3A-11
Canney M	S2B-3, S7A-6, P8-2
Carpentier A	S4A-2
Cassadó J	S3A-11
Casper A	S1-2
Chang F	S6B-5
Chapelon JY	S1-3, S8-4, S8-6, S8-7, S9-10, S3B-2, P9-2, P9-4
Charrel T	S8-4
Chau A	S7B-7
Chaussy C	S9-2
Chavrier F	S8-4
Chen C	S6B-5
Chen J	S10-6, S10-9
Chen P	S7B-2
Chen S	P9-3
Chenot J	P9-4
Cherasse A	P9-2
Chesnais S	S6B-6
Chiba T	P1-7
Chitnis P	P1-1
Choi J	S7B-1, S7B-5
Chopra R	S9-5, S9-8, S10-7, S7B-7, P4-5
Christensen D	S5-8, S6B-3, P8-1, P8-5, P10-1, S5-4
Chubb N	P4-8
Civale J	S8-8, S9-7, S5-10
Cleveland R	S10-5, P4-2,
Cochran S	P4-1
Cohard E	S5-1
Contag C	S4B-4

Conti G	S9-2
Coon J	P10-1
Corner G	P4-1
Couillaud F	S3B-4
Couppis A	S2B-6
Coussios C	S3A-6, S3A-7, S3B-3, S3B-7, S6A-2, S6A-5, S6B-7
Couture O	S3B-5, P1-2
Cranston D	S1-6
Crawford N	S4B-7
Crum L	S2B-3, S3A-5, S6A-1, S7A-6, P5-4, P8-2, P8-3
Culp W	S2A-5, P6-1
Cunitz B	S1-8, P5-1
Curriel L	S4B-2
Czarnota G	S9-6

## D

Damianou C	S2B-6
Darton N	P2-7
David M	P9-4
De Bever J	S5-4
Deckers R	S3B-4
Deguchi J	P4-6, P4-7
Demeester J	S4B-10
Deng C	S4B-3
Denis de Senneville B	S2B-7, S10-4, S10-3, S10-1
Desmedt S	S4B-10
Diederich C	P7-4, P10-3, P4-8
Dodds J	P2-6
Draudt A	S10-5
Drazic J	S7B-3
Dreher M	S2A-7, S3B-6, S4B-7, S4B-8
Dumontet C	P3-2
Durando G	P5-6
Duryea A	S2B-2

## E

Ebbini E	S1-2, S3A-3
Efros A	S6B-3
El Maalouf J	P3-1
Emberton M	S9-1
Endo H	P3-4
Endo Y	P2-4

Enholm J	S1-7
Ensing G	S1-9

## F

Fabiilli M	P2-2
Fan L	P10-2
Fan Z	S4B-3
Felmlee J	P9-3
Feril L	P3-4, P2-8
Ferrara K	S4B-4, S7A-4
Fillinger L	S7B-6
Fink M	S5-1, S5-3, S2A-2, S3A-4, S3A-8, S3B-5, S4A-3, S4A-4, S4A-7
Fossheim S	S6B-6
Fowlkes B	S2B-5
Fowlkes J	P2-2
Francischelli D	P4-7
Fredberg J	S6A-3
Frenkel V	S2A-7, S3B-6, S4B-7, S4B-8, P2-1
Fukuda H	S1-4
Fukunishi H	P9-1
Funaki K	P9-1
Furusawa H	S1-5

## G

Garapon P	P1-2
Gateau J	S2A-2
Gavrilov L	S2B-1
Geers B	S4B-10
Gélat P	S8-5
Gelet A	S9-10, S9-2, P9-2
Genis V	P7-1
Gennisson J	S3A-4
Giles A	S9-6
Gilles B	S2A-4, P3-1
Giridhar D	P5-2
Gleizal A	P1-3, P1-5
Goertz D	S2A-3, P3-5
Gorny K	P9-3
Gourlay T	P4-1
Gyöngy M	S3A-6

**H**

Hadjisavvas V	S2B-6
Hall T	S9-4
Hancock H	S4B-7, P2-1
Hand J	S2B-1
Hangiandreou N	P9-3
Harada Y	P3-4
Hariharan P	S8-9
Harris G	S5-2, S7A-1, P5-5
Hattel A	P4-7
Haw C	S3A-7
Hempel C	S9-4
Henderson P	P4-4
Herman B	S5-2, P5-5
Herveau S	P3-2
Hesley G	P9-3
Hey S	S2B-7
Hockham N	S6A-5
Hoelscher T	S2A-6
Holbrook A	S10-2
Horinouchi T	P1-11
Hotta S	P1-7
Hou Y	P9-6
Howard S	P5-3
Hu S	P2-3
Hua M	S7B-2
Huang C	S7B-2
Huang Y	S4B-9
Huang Z	P4-1
Huber P	S10-10, S7B-4
Hunter K	S4B-7
Hwang JH	S2B-3, S6B-1, S7A-6
Hynynen K	S8-11, S8-2, S2A-3, S4B-9, S6A-6, S7B-3, S7B-7, P1-6, P1-8, P3-5

**I**

Ignasi Corral-Baques M	S6A-2
Ioannides K	S2B-6
Iosif D	S2B-6
Irie Y	P3-4
Isern Quittlet J	S3A-11
Ito R	S1-4

**J**

Jaiswal D	S6B-2, P4-7
Jang B	S4B-8
Jayadewa C	P1-4
Jeanmonod D	S4A-6
Jenderka KV	S8-10
Jenne JW	S10-10, S7B-4
Jones G	S2A-7, P2-1
Jordao J	S4B-9
Juang T	P7-4, P4-8
Jung J	S6B-1

**K**

Kaczkowski P	S1-8, S3A-5, P5-4
Kaddur K	S6B-4
Kajiyama K	S6A-7
Kapoor A	S2A-7
Karaböce B	P5-6
Kargl S	P5-4
Karshafian R	S9-6
Kassell N	S4A-1
Katsuike Y	P1-7
Kaye E	S10-2, S10-6, S10-9
Kennedy A	S4B-5
Ketterling J	P4-2,
Khokhlova T	S2B-3, S7A-6, S2B-1, S2B-3
Khokhlova V	P8-2
Khuri-Yakub P	S8-1
Kickhefel A	S4A-8
Kimmel E	S6A-3
King R	P9-5
Kitazumi G	P1-7
Kobelevskiy I	S9-8
Koch C	P5-6
Köhler M	S1-7, S10-4, S10-3, S2B-7
Koizumi N	P4-3, P10-4
Komaki K	S1-5
Konings M	P5-7
Konofagou E	S7B-1, S7B-5, P9-6
Kostson E	S6A-8
Kovacheva R	S7A-5
Kraff A	S10-10, S7B-4
Krause N	S7B-4

Kreider W	P4-2, P8-3
Kruse D	S4B-4, S7A-4
Kudo T	P1-11
Kujawska T	P7-2
Kukic A	S8-2, S7B-7
Kulisa M	S9-10
Kumon R	S4B-3
Kurtenoks V	S7B-6
Kuwahara M	P1-11
Kyriakou ZM	S6A-2

## L

Lacoste F	S7A-5
Lafon C	S8-3, S8-4, S3B-2, S6B-6
Lai CY	S7A-4
Lai P	S10-5
Larrat B	S5-3, S4A-7
Laurent C	S10-1
Lavandier B	P1-3, P1-5
Lee D	P5-1
Lee K	S4B-2
Lee P	P4-2,
Lee Y	P2-3
Lentacker I	S4B-10
Lepetit-Coiffe M	S3B-4
Leskinen J	P1-6
Leslie T	S1-6, S3A-6
Lewis Jr G	S7B-6, P4-4
Li S	P1-3
Lin CY	S6B-5
Lin W	S6B-5, P2-3
Liu D	S3A-3
Liu HL	S7B-2
Liu T	S6B-5
Liu Y	P5-5
Lourenco de Oliveira P	S3B-4
Ludomirsky A	S1-9
Lugovaya M	P1-10

## M

Machida E	S1-5
Mackanos M	S4B-4
Maclair G	S10-3, S10-1
Maeda Y	S1-5

Maier F	S10-10, S7B-4
Maleke C	P9-6
Mamoru M	P10-4
Mamou J	P1-1
Marquet F	S3A-8
Marro K	P5-1
Marsac L	S4A-3
Martin E	S4A-6
Martin X	S9-10, P9-2
Martynov S	S6A-8
Maruvada S	P5-5
Maruyama H	P1-7
Maruyama K	S4B-1, S4B-6, P2-4, P2-5
Matias A	S3B-2
Matsumoto Y	S4A-5, S6A-7, P3-3, P4-3, P4-6, P4-7, P8-4
Matsuo M	P2-8
Maxwell A	S2B-2, S2B-5
Mayne K	P4-1
McLaughlan J	P1-1
McLaurin J	S4B-9
Meairs S	S2A-1, S2A-2
Medan Y	S10-9
Melodelima D	S1-3, S8-6, S8-7
Melzer A	P4-1
Merino M	P9-7
Merle M	S10-4
Mestas J	S3B-2, S6B-6, P3-1, P3-2
Miller N	S8-7
Miller R	S1-9
Mitsuishi M	P4-3
Miyata T	P4-6, P4-7
Mizrahi N	S6A-3
Mochizuki T	P1-7
Montaldo G	S5-3
Moonen C	S10-4, S10-1, S3B-4, S2B-7, S10-3
Morel A	S4A-6
Morris H	P5-3
Morris P	S5-10
Mougenot C	S1-7
Muchart J	S3A-11
Murat F	S9-10, P9-2
Murray T	S10-5, P1-1
Myers M	S5-2, S8-9, P5-2
Mylonas N	S2B-6
Mylonopoulou E	S3B-7

**N**

N'Djin WA	S1-3, S8-6, S8-7, P4-5
Nagata Y	S9-3, S9-9
Nakahara H	S1-5
Nakamura Y	S6A-4
Nakano M	S9-3, S9-9
Nakano O	P1-11
Nakayama J	P2-8
Nam K	S4B-5, S6B-3
Negishi Y	S4B-6, P2-4
Negussie A	S3B-6
Neuberger T	S10-8
Nishiie N	S4B-1, S4B-6
Noble A	S3A-7
Nowicki A	P7-2

**O**

O'Brien, Jr. W	S2A-5, S5-1, P6-1
O'Connell-Rodwell C	S4B-4
Oda Y	S4B-1, S4B-6, P2-5
Oelze M	S2A-5, P6-1
Ogawa K	P3-4
Ohto M	S1-4
Okamoto A	P3-3
Okita K	P8-4
Olbricht W	P4-4
Ono K	P8-4
O'Reilly M	S8-11
Otake S	P2-5
Owen N	S8-3
Owens G	S1-9

**P**

Paik C	S4B-8
Pannacci N	S3B-5
Park E	S10-8, S6B-2, P2-6, P4-7
Park J	S4B-3
Parker D	S5-4, S5-8, P8-5
Partanen A	S3B-6
Paun M	S1-8
Payne A	S5-4, P8-5, P10-1
Pernot M	S5-3, S3A-4, S3A-8, S4A-3, S4A-7

Pessarrodona A	S3A-11
Petruzzello J	S3A-10, S3A-2
Phillips R	S1-6
Pialat J	P1-3
Pichardo S	S4B-2, P1-8
Pinton G	S4A-4
Piron J	S6B-4
Poissonnier L	S9-10, P9-2
Prada C	S5-1
Prakash P	P7-4, P10-3, P4-8
Protheroe A	S1-6
Prus O	S10-9

**Q**

Quesson B	S10-1, S10-4, S10-3, S2B-7
-----------	----------------------------

**R**

Rapoport N	S4B-5, S6B-3
Rauschenberg J	S10-10
Razjouyan F	S4B-8, P2-1
Rebillard X	S9-2
Rémi S	P9-4
Reslan L	P3-2
Retat L	S9-7
Rieke V	S10-2, P9-5
Ries M	S10-3, S10-1, S2B-7
Rifai B	S3B-3, S6B-7
Ritchie R	S1-6, S3A-6
Rivens I	S8-5, S8-8, S9-7, S5-10, S3B-1, P1-4
Rivoire M	S1-3, S8-6
Robert B	S4A-3
Roberts W	S9-4
Robertson C	S9-2
Robinson R	P5-2
Rodriguez J	S3A-11
Roemer R	S5-8, P10-1
Roland J	S4A-8
Roujol S	S10-4
Roy R	S10-5, P1-1
Rybyanets A	P1-9, P1-10

**S**

Saffari N	S5-5, S5-6, S5-7, S8-5, S6A-8
Sakamoto A	S1-4
Saletes I	S2A-4
Sanders N	S4B-10
Santos J	S10-2
Sapin E	S3A-4
Sapozhnikov O	S1-8, P8-3
Sarvazyan A	S7B-6
Satoh M	P1-11
Scaife C	S4B-5
Schad K	S6A-6
Schenone F	S1-3
Schick F	S4A-8
Scott S	P4-8
Sebastian I	P2-2
Segars J	P9-7
Sekine S	P2-4
Sekins K	S3A-9, P10-2
Senoo N	P4-6, P4-7
Seo J	P4-3, P10-4
Servois V	S3B-5
Sethuraman S	S3A-10, S3A-2
Seymour L	S6B-7
Shah A	S1-8
Shaw A	S2B-1, S7A-2, P5-6
Shea J	S4B-5
Shin I	S4B-8
Shoji S	S9-3, S9-9
Sinden D	S5-6
Slater N	P2-7
Sliwa J	P5-2
Smith M	P2-7
Smith N	S10-8, S6B-2, P2-6, P4-7
Soini J	S1-7
Sokka S	P9-7
Somaglino L	S3B-2, S6B-6
Soneson J	S7A-3, P8-2
Souilah A	S4A-7
Speyer G	S3A-5, P5-4
Sprinkhuizen S	P5-7
Sridhar-Keralapura M	P4-8
Stephens D	S7A-4
Stone M	S2A-7
Stratton P	P9-7

Stride E	S5-6, S6A-8
Sugiyama K	P8-4
Sutcliffe P	S7A-4
Sutin A	S7B-6
Suzuki J	P4-6, P4-7
Suzuki R	S4B-1, S4B-6, P2-4, P2-5
Suzuki Y	P4-3

**T**

Tabeling P	S3B-5
Tachibana K	P2-8, P3-4
Tachibana R	P3-3
Taira Y	S4B-1, P2-5
Takagi R	S2B-4
Takagi S	S6A-7, P3-3, P4-6, P4-7, P8-4
Takahashi A	P2-8
Tamura Y	S4A-5
Tanter M	S5-3, S2A-2, S3A-4, S3A-8, S3B-5, S4A-3, S4A-4, S4A-7, P1-2
Ter Haar G	S3A-1, S3B-1, S5-5, S5-7, S8-5, S8-8, S9-7, S5-10, P1-4
Terachi T	S9-3, S9-9
Todd N	S5-4, P8-5
Tokarczyk A	S3B-1
Trillaud H	S1-7
Tung S	S2A-5, P6-1
Tung YS	S7B-1, S7B-5
Twomey R	P5-3

**U**

Uchida T	S9-3, S9-9
Uebayashi J	S4A-5
Umemura S	S2B-4
Usui Y	S9-3
Utashiro H	S6A-7
Utoguchi N	S4B-1, S4B-6, P2-5

**V**

Vedula S	S9-5
Venkatesan A	P9-7
Ventikos Y	S3B-3
Vilensky G	S5-5, S5-7

Vyas U S5-4, S5-8, P8-1, P8-5,  
P10-1

## W

Wang J S7B-2  
 Wang TY S2B-2, S2B-5  
 Wang Y S6B-1  
 Wang Z S1-4  
 Waspe A S7B-7  
 Webb A S10-8  
 Wei K S7B-2  
 Weihs D S6A-3  
 Weiß C S4A-8  
 Werner B S4A-6  
 Werner J S6B-2, P4-7  
 Wheat J S9-4  
 Winkler I P7-3  
 Wójcik J P7-2  
 Wood B S2A-7, S3B-6, S4B-7,  
P2-1, P9-7  
 Woodford S S5-5, S5-7, S8-8  
 Wootton J P7-4  
 Wright C S2A-3, P3-5  
 Wu F S1-1  
 Wu X P2-3

## X

Xu Z S1-9, S2B-2, S2B-5

## Y

Yamaguchi K P2-8  
 Yarmolenko P S3B-6  
 Yasuda Y S1-5  
 Yee C S7A-6  
 Yoichiro M P10-4  
 Yoshinaka K S6A-7, P3-3, P4-3  
 Yoshizawa S S2B-4  
 Yuan L S2B-2  
 Yudina A S3B-4  
 Yugo S P10-4

## Z

Zadicario E S4A-6

Zahur S S9-7  
 Zanelli C P5-3  
 Zderic V P5-2  
 Zehbe I S4B-2  
 Zeng X S3A-9  
 Zhou S S3A-10, S3A-2  
 Zhou Y S6B-1  
 Zhu H S1-4

Conception / Réalisation  
**Agence DORIQAM**  
Tél. 04 42 24 20 99  
[www.doriqam.fr](http://www.doriqam.fr)  
Septembre 2009



# CÉSAR

## le Rhône pour mémoire

20 ANS DE FOUILLES DANS LE FLEUVE À ARLES

MUSÉE DÉPARTEMENTAL ARLES ANTIQUE  
24 OCTOBRE 2009 / 19 SEPTEMBRE 2010  
Presqu'île du cirque romain 13200 Arles  
04 90 18 88 88 - arles-antique.cg13.fr

Cette exposition est reconnue d'intérêt national par le ministère de la culture et de la communication / Direction des musées de France. Elle bénéficie à ce titre d'un soutien financier exceptionnel de l'Etat



**CONSEIL  
GENERAL**  
BOUCHES-DU-RHÔNE

cg13.fr



Marseille  
Provence  
Musée  
de la culture  
2013

## What inspired our MR-HIFU innovation? A stress free non-invasive therapy.

Having uterine fibroids can be painful and established treatment options require long recovery. Philips MR-HIFU\* offers a non-invasive alternative treatment of uterine



fibroids that lets most patients return to normal life within two days.

Learn more at [www.healthcare.philips.com/mri](http://www.healthcare.philips.com/mri),  
or email to [mr-hifu.info@philips.com](mailto:mr-hifu.info@philips.com)

\* Because our innovations are inspired by you

**PHILIPS**

sense and simplicity



\* Investigational device; available for clinical use in selected countries soon.